UNIVERSIDAD NACIONAL AUTÓNOMA DE MÉXICO
DOCTORADO EN CIENCIAS BIOMÉDICAS
INSTITUTO DE INVESTIGACIONES BIOMÉDICAS

La cinasa de histidina CckA es inhibida por el regulador de respuesta Osp y forma un asa de retroalimentación negativa del sistema de CckA-CtrA en la bacteria *Rhodobacter sphaeroides.*

TESIS
QUE PARA OPTAR POR EL GRADO DE:
DOCTOR EN CIENCIAS

PRESENTA:
BENJAMÍN DE JESÚS VEGA BARAY

DIRECTOR DE TESIS
DRA. ROSA LAURA CAMARENA MEJÍA
INSTITUTO DE INVESTIGACIONES BIOMÉDICAS
COMITÉ TUTOR
DR. GEORGES DREYFUS CORTÉS
INSTITUTO DE FISIOLOGÍA CELULAR
DR. DIMITRIS GEORGELLIS
INSTITUTO DE FISIOLOGÍA CELULAR

CIUDAD DE MÉXICO, CDMX, SEPTIEMBRE DE 2022

Agradecimientos

A mi comité tutoral Dra. Laura Camarena Mejía, Dr. Georges Dreyfus Cortés y al Dr. Dimitris Georgelis, por todo el apoyo, dedicación, aportaciones y enseñanzas durante mi proceso de formación.

Al apoyo técnico de la QFB Aurora Osorio y la Dra. Clelia Domenzain y por sus valiosas aportaciones.

A mis compañeros de laboratorio, por su tiempo y su disposición a discutir ideas, resultados, experimentos y sobre todo por su compañía y todo su apoyo.

Al Dr. Sebastian Poggio, por todas sus aportaciones a este trabajo.

Al grupo del Dr. Georges Dreyfus, QFB Teresa Ballado y al Dr. Javier de la Mora, por sus comentarios en seminarios y apoyo técnico.

A la profesora Tzipe Govezensky Zack por su valiosa ayuda y asesoría de estadística.

A la Dra. Rosa Laura Camarena Mejía, por su apoyo invaluable, por su tiempo, enseñanzas, dedicación, por compartir su pasión por la ciencia, por no dejarme claudicar a pesar de los obstáculos, gracias.

Al CONACyT por otórgame la beca para poder realizar mis estudios de Doctorado.

Al Doctorado en Ciencias Biomédicas

Este estudio es parte de los requisitos para obtener el grado de doctor de Benjamín de Jesús Vega Baray (Doctorado en Investigación Biomédicas Básica UNAM), y se contó con el apoyo de la beca de CONACyT 587609.

Este trabajo se desarrolló en el Instituto de Investigaciones Biomédicas, en el Departamento de Biología Molecular y Biotecnología bajo la asesoría de la Dra. Rosa Laura Camarena.

Este trabajo se desarrolló en diferentes momentos gracias al apoyo de los donativos DGAPA-UNAM (PAPIIT IN204317, IG200420).

A mis padres: Alma y Fermín,

por su amor incondicional.

Contenido

Resumen

En las α-proteobacterias, el sistema de dos componentes (TCS) formado por la cinasa de histidina híbrida CckA, la fosfotransferasa ChpT y el regulador de respuesta CtrA. Está ampliamente distribuido. En estos microorganismos este sistema controla distintas funciones como motilidad, reparación de ADN y división celular. En las Caulobacterales y Rhizobiales, CckA es regulada por la pseudo-cinasa DivL y el regulador de respuesta DivK. Sin embargo, este circuito regulatorio difiere en otros grupos de bacterias. En las Rhodobacterales, DivK está ausente y DivL consiste solo en los dominios PAS. En este estudio reportamos que en *Rhodobacter sphaeroides,* la actividad de cinasa de CckA es inhibida por Osp, un regulador de respuesta de un solo dominio que directamente interacciona con el dominio de transmisión de CckA. *In vitro*, la actividad de cinasa de CckA se redujo considerablemente con concentraciones equimolares de Osp, mientras que la actividad de fosfatasa no se afectó. También describimos que la expresión de *osp* es activada por CtrA; lo que crea un asa de regulación negativa. Sin embargo, en condiciones en las cuales se activa el sistema de CckA-ChpT-CtrA el aumento de la transcripción de *osp* no es equivalente con la acumulación de Osp, lo que sugiere una regulación más compleja.

Un análisis filogenético de algunas especies de Rhodobacterales muestra que se distribuye en distintos géneros, en la mayoría de las especies que presentan *osp* se encontró un motivo similar al sitio de unión de CtrA en la región regulatoria de *osp.* Lo que sugiere que el sistema CckA-ChpT-CtrA es controlado por este nuevo circuito regulatorio que incluye a Osp en estas bacterias.

Abstract

In α-proteobacteria, the two-component system (TCS) formed by the hybrid histidine kinase CckA, the phosphotransfer protein ChpT, and the response regulator CtrA is widely distributed. In these microorganisms, this system controls diverse functions such as motility, DNA repair, and cell division. In *Caulobacterales* and *Rhizobiales*, CckA is regulated by the pseudo- histidine kinase DivL, and the response regulator DivK. However, this regulatory circuit differs for other bacterial groups. For instance, in *Rhodobacterales,* DivK is absent and DivL consists of only the regulatory PAS domain. In this study, we report that, in *Rhodobacter sphaeroides*, the kinase activity of CckA is inhibited by Osp, a single domain response regulator (SDRR) protein that directly interacts with the transmitter domain of CckA. *In vitro*, the kinase activity of CckA was severely inhibited with an equimolar amount of Osp, whereas the phosphatase activity of CckA was not affected. We also found that the expression of *osp* is activated by CtrA creating a negative feedback loop. However, under growth conditions known to activate the TCS, the increased expression of *osp* does not parallel Osp accumulation, indicating a complex regulation. Phylogenetic analysis of selected species of *Rhodobacterales* revealed that Osp is widely distributed in several genera. For most of these species, we found a sequence highly similar to the CtrA-binding site in the control region of *osp*, suggesting that the TCS CckA/ChpT/CtrA is controlled by a novel regulatory circuit that includes Osp in these bacteria.

Introducción

Sistemas de dos componentes

Una de las formas por las cuales las bacterias son capaces de percibir distintas señales tanto ambientales como intracelulares es a través de los sistemas de dos componentes. Estos sistemas están compuestos en su forma más básica por dos proteínas: una cinasa de histidina y un regulador de respuesta. La cinasa de histidina (HK) una vez activada es capaz de autofosforilarse o transfosforilarse en el residuo de Histidina conservado presente en el dominio de dimerización (DHp). El dominio DHp se encuentra asociado al dominio catalítico (CA) que lleva a cabo la hidrólisis del ATP, estos dominios en conjunto se denominan dominio de transmisión. Una vez fosforilada la HK transfiere el grupo fosforilo al regulador de respuesta (RR) a un residuo de ácido aspártico conservado presente en el dominio aceptor (REC)[1].

Los RR se dividen en dos grandes grupos, el primero cuenta con un dominio de salida el cual puede ser un dominio de unión a ADN, o enzimático los cuales modulan su actividad dependiendo del estado de fosforilación del ácido aspártico conservado del dominio REC. Por otro lado, existe otro grupo de RR que solo están formados por el dominio REC, a los cuales se les denomina reguladores de respuesta de un solo dominio (SDRR) por sus siglas en inglés. Estos últimos actúan generalmente modificando su capacidad de interacción con otras proteínas dependiendo de su estado de fosforilación como el caso del regulador de respuesta CheY[2,3].

Existen sistemas híbridos en los cuales la cinasa de histidina incluye un dominio REC y lleva a cabo la fosfotransferencia entre la histidina del dominio DHp y el ácido aspártico del dominio REC de la misma proteína. Dado que la transferencia del grupo fosforilo ocurre entre un residuo de histidina y un residuo de ácido aspártico, para que ocurra la transferencia entre el dominio REC de la cinasa de histidinas híbrida (HHK) y el dominio REC del RR, es necesaria la presencia de un dominio de

fosfotransferasa (HPt) que contiene un residuo de histidina conservado susceptible de ser fosforilado y llevar a cabo la transferencia del grupo fosforilo del REC de la HHK al REC del RR. El dominio HPt puede formar parte de la HHK o ser una proteína independiente (figura 1)[1].

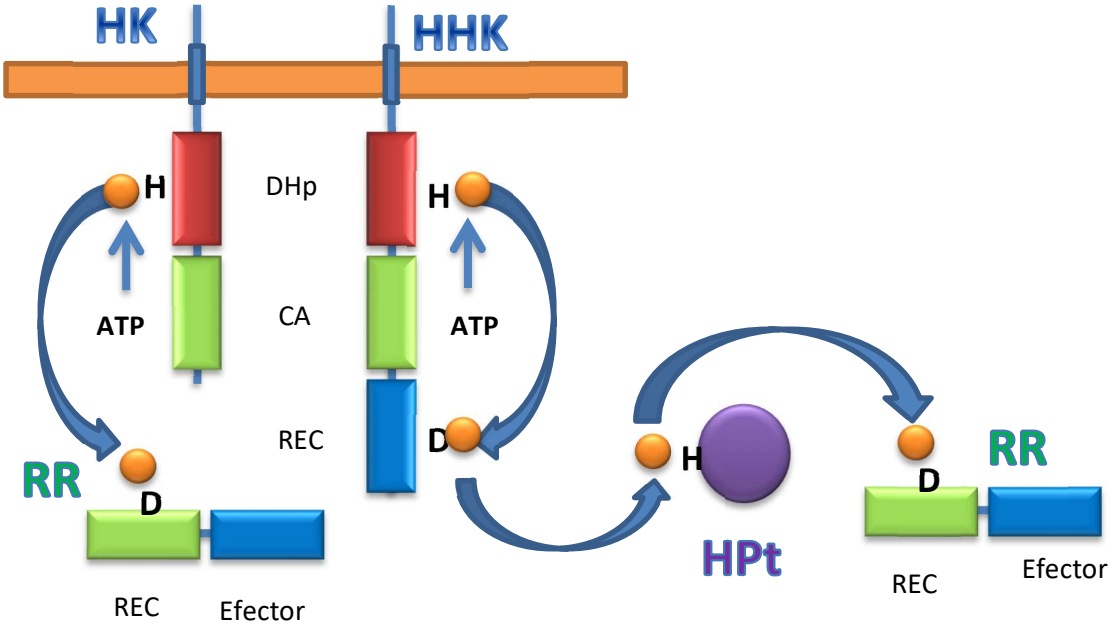

Figura 1. Esquema de las reacciones de fosfotransferencia de los sistemas de dos componentes. El sistema de dos componentes del lado izquierdo muestra el sistema canónico conformado por la cinasa de histidina (HK) y su regulador de respuesta (RR), y en el lado derecho se muestra un sistema de dos componentes híbrido con una cinasa de histidina híbrida (HHK) una fosfotransferasa(HPt) independiente y un RR. Los dominios de las proteínas se indican en forma de rectángulos de color: Dominio de dimerización DHp (rojo), dominio catalítico CA (verde) y dominio aceptor del grupo fosforilo REC (azul).

El sistema de dos componentes híbrido CckA-ChpT-CtrA

El sistema de dos componentes CckA-ChpT-CtrA (figura 2) se encuentra ampliamente distribuido en las α-proteobacterias [4].

CckA es una cinasa de residuos de histidina híbrida de membrana que posee dos cruces transmembranales con un asa periplásmica de entre 4 y 7 aminoácidos. En la región citoplásmica de CckA se encuentran dos dominios PAS importantes para modular la actividad de CckA[5]; el dominio de transmisión y el dominio REC se localizan en el carboxilo terminal.

La proteína CckA es la responsable de la fosforilación del RR CtrA usando como fosfotransferasa a la proteína ChpT [6]. Una vez que la proteína CtrA es fosforilada puede activar la transcripción de sus genes blanco, mediante la interacción directa con el ADN [7].

Debido a que el estado de fosforilación de CtrA es crucial para su actividad, el control de la actividad de CckA como cinasa o fosfatasa es esencial para el correcto funcionamiento del sistema.

Se han descrito diferentes mecanismos por los cuales el sistema de dos componentes CckA-ChpT-CtrA es regulado en diversas bacterias donde destacan miembros de las Rhizobiales, Caulobacterales, Rhodobacterales, Sphingomonadales, Rhodospirilares y Ricketsiales [4]. En cada uno de los órdenes mencionados existe por lo menos una especie en la que se ha obtenido evidencia experimental de la presencia del sistema de dos componentes CckA-ChpT-CtrA.

CckA-ChpT-CtrA se ha descrito su papel regulatorio en distintos procesos celulares dentro de las alfa-proteobacterias donde regula procesos como la progresión del ciclo celular, la división celular, vesículas de gas, la motilidad mediada por flagelo, agente de transferencia de genes, entre otras. Estos blancos regulatorios varían entre las especies[8–16].

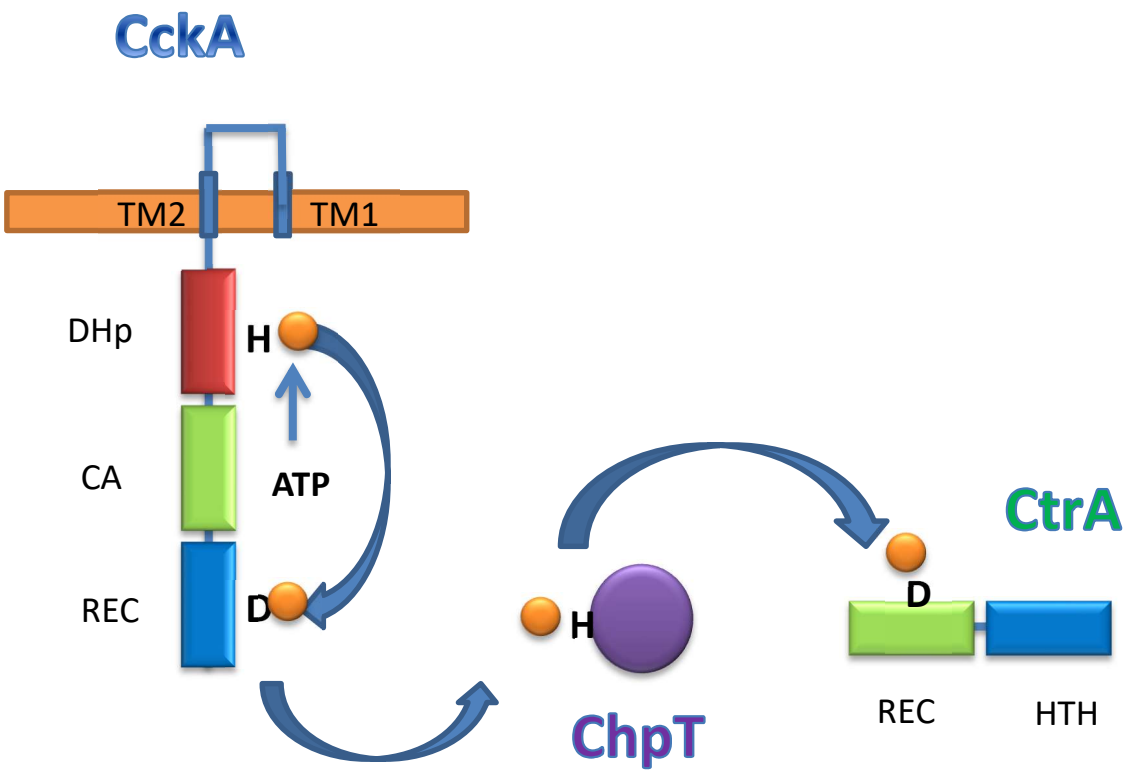

Figura 2. Esquema del sistema de dos componentes CckA-ChpT-CtrA. Las flechas azules representan las reacciones de fosfotransferencia, los grupos fosforilos están representados como círculos amarillos, los residuos fosforilables se muestran en negritas. Los dominios de las proteínas se indican en forma de rectángulos de color: Dominio de dimerización DHp (rojo), dominio catalítico CA (verde) y dominio aceptor del grupo fosforilo REC (azul) y los cruces transmembranales representados en la membrana interna (rectángulo anaranjado).

El TCS CckA-ChpT-CtrA fue descrito por primera vez en *Caulobacter crescentus* [6,17,18] en donde regula la motilidad, el inicio de la replicación y la progresión del ciclo celular. *C. crescentus* es una bacteria acuática que presenta una división celular asimétrica la cual resulta en dos células hijas diferentes, una célula sésil prostecada con la habilidad de iniciar un nuevo ciclo de replicación y una célula mótil flagelada no replicativa. En la célula flagelada de *C. crescentus* CtrA reprime el inicio de la replicación mediante su unión al origen de replicación [19] y es necesario un proceso

de diferenciación en el cual se acoplan distintos procesos regulatorios tanto transcripcionales, postranscripcionales, de degradación y de localización que modulan la actividad de las proteínas CckA, ChpT y CtrA, lo que permite la transición de la célula flagelada a prostecada y el inicio de la replicación del cromosoma.

La actividad de CckA en *C. crescentus* está regulada por otro sistema de dos componentes formado por las cinasas de histidina (HKs) PleC [20] y DivJ [21], el regulador de respuesta de un solo dominio DivK [15], el regulador de respuesta PleD, así como por la pseudocinasa de histidina DivL[22] (figura 3).

Regulación de CckA por el sistema de dos componentes DivJ/PleC-DivK y DivL en *C. crescentus*

En la bacteria *C. crescentus* DivL es esencial para modular la actividad de cinasa de CckA así como para localizarla [23] . El mecanismo por el cual DivL modula la actividad de cinasa/fosfatasa de CckA no es claro ya que no se ha demostrado una interacción directa entre DivL y CckA, pero se ha aportado evidencia experimental del mecanismo regulatorio que modula la capacidad de DivL para favorecer la actividad cinasa de CckA. La acción de DivL es controlada por el sistema de dos componentes PleC/DivJ-DivK mediante su interacción directa con DivK [24].

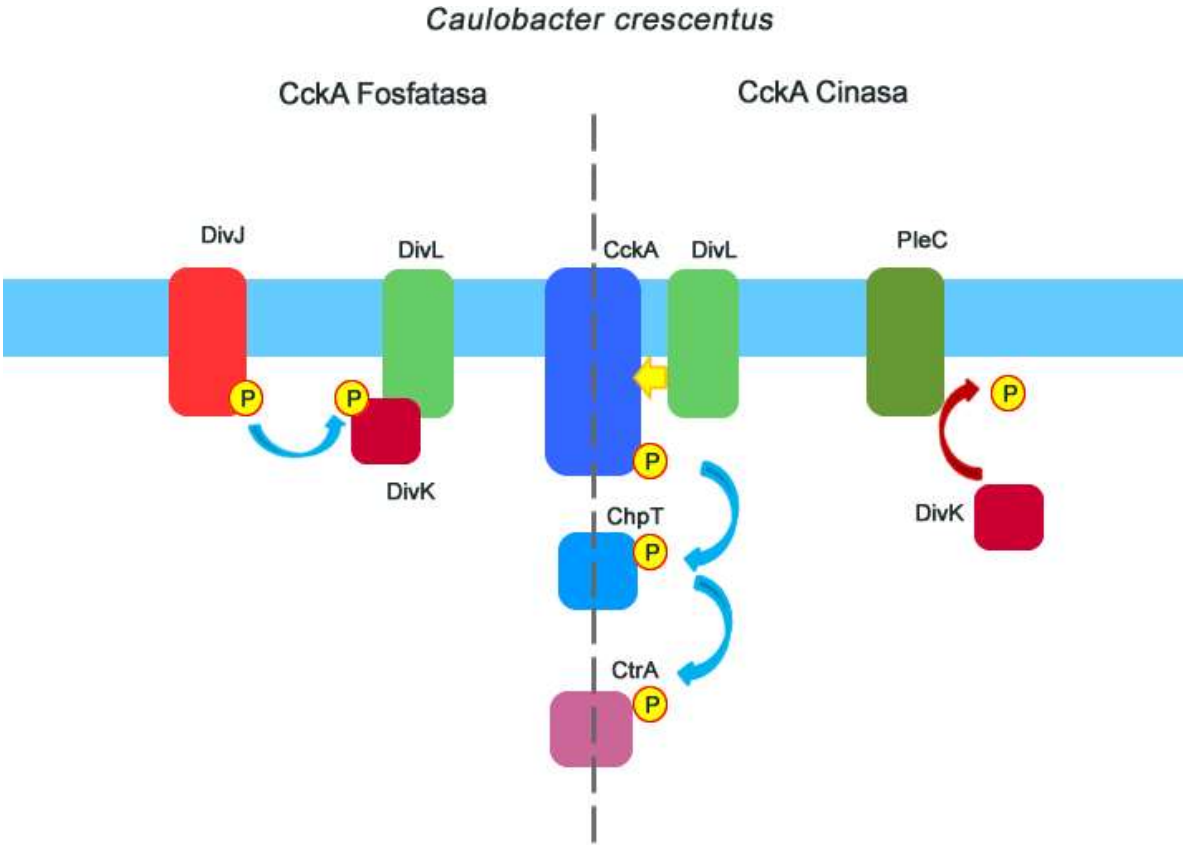

Figura 3. Regulación de CckA por el sistema de dos componentes DivJ/PleC-DivK y DivL en *C. crescentus*. Representación esquemática de la regulación de la actividad de CckA como fosfatasa a cinasa mediada por el sistema de dos componentes DivJ-DivK o PleC-DivK y la activación dependiente de DivL en ausencia de DivK-P.

La unión de DivK a DivL modula su capacidad de activar a CckA. La unión entre DivL y DivK requiere del estado fosforilado de DivK (DivK-P). Cuando la pseudocinasa DivL se encuentra unida a DivK-P es incapaz de promover la actividad de cinasa de CckA lo que resulta en que CckA se comporte predominatemente como una fosfatasa. En condiciones en las que DivK no es fosforilado, DivL es capaz de promover la actividad de cinasa de CckA lo que resulta en la acumulación de CtrA fosforilada [22].

DivL presenta un cruce transmembranal, y en el dominio citoplásmico se identifican 2 o 3 dominios PAS, cuyo número varía dependiendo de la especie, un dominio DHp y el dominio CA. El dominio DHp es el responsable de la interacción con el regulador

de respuesta DivK [22]; la presencia del dominio DHp de DivL es esencial para poder percibir el estado de fosforilación de DivK y de esta manera modular adecuadamente la actividad cianasa/fosfatas de CckA [22,25]. DivL no es una cinasa de histidina típica ya que presenta un residuo de tirosina en lugar del residuo de histidina fosforilable. El sistema CckA-ChpT-CtrA y la proteína DivL son esenciales para el crecimiento de *C. crescentus.* Sin embargo, es posible sustituir el alelo silvestre de *divL* por un alelo mutante que produzca una variante de DivL sin el dominio CA, sin perder viabilidad[26]. Esto sugiere una vez más que la actividad regulatoria de DivL sobre el sistema CckA-ChpT-CtrA es independiente de la actividad cinasa.

En una mutante nula de *divJ* en el que el estado fosforilado de DivK se encuentra alterado, y predomina en su estado desfosforilado se han identificado mutaciones secundarias en los dominio PAS de DivL que disminuyen la actividad del sistema CckA-ChpT-CtrA [27] esto sugiere que los dominios PAS son importantes pare el mecanismo mediante el cual DivL actúa para promover la actividad de cinasa de CckA.

Otra evidencia que sustenta la posible interacción entre DivL y CckA, a través de los dominios PAS de ambas, es que la colocalización de CckA con DivL en *C. crescentus* es dependiente de la región de los dominios PAS de CckA [28].

El aumento en la concentración de CckA en la superficie de membranas lipídicas promueve una mayor autofosforilación [5]. El dominio PAS-A de CckA es responsable de este fenómeno, el cual se identificó en experimentos *in vitro* usando liposomas [5]. La actividad de CckA dependiente de su concentración en la superficie celular podría ser el mecanismo por el cual DivL favorece la actividad cinasa de CckA al reclutarla en un polo celular y aumentar su concentración local.

Variaciones del sistema PleC/DivJ-DivL-DivK en diferentes α-proteobacterias

Se han encontrado homólogos de DivL en distintas α-proteobacterias[4], es interesante notar que en bacterias en las cuales se encuentran homólogos de DivL y también de DivK, DivL es una pseudocinasa con la tirosina 550 conservada, pero en aquellas en las no se encuentra un homólogo de DivK el homólogo más cercano de DivL solo presenta la región que contiene los dominios PAS y carece de los dominios DHp y CA lo que sugiere que los dominios DHp y CA de DivL son el dominio de unión a DivK [22] y posiblemente se seleccionan juntos.

Las Rhodobacterales y algunas especies de las Ricketsiales contienen homólogos de DivL que carecen del dominio DHp (denominados DivL-like [29]) y como se mencionó en el párrafo anterior, tampoco se encuentra un homólogo de DivK. La proteína DivL-like de *R. capsulatus* conserva su papel como modulador de la actividad de CckA [30].

En *C. crescentus*, el estado fosforilado de DivK está directamente regulado por las cinasas/fosfatasas DivJ y PleC. En esta bacteria se ha descrito que DivJ actúa principalmente como cinasa de DivK [31], mientras que la proteína PleC actúa preferencialmente como una fosfatasa [32].

La actividad de fosfatasa de PleC se observa cuando ésta es reclutada en el polo nuevo de las células predivisionales, para lo que es necesaria la presencia de factores adicionales que localizan a PleC, tales como la proteína de membrana PodJ [33]. Se ha reportado que la actividad de cinasa de PleC es importante durante la transición de célula flagelada a prostecada[25]. Un aumento en la concentración de DivK puede modular positivamente la actividad de PleC como cinasa favoreciendo la transición del polo flagelado a prostecado [34,35]. En la célula prostecada, la fosforilación de DivK depende de la cinasa DivJ, que se encargará de elevar los niveles de DivK fosforilado lo que favorecerá la actividad de fosfatasa de CckA [36] (figura 3).

El sistema de PleC y DivJ se ha estudiado también en otros miembros de las α–proteobacterias en especial en algunos miembros de las Rhizobiales. Además de PleC y DivJ algunas Rhizobiales cuentan con HK adicionales que se propone modulan el estado fosforilado de DivK[37 38 38] (figura 4). En *Sinorhizobium meliloti* la HK CbrA, y en *Brucella abortus* un homólogo de CbrA, denominado PdhS[38] son capaces de modular la actividad reguladora de DivK [37]. El papel propuesto de CbrA y PdhS se basa en evidencia genética relacionada a fenotipos dependientes de la actividad de CtrA. Además, se demostró la interacción directa de PdhS con DivK en ensayos de doble híbrido. *Agrobacterium tumefaciens* tiene a los parálogos PdhS1 y 2 que parecen estar involucrados en controlar el estado de fosforilación de DivK ya que las mutantes en *pdhS1* y *pdhS2* se ven afectadas en la motilidad y división celular; ambos procesos son modulados por DivK [10] y CtrA. No hay evidencia experimental que demuestre que efectivamente las cinasas PdhS1 y 2 son capaces de fosforilar a DivK y de esa manera regular al sistema de dos componentes CckA-ChpT-CtrA.

DivK se encuentra conservado en otras α–proteobacterias [4] como es el caso de *Magnetospirillum magneticum* miembro de las Rhodospirillares, donde la eliminación de *divK* resulta en una mayor cantidad de células nadadoras. En esta bacteria los genes flagelares están directamente regulados por CtrA, por lo que se propone que DivK regula negativamente la actividad de cinasa de CckA [13]. A diferencia de *C. crescentus*, *B. abortus*, *A. tumefaciens* y *S. meliloti* en *M. magneticum* no se encontró ningún homólogo de DivJ (figura 4).

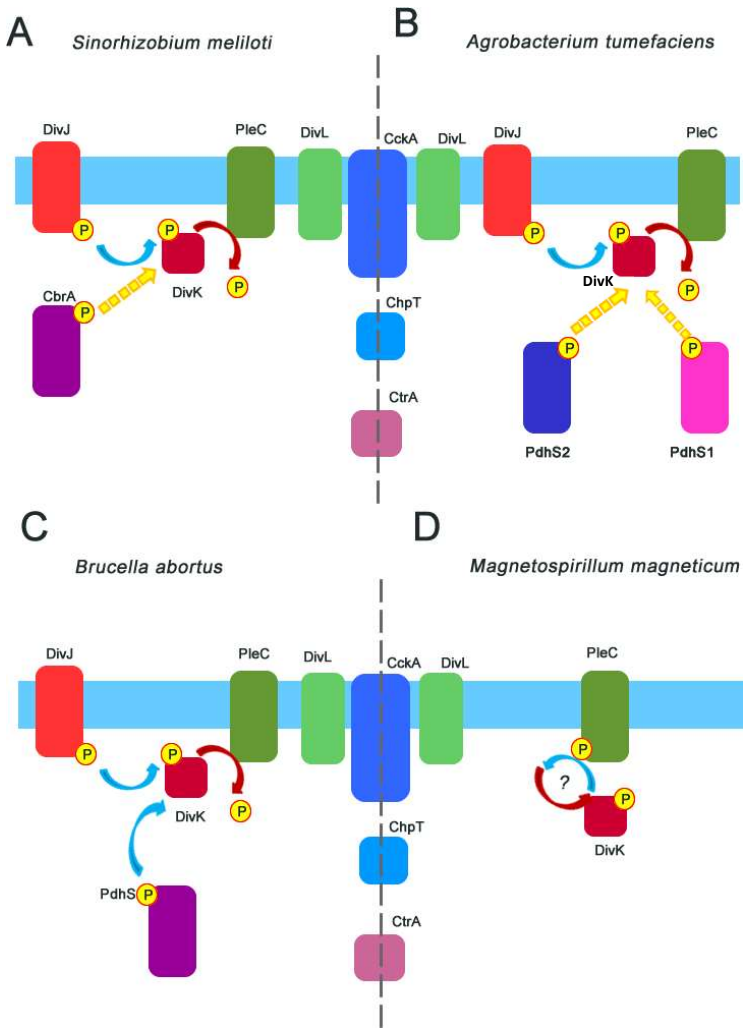

Figura 4. Distintas composiciones del sistema de dos componentes PleC/DivJ-DivK en diversas α-proteobacterias. A) *S. meliloti* con la presencia de la HK de DivK, llamada CbrA. B) *A. tumefaciens* con una pareja más de HKs de DivK, denominadas PdhS1 y PdhS2. C) *B. abortus* con la cinasa PdhS1. D) El sistema en *M.magneticum* con la presencia de la HK PleC y ausencia de DivJ.

Regulación por c-di-GMP de CckA.

Se ha determinado que CckA, al igual que otras HK, puede ser regulado directamente por c-di-GMP. En *C. crescentus* las proteínas PleD y DgcB están involucradas en la síntesis de c-di-GMP y cumplen un papel importante en el control de la motilidad y del ciclo celular [39]. PleD es un RR que contiene dos dominios REC y un dominio GGDEF necesario para la síntesis del segundo mensajero c-di-GMP.

PleD forma parte del circuito regulatorio PleC/DivJ-DivK y es fosforilado por las HK PleC y DivJ. Al igual que ocurre para DivK, PleC actúa principalmente como fosfatasa y DivJ como cinasa [40]. Los fenotipos asociados a la función de PleD como la eyección del flagelo y la correcta síntesis de la prosteca se ven alterados en una cepa que expresa el alelo mutante *pleD*-D53G, cuyo producto carece de residuo fosforilable [40]. Esto sugiere que la actividad de síntesis de c-di-GMP de PleD depende de su estado fosforilado.

Cepas mutantes con genotipo Δ*pleD* en *C. crescentus* tienen un fenotipo supermótil ya que no eyectan el flagelo durante la transición de célula flagelada a prostecada y son incapaces de formar la prosteca, procesos que son favorecidos por un aumento en la concentración de c-di-GMP [20]. La acción de PleD y el aumento en la concentración local de c-di-GMP ocasionada por la fosforilación de su dominio REC dan lugar a la remodelación del polo flagelado, que implica la eyección del flagelo y la formación de la prosteca [20].

La ausencia de PleC resulta en un incremento en los niveles de PleD fosforilado y por lo tanto en los niveles de c-di-GMP; este aumento en los niveles de c-di-GMP en ausencia de PleC afecta la actividad de CckA [41]. Esta alteración en la actividad de CckA en ausencia de PleC puede suprimirse mediante una mutación extragénica en CckA en el dominio CA[41]. El dominio CA de CckA une c-di-GMP mientras que la variante con el dominio CA mutante es incapaz de unir c-di-GMP y mantiene su actividad cinasa[41].

La diguanilato ciclasa DgcB se reconoció por su impacto sobre la motilidad y la adhesión. Su contribución al mantenimiento de la poza global de c-di-GMP es evidente en ausencia de la fosfodiesterasa PdeA, la cual se encuentra localizada en el polo flagelado y es degradada de forma preferencial ante un ligero incremento en la concentración de c-di-GMP mediada por PleD-P [42,43] . El incremento en la concentración de c-di-GMP ocasionado por DgcB da paso a la vía que conduce a la formación de la prosteca [39].

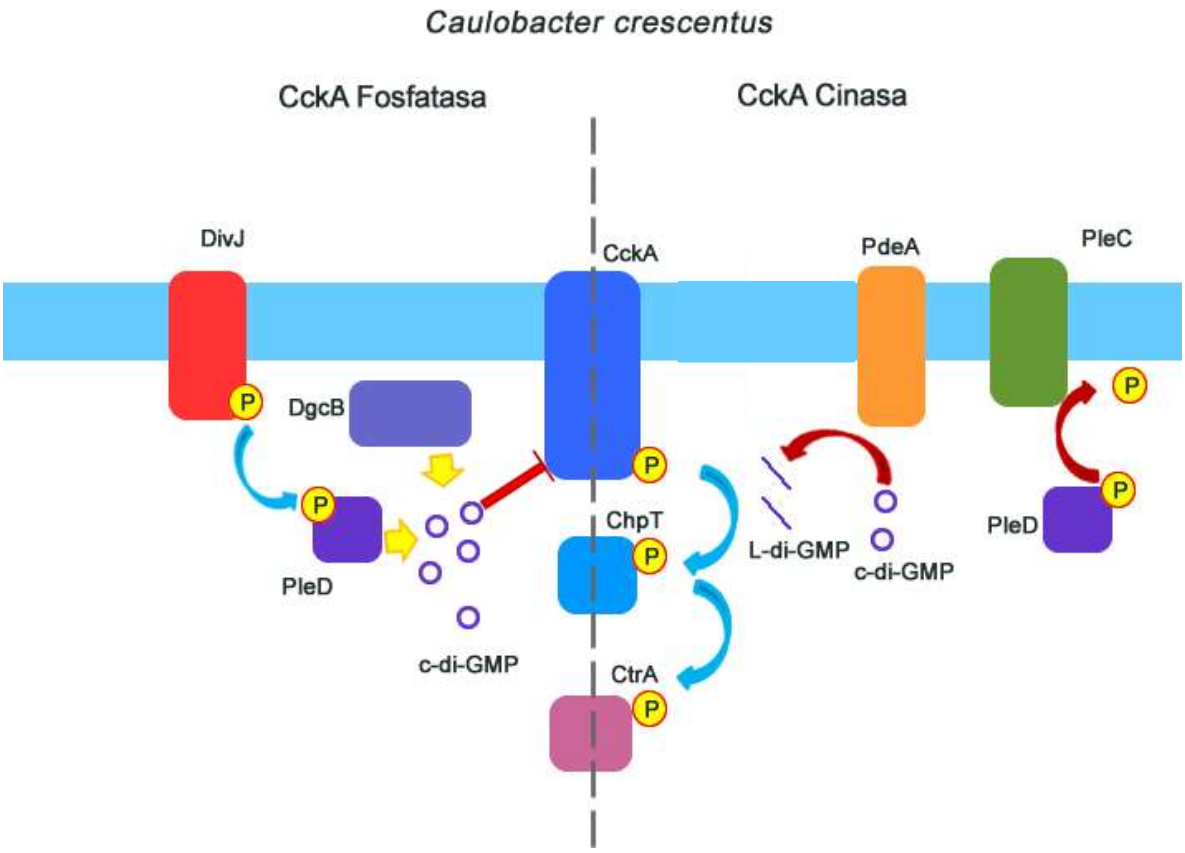

Figura 5. Regulación por c-di-GMP de CckA-CtrA. Regulación de la actividad de cinasa o fosfatasa mediada por la concentración de c-di-GMP. Las diguanilato ciclasas DgcB y PleD aumentan los niveles de c-di-GMP lo que mantiene a CckA como fosfatasa, mientras que la fosfodiesterasa PdeA degrada el c-di-GMP a GMP-GMP (L-di-GMP) y mantiene a CckA como cinasa.

Control de la estabilidad del sistema CckA-ChpT-CtrA

En *C. crescentus* la proteína CtrA se encuentra en distinta concentración a lo largo del ciclo celular. Los cambios en la concentración de CtrA están regulados a nivel transcripcional y a nivel post-traduccional. CtrA es blanco de un proceso activo de degradación que depende de una región presente en el extremo carboxilo terminal [43], así como de la actividad cinasa de CckA [44] y de los niveles de c-di-GMP [45].

La degradación de CtrA es dependiente de la peptidasa ClpP y la coproteasa ClpX [46] y está mediada por su propio carboxilo terminal, en especial por los dos últimos aminoácidos que son dos residuos de alanina. La sustitución de los residuos de alanina por aspártico o la eliminación de los últimos tres aminoácidos de la proteína, provocan que CtrA permanezca estable a lo largo del ciclo celular [43].

El estado de activación de CckA regula la degradación de CtrA al modular la interacción del RR CpdR y el complejo de degradación ClpX/P. Esto es mediado por la proteína de fosfotransferencia ChpT que es capaz de transferir el grupo fosfato tanto a CtrA como al RR de dominio único CpdR [6,47]. CpdR en su estado no fosforilado interacciona con el complejo ClpX/P [48] y funciona como acoplador para la degradación de proteínas específicas [49]. CpdR es necesario para la degradación de CtrA, así como de la fosfodiesterasa PdeA [42,50].

La degradación de CtrA mediada por la proteína acopladora CpdR (CpdR1) también ha sido descrita en *S. meliloti*, de forma similar a lo observado en *C. crescentus*, la degradación de CtrA está modulada por el nivel de fosforilación del RR CpdR, el cual es controlado por CckA [48].

El c-di-GMP modula la degradación de CtrA a través de la proteína efectora PopA [50]. PopA es un ortólogo de PleD [50]con un dominio GGDEF degenerado incapaz de sintetizar c-di-GMP pero con la capacidad de unirlo de manera alostérica [51]. PopA se une a un adaptador del complejo ClpX/P llamado RcdA [52] el cual también es esencial para llevar a cabo la degradación de CtrA [50]. La unión de c-di-GMP a PopA

favorece la formación del complejo RcdA-PopA-CtrA y la degradación de CtrA mediada por el complejo ClpX/P [45] (figura 6).

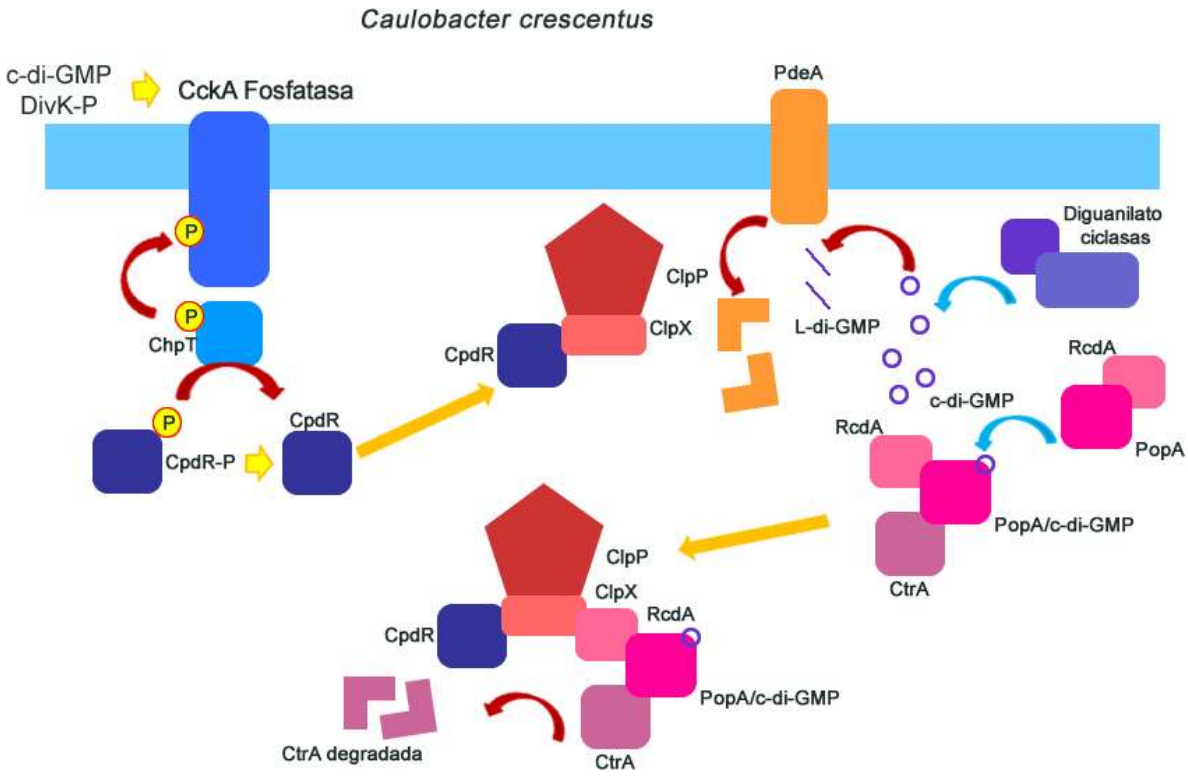

Figura 6. Control de la estabilidad del sistema CckA-ChpT-CtrA. CpdR defosforilado forma un complejo con ClpX/P el cual degrada a PdeA favoreciendo la acumulación de c-di-GMP. El c-di-GMP se une a PopA y favorece la unión de esta a CtrA, que en conjunto con RcdA se unen al complejo ClpX/P/CpdR y facilitan la degradación de CtrA.

Presencia de las proteínas accesorias que controlan el TCS CckA/ChpT/CtrA en α-proteobacterias

Como se mencionó en la sección anterior el TCS CckA/ChpT/CtrA ha sido estudiado de forma intensiva en la bacteria *C. crescentus* y se cuenta con una gran cantidad de información al respecto de las proteínas y moléculas que controlan la actividad, distribución y estabilidad de estas proteínas. Recientemente el estudio del sistema CckA/ChpT/CtrA y de sus proteínas regulatorias en otras especies bacterianas ha recibido gran atención.

La figura 7 presenta a modo de resumen, la presencia de proteínas homólogas que se sabe que en *C. crescentus* controlan el TCS CckA/ChpT/CtrA. Se puede observar que solamente PleC y PleD se encuentran de forma recurrente en los organismos analizados, mientras que DivJ, DivK y diversas proteínas adaptadoras necesarias para la degradación están ausentes en diversos órdenes, como es el caso de las Rhodobacterales.

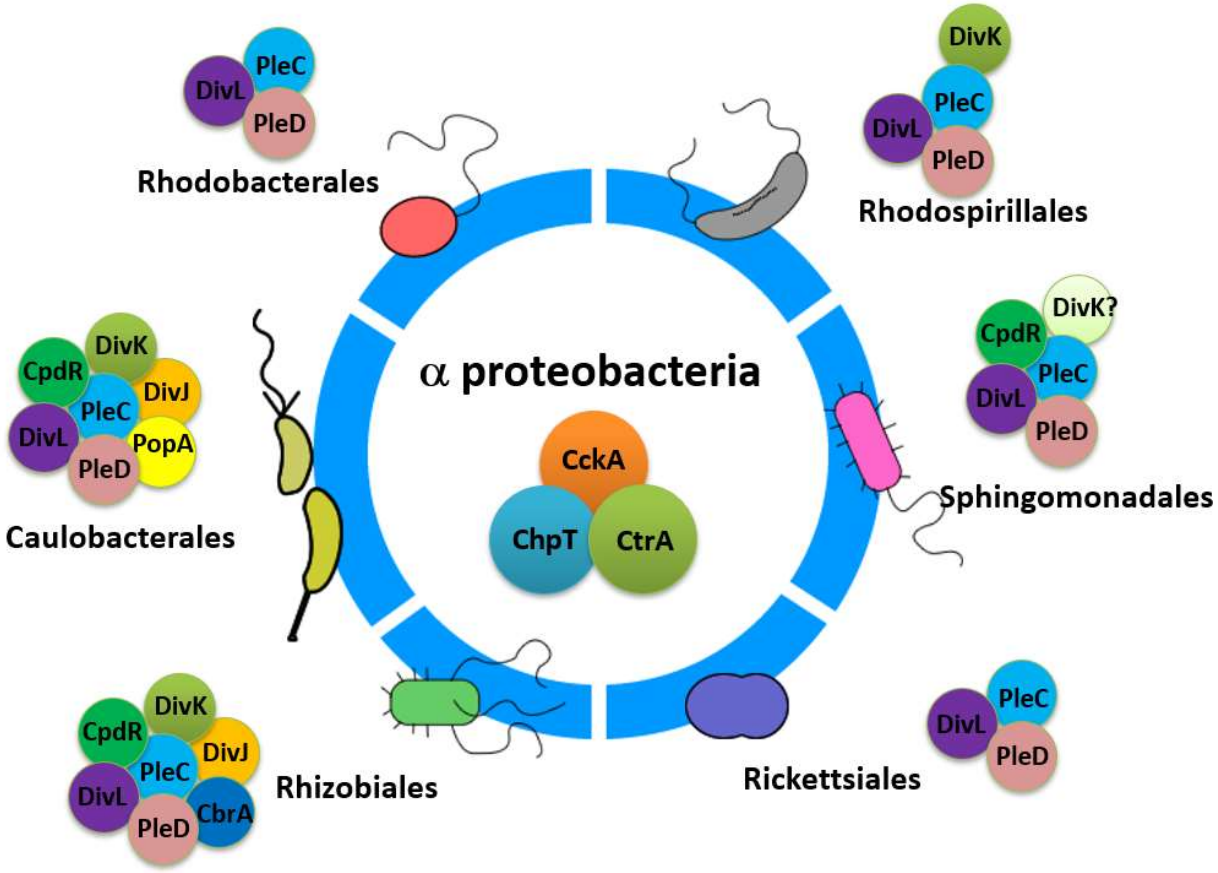

Figura 7. Las proteínas regulatorias del sistema CckA-ChpT-CtrA en distintos grupos de las α-proteobacterias. Se muestran representadas en círculos de colores las distintas proteínas regulatorias del sistema de CckA representadas por círculos. Los distintos órdenes están representados por un fragmento de dona.

R. sphaeroides

Rhodobacter sphaeroides es una α-proteobacteria purpura no sulfurosa, metabólicamente diversa con la capacidad de realizar respiración aeróbia y anaeróbia, fijar carbono y nitrógeno, así como producir hidrógeno y de llevar a cabo fotosíntesis anaeróbica anoxigénica [53].

Rhodobacter sphaeroides posee dos sistemas flagelares. El sistema flagelar 1 (Fla1) fue adquirido por transferencia horizontal, probablemente de una γ- o β-proteobacteria ancestral. El sistema *fla1* da lugar a la formación de un flagelo monótrico de ubicación subpolar. El sistema *fla1* se expresa de manera constitutiva y se encuentra regulado por el activador dependiente de sigma-54 FleQ [54,55]. En contraste, el sistema flagelar 2 (Fla2) ensambla un flagelo lofótrico de ubicación polar. Los genes *fla2* se expresan en cepas con mutaciones compensatorias que permiten el nado en ausencia del sistema Fla1, fenotipo denominado Fla2^{+}. El sistema *fla2* está regulado por CckA, ChpT y CtrA [56], y las cepas Fla2+ poseen mutaciones de ganancia de función en el dominio DHp de CckA, lo que permite la expresión de los genes flagelares 2 [56].

CtrA en *R. sphaeroides* controla la expresión de aproximadamente 321 genes, entre ellos, además de los genes *fla2,* se encuentran genes relacionados con la formación del sistema quimiotáctico, de las vesículas de gas, genes fotosintéticos, genes relacionados con la respuesta a estrés, etc [8].

A diferencia de las Caulobacterales y Rhizobiales en las cuales el sistema de CckA/ChpT/CtrA es esencial, en *R. sphaeroides* éste es dispensable e incluso se mantiene apagado en algunas condiciones de crecimiento. La activación de este sistema ocurre cuando se crece a las bacterias Fla2+ en presencia de una baja concentración de ácido succínico como única fuente de carbono en el medio de cultivo, o incluso cuando se sustituye el ácido succínico por cas aminoácidos. Además de estas características en la composición del medio, el crecimiento en

condiciones fotoheterotróficas vs quimioheterotróficas favorece la activación del TCS CckA/ChpT/CtrA [56,57].

La activación de CtrA en *R. sphaeroides* puede promoverse mediante la expresión en *trans* de una versión de CckA con actividad constitutiva de cinasa. Esto sugiere que, en condiciones de laboratorio, la actividad de cinasa CckA de *R. sphaeroides* es inhibida por proteínas reguladoras. *R. sphaeroides* no cuenta con genes homólogos a los reguladores canónicos del sistema PleC/DivJ-DivK, ni tampoco con los genes que codifican para las proteínas adaptadoras involucradas en la degradación CtrA. Esto sugiere que la regulación de la actividad de CckA en *R. sphaeroides* es contralada por reguladores novedosos. A partir de estas consideraciones, en este trabajo nos planteamos el identificar nuevas proteínas involucradas en la activación del TCS CckA-ChpT-CtrA.

Hipótesis

A partir de la cepa silvestre WS8N de *R. sphaeroides*, será posible aislar mutantes en las cuales el sistema de dos componentes CckA-ChpT-CtrA se encuentre activo sin alterar la identidad de residuos de la cinasa CckA.

Objetivo general

Valorar la existencia de posibles reguladores negativos de la cinasa CckA en la bacteria *R. sphaeroides*.

Objetivos particulares

Aislar mutantes en las cuales el sistema de dos componentes CckA-ChpT-CtrA se encuentre activo utilizando como reflejo de dicha activación la formación y funcionamiento del flagelo Fla2.

Realizar el tamizaje de las mutantes obtenidas para descartar aquellas que presenten mutaciones en los genes *cckA*, *chpT* y *ctrA*.

Identificar la mutación causante de la activación del sistema CckA-ChpT-CtrA mediante la secuenciación del genoma completo de la cepa mutante seleccionada.

Caracterizar el papel de la proteína afectada por la mutación que sea identificada.

Valorar si el gen afectado es controlado por reguladores transcripcionales conocidos en *R. sphaeroides*.

Resultados

Obtención de cepas Fla2+

Con el objetivo de encontrar nuevos elementos regulatorios del sistema CckA-ChpT-CtrA se decidió seleccionar cepas con la capacidad de nadar con el sistema Fla2 que es dependiente de CtrA [54,56]. Para este fin se utilizó a las cepas SP13 (Δ*fleQ*) [54,56,58], que carece del regulador maestro del sistema flagelar 1, y SP20 (Δ*fliF*1) [54,58] que carece de la proteína que ensambla el anillo MS Fla1. Ambas cepas son incapaces de nadar en condiciones de cultivo en el laboratorio dado que no expresan o ensamblan Fla1 y el sistema de CtrA se encuentra apagado. Estas dos cepas fueron inoculadas en cajas de medio de cultivo con agar suave (0.21% de agar en medio Sistrom con 0.1 mM de ácido succínico) y se incubaron por 7 días. Después de este tiempo se observaron pequeños halos de nado, como se muestra en la figura 8 A, que indican la presencia de células mótiles. Se aislaron células clonales de estos halos de nado y se inocularon en cajas de agar suave y se observó que generaban un halo de nado uniforme indicando la presencia de una población homogénea capaz de nadar con el sistema Fla2, como se muestra en la figura 8 B.

Como se había descrito previamente, con este método se obtienen mutantes de ganancia de función CckA, como es el caso de la cepa AM1 usada como control en la caja de nado de la figura 8 B, la cual presenta una mutación activadora en el dominio DHp que produce el cambio de la leucina 391 por una fenilalanina (L391F) [56] y que denominamos CckA*. De las nuevas cepas aisladas se descartaron aquellas que tenían mutaciones en CckA. Se obtuvieron 4 cepas nuevas que presentaban un fenotipo Fla2+ y el sistema CckA-ChpT-CtrA silvestre; estas cepas fueron denominadas BV6, BV7, BV8 y BV9. Se corroboró la presencia del flagelo 2 en estas cepas, mediante inmunodetección por Western blot de la proteína FlaA, que es una flagelina componente del filamento del sistema Fla2 (figura 8 C). Las cuatro nuevas cepas con fenotipo Fla2+ fueron positivas para FlaA al igual que la cepa control AM1. Al observar a la cepa BV6 por microscopía electrónica de

transmisión se puede observar la presencia de flagelos polares típicos del sistema Fla2 y la presencia de vesículas de gas (figura 9), ambas estructuras dependientes de la presencia de CtrA en estado fosforilado [8]. Para encontrar la mutación responsable de generar el fenotipo Fla2+ se secuenció el genoma de la cepa BV6, al comparar la secuencia de la cepa BV6 con el genoma de la cepa silvestre WS8N se encontró un cambio en el gen RSWS8N_09785 que generó una substitución del residuo de histidina 115 por un ácido aspártico. RSWS8N_09785 codifica para una proteína de 120 aminoácidos que predice ser un regulador de respuesta de un solo dominio (figura 10).

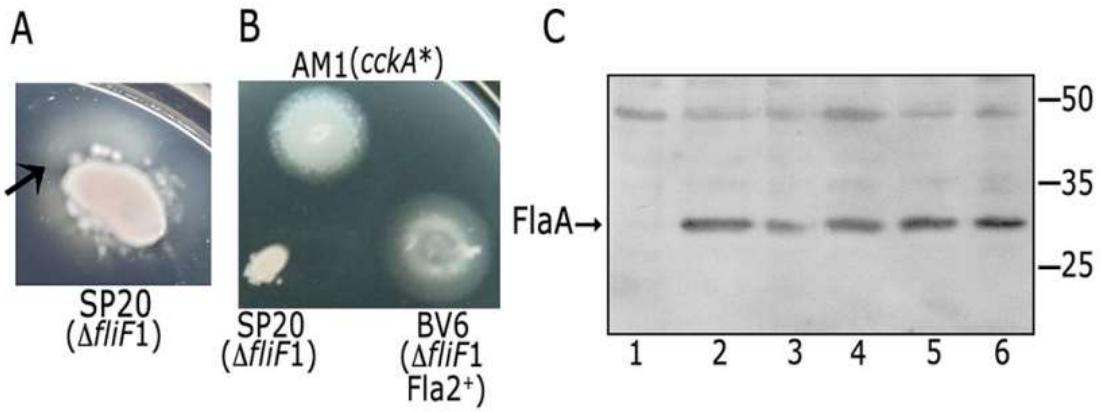

Figura 8. Obtención de mutantes Fla2+ (A) Aislamiento de mutantes capaces de expresar el sistema flagelar 2 a partir de la cepa SP20. Las células fueron inoculadas en cajas de Petri con agar suave (0.21% agar) en medio mínimo de Sistrom con 0.1mM de ácido succínico como fuente de carbono e incubadas por 7 días, la flecha indica la aparición de células nadadoras que se desplazan fuera del inóculo. (B) Fenotipo de nado de la cepa BV6 (SP20 Fla2+) en cajas de agar suave (0.21%) en medio de Sistrom con 0.1mM de ácido succínico e incubada 48 horas. En la misma caja se incluyó para su comparación la cepa parental SP20 y AM1 (CckA* Fla2+). (C) Western blot anti-FlaA del extracto total de las cepas LC7(*ctrA*::hyg) línea 1, AM1 línea 2, y BV6 a BV9 líneas 3 a 6 respectivamente, los extractos fueron tomados de cultivos a D.O. 0.6 crecidos en condiciones fotoheterotróficas por 16 horas en medio de Sistrom con 0.1mM de ácido succínico.

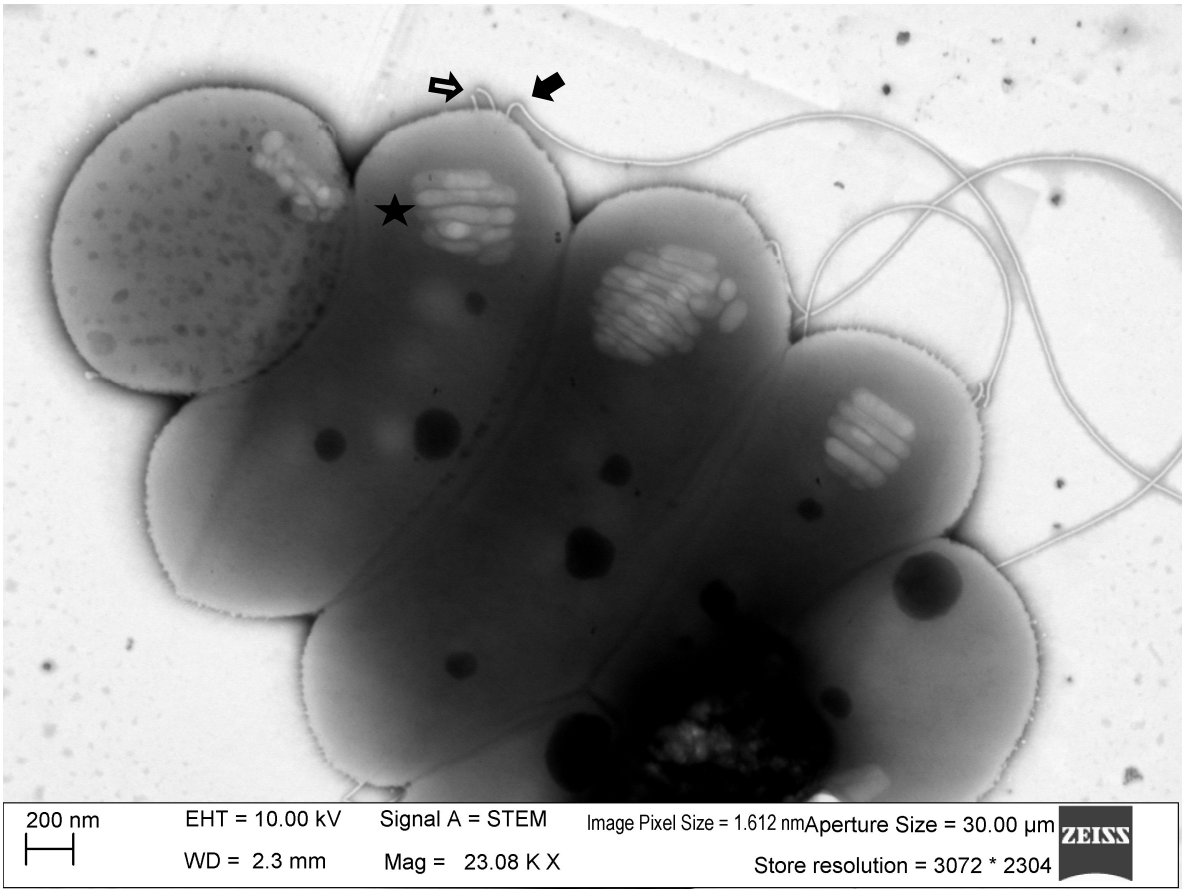

Figura 9. Microscopía electrónica de transmisión de células de la cepa BV6. La cepa BV6fue en condiciones fotoheterotróficas en medio de Sistrom 0.1mM ácido succínico, se muestran los flagelos polares, en la célula de la izquierda se indica con la flecha negra el filamento y con la flecha vacía se muestran los ganchos flagelares que han perdido el filamento y aún continúan unidos al cuerpo celular y las vesículas de gas, regiones elípticas claras en el polo de la célula marcadas con una estrella negra en la misma célula.

Valor E = 4.78e-07

Figura 10. Predicción de dominios de RSWS8N_09785. Se indica el valor E de la predicción de dominios de Blast, la flecha azul muestra el cambio encontrado en la cepa BV6, en verde se observa la predicción del dominio REC en RSWS8N_09785.

La pérdida de RSWS8N_09785 es la responsable de la activación del sistema de dos componentes CckA-ChpT-CtrA.

La posible función de la proteína codificada por RSWS8N_09785 fue descrita originalmente en la cepa de *R. sphaeroides* 2.4.1, en donde el gen homólogo, RSP_0869, fue nombrado *osp*[59] por favorecer la expresión óptima de los genes del aparato fotosintético. En dicho reporte, no se describió su mecanismo de acción ni se ligó al sistema de dos componentes CckA-ChpT-CtrA.

Para demostrar que el cambio observado en RSWS8N_09785, el cual será denominado *osp* a partir de este punto en adelante, es el responsable de la activación del sistema de CckA-ChpT-CtrA en la cepa BV6, se procedió a aislar la cepa mutante Δ*osp*::hyg, intercambiando al gen silvestre por el gen de resistencia a higromicina (*hyg*) en las cepas SP13 y SP20. Como se puede observar en la figura 11, las mutantes BV10 (SP20 Δ*osp*) y BV11 (SP13 Δ*osp*) son mótiles a diferencia de las cepas parentales SP20 y SP13. Además, al complementar las cepas BV10 y BV11 utilizando el plásmido pRK415_osp, se observó que ambas cepas mostraron una reducción significativa del halo de nado (figura 11). Estos resultados indican que *osp* es el responsable del fenotipo de nado observado en la cepa mutante BV6, y sugieren que Osp es un regulador negativo del TCS CckA-ChpT-CtrA.

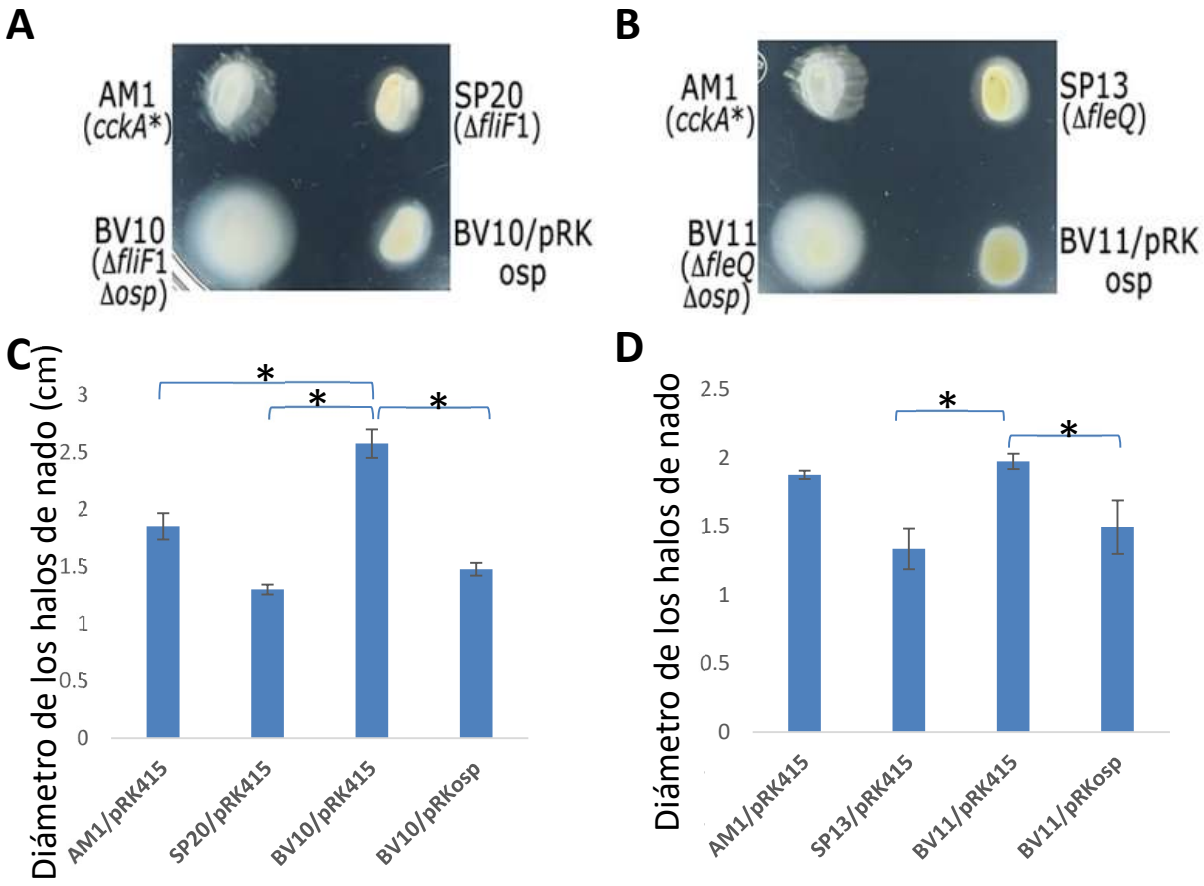

Figura 11. Fenotipo de las mutantes en osp BV10 y BV11. Cajas de nado de las cepas derivadas de SP20 (A) y SP13 (B) que llevan el alelo Δ*osp*::hyg, denominadas BV10 y BV11. En la caja de nado se incluyeron las cepas controles SP20, SP13 y la cepa AM1 que tiene el alelo *cckA**. Todas las cepas llevan el plásmido vacío pRK415. Las cajas de agar suave conteniendo 0.21% de agar en medio de Sistrom con 0.1mM de ácido succínico fueron incubadas 48 horas en condiciones fotoheterotróficas. El panel C y D muestran las mediciones de los diámetros de los halos de nado en centímetros. Los resultados fueron analizados mediante un análisis de varianza y una prueba de Tukey, la cepa BV10 mostró diferencias significativas con un pval<0.01 respecto a las cepas AM1, SP20 Y BV10/pRK_osp panel C, mientras que la cepa BV11 mostró diferencias significativas en comparación con las cepas SP13 y BV11/pRK_osp.

Dado que la cepa AM1 presenta el alelo constitutivo de *cckA* y mantiene el gen *osp* silvestre decidimos evaluar si esta versión de CckA aún respondía al efecto inhibitorio ejercido por la presencia de Osp. En la figura 12A se observa que la cepa BV12 (AM1 Δ*osp*) presenta un halo de nado de mayor tamaño que su cepa parental AM1; además, cuando *osp* se expresa en *trans* en el vector pRK415 podemos observar que disminuye significativamente el diámetro del halo de nado en las cepas AM1/pRK_osp y BV12/pRK_osp (figura 12B), lo que indica que la forma constitutiva de CckA aún es susceptible de ser inhibida por Osp.

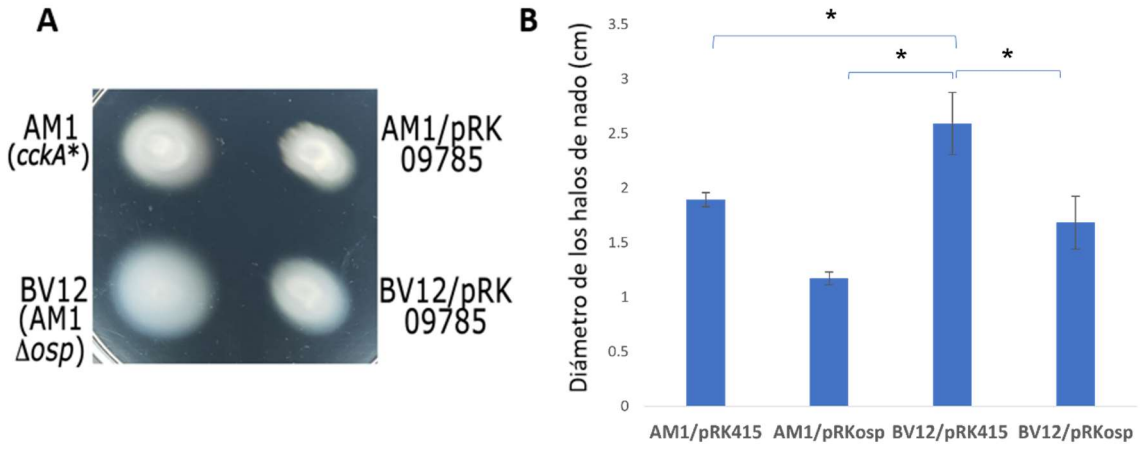

Figura 12. Efecto de Osp en la cepa AM1. Caja de nado de la cepa AM1 con el vector vacío y con el vector pRK_osp. (A) Las cajas de nado fueron preparadas con 0.21% de agar y medio de Sistrom con 0.1mM de ácido succínico, las cepas fueron incubadas 48 horas en condiciones foto heterotróficas. (B) mediciones de los halos de nado de las cepas AM1 y BV12 con el pRK vacío y con pRK_osp, los resultados se analizaron con un análisis de varianza de una vía dando diferencias significativas entre BV12 y el resto de las cepas con un pval<0.01.

Para evaluar si el regulador Osp afecta de forma negativa al sistema CckA/ChpT/CtrA y no solo la expresión de los genes *fla2*, se procedió a determinar si otros promotores o aspectos fisiológicos controlados por CtrA son afectados de la misma manera por esta proteína. Para ello, se midió la actividad del promotor del

gen *mcpB,* el cual es directamente controlado por CtrA [8,57], mediante una fusión transcripcional con el gen reportero *uidA*, que codifica la enzima β-glucuronidasa. Se observó una disminución significativa de la expresión de *mcpB* al introducir el plásmido pRK_osp en la cepa JHV3 (AM1*mcpB::uidAaadA*) (figura 13 A) lo que confirma que Osp interfiere con la activación de CtrA. Por otro lado, en la cepa BV11 se observó un aumento en la expresión de *mcpB* respecto a la cepa parental SP13 que no expresa a *mcpB* (figura 13B). Para explorar otro fenómeno controlado por CtrA se midieron los pigmentos fotosintéticos, ya que se demostró que CtrA reprime su expresión [8], dato que correlaciona con el papel anteriormente descrito para Osp relativo a que su presencia favorece la expresión óptima de los genes del aparato fotosintético. La absorbancia en las longitudes de 800nm, 850nm y 875nm de las muestras de pigmentos provenientes de las cepas BV11 y SP13 mostraron una reducción con respecto a la absorbancia observada para la muestra proveniente de la cepa BV13 (BV11Δ*ctrA*) (figura 13 C) lo que corrobora el efecto negativo de Osp sobre la actividad de CtrA.

De acuerdo con la idea de que Osp es el responsable de reprimir la actividad de CtrA y que su ausencia provoca la activación del sistema de CckA-ChpT-CtrA, se decidió secuenciar en el resto de las cepas seleccionadas inicialmente como Fla2+ el gen *osp*. En estas cepas, denominadas BV7, BV8 y BV9 también se observaron cambios en la secuencia codificadora del gen *osp*. La cepa BV7 tiene una inserción de un nucleótido que provoca un cambio de marco de lectura y un producto de 77 residuos; para la cepa BV8 se detectó una inserción de 6 nucleótidos que dan lugar a la adición de dos codones, uno para valina y el segundo para alanina, en la posición 64 y 65 de Osp, por último, la cepa BV9 tiene una deleción de 1 nucleótido que cambia el marco de lectura a partir del aminoácido de 11 de Osp. Las tres cepas fueron complementadas en *trans* con el alelo silvestre de *osp* usando el pRK_osp como se muestra en la figura 14.

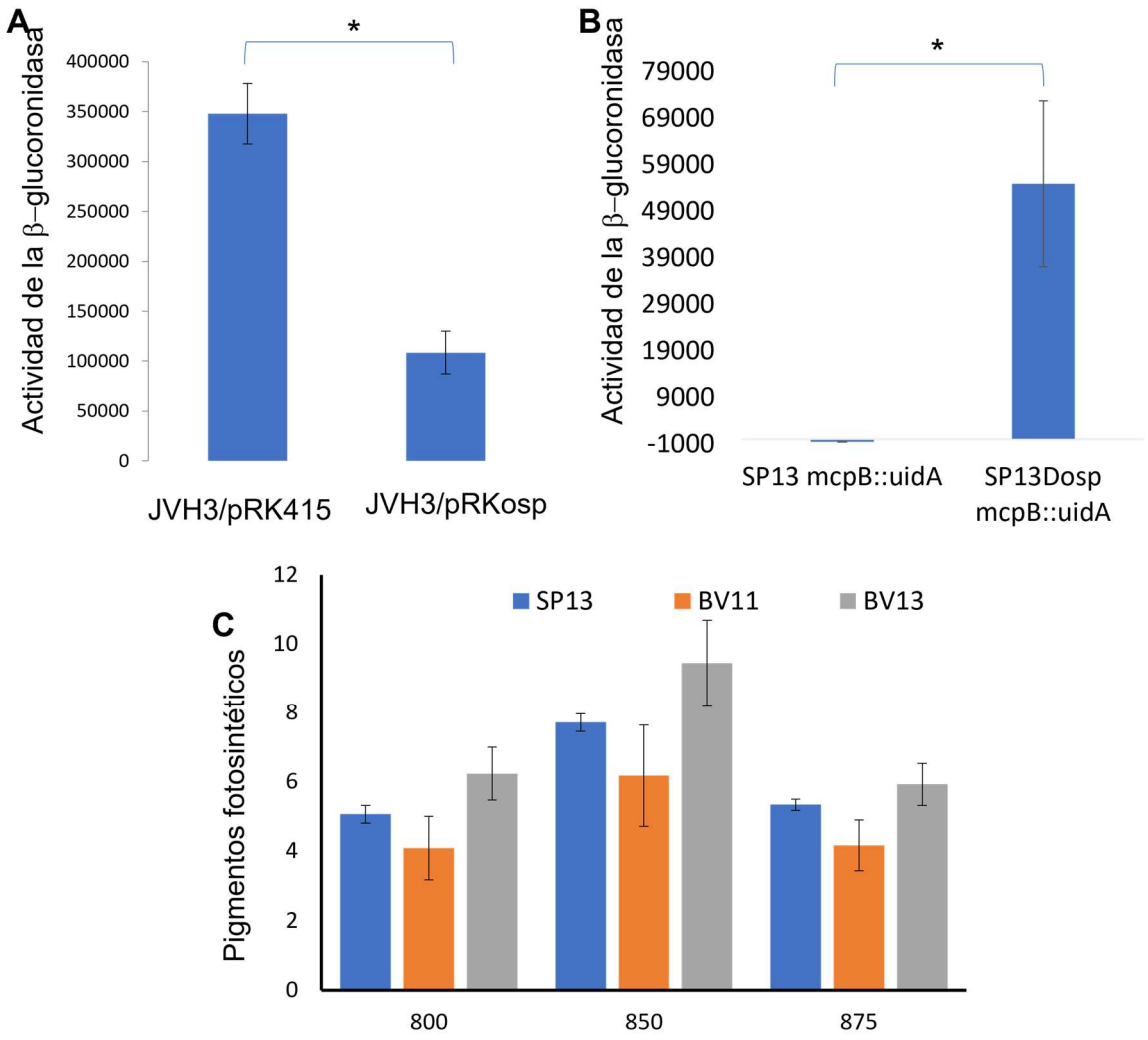

Figura 13. Efecto de Osp en blancos regulatorios de CtrA. (A) Actividad específica de la β–glucuronidasa (expresada en pico moles de metilumbelliferona formada por minuto por mg de proteína) detectada en extractos totales de las cepas JVH3 con el vector vacío pRK415 y con el plásmido pRK_osp. Las cepas fueron crecidas en medio de Sistrom con 0.1mM de ácido succínico en condiciones fotoheterotróficas hasta alcanzar una densidad óptica de 0.7. Los resultados se analizaron usando una prueba de t de dos colas, la diferencia mostró un pval<0.01 (B) Actividad específica de la β–glucuronidasa (expresada en pico moles de metilumbelliferona formada por minuto por mg de proteína) detectada en extractos totales de las cepas SP13 y BV11. Las cepas fueron crecidas en medio de Sistrom con 0.1mM de ácido succínico en condiciones fotoheterotróficas hasta alcanzar una densidad óptica de 0.7. Los resultados se analizaron usando una prueba de t de dos colas, la diferencia mostró un pval<0.01 (C). Determinación de la abundancia de los pigmentos fotosintéticos valorada mediante los valores de absorbancia de los extractos de las cepas SP13, BV11 y BV13 en las longitudes de onda de 800, 850 y 875nm y dividida entre miligramos de proteína. Se hizo una prueba de ANOVA posterior una prueba Tukey y se obtuvo una diferencia significativa entre las cepas BV13 respecto a las cepas BV11 y SP13 pval<0.05.

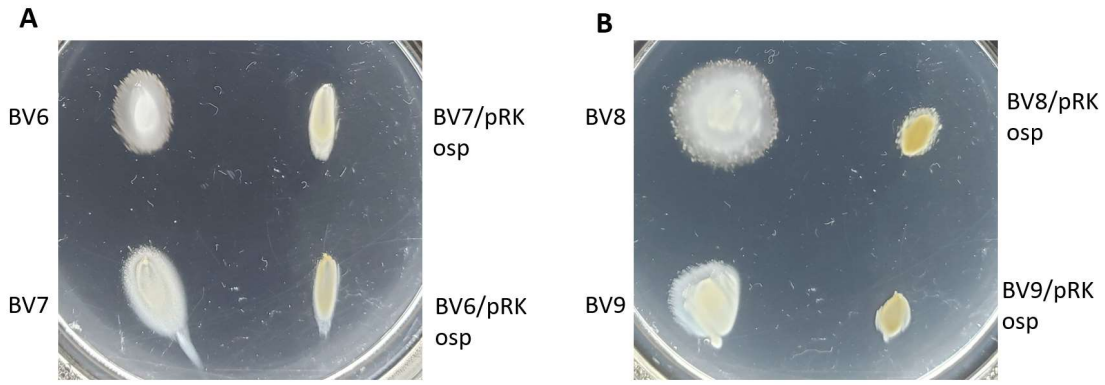

Figura 14. Complementación de las cepas BV6-9. Cajas de nado de las complementaciones de las cepas BV6, BV7, BV8 y BV9 portando el vector pRK415 o complementadas con el vector pRK_osp. Las cajas de nado contenían 0.21% de agar en medio mínimo de Sistrom con 0.1mM de ácido succínico. Las cajas fueron incubadas 48 horas en condiciones fotoheterotróficas.

Osp es similar a un regulador de respuesta de un solo dominio (SDRR).

La predicción de dominios de la secuencia de Osp utilizando el algoritmo BLAST en el servidor del NCBI reveló la presencia de un dominio REC, aunque la cobertura del dominio no es total y presenta mayor similitud en el extremo amino terminal respecto al carboxilo (figura 10).

Para determinar si Osp se pliega como un dominio REC o si la parte carboxilo es una parte no estructurada se hizo una predicción de la estructura terciaria de Osp usando SWISS-MODEL. Como se muestra en la figura 15A el modelo obtenido usando a la proteína CheY de *Escherichia coli* como templado, concuerda con la estructura característica de los dominios REC. La estructura presenta un plegamiento (α/β) con un núcleo central de 5 láminas β paralelas rodeadas por 5 hélices α (β/α)5. En CheY, el sitio activo lo conforman el residuo de ácido aspártico fosforilable al final de la lámina β3, y otros dos residuos de ácido aspártico (DD) al

final de la lámina β1, necesarios para coordinar el ATP-Mg. Sin embargo, Osp carece de algunos de los residuos altamente conservados en los dominios REC como son los dos residuos de ácido aspártico (DD) al final de la lámina β1, y la lisina (K) al final de la lámina β5 que no está presente [60,61], como se muestra en el alineamiento de Osp con CheY en la figura 15B. La falta de estos residuos sugiere que Osp no se fosforila. En este sentido, en *R. sphaeroides* 2.4.1 la activación del aparato fotosintético fue indistinguible entre las cepas que expresaban la versión silvestre de Osp o la versión mutante D51A[59]. De acuerdo con lo anterior, algunos homólogos de Osp no presentan el residuo de ácido aspártico al final de la lámina β3, como en *Dinoroseobacter shibae* donde en esta posición hay una serina (S) y en el caso de *Marinovum algicola* hay un residuo de asparagina (N). Existen algunos trabajos en donde se han hecho las sustituciones del ácido aspártico fosforilable por asparagina lo cual resulta en un RR no fosforilable y por ende, no complementa los fenotipos dependientes del RR fosforilado [62–64]. La expresión en trans del alelo *ospD51N* en la cepa hipermótil BV12 (AM1Δ*osp*) inhibe la motilidad de forma comparable al efecto de la expresión en *trans* del alelo silvestre *osp*. Esto sugiere que la regulación de la motilidad mediada por Osp no requiere de su fosforilación en el residuo D51 (figura 16).

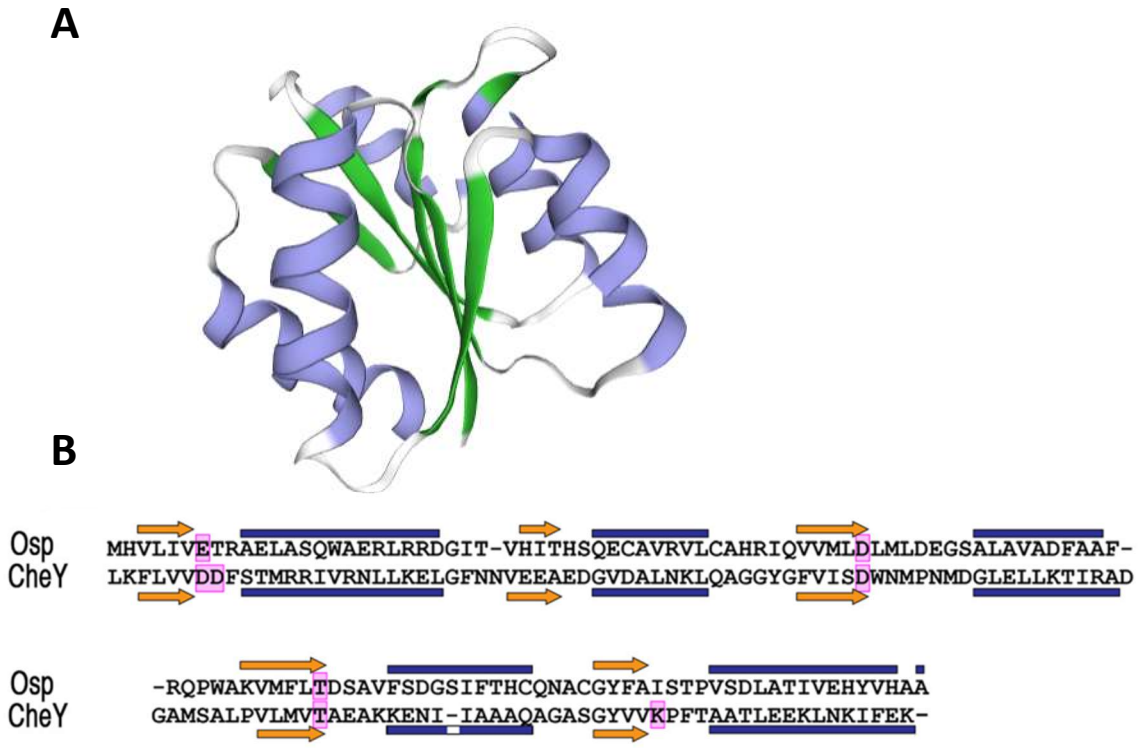

Figura 15. Osp es similar a un SDRR. (A) Modelo de estructura de Osp usando como templado a la proteína CheY predicción hecha con Swiss-Model [65], en lila se representan las α hélices y en verde las láminas β. (B) Alineamiento de aminoácidos de Osp y CheY de *E. coli* la estructura secundaria de cada una está marcada en flechas naranjas para las láminas β y las α hélices en rectángulos azules, los aminoácidos conservados funcionales están enmarcados en rosa. La estructura secundaria se obtuvo usando Psipred [66] y el alineamiento se obtuvo usando Swiss-Model [65].

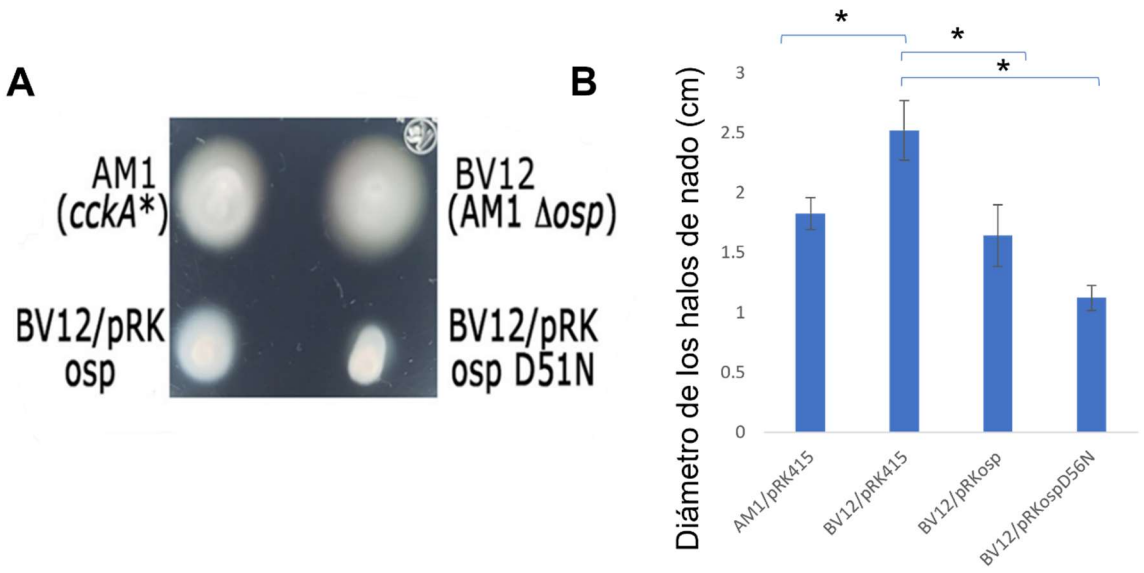

Figura 16. Efecto de la expresión de *ospD51N* en AM1. (A) Nado de la cepa BV12 complementada con el alelo silvestre de *osp* y el alelo *ospD51N*. Las cepas fueron inoculadas en cajas de agar suave (0.21% agar) en medio mínimo de Sistrom con 0.1mM de ácido succínico e incubadas por 48 horas. (B) Gráfica de barras de la longitud del diámetro de los halos de nado en cm, se analizaron los datos mediante una análisis de varianza donde tanto la cepa BV12 complementada con el alelo silvestre, así como con la versión D51N son diferentes significativamente de la cepa BV12 con el vector vacío.

CtrA regula la expresión de *osp.*

El gen *osp* se encuentra 243 pares de bases (pb) río abajo de un posible regulador transcripcional de la familia TetR y 111 pb río arriba de un gen que codifica para una proteína hipotética (figura17A). Tomando en cuenta estas distancias intercistrónicas se podría considerar que *osp* se transcribe como un mRNA monocistrónico. El análisis del regulón de CtrA, reveló que la expresión de *osp* es activada por CtrA mientras que la expresión de sus genes vecinos no se ve influenciada por los niveles de este regulador [8]. Esto es evidencia adicional que sustenta que *osp* se transcribe como un mRNA monocistrónico. Para evaluar el control de CtrA sobre *osp* se hizo una fusión transcripcional del promotor de *osp* con el gen *uidA*; esta fusión transcripcional fue clonada en el vector pRK415 e introducida en las cepas AM1 y

LC7 (AM1∆*ctrA*::*hyg*). Como se muestra en la figura 17B la actividad del promotor de *osp* disminuye drásticamente en la mutante con genotipo ∆*ctrA*::*hyg*; además que en la cepa AM1 se observa el comportamiento típico de los genes controlados por CtrA ya que se induce su expresión cuando se cultivan en medio mínimo de Sistrom con 0.1mM de ácido succínico en comparación con el medio que contiene 15 mM de ácido succínico tanto en condiciones heterotróficas como fotoheterotróficas [8,56].

Al analizar la región intercistrónica entre RSWS8N_09785 y *osp* se encuentra un motivo TTAA N7 TTAA que es el motivo descrito para la unión de CtrA [8,67,68], este motivo se encuentra a 54 pb río arriba del ATG de *osp* lo que podría indicar que CtrA regula directamente a *osp* (figura 17C). Con el objetivo de encontrar en la región regulatoria de *osp* otros elementos correspondientes a las secuencias conservadas del promotor, se alinearon las regiones río arriba del gen *osp* identificado en especies que pertenecen al mismo género de *R. sphaeroides*. Cabe mencionar que el género *Rhodobacter* recientemente fue renombrado como *Cereibacter* [69].

En la figura 17D se muestra el alineamiento de la región regulatoria de *osp* de cinco especies del género Cereibacter. Se observa que existen distintas regiones conservadas de las cuales dos de ellas podrían ser la caja -35 y la caja -10, además de una purina (A) conservada que coincide con el posible +1. El motivo de CtrA encontrado río arriba de la posible caja -35 coincide con lo antes ya reportado en *C. crescentus* donde la caja de CtrA se ubica sobre o aledaña a la caja -35 [70].

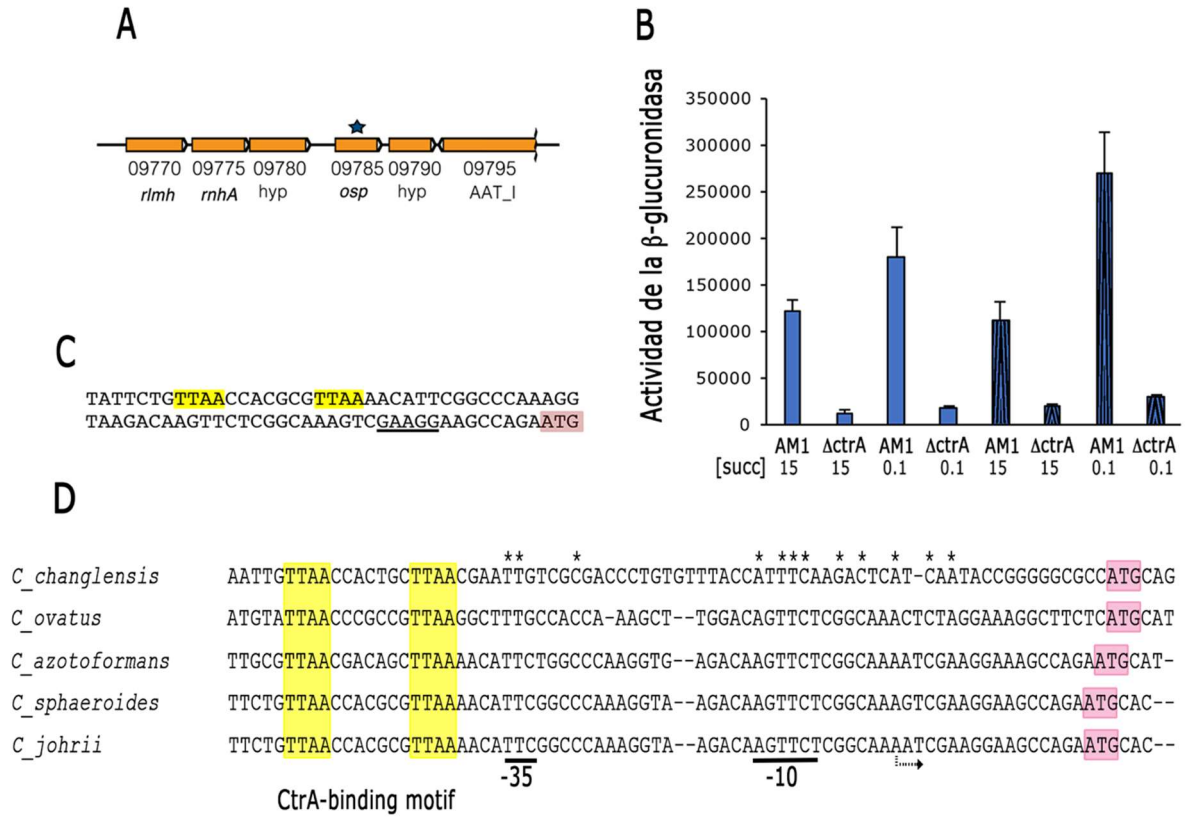

Figura 17 Contexto genómico de *osp* y actividad del promotor de *osp* (A) Contexto genómico de *osp*. Indicado con una estrella se encuentra *osp*. (B) Actividad de la β-glucuronidasa (pico moles de MU por minuto por mg de proteína) de las cepas AM1 y LC7 que llevan el plásmido pRK_osp::uidA-aadA. Las células fueron crecidas en medio mínimo de Sistrom conteniendo 15 mM y 0.1 mM de ácido succínico en condiciones heterotróficas barras sólidas y en condiciones fotoheterotróficas barras rayadas. Los datos fueron analizados con un análisis de varianza de una vía, la actividad del promotor de *osp* en la cepa AM1 es mayor significativamente con respecto a la cepa LC7 en todas las condiciones con un pval<0.01. (C) Secuencia intercistrónica río arriba de *osp,* las cajas amarillas muestran el posible motivo de unión de CtrA, en rosa se marca el codón de inicio de la traducción (ATG) y subrayado la posible secuencia Shine-Dalgarno. (D) Alineamiento de las regiones regulatorias de *osp* presentes en distintas especies de bacterias del género Cereibacter, se muestra subrayado las posibles cajas -10 y -35. Se indica la purina que posiblemente sea el +1 y en amarillo se muestra la posible caja de CtrA conservada.

La acumulación de Osp no correlaciona con las actividades transcripcionales del promotor de *osp.*

El promotor P_{osp} tiene una expresión basal y esta se induce por la acción de CtrA [8]. En principio, Osp es capaz de modular negativamente la expresión del promotor P_{osp} indirectamente a través de la inhibición del sistema CckA-ChpT-CtrA. Esto lleva a cuestionarse como es la dinámica de activación de *osp* y la acumulación de su producto en diferentes condiciones. Para valorar los niveles de la proteína Osp se construyó una fusión con la etiqueta 3xFLAG, la cual se fusionó en el amino terminal de Osp y se integró en el cromosoma de la cepa AM1 y de la cepa SP13 derivando en las cepas BV18 (AM1 FLAG-Osp) y BV19 (SP13FLAG-Osp). La cepa BV19 (SP13 FLAG-Osp) es capaz de formar un halo de nado mayor que su cepa parental SP13, lo cual sugiere que la variante FLAG-Osp es menos activa que su contraparte silvestre. Sin embargo, el halo de nado de la cepa BV19 es mucho menor que el de la cepa BV11 (SP13Δ*osp*) la cual carece del gen *osp*. Estas observaciones sugieren que la versión FLAG-Osp es parcialmente funcional.

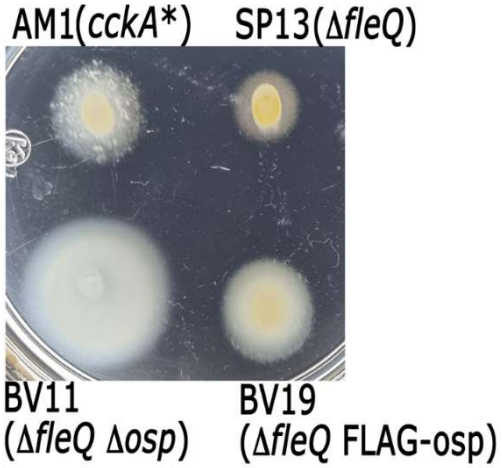

Figura 18. Nado de la cepa BV19. Las cepas AM1, SP13, BV11 y BV19 fueron inoculadas en cajas de agar suave (0.21% agar) en medio mínimo de Sistrom con 0.1mM de ácido succínico. Las cajas fueron incubadas en condiciones fotoheterotróficas por 48 horas.

Para evaluar si un aumento en la acumulación de Osp se correlaciona con condiciones que favorecen su transcripción, se analizó mediante Western blot la presencia de FLAG-Osp en la cepa BV18 (AM1 FLAG-Osp), en condiciones de crecimiento en las que el sistema CckA/ChpT/CtrA se encuentra inhibido o activado. En la figura 17B se observó que la expresión de osp se ve favorecida en condiciones de crecimiento fotoheterotróficas a bajas concentraciones de ácido succínico de manera dependiente de CtrA. En contraste, en la figura 19A observamos que FLAG-Osp se acumula, casi exclusivamente, en la condición de crecimiento heterotrófica con 15 mM de ácido succínico, la condición menos favorable para la activación del sistema CckA/ChpT/CtrA. Como control de que las condiciones de crecimiento usadas resultan en diferentes niveles de activación de CtrA analizamos la abundancia de uno de sus blancos de regulación, la proteína del gancho del flagelo 2 (FlgE2). Los niveles de FlgE2 fueron mayores en células crecidas en condiciones de baja concentración de ácido succínico (figura 19B), lo cual favorece la activación de CtrA. Estos resultados sugieren que los niveles de Osp podrían estar controlados a nivel post-transcripcional, traduccional o post-traduccional. Como se muestra en la figura 10 los últimos dos aminoácidos de Osp son alaninas (AA) lo cual se ha propuesto que es una señal reconocida por el sistema de proteasa ClpXP en algunas proteínas como es el caso de CtrA en *C. crescentus* [49,71].

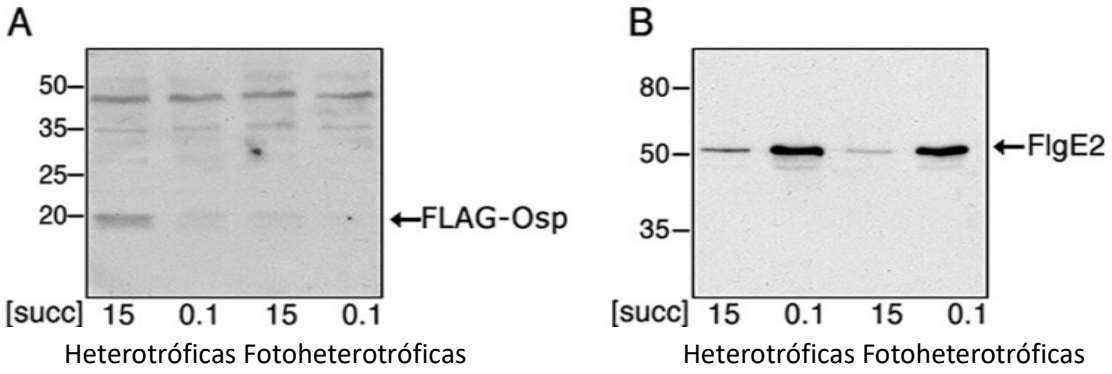

Figura 19. Inmunotección de Osp y FlgE2. Western blot de extractos totales de la cepa BV18 (AM1 FLAG-Osp) crecida en medio mínimo de Sistrom adicionado con 15 o 0.1 mM ácido succínico en las condiciones de cultivo indicadas. La detección de la proteína FLAG-Osp (A) y de la proteína del gancho del sistema flagelar 2, FlgE2 (B) se realizó utilizando anticuerpos αFLAG y αFlgE2.

Osp interacciona con el dominio de transmisión de CckA.

Para entender la forma como Osp regula negativamente la actividad del sistema de CckA-ChpT-CtrA y dada su naturaleza como un RR se decidió hacer ensayos de interacción entre CckA y Osp usando el sistema de doble híbrido de levadura.

Para esto se fusionó Osp con el dominio de activación de GAL4 (AD) y diferentes versiones de CckA se fusionaron al dominio de unión a ADN (BD) del regulador GAL4, una interacción positiva entre ambas proteínas reconstituye al regulador Gal4 y permite la expresión de los genes reporteros HIS3 y ADE2 cuyo promotor está controlado por GAL4[72]. La cepa de levadura AH109 crecida en ausencia de leucina(L) y triptófano(W) permite seleccionar a los vectores que llevan las fusiones de BD y AD de GAL4. La interacción entre ambas proteínas probadas permite a la cepa AH109 crecer en medio sin histidina (H) y sin adenina (A) debido a la expresión de HIS3 y ADE2. Sabiendo esto se fusionaron distintos dominios de CckA (figura

20A) con el dominio BD de GAL4. Siendo la composición de dominios de CckA: 2 cruces transmembranales, dos dominios PAS, el dominio DHp, el dominio CA y por último el dominio REC.

Cuando la cepa AH109 expresa GAL4AD-Osp y GAL4BD-CckA(ΔTM), observamos crecimiento en ausencia de histidina y adenina, indicando una interacción fuerte entre ambas proteínas (figura 20B).

Además, la remoción de los dominios PAS y del dominio REC de CckA no evitó que esas versiones de CckA continuaran interaccionando con Osp, lo que indica que Osp se une al dominio de transferencia de CckA (figura 20B). No se observó crecimiento cuando se probó la interacción entre el dominio REC de CckA y Osp (figura 20B), aunque hubo un ligero crecimiento este fue similar al observado en la cepa que solo expresaba la fusión del dominio AD con el dominio REC de CckA (datos no mostrados). Con el objetivo de probar que la interacción del dominio de transmisión de CckA con Osp es específica, se probó la interacción con el dominio REC del RR DctR de *Rhodobacter sphaeroides* WS8N, la expresión de estas fusiones en la cepa AH109 no permitió su crecimiento en ausencia de adenina (figura 20B) lo que sugiere fuertemente que la interacción entre el dominio de transmisión de CckA y Osp es específica.

Por otro lado, se decidió probar la interacción de CckA* de la cepa AM1 ($CckA_{L391F}$) con Osp utilizando esta misma metodología. No se mostró ninguna diferencia al comparar la interacción de CckA silvestre o CckA* con Osp, lo que corrobora la observación de que el nado de la cepa AM1 sigue siendo sensible a la presencia de Osp. No obstante, queda la duda de porque la cepa que expresa CckA* puede nadar aun expresando *osp* del cromosoma, mientras la cepa que expresa CckA silvestre no. Posiblemente este ensayo no es lo suficientemente sensible para identificar si hay un ligero cambio en la afinidad de CckA* por Osp (figura 20B).

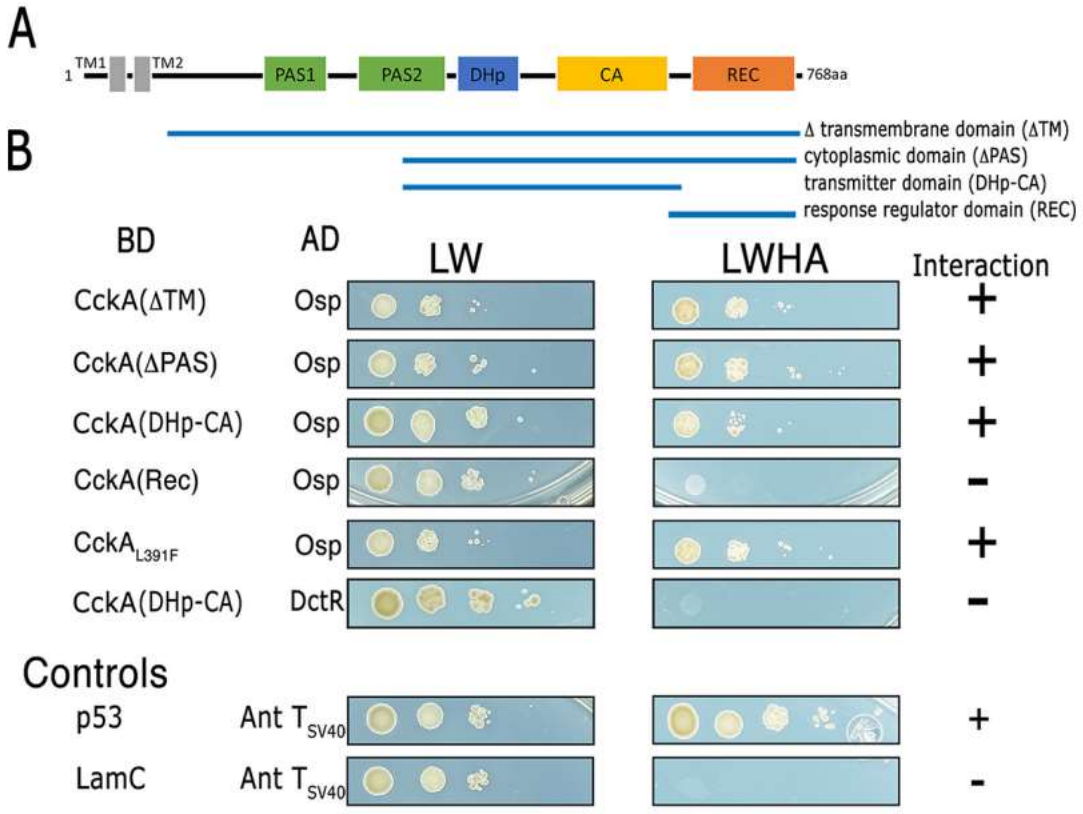

Figura 20. Interacción entre CckA y Osp. (A) Diagrama de la arquitectura de dominios de CckA, debajo se muestran las regiones que se fusionaron al dominio BD de Gal4. (B) Las levaduras transformadas con los plásmidos con las fusiones indicadas BD y AD se crecieron en cajas de medio SD sin leucina y triptófano (LW) como control de crecimiento, y en cajas de agar eliminando además la histidina y la adenina (LWHA). A la derecha se indica con un signo (+) la interacción positiva y una falta de interacción con signo (-). En la parte inferior se muestran los controles incluidos en el kit para probar la interacción positiva utilizando las fusiones BD-p53 con el AD-antígeno T y el control negativo con las fusiones BD-LamC con AD-antígeno T.

Para corroborar los resultados del ensayo de doble híbrido de levadura se decidió hacer un experimento de co-precipitación (pull down) *in vivo* con el dominio de transmisión de CckA y Osp, para ello se construyó el vector pET28a-His-CckA-Osp, este plásmido expresa a cada una de las proteínas desde un promotor dependiente de la polimerasa T7, en este caso CckA está fusionada a la etiqueta de 6 histidinas, lo que nos permite purificarla del extracto total usando perlas de Ni-NTA-Agarosa, la proteína Osp no tiene ninguna etiqueta; como se muestra en la figura 21 Osp se copurifica con His_6-CckA (línea 3), mientras que del extracto de la cepa que solo produce Osp, esta no se obtiene (línea 2). Esta evidencia confirma que el dominio de transmisión de CckA interacciona con Osp.

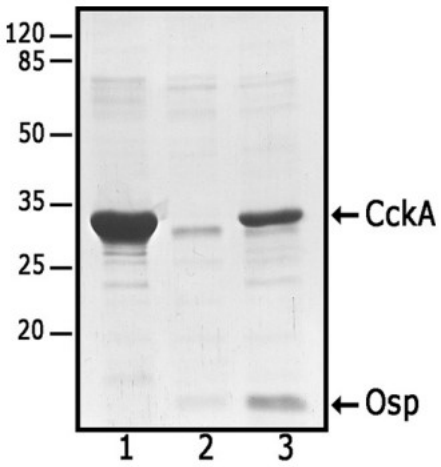

Figura 21. Coprecipitación *in vivo* de Osp usando His_6-CckA. Extractos totales obtenidos de *E. coli* Rosetta sobreexpresando His_6-CckA línea 1, Osp línea 2 y sobreexpresando ambas proteínas His_6-CckA y Osp desde el mismo vector línea 3, fueron usados para purificar His_6-CckA por cromatografía de afinidad con perlas de Ni-NTA-agarosa, las proteínas purificadas fueron sometidas a electroforesis en un gel de poliacrilamida con SDS (SDS-PAGE). El gel fue teñido con Azul de Coomassie (Brilliant Blue).

Osp inhibe la autofosforilación de CckA y la fosforlición de CtrA.

Con el objetivo de determinar el efecto de Osp sobre la actividad cinasa de CckA se hicieron ensayos de fosforilación *in vitro*. En estos ensayos se usó la versión citoplásmica de CckA (figura 20A), que lleva el dominio de transmisión y el dominio REC que se demostró que se fosforila *in vitro* [56], y diferentes concentraciones de Osp. En estos ensayos, la reacción se inició al añadir (γ-^{32}P) ATP. Como se observa en la figura 22, Osp inhibe la fosforilación de CckA. Se determinó que basta un cuarto de la concentración de Osp respecto a CckA para reducir la fosforilación de CckA aproximadamente un 50% (Figura 22B) y una concentración equimolar de ambas proteínas prácticamente inhibe por completo la fosforilación de CckA.

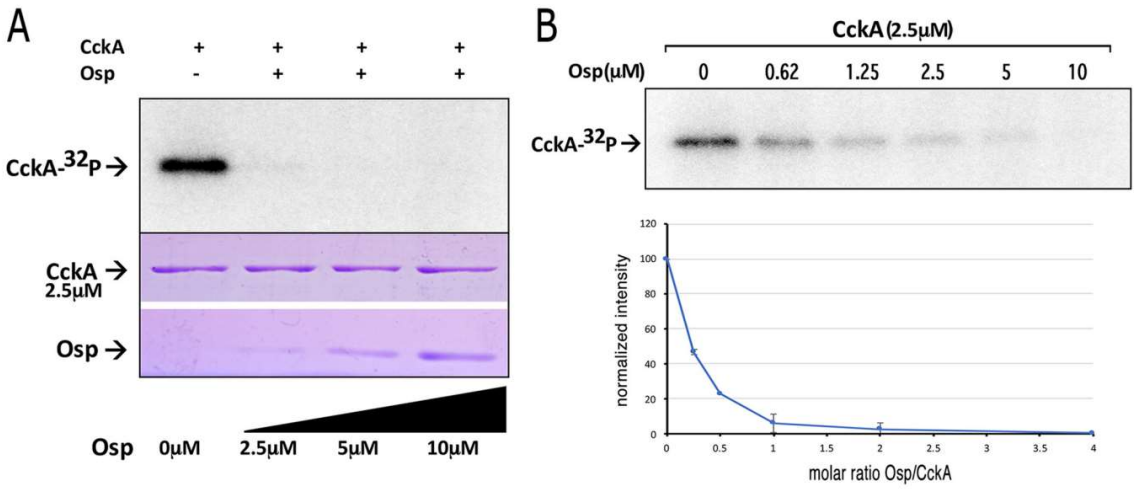

Figura 22. Fosforilación *in vitro* de CckA en presencia de Osp. (A) Fosforilación de CckA en presencia de Osp en concentraciones crecientes de Osp a partir de concentraciones equimolares (2.5 μM) hasta un aumento de cuatro veces más de Osp en la reacción (10μM). (B) Fosforilación de CckA en presencia de concentraciones subequimolares (menores a 2.5 μM) y con un exceso de 2 y 5 veces de Osp.

Para demostrar que esta inhibición de Osp sobre CckA es específica, se realizó el ensayo de fosforilación sustituyendo a CckA por la parte citoplásmica de la HK PhoR de *C. crescentus* [73]. Como se observa en la figura 23 el patrón de fosforilación de PhoR no se modifica por la adición de Osp. De igual manera, la fosforilación de CckA no se modifica en presencia de un RR distinto a Osp, en este caso se usó DctR [74] de *R. sphaeroides*.

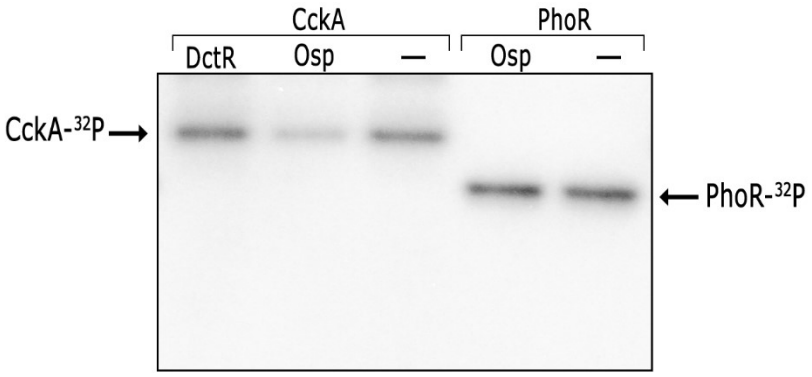

Figura 23. Especificidad de la inhibición de Osp sobre CckA. Fosforilación de CckA en presencia del RR DctR (parte izquierda del gel). Fosforilación de la HK PhoR en presencia de Osp. Todas las proteínas se usaron a una concentración de 2.5μM y fueron incubadas durante 30 minutos en presencia de (γ-^{32}P) ATP.

Osp inhibe la fosforilación de CckA aún en presencia de ChpT y CtrA. En presencia de Osp la inhibición de la actividad cinasa de resulta en una disminución en CtrA-P y el sistema CckA-ChpT-CtrA permanece apagado. En este ensayo se comprobó también la dependencia de ChpT para la fosfotransferencia del grupo fosforilo entre CckA y CtrA (figura 24).

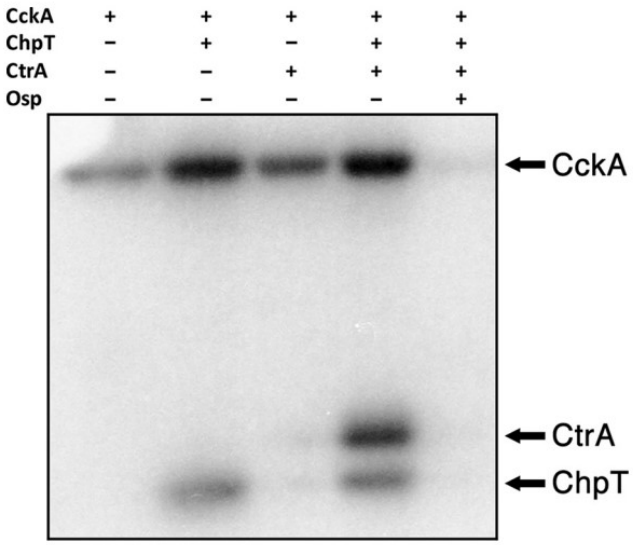

Figura 24. Reconstuitución del sistema de CckA-ChpT-CtrA en presencia o ausencia de Osp. La presencia de cada proteína está indicada con un símbolo (+) en la parte superior de la figura. Las reacciones se incubaron 30 minutos en presencia de (γ-^{32}P) ATP.

Para evaluar el papel de Osp como un regulador alostérico de la transición de CckA entre los estados de cinasa/fosfatasa, analizamos la actividad fosfatasa de CckA en presencia de una concentración equimolar de Osp. Para este análisis, CckA fue fosforilada utilizando (γ-^{32}P)ATP y posteriormente el ATP libre fue eliminado mediante cromatografía de filtración. CckA-P fue mezclada con amortiguador o con una concentración equimolar de Osp. La cantidad de CckA-P remanente a diferentes tiempos fue determinada. Como se observa en la figura 25, no se observó una aceleración en la desfosforilación de CckA en presencia de Osp, por lo que esta proteína no parece estimular la actividad de fosfatasa de CckA.

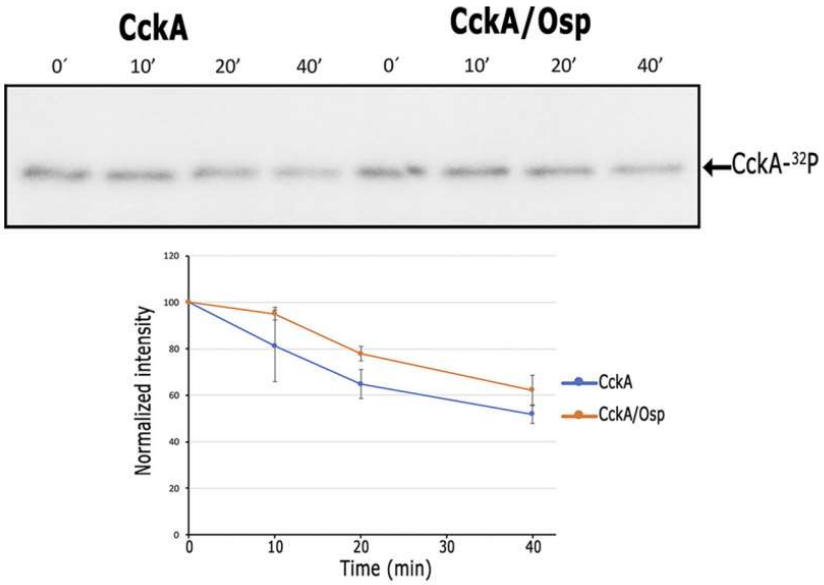

Figura 25. Curso temporal de desfosforilación de CckA presencia y ausencia de Osp. CckA fue fosforilada con (γ-^{32}P) ATP durante 30 minutos y posteriormente el ATP libre fue elimindo mediante cromatografía. La proteína fosforilada se coincubó en presencia o ausencia de concentraciones equimolares de Osp. Una alícuota de la reacción fue tomada a los 10, 20 y 40 minutos después de ser añadida Osp. La gráfica de las densitometrías se muestra en la parte inferior, se analizaron las pendientes de las gráficas mediante una prueba de t de dos colas no se encontró diferencia significativa entre ambas.

CckA*(L391F) es parcialmente resistente a Osp.

Para comprender por qué la cepa AM1 enciende el sistema flagelar 2 aún en presencia del gen silvestre de *osp*, se analizó si la variante CckA* es igualmente sensible a la inhibición por Osp que la versión silvestre (figura 20B). Como se muestra en la figura 26A, la concentración equimolar de Osp no es suficiente para inactivar a CckA*. Para alcanzar un nivel de inhibición similar al observado para CckA silvestre en presencia de concentraciones equimolares de Osp, es necesario que Osp esté por lo menos 4 veces más concentrado que CckA* (figura 26C). De forma similar, al reconstituir el sistema CckA*-ChpT-CtrA se logró observar CtrA

fosforilada aún en presencia de Osp (figura 26B). Estos resultados explican por qué la cepa AM1 enciende al sistema Fla2 por lo que la mutación encontrada en el alelo *cckA** (L391F) no solo activa a CckA [56] sino que también la hace parcialmente más resistente a la presencia de Osp.

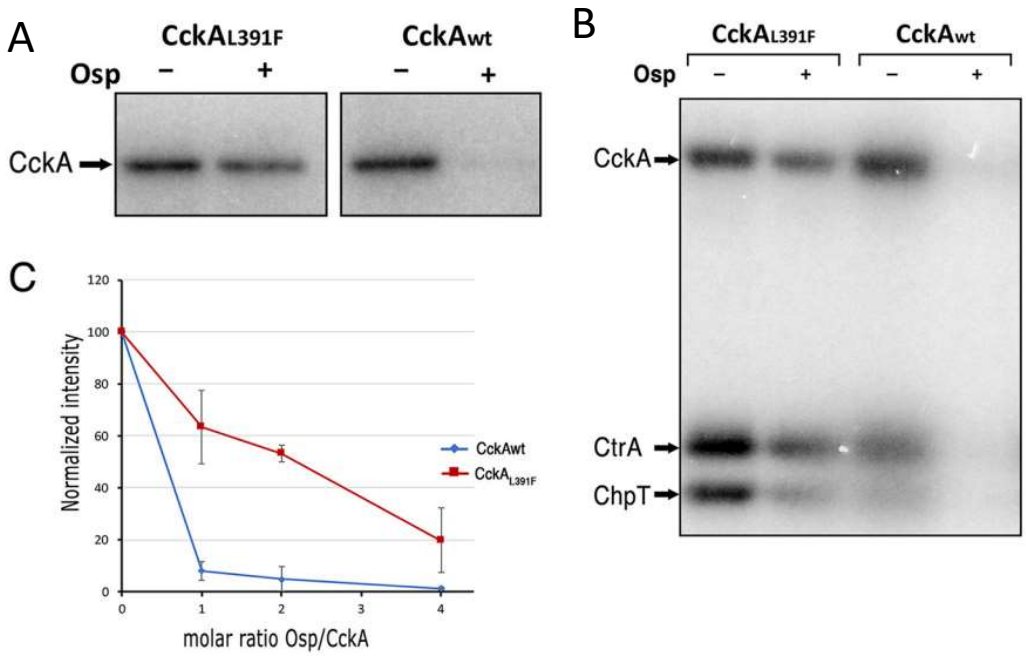

Figura 26. Forsforilación de CckA* en ausencia y presencia de Osp. (A) Efecto de Osp en la fosforilación de CckA*(L391F) y de CckA silvestre, las proteínas fueron utilizadas en una concentración equimolar de 2.5 μM. Las reacciones se incubaron 30 minutos en presencia de (γ-^{32}P)ATP. (B) Reconstitución del sistema CckA-ChpT-CtrA y CckA*-ChpT-CtrA en presencia y ausencia de Osp, todas las proteínas fueron utilizadas a una concentración de 2.5 μM. Las reacciones se incubaron 30 minutos en presencia de (γ–^{32}P)ATP. (C) Cuantificación de la cantidad de CckA y CckA* fosforilada en presencia de diferentes proporciones molares de Osp/CckA.

Osp se encuentra conservado en algunos géneros de las Rhodobacterales.

CtrA está conservada en distintos grupos de las α-proteobacterias pero la presencia de las proteínas que la regulan varía entre estos grupos y en algunos casos se encuentran ausentes [4]. Por lo anterior, decidimos buscar los ortólogos de Osp en las α-proteobacterias. Solo se encontraron ortólogos de Osp en bacterias en el orden de las Rhodobacterales en las familias de las *Rhodobacteraceae* y las *Roseobacteraceae*. Dentro de las *Rhodobacteraceae* se encuentra en especies muy cercanas a *Rhodobacter sphaeroides* ahora denominada *Cereibacter sphaeroides* [69] y en algunas especies del género de las *Defluviimonas*, sin embargo, no se encontró en otros géneros dentro de la familia *Rhodobacteraceae*. A diferencia de las *Rhodobacteraceae,* en las *Roseobacteraceae* Osp se encuentra distribuido en una mayor cantidad de géneros, como se muestra en la figura 27 (especies cuyos nombres se encuentran marcados en azul). Dentro de las Rhodobacterales también se encontró su presencia en *Amylibacter kogurei* que diverge antes de que se separen las familias de las *Rhodobacteraceae* y las *Roseobacteraceae* lo que podría sugerir que Osp apareció antes de la divergencia de estos dos grupos y pudo haberse perdido en diversos géneros de las *Rhodobacteraceae* quedando en solo algunos pocos como *Defluviimonas* y *Cereibacter* mientras que permaneció y se distribuyó en un mayor número de géneros de la familia de las *Roseobacteraceae* (figura 27).

También se evaluó la región regulatoria de *osp* de las bacterias incluidas en la figura 27 usando MEME, y se encontró un motivo similar a la caja de unión de CtrA que tiene como consenso la secuencia TTAA N7 TTAA, en la figura se indican las especies en las cuales se encontró este motivo con una estrella azul y en el anexo 1 se muestran los resultados arrojados por MEME. Si este motivo es funcional, *osp* estaría controlado por CtrA en todas estas especies y probablemente la existencia de un asa de regulación negativa tal y como la observamos en *R. sphaeroides* sería una forma de regulación conservada en todas ellas.

Como se mencionó antes, las Rhodobacterales carecen de DivK, que es el regulador negativo del sistema de CckA-ChpT-CtrA en algunos órdenes de las α-proteobacterias como en las Rhizobiales y Caulobacterales. Interesantemente, en algunas especies que carecen de DivK se encuentra presente una versión trunca de DivL la cual perdió el dominio de trasmisión (DHp y CA) involucrado en la percepción de DivK en el estado fosforilado [5,30,75]. La ocurrencia de estas proteínas también se muestra en las especies incluidas en la figura 27 (DivK representada por un recuadro verde, DivL rojo, y DivL trunca en amarillo).

A partir de los resultados presentados, se puede apreciar un posible orden de eventos evolutivos que precedieron a la aparición de Osp. Inicialmente, después de la pérdida de DivK en las Rhodobacterales encontramos dos versiones de DivL una versión larga con el dominio de transmisión degenerado pero que aún es reconocible utilizando predicciones bioinformáticas, tal es el caso de *Oceanicella actignis* y *Albimonas pacifica*; y por otro lado una versión corta de DivL la cual ya no posee ninguno de los dominios del dominio de transmisión. Esta forma trunca está presente en el resto de las Rhodobacterales. Seguido de la aparición de una DivL corta, Osp pudo haber aparecido antes de la divergencia de las *Rhodobacteraceae* y *Roseobacteraceae* o después posiblemente en las *Roseobacterace* y luego adquirirse por algunos géneros como Amylibacter, Cereibacter y Defluviimonas por transferencia horizontal. En la figura 28 se ilustran los posibles eventos en la evolución de DivL que antecedieron a la aparición de Osp.

En la búsqueda de ortólogos de estos reguladores se encontró un posible evento de transferencia horizontal de DivK en *Thalassobius mediterraneum* (*Roseobacteraceae*) ya que es la única especie en su género y familia que tiene a DivK en conjunto con una DivL corta. Se buscó el mejor ortólogo de DivK mediante BlastP y se encontró que DivK de *Henricella marina*, miembro de la familia de las *Hyphomonadaceae,* es el ortólogo más parecido a DivK de *T. mediterraneum;* además que en las *Hypomonadaceae* como en las *Caulobacteraceae divK* se encuentra contiguo a *pleD,* lo que también ocurre *en T. mediterraneum* y PleD de

H. marina, al igual que ocurre con DivK, es ortólogo más parecido al de *T. mediterraneum* lo que indica que posiblemente ambos genes se transfirieron juntos.

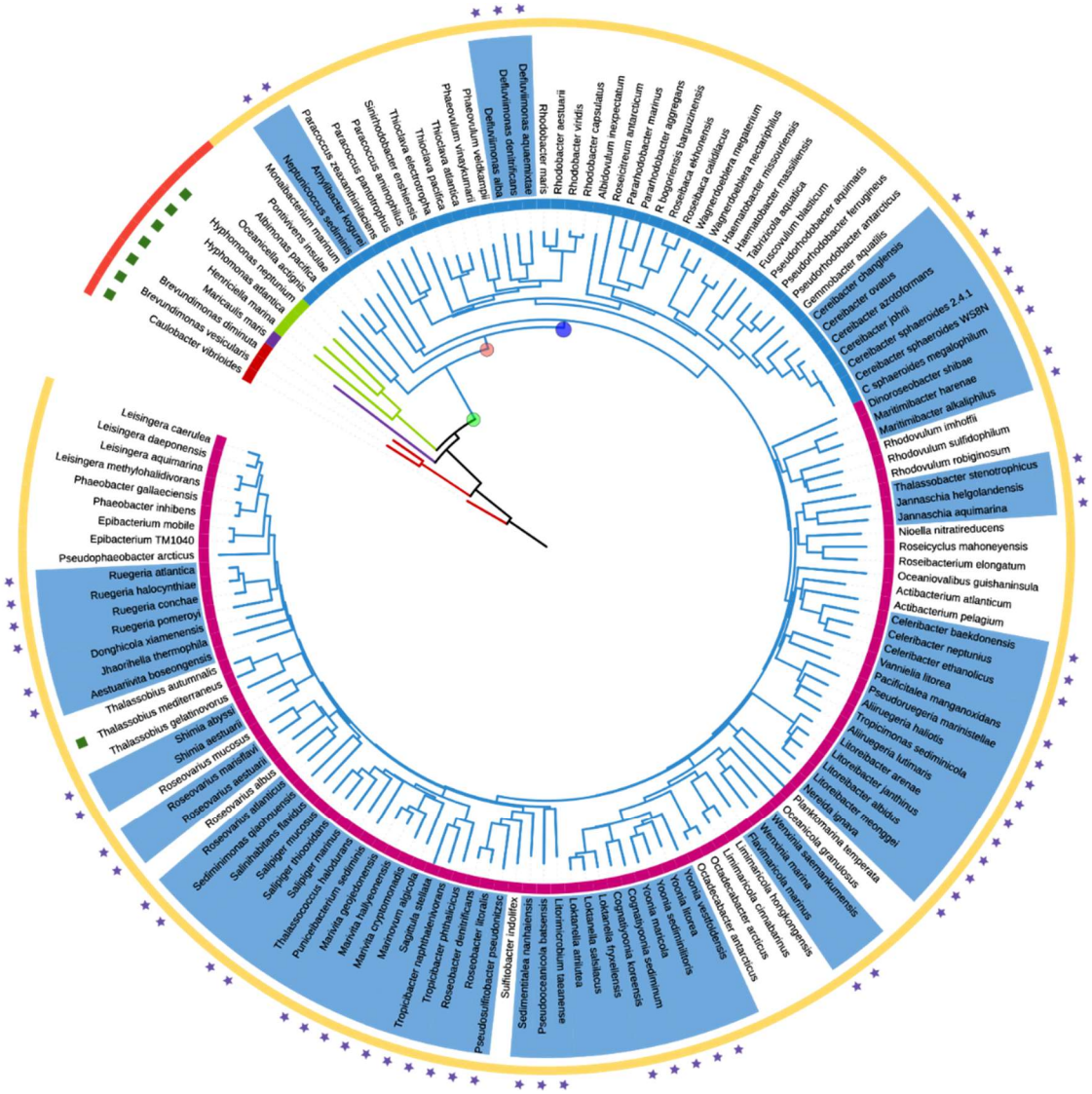

Figura 27. Distribución filogenética de *osp* en las Rhodobacterales. Filogenia basada en RpoC, el árbol se generó usando simple phylogeny de clustal y fue editado usando la herramienta iTOL. De dentro hacia fuera los colores de las ramas indican el orden: Caulobacterales (rojo), Maricaulales (morado), Hyphomonadales (verde) y Rhodobacterales (azul). El círculo debajo del nombre de las especies indica las familias: *Caulobacteraceae* (rojo), *Maricaulaceae* (morado), *Hyphomonadaceae* (verde), *Rhodobacteraceae* (azul) y *Roseobacteraceae* (magenta). En los nombres de las especies, aquellos marcados con azul indican la presencia de Osp. DivK está representado por un cuadrado verde arriba del nombre de la especie. La presencia de DivL larga está marcado en rojo en el círculo arriba de las especies y DivL corta (amarillo). El punto verde representa

el posible evento de pérdida de DivK, el punto rosa la aparición de DivL corta y el punto azul el posible evento de aparición de Osp. Las estrellas azules indican la presencia de la caja de CtrA en la región regulatoria de *osp*. Los números de acceso de las proteínas, el MEME de la región regulatoria de *osp* y la tabla de posiciones del motivo de CtrA encontrado por meme se muestran en el anexo 1 y 2 respectivamente.

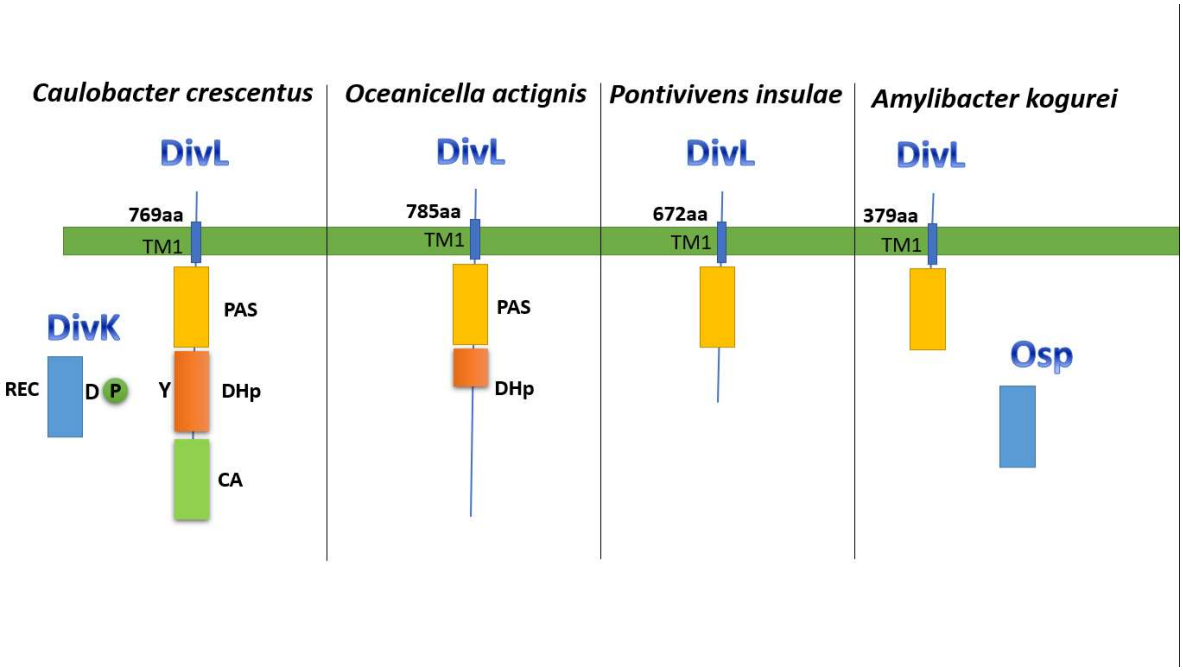

Figura 28. Posibles eventos de evolución de DivL que antecedieron a la aparición de Osp. De izquierda a derecha se representa la proteína DivL desde *C. crescentus* con presencia de los dominios DHp, CA y con la proteína DivK, seguida de *O. actignis* con una degeneración de los dominios DHp y CA y la pérdida de DivK, después el sistema en *P. insulae* con DivL trunca y después *A. kogurei* en presencia de Osp.

Discusión y conclusiones.

El control negativo de los sistemas de dos componentes en bacterias es normalmente llevado por distintos tipos de proteínas que modulan la actividad de las HKs. En el caso de *E. coli* la cinasa NtrB cambia a su estado de fosfatasa cuando se une a la proteína PII [76,77]. En *Bacillus subtilis* la cinasa KinA es inhibida por Sda y KipI [78,79]. Ninguna de estas proteínas tiene homología entre ellas y tampoco son parecidas estructuralmente; sin embargo, todas se unen al dominio de transmisión de sus respectivas HKs [76,79–82]. Estos ejemplos muestran cómo distintos tipos de proteínas pueden llevar a cabo la función de inhibir la actividad cinasa de las HKs.

FixT es una proteína que al igual que Osp es un SDRR y es el regulador negativo de FixL tanto en *C. crescentus* como como en *S. meliloti* [83–85]. Se sabe que FixT inhibe la autofosforilación de la HK FixL sin afectar su capacidad de desfosforilación [84,86]. Dado que FixT fosforilado no fue observado en los ensayos de fosforilación, se descartó que esta proteína funcione como una poza de fosfatos [84,86].

En este trabajo mostramos que Osp un SDRR es responsable de inhibir al sistema de dos componentes CckA-ChpT-CtrA en *R sphaeroides*. Encontramos que una mutación que inactiva a Osp es suficiente para favorecer la fosforilación de CtrA y de este modo permitir la expresión de los genes regulados por CtrA, *i.e.* los genes del sistema Fla2, los genes quimiotácticos, de vesículas de gas, del agente de transferencia de genes, etc. y de reprimir los genes del fotosistema. Congruente con este resultado los ensayos *in vitro* mostraron que Osp directamente inhibe la actividad de cinasa de CckA mientras que su actividad de fosfatasa parece no estar afectada. Además, mostramos que la presencia de ChpT y CtrA no afecta la actividad inhibitoria de Osp.

El efecto inhibitorio de las proteínas FixT y Osp sobre HKs específicas, lleva a considerar la posibilidad de que un cierto número de SDRRs pudieran cumplir una función similar sobre HKs específicas, sean estas canónicas como FixL, o híbridas como CckA. En consecuencia, sería factible suponer que algunos de los SDRRs

huérfanos presentes en los genomas bacterianos pudieran cumplir este tipo de función.

En este trabajo se determinó que Osp interacciona con el dominio transmisor de CckA. Dado que Osp interacciona con este dominio y dada su naturaleza de SDRR creemos que se une a las mismas regiones a las cuales se une el dominio REC de CckA y de esa manera imposibilitaría el acceso al residuo de histidina fosforilable, tanto para el propio dominio REC de CckA como para el dominio CA de CckA, impidiendo así la autofosforilación del residuo de histidina. Sin embargo, es factible que Osp no solo impida el acceso del dominio CA al dominio DHp, debido a que Osp puede inhibir en un 50% la actividad de CckA cuando estas proteínas se encuentran en relación molar 1:4. Lo anterior sugiere que la unión de un monómero de Osp podría generar un cambio conformacional en el dímero de CckA que impida su fosforilación. La determinación de la estructura cristalográfica nos ayudaría a elucidar la forma en la cual interaccionan estas proteínas y de este modo entender cómo es que funcionan este tipo de SDRR inhibidores.

La disponibilidad en la célula de Osp es también uno de los aspectos que será necesario elucidar con el fin de generar un modelo preciso al respecto del funcionamiento y control del sistema. Nuestros resultados nos mostraron que CtrA es necesaria para inducir la expresión del gen *osp*, pero en su ausencia es posible detectar expresión. Este nivel basal de Osp podría ser importante para mantener el sistema inactivo hasta que ocurra el estímulo apropiado para su activación. Por otro lado, la mayor expresión de *osp* ocurre en condiciones de cultivo que correlacionan con la activación de CtrA, no obstante, la proteína Osp en esas condiciones fue indetectable (*i.e*. en presencia de 0.1 mM ácido succínico). Lo anterior podría indicar que Osp podría estar sujeta a degradación proteolítica cuando el sistema es activado. Dado que Osp posee en el carboxilo terminal dos residuos de alanina, es factible suponer que el sistema ClpXP podría ser responsable de su degradación debido a que se ha documentado que esta proteasa reconoce este tipo de sustratos [71,87]. Sí este fuera el caso compartiría esta cualidad con FixT y Sda que son degradadas para permitir la activación de sus respectivas cinasas [86,88]. Hace falta

más exploración para entender cuáles son las señales que hacen que Osp no se acumule en condiciones en donde el ácido succínico es bajo y en condiciones fotoheterotróficas.

La presencia de Osp en diversos géneros de bacterias que carecen del circuito regulatorio formado por el par de proteínas DivK-DivL sugiere que la regulación negativa de la actividad de CckA debe ser fisiológicamente importante. En este caso Osp cumple con una función análoga a la de DivK-P de *C. crescentus* pero a diferencia de ésta, el sistema CckA/ChpT/CtrA es altamente sensible a señales ambientales, lo cual podría ser adscrito a la capacidad de Osp de ser regulado postraduccionalmente. En este contexto Osp representa una alternativa del sistema DivK-DivL para el control de CckA, pero que es altamente sensible a los estímulos ambientales.

Material y Métodos.

Cepas, oligonucleótidos y condiciones de crecimiento bacteriano. Las cepas utilizadas en este trabajo se enlistan en la Tabla 1. Los cultivos de *R. sphaeroides* se realizaron en medio mínimo de Sistrom [89], sin cas aminoácidos y suplementado con ácido succínico 15 mM o 0.1 mM como fuente de carbono. Las condiciones de cultivo para el crecimiento heterótrofo o fotoheterótrofo han sido reportadas previamente y brevemente consisten en el crecimiento en matraces con agitación en la obscuridad, o en viales de tapón de rosca completamente llenos e iluminados de forma continua, respectivamente [8]. Se cultivaron las cepas de *E. coli* en medio LB a 37°C. Para *R. sphaeroides* y *E coli* se adicionaron los antibióticos a las concentraciones indicadas en la Tabla 2. *Saccharomyces cerevisiae* fue crecida a 30°C en YPDA o en medio mínimo definido sintético (Clontech). Los oligonucleótidos utilizados en este trabajo se muestran en la Tabla 3.

Tabla 1. Cepas utilizadas en este trabajo

Cepa o Plásmido	Descripción	Fuente
Rhodobacter sphaeroides		
AM1	Derivada de SP13; Δ*fleQ*::Kan, *cckA*L391F	[90]
BV6	Derivada de SP20 ; Δ*fliF1*::aadA, *osp*H115D	Este trabajo
BV7	Derivada de SP13 ; Δ*fleQ*::Kan, *osp*77aa	Este trabajo
BV8	Derivada de SP20 ;Δ*fliF1*::*aadA*, *osp*AV+	Este trabajo
BV9	Derivada de SP13 ; Δ*fleQ*::Kan, *osp*11shift	Este trabajo
BV10	Derivada de SP20 ;Δ*fliF1*::*aadA*, Δ*osp*::hyg	Este trabajo
BV11	Derivada de SP13; Δ*fleQ*::Kan, Δ*osp*::hyg	Este trabajo
BV12	Derivada de AM1; Δ*fleQ*::Kan, *cckA*L391F, Δ*osp*::hyg	Este trabajo
BV13	Derivada de SP13; Δ*fleQ*::Kan, Δ*osp*::hyg, Δ*ctrA*::*aadA*	Este trabajo
BV14	Derivada de BV11; Δ*ctrA*::*aadA*	Este trabajo
BV15	Derivada de BV11; Δ*chpT*::*aadA*	Este trabajo
BV16	Derivada de BV6; Δ*cckA*::hyg	Este trabajo
BV17	Derivada de SP13; Δ*ctrA*::hyg	Este trabajo
BV18	Derivada de AM1; FLAG-*osp*	Este trabajo
BV19	Derivada de SP13; FLAG-*osp*	Este trabajo
JHV3	Derivada de AM1; Δ*fleQ*::Kan, *cckA*L391F, *mcpB*::*uidA*-*aadA*	[8]
LC7	Derivada de AM1; Δ*fleQ*::Kan, *cckA*L391F, Δ*ctrA*::hyg	colección lab
SP13	Derivada de WS8N; Δ*fleQ*::Kan	[58]
SP20	Derivada de WS8N; Δ*fliF1*::*aadA*	Colección lab
Escherichia coli		
LMG194	Cepa para expresión de proteínas	Invitrogen
TOP10	Cepa para clonación	Invitrogen
Rosetta	Cepa para expresión de proteínas	Novagen
Levaduras		
AH109	Cepa reportera para el ensayo de doble híbrido *HIS3*, *ADE2,* and *lacZ*	Clontech
Plasmidos		
pBAD HisB	Vector de expresión de proteínas etiqueta His6X; Ap^R	Invitrogen
pBAD_chpT	pBAD/HisB expresando His6x-ChpT	Colección Lab
pBAD_ctrA	pBAD/HisA expresando His6X-CtrA	[91]
pBAD/His-CckA	pBAD/HisB expresando el dominio citoplásmico de CckA fusionado a His6x	[56]

pBAD/His-CckA L391F	pBAD/HisB expresando el dominio citoplásmico deCckAL391F fusionado a His6x	[56]
pBADHis-dctR	pBAD-His expresando DctR fusionado a His6x	[74]
pET28a	Vector de expresión para la etiqueta His6x, Kan	Novagen
pET28A_6XHis-cckA_osp	pET28 expresando el dominio transmisor de CckA fusionado a His6x, and Osp	Este trabajo
pET28A_6xHis-cckA	pET28 expresando el dominio transmisor de CckA fusionado a His6x	Este trabajo
pET28a_His6x-PhoR	pET28a expresando el dominio citoplásmico de PhoR fusionado a His6x	Este trabajo
pET28a_osp	pET28a expresando Osp	Este trabajo
pET28a_osp6xHis	pET28a expresando Osp fusionado a His6x	Este trabajo
pGADT7	Plásmido para el ensayo de doble híbrido con el dominio de activación de Gal4, *LEU2*	Clontech
pGADT7_osp	pGADT7 expresando la fusión Gal4AD-Osp	Este trabajo
pGADT7_REC-DctR	pGADT7 expresando la fusión Gal4AD-REC-DctR	Este trabajo
pGBKT7	Plásmido para el ensayo de doble híbrido con el dominio de unión a DNA de Gal4, *TRP1*	Clontech
pGBKT7_cckA_DHp-CA	pGBKT7 expresando la fusión GAL4AD-CckA-DHp	Este trabajo
pGBKT7_cckA-REC	pGBKT7 expresando la fusión Gal4AD-CckA-REC	Este trabajo
pGBKT7_cckADPas	pGBKT7 expresando la fusión Gal4BD-CckAΔPAS	Este trabajo
pGBKT7_cckAΔTM	pGBKT7 expresando la fusión Gal4BD-CckAΔTM	Este trabajo
pIJ963	Plásmido fuente del casete de hygromicina (hyg)	[92]
pJQ200mp18	Plásmido suicida en *R. sphaeroides*	[93]
pJQ200_Δosp::hyg	pJQ200mp18 llevando Δ*osp*::hyg	Este trabajo
pRK415	Vector de expresión en *R. sphaeroides*, Tc^R	[94]
pRK_osp	pRK415 expresando Osp	Este trabajo
pRK_osp D51N	pRK415 expresando Osp D51N	Este trabajo
pRK_osp::uidA-aadA	pRK415 llevando la fusión transcripcional *osp-uidA*	Este trabajo
pSUP11	Plásmido para etiquetar con FLAG	[95]
pTZ18R_Δosp::hyg	pTZ18R llevando Δ*osp*::hyg	Este trabajo
pTZ18R_ospUPDW	pTZ18R llevando las regiones río abajo y río arriba de *osp*	Este trabajo
pTZ18R/19R	Cloning vectors, Ap^R	[96]
pTZ19R Bam-	pTZ19R sin sitio BamHI	Colección Lab
pTZospFLAG_1.7	pTZ19RBamHI- conteniendo las regiones río arriba y codificadora de FLAG-osp	Este trabajo
pWM5	Plásmido fuente del casete *uidA-aad*	[97]

Tabla 2. Concentraciones de antibióticos utilizadas en este trabajo

R. sphaeroides	kanamicina	25 μg/ml
	tetraciclina	1 μg/ml
	espectinomicina	50 μg/ml
	higromicina	
E. coli	kanamicina	50 μg/ml
	tetraciclina	12 μg/ml
	espectinomicina	50 μg/ml
	higromicina	
	ampicilina	100 μg/ml
	gentamicina	30 μg/ml

Tabla 3. Oligonucleótidos utilizados en este trabajo

FwUPospEco	GCGAATTCCGCTCGGTCACTTCTGGGAC
RvUPospBam	GCGGATCCCTCCACGATCAGGACGTGCAT
FwDWospBam	GCGGATCCGACGGGTCCATCTTCACCCAT
RvDWospXba	GCTCTAGACTCGAGCCAGAAATCGAGCG
Fw_hygrouniv	GCGGATCCCGGGCCAGCTCCGCCATCGCC
Rv_hygrouniv	GCGGATCCGGCGGCCCGGGGCGTCAGGC
FWospQE	GCCCATGGACGTCCTGATCGTGGAGAC
Rv osp Hind	GCAAGCTTGGCCGCGTGAACGTAATGCTC
Fw Ccka cristal NdeI	GCCATATGAAGACGCTCGAGGCTCAGTTC
Rv CckA cristal XbaI	GCTCTAGATCACGGCTCTTCATTGATGGG
FWospQE	GCCCATGGACGTCCTGATCGTGGAGAC
Rv osp pBAD HindIII	GCAAGCTTCTCAGGCCGCGTGAACGTAATG
T7 prom BglII	GCAGATCTTTAATACGACTCACTATAGGG
T7 ter BglII	GCAGATCTGATATAGTTCCTCCTTTCAGC
Fw CckA DH NdeI	GCCATATGCTCGATCTGCGGTTCGCGC

454 B	GGAGCTCGGCTCAACGTCTCGCCCTGT
Fw DPasCckA DH NdeI	GCCATATGGATGTCGCCGCCGAGCGGATG
Rv CckADrec NcoI	GCCCATGGTCACTCGACGGGAAGCGGCTC
Fw CckA REC NdeI	GCCATATGGAAGAGCCGCTTCCCGTCGAG
Fw osp NdeI	GCCATATGCACGTCCTGATCGTG
Rv OspDH BamHI	GCGGATCCCTCAGGCCGCGTGAACGTAATG
Rv Met osp Eco	GCGAATTCCATTCTGGCTTCCTTCGACTTTG
Rv Flag Nde	GCCATATGTTTATCGTCGTCATCTTTGTAG
Fw osp Nde	GCCATATGCACGTCCTGATCGTG
Fw dw ospflag Bam	GCGGATCCCCGCGCAGCATTCGTAACGCC
Rv dw ospflag Xba	GCTCTAGATTCGACTCGCGGATCAACGCG
Fw_phoR_BamHI	GCGGATCCCTGAACCGGCGAAAGGCCGTC
Rv_PhoR_EcoRI	GCGAATTCTCAGGCGCTTCCCGCTTCCGC
DctR_DHTH_EcoRI	GCGAATTCTCAGCGCGCGCCGCTGTGGGCCAG
DctRA	CCGGAATTCACAGGGTGCGTCCATATCAT
Fw_osp_Hind	GCAAGCTTCTTTTCCCCGCCTCTTTCGG
Rv_osp_Xba	GCTCTAGAAGACTGGGTGCGGGCGTTAC
Fw ospD51N	CAGGTCGTGATGCTGAATCTGATGCTCGACG
Rv ospD51N	CGTCGAGCATCAGATTCAGCATCACGACCTG

Las cepas mutantes obtenidas en este trabajo. Para obtener el alelo ∆*osp*::hyg, las regiones río arriba y río abajo de *osp* se amplificaron mediante PCR utilizando los oligonucleótidos FwUPospEco y RvUPospBam para la región río arriba, y FwDWospBam y RvDWospXba para la región río abajo, se utilizó como sustrato de amplificación el DNA total purificado de la cepa WS8N de *R. sphaeroides*. Los productos de 584 y 534 pb se clonaron juntos a través de un sitio BamHI presente en los oligonucleótidos RvUPospBam y FwDWospBam en el plásmido pTZ18R. El plásmido resultante denominado pTZ_ospUPDW lleva clonado un fragmento de 1118 pb y su identidad fue confirmada por secuenciación. Este plásmido fue digerido con BamHI y ligado con un casete de higromicina (hygR) previamente digerido con BamHI, para obtener pTZBam_∆osp::hyg. El casete hyg se obtuvo por PCR utilizando los oligonucleótidos Fw_hygrouniv y Rv_hygrouniv y el plásmido pIJ963, que lleva el casete de resistencia a higromicina [92]. El fragmento de DNA que lleva el alelo ∆osp::hyg se obtuvo por PCR con los oligonucleótidos FwUPospEco y RvDWospXba, y pTZBam_∆osp::hyg como sustrato de amplificación. EL producto de amplificación se clonó en el sitio SmaI del plásmido suicida pJQ200mp18, el cual es incapaz de replicarse en *R. sphaeroides*. El plásmido resultante se introdujo en *R. sphaeroides* mediante conjugación y se seleccionaron eventos de doble recombinación mediante la selección de las transconjugantes resistentes a hyg y sensibles a Gm (que es la resistencia del plásmido pJQ200mp18). La presencia del alelo mutante en la cepa seleccionada se confirmó mediante PCR.

Para marcar Osp con 3XFLAG, se obtuvo un producto de PCR de 566 pb que lleva la región río arriba de *osp* desde la posición -563 (considerando el sitio de inicio de la traducción como +1) hasta el codón de inicio de *osp*, usando los oligonucleótidos FwUPospEco y RvMetospEco. La fusión entre el codón inicial de osp y la secuencia codificante de la etiqueta FLAG se generó mediante la ligación del producto de PCR de 566 pb y el plásmido pSUB11 previamente digeridos ambos con EcoRI. El producto de ligación se usó para amplificar por PCR el fragmento que abarca la región río arriba de *osp* y la región codificante de la secuencia FLAG-tag, para esta reacción se utilizaron los oligonucleótidos FwUPospEco y RvFlagNde. El producto fue clonado en pTZ18R previamente digerido con SmaI. El plásmido resultante se

digirió con la enzima de restricción NdeI y la región codificante de *osp* obtenida por PCR con los oligonucleótidos FwospNde y RvOspDHBamHI fue digerida con NdeI y ligada a este plásmido. La reacción de ligación fue amplificada con los oligonucleótidos FwUPospEco y RvOspDHBamHI para generar un producto de 1,000 pb que lleva la región río arriba de *osp*, la secuencia FLAG, y la región codificadora de *osp*. Este producto de PCR se digirió con BamHI y se ligó con la región río abajo de *osp*, la cual se obtuvo por PCR con los oligonucleótidos FwdwospflagBam y RvdwospflagXba y para su ligación fue digerida con BamHI. El producto de PCR de la reacción de ligación obtenido con los oligonucleótidos FwUPospEco y RvdwospflagXba de 1.7 Kb se ligó a pTZ19RBamHI- en el único sitio SmaI para obtener el plásmido pTZospFlag_1.7. Por otro lado, se obtuvo un casete de espectinomicina por PCR flanqueado por sitios BamHI y se clonó en el sitio BamHI de pTZospFlag_1.7, el cual se encuentra presente después del codón de paro de la región codificadora de *osp*. El fragmento presente en el plásmido pTZospFlag_1.7_aadA que contiene FLAG-osp y el casete de espectinomicina, se subclonó en el plásmido suicida pJQ200mp18. El plásmido resultante se introdujo por conjugación a las cepas AM1 o SP13 para obtener las cepas BV18 y BV19, respectivamente. Se seleccionaron eventos de doble recombinación y se verificó la exactitud de las mutantes mediante PCR.

Sobreexpresión y purificación de proteínas. La región codificadora de *osp* se amplificó por PCR utilizando los oligonucleótidos FwospQE y RvospHind. El producto se clonó en el plásmido pET28a para generar la fusión entre Osp y la etiqueta His6x codificada en este vector. El plásmido resultante pET28a_osp-His6 se usó para transformar células de *E coli* Rosetta, esta cepa permite la expresión de la fusión Osp-His6 a partir del promotor del bacteriófago T7. Una vez elegida una clona en la cual se confirmó la inducción de la proteína de interés por la adición de IPTG, se procedió a la purificación de la misma. Para ello, se creció un cultivo de la cepa que expresa Osp-His en medio LB a 37°C hasta la fase de crecimiento exponencial y se adicionó 1 mM IPTG, el cultivo se incubó durante 4 horas mas. Las células se colectaron por centrifugación y se suspendieron en 1/10 del volumen de buffer TEG (Tris 50 mM pH 8, NaCl 50 mM y glicerol al 5%). La suspensión celular

se sonicó en hielo utilizando una micropunta (3 mm), con tres pulsos de 10 s, los desechos se eliminaron mediante centrifugación a baja velocidad a 5,000 rpm durante 2 min. Aunque la mayor parte de la proteína era insoluble, una pequeña cantidad de proteína permanece soluble; por lo tanto, el sobrenadante se incubó con agarosa Ni-NTA durante 2 h a 4 °C. Las perlas se lavaron tres veces con PBS pH 7.4. La proteína se eluyó utilizando PBS/glicerol al 10%/imidazol 200 mM. El dominio citoplasmático de CckA fusionado a la etiqueta His6x (His6-CckA) se purificó como se describió anteriormente utilizando el plásmido pBAD_His-cckA y pBAD_His-cckA F391L [56]. La proteína His6-CtrA se purificó utilizando el plásmido pBAD_ctrA y siguiendo el procedimiento descrito anteriormente [91]. His6x-ChpT se obtuvo utilizando el plásmido pBAD_His-chpT en la cepa de *E. coli* LMG194. Para ello, se creció un cultivo de la cepa que expresa His-ChpT en medio LB a 37°C hasta la fase de crecimiento exponencial y se indujo la expresión de la proteína con arabinosa al 0.2 % durante 4h a 37°C. Las células se cosecharon a 12,000 rpm durante 10 min. Las células se suspendieron en 1/10 del volumen en buffer TEG (Tris 50 mM, pH 8, NaCl 50 mM y glicerol al 5 %), se sonicaron y se centrifugaron a 12,000 rpm durante 10 min a 4°C para eliminar los restos celulares. El sobrenadante se incubó con agarosa Ni-NTA, durante 2 h a 4°C. Las perlas de agarosa se lavaron tres veces con PBS pH 7.4. La proteína se eluyó con PBS/glicerol al 10%/imidazol 200 mM. Antes de los ensayos de fosforilación, la proteína purificada se dializó utilizando el buffer de PBS con glicerol al 10 % durante 2 h. Para obtener His6-PhoR, la región de DNA que codifica el dominio citoplasmático de PhoR se amplificó por PCR utilizando los oligonucleótidos Fw_phoR BamHI y Rv_phoR_EcoRI. El producto de 1248 pb se purificó y clonó en pET28a. El plásmido resultante se introdujo en *E. coli* Rosetta. La proteína se obtuvo mediante la inducción de un cultivo en fase exponencial, utilizando IPTG 1 mM durante 2 h a 37°C. Las células se cosecharon y se resuspendieron en PBS pH 7.4, las células se lisaron mediante sonicación como se indicó antes. La fracción soluble fue incubada con Ni-NTA agarosa durante 2 h a 4°C. Las perlas de agarosa se lavaron tres veces con PBS pH 7.4. La proteína se eluyó con PBS/glicerol al 10%/imidazol 200 mM . Se utilizó el protocolo previamente publicado para la obtención de la proteína His6-DctR [74].

Copurificación de proteínas. EL procedimiento para la obtención de los plásmidos necesarios para este ensayo se describe brevemente a continuación: El dominio transmisor de CckA fue obtenido mediante PCR utilizando los oligonucleótidos Fw CckA_cristal_NdeI y Rv_CckA cristal_XbaI, dicho producto de PCR fue clonado en el plásmido pTZ18R SmaI. El plásmido resultante fue digerido con las enzimas NdeI y BamHI y el inserto se subclonó en pET28a, previamente digerido con las enzimas NdeI y BamHI. Por otro lado, el plásmido pET28a_osp que sobre-expresa la proteína Osp (sin etiqueta) fue obtenido mediante la clonación del producto de PCR que lleva la región codificadora de *osp* en pET28a, la reacción de amplificación de *osp* se llevó a cabo utilizando los oligonucleótidos FWospQE y Rv osp pBAD HindIII, para la clonación, el plásmido y el producto de PCR fueron digeridos con las enzimas NcoI y HindIII. Finalmente, el vector pET28a_His6-cckA_osp se construyó clonando en el plásmido pET28a_His6x-CckA, el producto de PCR que lleva *osp* así como las regiones río arriba y río abajo que incluyen el promotor y el terminador T7. Para la obtención de este plásmido se amplificó la región codificadora de *osp*, junto con las regiones de control 5' y 3' que incluyen el promotor y el terminador de T7, presentes en el plásmido pET28a_Osp, utilizando los oligonucleótidos T7 prom BglII y T7 ter BglII. El producto de PCR fue clonado en el sitio BglII de pET28a_6xHis-cckA. La sobreexpresión de His6x-CckA, Osp, así como de His6-CckA y Osp se realizó induciendo cultivos celulares de *E. coli* Rosetta llevando pET28a_6xHis-CckA, pET28a_osp, o pET28a_His6x-cckA_osp con IPTG 1 mM. Los tres extractos celulares obtenidos de cultivos inducidos se procesaron de acuerdo a los protocolos establecidos de purificación con NI-NTA descritos en la sección anterior. Las proteínas purificadas se sometieron a SDS-PAGE [98] y se tiñeron con azul brillante de Coomassie R-250.

Plásmidos obtenidos para el ensayo de doble híbrido de levaduras. Los plásmidos pGBKT7_cckAΔTM, pGBKT7_cckAΔPAS, pGBKT7_cckA DHp-CA y pGBKT7_cckA Rec (ver figura 20 la estructura de dominios de CckA) se construyeron clonando en el plásmido pGBKT7 los productos de amplificación

obtenidos con los oligonucleótidos indicados en la Tabla 3. El plásmido pGADT7_osp se construyó clonando en pGADT7 la región codificante de *osp* obtenida mediante PCR usando los oligonucleótidos FwospNdeI y RvospDHBam. El plásmido pGADT7_REC-dctR se obtuvo clonando la región de DNA que codifica para el dominio REC de DctR en pGADT7, para ello se utilizaron los oligonucleótidos DctR_ΔHTH_EcoRI y DctRA. La secuencia de estos plásmidos y la fusión con el domio GAL4 correcta se confirmó mediante secuenciación.

Plásmidos obtenidos en este trabajo derivados de pRK415. El plásmido pRK_osp se obtuvo clonando en pRK415 el producto de amplificación de 542 pb generado utilizando los oligonucleótidos Fw_osp_HindIII, Rv_osp_Xba y el DNA total de WS8N. El plásmido pRK_osp D51N se obtuvo mediante mutagénesis dirigida del residuo de interés utilizando los oligonucleótidos Fw ospD51N y Rv ospD51N. Para generar el plásmido pRK_osp::uidA-aadA, el casete *uidA-aadA* fue obtenido a partir del plásmido pWM5 como un fragmento BamHI de 4.2 kb, este fragmento se clonó en pTZ18R_ospUPDW previamente digerido con BamHI. Se realizó un tamizaje de las clonas obtenidas para seleccionar el plásmido en el cual el gen reportero *uidA* estuviera orientado apropiadamente para dejar la región de control de *osp* adyacente al reportero. El plásmido seleccionado fue purificado y se digirió con las enzimas XbaI y EcoRI para liberar el inserto; el fragmento de DNA de 4.7 kb (osp::uidA-aadA) se subclonó en pRK415. La secuencia de estos plásmidos se confirmó mediante secuenciación.

Ensayos de nado. La capacidad de nado de las bacterias fue probada en cajas de agar suave, las cuales fueron preparadas utilizando el medio indicado para cada experimento y adicionadas con 0.22% agar.

Secuenciación y análisis del genoma de la cepa BV6. EL DNA cromosomal total de la cepa BV6 fue aislado utilizando el estuche de purificación de DNA cromosomal (Sigma-Aldrich). El DNA fue utilizado para la obtención de una biblioteca genómica utilizando los adaptadores recomendados por el fabricante. Dicha biblioteca fue secuenciada en el equipo Illumina NexSeq 500 y se obtuvieron lecturas (reads) pareados de 2X76 pb. Las lecturas se mapearon contra el genoma de *R.*

sphaeroides WS8N usando el programa bowtie2 [99]. Una vez mapeadas las lecturas, se identificaron las variantes (SNP e indels) usando las herramientas de BCFtools [100,101]. Los cambios detectados en la secuencia nucleotídica se confirmaron mediante PCR y secuenciación del producto mediante la técnica de Sanger.

Determinación enzimática de la β-glucuronidasa. El ensayo para determinar la actividad de la β-glucuronidasa se realizó con extractos celulares totales que fueron obtenidos a partir de cultivos en fase exponencial. La actividad enzimática se determinó siguiendo el protocolo descrito previamente [8,102], en el cual se utiliza 4-metilumbeliferil- β-D-glucurónido (MUG) como sustrato y se incuba a 37 C con extractos de células sonicadas. La reacción se detiene a diferentes tiempos con buffer de Na_2CO_3 0.2 M. La fluorescencia de las muestras se determinó utilizando las longitudes de 360 nm de exitación y 446 nm de emisión. La cantidad de producto se calculó en base a una curva estándar de 4-metilumbeliferona (Sigma-Aldrich). La actividad enzimática específica se expresó como picomoles de metilumbeliferona por minuto por miligramo de proteína. El contenido de proteína se determinó mediante el método de Bradford con un ensayo de proteínas comercial, utilizando albúmina de suero bovino como estándar.

Reacciones de fosforilación. La concentración de His6-CckA o la versión mutante His6-$CckA_{L391F}$, se ajustó a 2.5 μM en buffer HEPES (HEPES 33 mM, MgCl2 10 mM, KCl 50 mM, ditiotreitol 1 mM y glicerol al 10%, pH 7.5). Se añadió Osp-His6x a la concentración indicada en cada figura. La reacción de fosforilación se inició agregando 500 μM de ATP con 1 μl de (γ-^{32}P)ATP hasta un volumen final de 30 μl. En los puntos de tiempo deseados, se extrajo una muestra de 5 μl y la reacción se detuvo mediante la adición de 5 μl de buffer de muestra de Laemmli (4X) [98]. Las muestras fueron sometidas a electroforesis, SDS-PAGE, y el gel se secó y la radiactividad se visualizó y cuantificó utilizando pantallas de imágenes de fósforo (Typhoon, GE). Las reacciones de fosfotransferencia se realizaron mezclando His6-CckA o His6-CckA y 2.5 μM Osp-His6, junto con His6-ChpT purificado (2.5 μM) y His6-CtrA (2.5 μM) en buffer HEPES. La reacción de fosforilación se inició agregando ATP 500 μM con 1 μl de (γ-^{32}P)ATP hasta un volumen final de 30 μl.

Después de 20 min, la reacción se detuvo mediante la adición de 30 μl de buffer de muestra de Laemmli (4X). Alternativamente, para el experimento que se muestra en la Fig., se fosforilaron 2.5 μM de CckA con (γ-^{32}P)ATP durante 30 min y la muestra se sometió a cromatografía de exclusión en Sephadex G-250. El volumen de elución se dividió en dos y se mezcló con 2.5 μM de ChpT y CtrA o con 2.5 μM de ChpT, CtrA y Osp. Después de mezclar, se tomaron muestras en los tiempos indicados y se sometieron a electroforesis, SDS-PAGE.

Actividad fosfatasa de CckA. Se fosforilaron 2.5 μM de His6-CckA utilizando (γ-^{32}P)ATP durante 20 min. Después de este tiempo, el ATP restante se eliminó por cromatografía de exclusión en Sephadex G-250. El volumen de elución de 40 μl se dividió en dos y se mezcló con buffer o con 2.5 μM Osp-His6 hasta un volumen final de 30 μl. Después de mezclar, se tomaron muestras cada 10 min y la reacción se detuvo con 5 μl de buffer de muestra Laemmli (4X). Alternativamente, también se evaluó la actividad fosfatasa iniciando la reacción con 2.5 μM de CckA, ChpT y CtrA, previamente fosforilados con (γ-^{32}P)ATP durante 30 min y sometidos a cromatografía de exclusión usando Sephadex G-250. El volumen de elución se dividió en dos y se mezcló con buffer o con Osp-His6x 2.5 μM. Se tomaron muestras en los tiempos indicados y se analizaron por SDS-PAGE.

Ensayos de doble híbrido de levadura. Las interacciones entre proteínas utilizando el ensayo de doble híbrido de levaduras se probaron utilizando el sistema Matchmaker GAL4 3 siguiendo las instrucciones del fabricante (Clontech).

Inmunodetección de proteínas mediante Western blot. Los extractos celulares totales se sometieron a electroforesis en SDS-PAGE [98]. Las proteínas se transfirieron a una membrana de nitrocelulosa y se probaron usando inmunoglobulinas anti-FLAG (1:10.000) (Sigma-Aldrich), anti-FlgE2 o anti-FliA (1:30,000) obtenidas en ratón [103,104]. La detección se realizó utilizando un anticuerpo secundario anti-IgG de ratón conjugado con fosfatasa alcalina y desarrollado con CDP-Star (Applied Biosystems).

Análisis filogenético. Se seleccionaron diferentes especies de Rhodobacterales para realizar el análisis filogenético de la distribución de Osp y otras proteínas reguladoras. Se buscó contar con una buena distribución y se tomó en cuenta que los genomas estuvieran completos (o casi completos > 95 %) y con un bajo nivel de contaminación (< 5 %), de acuerdo a los criterios establecidos en el algoritmo CheckM [105]. La proteína RpoC fue identificada por BLASTP. Las proteínas RpoC de todas las especies seleccionadas se alinearon con MUSCLE versión 3.8 [106]. El árbol filogenético se construyó mediante el método de neighbor joining [107].

Análisis bioinformático de las secuencias. Para cada genoma de la figura 27, la región intergénica entre *osp* y el gen río arriba se obtuvo de la base de datos del NCBI. En estas regiones se buscó la presencia de motivos conservados utilizando el algoritmo MEME versión 5.4.1 [108]. Por otro lado, el análisis de las secuencias en relación a la predicción de la estructura secundaria se llevó a cabo utilizando el servidor Psipred [66] y la homología de proteínas se evaluó utilizando Swiss-Model [65] y la estructura cristalina de CheY (PDB 6TG7).

Anexos

Anexo 1. Especies y números de acceso del ensamble y de las proteínas usadas para construir el árbol figura 27.

Cepa	Nombre en el árbol	Número de acceso del genóma	RpoC	Osp	DivK
Actibacterium atlanticum 22II-S11-z10	Actibacterium_atlanticum	GCA_000671395.1	KCV80777		
Actibacterium pelagium JN33	Actibacterium_pelagium	GCA_002285415.1	WP_095593921		
Aestuariivita boseongensis BS-B2	Aestuariivita_boseongensis	GCA_001262635.1	WP_050931493	WP_050928652	
Albidovulum inexpectatum DSM 12048	Albidovulum_inexpectatum	GCA_002927635.1	PPB79601		
Albimonas pacifica CGMCC 1.11030	Albimonas_pacifica	GCA_900113695.1	SFI00853		
Amylibacter kogurei strain 4G11	Amylibacter_kogurei	GCA_002742285.1	PIB25196	PIB23191	
Brevundimonas diminuta ATCC(B) 19146	Brevundimonas_diminuta	GCA_004102925.1	WP_076224664		WP_003164449
Brevundimonas vesicularis FDAARGOS_289	Brevundimonas_vesicularis	GCA_002208825.2	WP_055754901		ASE40561
Caulobacter vibrioides NA 1000	Caulobacter_vibrioides	GCA_000022005.1	YP_002515910		YP_002517920
Celeribacter baekdonensis DSM 27375	Celeribacter_baekdonensis	GCA_900102315.1	WP_066707218	SDF70266	
Celeribacter ethanolicus NH195	Celeribacter_ethanolicus	GCA_001550095.1	SFK27297	WP_066707909	
Celeribacter manganoxidans DY25	Pacificitalea_manganoxidans	GCA_002504165.1	ATI42951	ATI43176	
Celeribacter neptunius DSM 26471	Celeribacter_neptunius	GCA_900113955.1	PTR18330	SFK13407	
Cereibacter changlensis DSM 18774	Cereibacter_changlensis	GCA_003254335.1	ODM41211	PZX58697	

Cognatiyoonia koreensis DSM 17925	Cognatiyoonia_koreensis	GCA_900109295.1	SEW47652	SEW38493	
Cognatiyoonia sediminum DSM 28715	Cognatiyoonia_sediminum	GCA_900129845.1	SHH27645	SHH04478	
Defluviimonas alba cai42	Frigidibacter_mobilis	GCA_001620265.1	AMY67679	SMY06504	
Defluviimonas aquaemixtae CECT 8626	Defluviimonas_aquaemixtae	GCA_900302475.1	SPH25099	SPH16573	
Defluviimonas denitrificans DSM 18921	Defluviimonas_denitrificans	GCA_002973535.1	PQV55337	PQV55803	
Dinoroseobacter shibae DFL 12	Dinoroseobacter_shibae	GCA_000018145.1	ABV92018	ABV91917	
Epibacterium mobile DSM 23403	Epibacterium_mobile	GCA_900106635.1	WP_009176501		
Flavimaricola marinus CECT 8899	Flavimaricola_marinus	GCA_900184895.1	SMY06435		
Gemmobacter aquatilis DSM 3857	Gemmobacter_aquatilis	GCA_900110025.1	SEO31615		
Gemmobacter megaterium DSM 26375	Wagnerdoeblera_megaterium	GCA_900156815.1	WP_028031864		
Gemmobacter nectariphilus DSM 15620	Wagnerdoeblera_nectariphilus	GCA_000429765.1	SIS52537		
Haematobacter massiliensis CCUG 47968	Haematobacter_massiliensis	GCA_000740795.1	KFI25179		
Haematobacter missouriensis H1892	Haematobacter_missouriensis	GCA_002196895.1	OWJ74397		
Henriciella marina DSM 19595	Henriciella_marina	GCA_000376805.1	WP_018146781		WP_040500691
Hyphomonas atlantica 22II1-22F38	Hyphomonas_atlantica	GCA_000682715.1	KCZ61886		KCZ60428
Hyphomonas neptunium ATCC15444	Hyphomonas_neptunium	GCA_000013025.1	ABI76613		ABI78279
Jannaschia aquimarina GSW-M26	Jannaschia_aquimarina	GCA_000877395.1	KIT15263	KIT16437	

Jannaschia helgolandensis DSM 14858	Jannaschia_helgolandensis	GCA_900109285.1	SEL80859	SEK67075	
Jhaorihella thermophila DSM 23413	Jhaorihella_thermophila	GCA_900108275.1	SEG11334	SEF81904	
Leisingera aquimarina DSM 24565	Leisingera_aquimarina	GCA_000473165.1	WP_027257334		
Leisingera caerulea DSM 24564	Leisingera_caerulea	GCA_000473325.1	WP_027236234		
Leisingera daeponensis DSM 23529	Leisingera_daeponensis	GCA_000473145.1	WP_008557437		
Leisingera methylohalidivorans DSM 14336	Leisingera_methylohalidivorans	GCA_000511355.1	AHC99464		
Limimaricola cinnabarinus LL-001	Limimaricola_cinnabarinus	GCA_000466965.1	GAD57028		
Limimaricola hongkongensis DSM 17492	Limimaricola_hongkongensis	GCA_000600975.2	EYD73484		
Litoreibacter albidus DSM 26922	Litoreibacter_albidus	GCA_900107015.1	SDX68687	SDW66021	
Litoreibacter arenae DSM 19593	Litoreibacter_arenae	GCA_000442275.2	EPX76904	EPX77261	
Litoreibacter janthinus DSM 26921	Litoreibacter_janthinus	GCA_900111945.1	SFR65490	SFR33360	
Litoreibacter meonggei DSM 29466	Litoreibacter_meonggei	GCA_003663885.1	RLJ40761	RLJ41125	
Litorimicrobium taeanense DSM 22007	Litorimicrobium_taeanense	GCA_900110775.1	SEQ04336	SEP84051	
Loktanella atrilutea DSM 29326	Loktanella_atrilutea	GCA_900128995.1	SHF20753	SHE82228	
Loktanella fryxellensis DSM 16213	Loktanella_fryxellensis	GCA_900110065.1	SEN76788	SEM75348	
Loktanella salsilacus DSM 16199	Loktanella_salsilacus	GCA_900114485.1	SFL66905	SFL47365	
Maricaulis maris MCS10	Maricaulis_maris	GCA_000014745.1	ABI66093		ABI65568

Marinovum algicola FF3	Marinovum_algicola	GCA_900109145.1	WP_074840290	SEJ56271	
Maritimibacter alkaliphilus HTCC2654	Maritimibacter_alkaliphilus	GCA_008124775.1	EAQ13073	EAQ13089	
Maritimibacter harenae DP07	Maritimibacter_harenae	GCA_009882975.1	MZR15458	MZR13594	
Marivita cryptomonadis CL-SK44	Marivita_cryptomonadis	GCA_002115725.1	WP_085628840	WP_085627934	
Marivita geojedonensis DPG-138	Marivita_geojedonensis	GCA_002115805.1	OSQ44098	OSQ53142	
Marivita hallyeonensis DSM 29431	Marivita_hallyeonensis	GCA_900129875.1	SHI07924	SHH97511	
Monaibacterium marinum C7	Monaibacterium_marinum	GCA_900231835.1	SOH94638		
Neptunicoccus sediminis CY02	Neptunicoccus_sediminis	GCA_001719615.1	WP_083225714	WP_069298779	
Nereida ignava CECT 5292	Nereida_ignava	GCA_001049735.1	CRK76475	CRK74950	
Nioella nitratireducens SSW136	Nioella_nitratireducens	GCA_001879715.1	WP_071673921		
Oceanicella actignis CGMCC 1.10808	Oceanicella_actignis	GCA_900143155.1	SHN73248		
Oceanicola granulosus HTCC2516	Oceanicola_granulosus	GCA_000153305.1	EAR49402		
Oceanicola litoreus DSM 29440	Vannielia_litorea	GCA_900142295.1	SIO22111	SIO31853	
Oceaniovalibus guishaninsula JLT2003	Oceaniovalibus_guishaninsula	GCA_000299575.1	EKE45246		
Octadecabacter antarcticus 307	Octadecabacter_antarcticus	GCA_000155675.2	AGI69804		
Octadecabacter arcticus 238	Octadecabacter_arcticus	GCA_000155735.2	AGI70526		
Paenirhodobacter enshiensis DW2-9	Sinirhodobacter_enshiensis	GCA_000740785.1	KFI25542		

Paracoccus aminophilus JCM 7686	Paracoccus_aminophilus	GCA_000444995.1	AGT10255		
Paracoccus pantotrophus DSM 2944	Paracoccus_pantotrophus	GCA_008824185.1	QFG37979		
Paracoccus zeaxanthinifaciens ATCC 21588	Paracoccus_zeaxanthinifaciens	GCA_000420145.1	WP_022705690		
Pararhodobacter aggregans D1-19	Pararhodobacter_aggregans	GCA_003075525.1	PVE46209		
Pararhodobacter marinus CIC4N-9	Pararhodobacter_marinus	GCA_003122215.1	PWE27682		
Phaeobacter gallaeciensis DSM 26640	Phaeobacter_gallaeciensis	GCA_000511385.1	AHD08079		
Phaeobacter inhibens DSM 16374	Phaeobacter_inhibens	GCA_000473105.1	WP_014876024		
Planktomarina temperata RCA23	Planktomarina_temperata	GCA_000738435.1	AII88242		
Pontivivens insulae CECT 8812	Pontivivens_insulae	GCA_900302495.1	SPF27778		
Pseudodonghicola xiamenensis DSM 18339	Donghicola_xiamenensis	GCA_000429365.1	WP_028094067	WP_028092610	
Pseudooceanicola batsensis HTCC2597	Pseudooceanicola_batsensis	GCA_000152725.1	EAQ04072	EAQ04522	
Pseudophaeobacter arcticus DSM 23566	Pseudophaeobacter_arcticus	GCA_000473205.1	WP_027238987		
Pseudorhodobacter antarcticus CGMCC 1.10836	Pseudorhodobacter_antarcticus	GCA_900110135.1	SEN21862		
Pseudorhodobacter aquimaris KCTC 23043	Pseudorhodobacter_aquimaris	GCA_001202025.1	WP_050526161		
Pseudorhodobacter ferrugineus DSM 5888	Pseudorhodobacter_ferrugineus	GCA_000420745.1	WP_022705587		
Pseudoruegeria haliotis DSM 29328	Aliiruegeria_haliotis	GCA_003003255.1	PRY21164	PRY21154	

Pseudoruegeria lutimaris DSM 25294	Aliiruegeria_lutimaris	GCA_900099935.1	SDL19643	SDI72855	
Pseudoruegeria marinistellae SF-16	Pseudoruegeria_marinistellae	GCA_001509585.1	WP_068117056	WP_068118168	
Puniceibacterium sediminis DSM 29052	Puniceibacterium_sediminis	GCA_900188035.1	SNR33780	SNR78869	
Rhodobaca barguzinensis alga05	R_bogoriensis_barguzinensis	GCA_001870665.2	ATX65164		
Rhodobacter aestuarii DSM 19945	Rhodobacter_aestuarii	GCA_900156655.1	SIT14655		
Rhodobacter azotoformans KA25	Cereibacter_azotoformans	GCA_003050905.1	WP_107664828	PTR20745	
Rhodobacter blasticus DSM 2131	Fuscovulum_blasticum	GCA_003034965.1	PTE12759	AMY67619	
Rhodobacter capsulatus DSM 1710	Rhodobacter_capsulatus	GCA_003254295.1	WP_055209135		
Rhodobacter johrii JA192	Cereibacter_johrii	GCA_003046325.1	SNX68436	ODM43394	
Rhodobacter maris JA276	Rhodobacter_maris	GCA_900217815.1	SOB94876		
Rhodobacter megalophilus DSM 18937	C_sphaeroides_megalophilum	GCA_900188265.1	SDG50138	SNS57577	
Rhodobacter ovatus JA234	Cereibacter_ovatus	GCA_900207575.1	ABA77855	SNX72866	
Rhodobacter sphaeroides 2.4.1	Cereibacter_sphaeroides_2.4.1	GCA_003324715.1	SNT06771	ABA80052	
Rhodobacter sphaeroides WS8N	Cereibacter_sphaeroides_WS8N	GCA_000212605.1	*EGJ23160*	EGJ22365	
Rhodobacter veldkampii DSM 11550	Phaeovulum_veldkampii	GCA_004363195.1	MBK5946872		
Rhodobacter vinaykumarii JA123	Phaeovulum_vinaykumarii	GCA_900217755.1	SOC01150		
Rhodobacter viridis JA737	Rhodobacter_viridis	GCA_003217355.1	PYF10957		

Rhodovulum imhoffii DSM 18064	Rhodovulum_imhoffii	GCA_003046545.1	MBK5934866		
Rhodovulum robiginosum DSM 12329	Rhodovulum_robiginosum	GCA_003944755.1	RSK40797		
Rhodovulum sulfidophilum DSM 1374	Rhodovulum_sulfidophilum	GCA_001633165.1	ANB32827		
Roseibaca calidilacus HL-91	Roseibaca_calidilacus	GCA_001517585.1	CUX79508		
Roseibaca ekhonensis CECT 7235	Roseibaca_ekhonensis	GCA_900499075.1	SUZ33085		
Roseibacterium elongatum DSM 19469	Roseibacterium_elongatum	GCA_000590925.1	AHM03926		
Roseicitreum antarcticum CGMCC 1.8894	Roseicitreum_antarcticum	GCA_014681765.1	SDX78784		
Roseicyclus mahoneyensis DSM 16097	Roseicyclus_mahoneyensis	GCA_003148775.1	PWK59086		
Roseobacter denitrificans OCh 114 DSM 7001	Roseobacter_denitrificans	GCA_900113215.1	ABG33465	ABG30975	
Roseobacter litoralis Och 149	Roseobacter_litoralis	GCA_000154785.2	AEI92452	AEI95393	
Roseovarius aestuarii CECT 7745	Roseovarius_aestuarii	GCA_900172285.1	SMC13673	SMC10772	
Roseovarius albus CECT 7450	Roseovarius_albus	GCA_900172335.1	SLN32545		
Roseovarius atlanticus R12B	Roseovarius_atlanticus	GCA_001441615.1	KRS10392	KRS14116	
Roseovarius marisflavi DSM 29327	Roseovarius_marisflavi	GCA_900142625.1	SHL62188	SHL07066	
Roseovarius mucosus DSM 17069	Roseovarius_mucosus	GCA_000768555.3	KGM88858		
Ruegeria atlantica CECT 4292	Ruegeria_atlantica	GCA_001458195.1	CUH50561	CUH49563	
Ruegeria conchae TW15	Ruegeria_conchae	GCA_000192475.2	RLK07784	RLK08113	

Ruegeria halocynthiae DSM 27839	Ruegeria_halocynthiae	GCA_900106805.1	SDX50253	SDX57655	
Ruegeria pomeroyi DSS-3	Ruegeria_pomeroyi	GCA_000011965.2	AAV96732	AAV96458	
Ruegeria sp. TM1040	Epibacterium_TM1040	GCA_000014065.1	*ABF62968*		
Sagittula stellata E-37	Sagittula_stellata	GCA_000169415.1	EBA06220	EBA10546	
Salinihabitans flavidus DSM 27842	Salinihabitans_flavidus	GCA_900110425.1	SEO74159	SEP07844	
Salipiger marinus DSM 26424	Salipiger_marinus	GCA_900100085.1	SDJ50631	SDI13184	
Salipiger mucosus DSM 16094	Salipiger_mucosus	GCA_000442255.1	EPX86859	EPX87036	
Salipiger thiooxidans DSM 10146	Salipiger_thiooxidans	GCA_900102075.1	SDF60425	SDF14621	
Sedimentitalea nanhaiensis DSM 24252	Sedimentitalea_nanhaiensis	GCA_000473225.1	SFU18154	SFT33342	
Sediminimonas qiaohouensis DSM 21189	Sediminimonas_qiaohouensis	GCA_000423645.1	WP_026759055	MTJ05468	
Shimia abyssi DSM 100673	Shimia_abyssi	GCA_003014475.1	PSL14268	PSL17838	
Shimia aestuarii DSM 15283	Shimia_aestuarii	GCA_900114635.1	SFM75650	SFL67127	
Sulfitobacter indolifex HEL-45	Sulfitobacter_indolifex	GCA_000172095.1	EDQ06754		
Sulfitobacter pseudonitzschiae H3	Pseudosulfitobacter_pseudonitzsc	GCA_000712315.1	KEJ93792	KEJ95091	
Tabrizicola aquatica RCRI19	Tabrizicola_aquatica	GCA_002900975.1	WP_103259205		
Thalassobacter stenotrophicus CECT 5294	Thalassobacter_stenotrophicus	GCA_001458315.1	CUH59300	CUH61837	
Thalassobius autumnalis CECT 5118	Thalassobius_autumnalis	GCA_001458255.1	CUH64467		

Thalassobius gelatinovorus CECT 4357	Thalassobius_gelatinovorus	GCA_001458355.1	CUH65788		
Thalassobius mediterraneus CECT 5383	Thalassobius_mediterraneus	GCA_001458435.1	CUH83498		QYJ00542
Thalassococcus halodurans DSM 26915	Thalassococcus_halodurans	GCA_900108225.1	SEG52122	SEF72868	
Thioclava atlantica 13D2W-2	Thioclava_atlantica	GCA_000737065.1	KFE33472		
Thioclava electrotropha Elox9	Thioclava_electrotropha	GCA_002085925.2	QPZ92658		
Thioclava pacifica DSM 10166	Thioclava_pacifica	GCA_000714535.1	KEO54608		
Tropicibacter naphthalenivorans DSM 19561	Tropicibacter_naphthalenivorans	GCA_900176475.1	SMD10375	SMC79686	
Tropicibacter phthalicicus CECT 8649	Tropicibacter_phthalicicus	GCA_900184825.1	SMX29721	SMX26862	
Tropicimonas sediminicola DSM 29339	Tropicimonas_sediminicola	GCA_900188335.1	SNT38898	SNS88829	
Wenxinia marina DSM 24838	Wenxinia_marina	GCA_000836695.1	KIQ67536	KIQ68055	
Wenxinia saemankumensis DSM 100565	Wenxinia_saemankumensis	GCA_900141735.1	SHI56608	SHI84376	
Yoonia litorea DSM 29433	Yoonia_litorea	GCA_900114675.1	SFS22108	SFS21443	
Yoonia maricola DSM 29128	Yoonia_maricola	GCA_002797915.1	PJI85399	PJI92990	
Yoonia sediminilitoris DSM 29955	Yoonia_sediminilitoris	GCA_003058085.1	PUB11492	PUB14161	
Yoonia vestfoldensis DSM 16212	Yoonia_vestfoldensis	GCA_000382265.1	WP_019956812	ART99670	

Anexo 2. Análisis de la region intergénica río arriba de osp. (A) Las cajas rojas indican el mejor motive encontrado por MEME con el consenso TTAACCHTTYGTTAA con su respectivo valor-e. (B) Resultados de MEME mostrando la distancia entre el motivo y el ATG de *osp*.

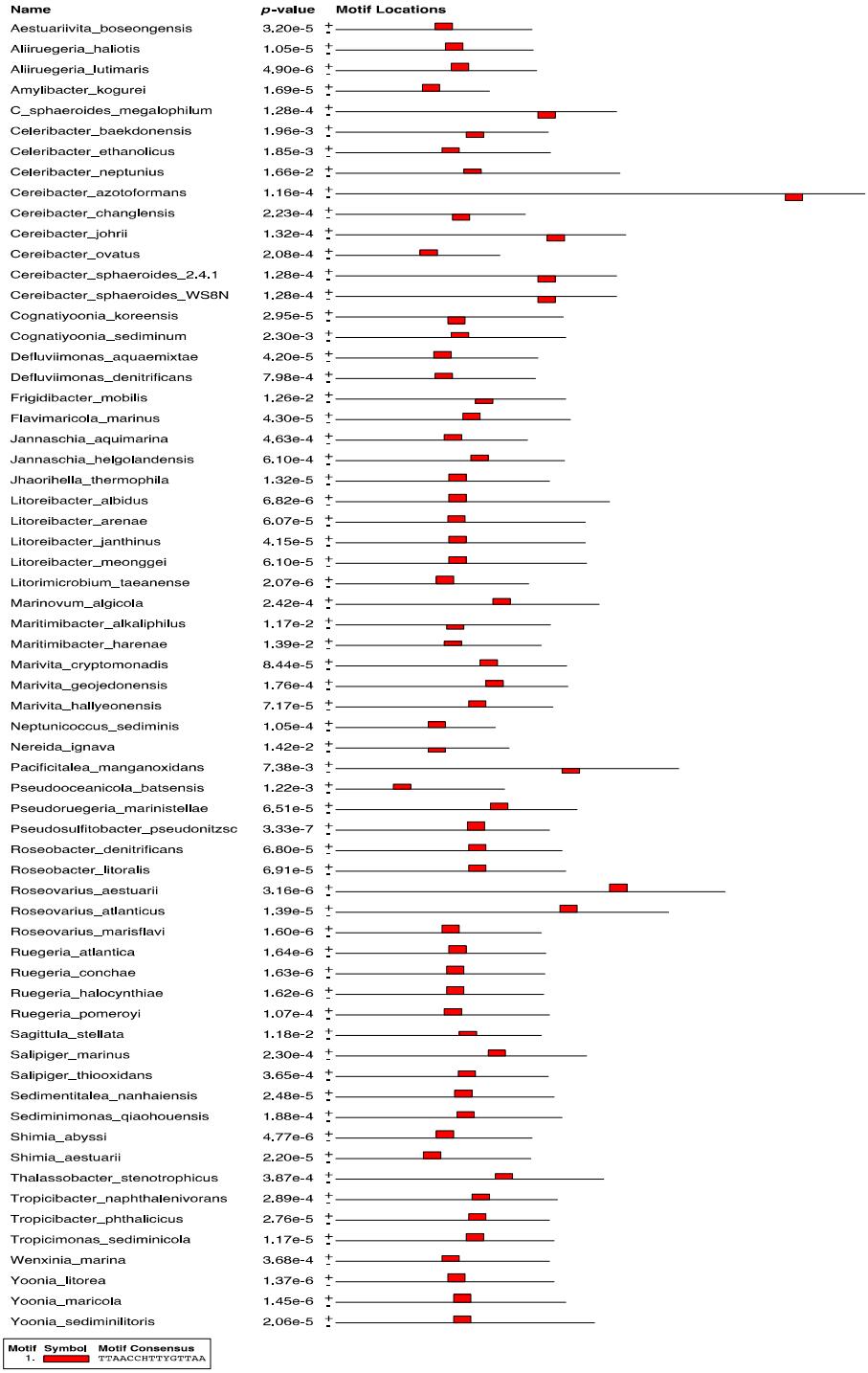

B

Motif TTAACCHTTYGTTAA MEME-1 block diagrams

SEQUENCE NAME	POSITION P-VALUE	MOTIF DIAGRAM
Pseudosulfitobacter_pseu	9.7e-10	114_[+1]_56
Yoonia_maricola	3.9e-09	102_[+1]_82
Yoonia_litorea	3.9e-09	97_[+1]_77
Ruegeria_halocynthiae	4.9e-09	96_[+1]_69
Ruegeria_conchae	4.9e-09	96_[+1]_70
Ruegeria_atlantica	4.9e-09	98_[+1]_69
Roseovarius_marisflavi	4.9e-09	92_[+1]_71
Roseovarius_aestuarii	4.9e-09	237_[+1]_85
Litorimicrobium_taeanens	6.8e-09	87_[+1]_65
Shimia_abyssi	1.5e-08	87_[+1]_68
Litoreibacter_albidus	1.5e-08	98_[+1]_124
Aliiruegeria_lutimaris	1.5e-08	100_[+1]_59
Roseovarius_atlanticus	2.5e-08	194_[+1]_79
Tropicimonas_sediminicol	3.3e-08	113_[+1]_61
Aliiruegeria_haliotis	3.3e-08	95_[+1]_61
Jhaorihella_thermophila	3.9e-08	98_[+1]_72
Yoonia_sediminilitoris	4.9e-08	102_[+1]_107
Shimia_aestuarii	7.1e-08	76_[+1]_78
Sedimentitalea_nanhaiens	7.1e-08	103_[+1]_71
Amylibacter_kogurei	7.1e-08	75_[+1]_43
Tropicibacter_phthalicic	8.1e-08	115_[+1]_55
Cognatiyoonia_koreensis	8.1e-08	97_[-1]_85
Litoreibacter_janthinus	1e-07	98_[+1]_103
Aestuariivita_boseongens	1e-07	86_[+1]_69
Flavimaricola_marinus	1.1e-07	110_[+1]_78
Defluviimonas_aquaemixta	1.3e-07	85_[+1]_75
Cereibacter_azotoformans	1.3e-07	389_[-1]_54
Litoreibacter_meonggei	1.5e-07	98_[+1]_104
Litoreibacter_arenae	1.5e-07	97_[+1]_104
Pseudoruegeria_mariniste	1.7e-07	134_[+1]_60
Roseobacter_litoralis	1.9e-07	115_[+1]_69
Roseobacter_denitrifican	1.9e-07	115_[+1]_66
Marivita_hallyeonensis	2.1e-07	115_[+1]_58
Marivita_cryptomonadis	2.3e-07	125_[+1]_60
Cereibacter_sphaeroides_	2.8e-07	175_[-1]_53
Cereibacter_sphaeroides_	2.8e-07	175_[-1]_53
Cereibacter_johrii	2.8e-07	183_[-1]_53
C_sphaeroides_megalophil	2.8e-07	175_[-1]_53
Ruegeria_pomeroyi	3.1e-07	94_[+1]_76
Neptunicoccus_sediminis	4.3e-07	80_[+1]_43
Marivita_geojedonensis	4.7e-07	130_[+1]_56
Sediminimonas_qiaohouens	5.2e-07	105_[+1]_76
Salipiger_marinus	5.7e-07	132_[+1]_70

Marinovum_algicola	5.7e-07	136_[+1]_77
Cereibacter_changlensis	7.4e-07	101_[-1]_48
Tropicibacter_naphthalen	8.1e-07	118_[+1]_59
Cereibacter_ovatus	8.1e-07	73_[+1]_54
Thalassobacter_stenotrop	8.9e-07	138_[+1]_79
Wenxinia_marina	1.1e-06	92_[+1]_78
Salipiger_thiooxidans	1.1e-06	106_[+1]_63
Jannaschia_aquimarina	1.5e-06	94_[+1]_57
Jannaschia_helgolandensi	1.7e-06	117_[+1]_66
Defluviimonas_denitrific	2.5e-06	86_[+1]_72
Pseudooceanicola_batsens	4.6e-06	50_[+1]_81
Celeribacter_ethanolicus	5.4e-06	92_[+1]_79
Celeribacter_baekdonensi	5.8e-06	113_[-1]_56
Cognatiyoonia_sediminum	6.2e-06	100_[+1]_84
Pacificitalea_manganoxid	1.3e-05	196_[-1]_86
Maritimibacter_alkaliphi	3.4e-05	96_[-1]_75
Frigidibacter_mobilis	3.4e-05	121_[-1]_63
Sagittula_stellata	3.6e-05	107_[+1]_56
Celeribacter_neptunius	3.6e-05	111_[+1]_120
Maritimibacter_harenae	4.3e-05	94_[+1]_69
Nereida_ignava	5.3e-05	80_[-1]_55

Bibliografía

1. Stock, A. M., Robinson, V. L. & Goudreau, P. N. Two-component signal transduction. *Annu. Rev. Biochem.* **69**, 183–215 (2000).
2. Welch, M., Oosawa, K., Aizawa, S. I. & Eisenbach, M. Effects of phosphorylation, Mg2+, and conformation of the chemotaxis protein CheY on its binding to the flagellar switch protein FliM. *Biochemistry* **33**, 10470–10476 (1994).
3. Welch, M., Oosawa, K., Aizawa, S. & Eisenbach, M. Phosphorylation-dependent binding of a signal molecule to the flagellar switch of bacteria. *Proc. Natl. Acad. Sci. U. S. A.* **90**, 8787–8791 (1993).
4. Brilli, M. *et al.* The diversity and evolution of cell cycle regulation in alpha-proteobacteria: a comparative genomic analysis. *BMC Syst. Biol.* **4**, 52 (2010).
5. Mann, T. H., Seth Childers, W., Blair, J. A., Eckart, M. R. & Shapiro, L. A cell cycle kinase with tandem sensory PAS domains integrates cell fate cues. *Nat. Commun.* **7**, 11454 (2016).
6. Biondi, E. G. *et al.* Regulation of the bacterial cell cycle by an integrated genetic circuit. *Nature* **444**, 899–904 (2006).
7. Reisenauer, A., Quon, K. & Shapiro, L. The CtrA Response Regulator Mediates Temporal Control of Gene Expression during the *Caulobacter* Cell Cycle. *J. Bacteriol.* **181**, 2430–2439 (1999).
8. Hernández-Valle, J., Sanchez-Flores, A., Poggio, S., Dreyfus, G. & Camarena, L. The CtrA Regulon of *Rhodobacter sphaeroides* Favors Adaptation to a Particular Lifestyle. *J. Bacteriol.* **202**, e00678-19 (2020).
9. Mercer, R. G. *et al.* Regulatory systems controlling motility and gene transfer agent production and release in *Rhodobacter capsulatus*. *FEMS Microbiol. Lett.* **331**, 53–62 (2012).

10. Kim, J., Heindl, J. E. & Fuqua, C. Coordination of Division and Development Influences Complex Multicellular Behavior in *Agrobacterium tumefaciens*. *PLOS ONE* **8**, e56682 (2013).

11. Bird, T. H. & MacKrell, A. A CtrA homolog affects swarming motility and encystment in *Rhodospirillum centenum*. *Arch. Microbiol.* **193**, 451–459 (2011).

12. Cheng, Z., Miura, K., Popov, V. L., Kumagai, Y. & Rikihisa, Y. Insights into the CtrA regulon in development of stress resistance in obligatory intracellular pathogen *Ehrlichia chaffeensis*. *Mol. Microbiol.* **82**, 1217–1234 (2011).

13. Greene, S. E., Brilli, M., Biondi, E. G. & Komeili, A. Analysis of the CtrA pathway in *Magnetospirillum* reveals an ancestral role in motility in alphaproteobacteria. *J. Bacteriol.* **194**, 2973–2986 (2012).

14. Barnett, M. J., Hung, D. Y., Reisenauer, A., Shapiro, L. & Long, S. R. A Homolog of the CtrA Cell Cycle Regulator Is Present and Essential in *Sinorhizobium meliloti. J. Bacteriol.* **183**, 3204–3210 (2001).

15. Hecht, G. B., Lane, T., Ohta, N., Sommer, J. M. & Newton, A. An essential single domain response regulator required for normal cell division and differentiation in *Caulobacter crescentus*. *EMBO J.* **14**, 3915–3924 (1995).

16. Koppenhöfer, S. *et al.* Integrated Transcriptional Regulatory Network of Quorum Sensing, Replication Control, and SOS Response in *Dinoroseobacter shibae*. *Front. Microbiol.* **10**, 803 (2019).

17. Quon, K. C., Marczynski, G. T. & Shapiro, L. Cell Cycle Control by an Essential Bacterial Two-Component Signal Transduction Protein. *Cell* **84**, 83–93 (1996).

18. Jacobs, C., Domian, I. J., Maddock, J. R. & Shapiro, L. Cell cycle-dependent polar localization of an essential bacterial histidine kinase that controls DNA replication and cell division. *Cell* **97**, 111–120 (1999).

19. Quon, K. C., Yang, B., Domian, I. J., Shapiro, L. & Marczynski, G. T. Negative control of bacterial DNA replication by a cell cycle regulatory protein that binds at the chromosome origin. *Proc. Natl. Acad. Sci.* **95**, 120–125 (1998).

20. Sommer, J. M. & Newton, A. Turning off flagellum rotation requires the pleiotropic gene pleD: pleA, pleC, and pleD define two morphogenic pathways in *Caulobacter crescentus*. *J. Bacteriol.* **171**, 392–401 (1989).

21. Ohta, N., Lane, T., Ninfa, E. G., Sommer, J. M. & Newton, A. A histidine protein kinase homologue required for regulation of bacterial cell division and differentiation. *Proc. Natl. Acad. Sci. U. S. A.* **89**, 10297–10301 (1992).

22. Childers, W. S. *et al.* Cell Fate Regulation Governed by a Repurposed Bacterial Histidine Kinase. *PLoS Biol.* **12**, (2014).

23. Iniesta, A. A., Hillson, N. J. & Shapiro, L. Cell pole-specific activation of a critical bacterial cell cycle kinase. *Proc. Natl. Acad. Sci. U. S. A.* **107**, 7012–7017 (2010).

24. Ohta, N. & Newton, A. The core dimerization domains of histidine kinases contain recognition specificity for the cognate response regulator. *J. Bacteriol.* **185**, 4424–4431 (2003).

25. Tsokos, C. G., Perchuk, B. S. & Laub, M. T. A dynamic complex of signaling proteins uses polar localization to regulate cell-fate asymmetry in *Caulobacter crescentus. Dev. Cell* **20**, 329–341 (2011).

26. Reisinger, S. J., Huntwork, S., Viollier, P. H. & Ryan, K. R. DivL performs critical cell cycle functions in *Caulobacter crescentus* independent of kinase activity. *J. Bacteriol.* **189**, 8308–8320 (2007).

27. Pierce, D. L. *et al.* Mutations in DivL and CckA rescue a divJ null mutant of *Caulobacter crescentus* by reducing the activity of CtrA. *J. Bacteriol.* **188**, 2473–2482 (2006).

28. Angelastro, P. S., Sliusarenko, O. & Jacobs-Wagner, C. Polar localization of the CckA histidine kinase and cell cycle periodicity of the essential master regulator CtrA in *Caulobacter crescentus*. *J. Bacteriol.* **192**, 539–552 (2010).

29. Christensen, S. & Serbus, L. R. Comparative analysis of wolbachia genomes reveals streamlining and divergence of minimalist two-component systems. *G3 Bethesda Md* **5**, 983–996 (2015).

30. Westbye, A. B. *et al.* The Protease ClpXP and the PAS Domain Protein DivL Regulate CtrA and Gene Transfer Agent Production in *Rhodobacter capsulatus*. *Appl. Environ. Microbiol.* **84**, e00275-18 (2018).

31. Wu, J., Ohta, N. & Newton, A. An essential, multicomponent signal transduction pathway required for cell cycle regulation in *Caulobacter*. *Proc. Natl. Acad. Sci. U. S. A.* **95**, 1443–1448 (1998).

32. Lam, H., Matroule, J.-Y. & Jacobs-Wagner, C. The Asymmetric Spatial Distribution of Bacterial Signal Transduction Proteins Coordinates Cell Cycle Events. *Dev. Cell* **5**, 149–159 (2003).

33. Lawler, M. L., Larson, D. E., Hinz, A. J., Klein, D. & Brun, Y. V. Dissection of functional domains of the polar localization factor PodJ in *Caulobacter crescentus. Mol. Microbiol.* **59**, 301–316 (2006).

34. Paul, R. *et al.* Allosteric Regulation of Histidine Kinases by Their Cognate Response Regulator Determines Cell Fate. *Cell* **133**, 928 (2008).

35. Subramanian, K., Paul, M. R. & Tyson, J. J. Potential role of a bistable histidine kinase switch in the asymmetric division cycle of *Caulobacter crescentus. PLoS Comput. Biol.* **9**, e1003221 (2013).

36. Chen, Y. E., Tsokos, C. G., Biondi, E. G., Perchuk, B. S. & Laub, M. T. Dynamics of two Phosphorelays controlling cell cycle progression in *Caulobacter crescentus*. *J. Bacteriol.* **191**, 7417–7429 (2009).

37. Schallies, K. B., Sadowski, C., Meng, J., Chien, P. & Gibson, K. E. *Sinorhizobium meliloti* CtrA Stability Is Regulated in a CbrA-Dependent Manner That Is Influenced by CpdR1. *J. Bacteriol.* **197**, 2139–2149 (2015).

38. Hallez, R. *et al.* The asymmetric distribution of the essential histidine kinase PdhS indicates a differentiation event in *Brucella abortus*. *EMBO J.* **26**, 1444–1455 (2007).

39. Abel, S. *et al.* Regulatory cohesion of cell cycle and cell differentiation through interlinked phosphorylation and second messenger networks. *Mol. Cell* **43**, 550–560 (2011).

40. Aldridge, P., Paul, R., Goymer, P., Rainey, P. & Jenal, U. Role of the GGDEF regulator PleD in polar development of *Caulobacter crescentus. Mol. Microbiol.* **47**, 1695–1708 (2003).

41. Lori, C. *et al.* Cyclic di-GMP acts as a cell cycle oscillator to drive chromosome replication. *Nature* **523**, 236–239 (2015).

42. Rood, K. L., Clark, N. E., Stoddard, P. R. & Garman, S. C. Adaptor-Dependent Degradation of a Cell-Cycle Regulator Uses a Unique Substrate Architecture. **20**, 1223–1232 (2013).

43. Domian, I. J., Quon, K. C. & Shapiro, L. Cell-type specific phosphorylation and proteolysis of a transcriptional regulator controls the G1 to S transition in a bacterial cell cycle. *Cell* **90**, 415–424 (1997).

44. Jacobs, C., Ausmees, N., Cordwell, S. J., Shapiro, L. & Laub, M. T. Functions of the CckA histidine kinase in Caulobacter cell cycle control. *Mol. Microbiol.* **47**, 1279–1290 (2003).

45. Smith, S. C. *et al.* Cell cycle-dependent adaptor complex for ClpXP-mediated proteolysis directly integrates phosphorylation and second messenger signals. *Proc. Natl. Acad. Sci.* **111**, 14229–14234 (2014).

46. Jenal, U. & Fuchs, T. An essential protease involved in bacterial cell-cycle control. *EMBO J.* **17**, 5658–5669 (1998).

47. Blair, J. A. *et al.* Branched signal wiring of an essential bacterial cell-cycle phosphotransfer protein. *Struct. Lond. Engl. 1993* **21**, 1590–1601 (2013).

48. Iniesta, A. a, McGrath, P. T., Reisenauer, A., McAdams, H. H. & Shapiro, L. A phospho-signaling pathway controls the localization and activity of a protease complex critical for bacterial cell cycle progression. *Proc. Natl. Acad. Sci. U. S. A.* **103**, 10935–10940 (2006).

49. Bhat, N. H., Vass, R. H., Stoddard, P. R., Shin, D. K. & Chien, P. Identification of ClpP substrates in *Caulobacter crescentus* reveals a role for regulated proteolysis in bacterial development. *Mol. Microbiol.* **88**, 1083–1092 (2013).

50. Folcher, M., Nicollier, M., Schwede, T., Amiot, N. & Duerig, A. Second messenger-mediated spatiotemporal control of protein degradation regulates bacterial cell cycle progression. *Gene Dev.* **23**, 93–104 (2009).

51. Ozaki, S. *et al.* Activation and polar sequestration of PopA, a c-di-GMP effector protein involved in *Caulobacter crescentus* cell cycle control. *Mol. Microbiol.* **94**, 580–594 (2014).

52. Joshi, K. K., Bergé, M., Radhakrishnan, S. K., Viollier, P. H. & Chien, P. An Adaptor Hierarchy Regulates Proteolysis during a Bacterial Cell Cycle. *Cell* **163**, 419–431 (2015).

53. Mackenzie, C. *et al.* The home stretch, a first analysis of the nearly completed genome of *Rhodobacter sphaeroides 2.4.1. Photosynth. Res.* **70**, 19–41 (2001).

54. Poggio, S. *et al.* A Complete Set of Flagellar Genes Acquired by Horizontal Transfer Coexists with the Endogenous Flagellar System in *Rhodobacter sphaeroides*. *J. Bacteriol.* **189**, 3208–3216 (2007).

55. Poggio, S., Osorio, A., Dreyfus, G. & Camarena, L. The flagellar hierarchy of *Rhodobacter sphaeroide*s is controlled by the concerted action of two enhancer-binding proteins. *Mol. Microbiol.* **58**, 969–983 (2005).

56. Vega-Baray, B. *et al.* The flagellar set Fla2 in *Rhodobacter sphaeroides* is controlled by the CckA pathway and is repressed by organic acids and the expression of Fla1. *J. Bacteriol.* **197**, 833–847 (2015).

57. Hernandez-Valle, J. *et al.* The Master Regulators of the Fla1 and Fla2 Flagella of *Rhodobacter sphaeroides* Control the Expression of Their Cognate CheY Proteins. *J. Bacteriol.* **199**, e00670-16 (2017).

58. Poggio, S., Osorio, A., Dreyfus, G. & Camarena, L. The flagellar hierarchy of *Rhodobacter sphaeroides* is controlled by the concerted action of two enhancer-binding proteins. *Mol. Microbiol.* **58**, 969–983 (2005).

59. Oh, J.-I., Ko, I.-J. & Kaplan, S. 2003. Digging deeper: uncovering genetic loci which modulate photosynthesis gene expression in *Rhodobacter sphaeroides 2.4.1*. *Microbiology* **149**, 949–960.

60. Bourret, R. B. Receiver domain structure and function in response regulator proteins. *Curr. Opin. Microbiol.* **13**, 142–149 (2010).

61. Gao, R., Bouillet, S. & Stock, A. M. Structural Basis of Response Regulator Function. *Annu. Rev. Microbiol.* **73**, 175–197 (2019).

62. Janausch, I. G., Garcia-Moreno, I., Lehnen, D., Zeuner, Y. & Unden, G. 2004. Phosphorylation and DNA binding of the regulator DcuR of the fumarate-responsive two-component system DcuSR of Escherichia coli. *Microbiology* **150**, 877–883.

63. Plate, L. & Marletta, M. A. Nitric Oxide Modulates Bacterial Biofilm Formation through a Multicomponent Cyclic-di-GMP Signaling Network. *Mol. Cell* **46**, 449–460 (2012).

64. Hernández-Eligio, A., Andrade, Á., Soto, L., Morett, E. & Juárez, K. The unphosphorylated form of the PilR two-component system regulates pilA gene expression in *Geobacter sulfurreducens*. *Environ. Sci. Pollut. Res.* **24**, 25693–25701 (2017).

65. Waterhouse, A. *et al.* SWISS-MODEL: homology modelling of protein structures and complexes. *Nucleic Acids Res.* **46**, W296–W303 (2018).

66. Buchan, D. W. A. & Jones, D. T. The PSIPRED Protein Analysis Workbench: 20 years on. *Nucleic Acids Res.* **47**, W402–W407 (2019).

67. Laub, M. T., Chen, S. L., Shapiro, L. & McAdams, H. H. Genes directly controlled by CtrA, a master regulator of the Caulobacter cell cycle. *Proc. Natl. Acad. Sci.* **99**, 4632–4637 (2002).

68. Ouimet, M.-C. & Marczynski, G. T. Analysis of a cell-cycle promoter bound by a response regulator11Edited by M. Yaniv. *J. Mol. Biol.* **302**, 761–775 (2000).

69. Liang, K. Y. H., Orata, F. D., Boucher, Y. F. & Case, R. J. Roseobacters in a Sea of Poly- and Paraphyly: Whole Genome-Based Taxonomy of the Family Rhodobacteraceae and the Proposal for the Split of the 'Roseobacter Clade' Into a Novel Family, Roseobacteraceae fam. nov. *Front. Microbiol.* **12**, 683109 (2021).

70. Zhou, B. *et al.* The Global Regulatory Architecture of Transcription during the Caulobacter Cell Cycle. *PLOS Genet.* **11**, e1004831 (2015).

71. Smith, S. C. *et al.* Cell cycle-dependent adaptor complex for ClpXP-mediated proteolysis directly integrates phosphorylation and second messenger signals. *Proc. Natl. Acad. Sci. U. S. A.* **111**, 14229–14234 (2014).

72. James, P., Halladay, J. & Craig, E. A. Genomic Libraries and a Host Strain Designed for Highly Efficient Two-Hybrid Selection in Yeast. *Genetics* **144**, 1425–1436 (1996).

73. Hsieh, Y.-J. & Wanner, B. L. Global regulation by the seven-component Pi signaling system. *Curr. Opin. Microbiol.* **13**, 198–203 (2010).

74. Sánchez-Ortiz, V. J., Domenzain, C., Poggio, S., Dreyfus, G. & Camarena, L. 2021. The periplasmic component of the DctPQM TRAP-transporter is part of the DctS/DctR sensory pathway in *Rhodobacter sphaeroides*. *Microbiology* **167**, 001037.

75. Brilli, M. *et al.* The diversity and evolution of cell cycle regulation in alpha-proteobacteria: a comparative genomic analysis. *BMC Syst. Biol.* **4**, 52 (2010).

76. Pioszak, A. A., Jiang, P. & Ninfa, A. J. The Escherichia coli PII Signal Transduction Protein Regulates the Activities of the Two-Component System Transmitter Protein NRII by Direct Interaction with the Kinase Domain of the Transmitter Module. *Biochemistry* **39**, 13450–13461 (2000).

77. Jiang, P. & Ninfa, A. J. Regulation of Autophosphorylation of *Escherichia coli* Nitrogen Regulator II by the PII Signal Transduction Protein. *J. Bacteriol.* **181**, 1906–1911 (1999).

78. Burkholder, W. F., Kurtser, I. & Grossman, A. D. Replication Initiation Proteins Regulate a Developmental Checkpoint in Bacillus subtilis. *Cell* **104**, 269–279 (2001).

79. Wang, L., Grau, R., Perego, M. & Hoch, J. A. A novel histidine kinase inhibitor regulating development inBacillus subtilis. *Genes Dev.* **11**, 2569–2579 (1997).

80. Martínez-Argudo, I., Salinas, P., Maldonado, R. & Contreras, A. Domain Interactions on the ntr Signal Transduction Pathway: Two-Hybrid Analysis of Mutant and Truncated Derivatives of Histidine Kinase NtrB. *J. Bacteriol.* **184**, 200–206 (2002).

81. Cunningham, K. A. & Burkholder, W. F. The histidine kinase inhibitor Sda binds near the site of autophosphorylation and may sterically hinder autophosphorylation and phosphotransfer to Spo0F. *Mol. Microbiol.* **71**, 659–677 (2009).

82. Whitten, A. E. *et al.* The Structure of the KinA-Sda Complex Suggests an Allosteric Mechanism of Histidine Kinase Inhibition. *J. Mol. Biol.* **368**, 407–420 (2007).

83. Foussard, M. *et al.* Negative autoregulation of the *Rhizobium meliloti* fixK gene is indirect and requires a newly identified regulator, FixT. *Mol. Microbiol.* **25**, 27–37 (1997).

84. Garnerone, A.-M., Cabanes, D., Foussard, M., Boistard, P. & Batut, J. Inhibition of the FixL Sensor Kinase by the FixT Protein in *Sinorhizobium meliloti* *. *J. Biol. Chem.* **274**, 32500–32506 (1999).

85. Crosson, S., McGrath, P. T., Stephens, C., McAdams, H. H. & Shapiro, L. Conserved modular design of an oxygen sensory/signaling network with species-specific output. *Proc. Natl. Acad. Sci.* **102**, 8018–8023 (2005).

86. Stein, B. J., Fiebig, A. & Crosson, S. Feedback Control of a Two-Component Signaling System by an Fe-S-Binding Receiver Domain. *mBio* **11**, e03383-19 (2020).

87. Gottesman, S., Roche, E., Zhou, Y. & Sauer, R. T. The ClpXP and ClpAP proteases degrade proteins with carboxy-terminal peptide tails added by the SsrA-tagging system. *Genes Dev.* **12**, 1338–1347 (1998).

88. Ruvolo, M. V., Mach, K. E. & Burkholder, W. F. Proteolysis of the replication checkpoint protein Sda is necessary for the efficient initiation of sporulation after transient replication stress in *Bacillus subtilis. Mol. Microbiol.* **60**, 1490–1508 (2006).

89. Sistrom, W. R. Y. 1962. The Kinetics of the Synthesis of Photopigments in *Rhodopseudomonas spheroides*. *Microbiology* **28**, 607–616.

90. del Campo, A. M. *et al.* Chemotactic Control of the Two Flagellar Systems of *Rhodobacter sphaeroides* Is Mediated by Different Sets of CheY and FliM Proteins. *J. Bacteriol.* **189**, 8397–8401 (2007).

91. Rivera-Osorio, A., Osorio, A., Poggio, S., Dreyfus, G. & Camarena, L. Architecture of divergent flagellar promoters controlled by CtrA in *Rhodobacter sphaeroides. BMC Microbiol.* **18**, 129 (2018).

92. Lydiate, D. J., Ashby, A. M., Henderson, D. J., Kieser, H. M. & Hopwood, D. A. Y. 1989. Physical and Genetic Characterization of Chromosomal Copies of the *Streptomyces coelicolor* Mini-circle. *Microbiology* **135**, 941–955.

93. Quandt, J. & Hynes, M. F. Versatile suicide vectors which allow direct selection for gene replacement in Gram-negative bacteria. *Gene* **127**, 15–21 (1993).

94. Keen, N. T., Tamaki, S., Kobayashi, D. & Trollinger, D. Improved broad-host-range plasmids for DNA cloning in Gram-negative bacteria. *Gene* **70**, 191–197 (1988).

95. Uzzau, S., Figueroa-Bossi, N., Rubino, S. & Bossi, L. Epitope tagging of chromosomal genes in Salmonella. *Proc. Natl. Acad. Sci.* **98**, 15264–15269 (2001).

96. Mead, D. A., Szczesna-Skorupa, E. & Kemper, B. Single-stranded DNA 'blue' T7 promoter plasmids: a versatile tandem promoter system for cloning and protein engineering. *Protein Eng. Des. Sel.* **1**, 67–74 (1986).

97. Metcalf, W. W. & Wanner, B. L. Construction of new β-glucuronidase cassettes for making transcriptional fusions and their use with new methods for allele replacement. *Gene* **129**, 17–25 (1993).

98. Laemmli, U. K. Cleavage of Structural Proteins during the Assembly of the Head of Bacteriophage T4. *Nature* **227**, 680–685 (1970).

99. Langmead, B. & Salzberg, S. L. Fast gapped-read alignment with Bowtie 2. *Nat. Methods* **9**, 357–359 (2012).

100. Li, H. *et al.* The Sequence Alignment/Map format and SAMtools. *Bioinformatics* **25**, 2078–2079 (2009).

101. Danecek, P. *et al.* Twelve years of SAMtools and BCFtools. *GigaScience* **10**, giab008 (2021).

102. Jefferson, R. A., Burgess, S. M. & Hirsh, D. beta-Glucuronidase from Escherichia coli as a gene-fusion marker. *Proc. Natl. Acad. Sci.* **83**, 8447–8451 (1986).

103. Towbin, H., Staehelin, T. & Gordon, J. Electrophoretic transfer of proteins from polyacrylamide gels to nitrocellulose sheets: procedure and some applications. *Proc. Natl. Acad. Sci.* **76**, 4350–4354 (1979).

104. Wright, K. Antibodies a laboratory manual: By E Harlow and D Lane. pp 726. Cold Spring Harbor Laboratory. 1988. ISBN 0-87969-314-2. *Biochem. Educ.* **17**, 220–220 (1989).

105. Parks, D. H., Imelfort, M., Skennerton, C. T., Hugenholtz, P. & Tyson, G. W. CheckM: assessing the quality of microbial genomes recovered from isolates, single cells, and metagenomes. *Genome Res.* **25**, 1043–1055 (2015).

106. Edgar, R. C. MUSCLE: multiple sequence alignment with high accuracy and high throughput. *Nucleic Acids Res.* **32**, 1792–1797 (2004).

107. Saitou, N. & Nei, M. The neighbor-joining method: a new method for reconstructing phylogenetic trees. *Mol. Biol. Evol.* **4**, 406–425 (1987).

108. Bailey, T. L. *et al.* MEME Suite: tools for motif discovery and searching. *Nucleic Acids Res.* **37**, W202–W208 (2009).

Publicaciones

The Flagellar Set Fla2 in Rhodobacter sphaeroides Is Controlled by the CckA Pathway and Is Repressed by Organic Acids and the Expression of Fla1.

The Histidine Kinase CckA Is Directly Inhibited by a Response Regulator-like Protein in a Negative Feedback Loop.

JB
Journals.ASM.org

The Flagellar Set Fla2 in *Rhodobacter sphaeroides* Is Controlled by the CckA Pathway and Is Repressed by Organic Acids and the Expression of Fla1

Benjamín Vega-Baray,[a] Clelia Domenzain,[a] Anet Rivera,[a] Rocío Alfaro-López,[a] Elidet Gómez-César,[a] Sebastián Poggio,[a] Georges Dreyfus,[b] Laura Camarena[a]

Instituto de Investigaciones Biomédicas[a] and Instituto de Fisiología Celular,[b] Universidad Nacional Autónoma de México, Mexico City, Mexico

Rhodobacter sphaeroides **has two different sets of flagellar genes. Under the growth conditions commonly used in the laboratory, the expression of the *fla1* set is constitutive, whereas the *fla2* genes are not expressed. Phylogenetic analyses have previously shown that the *fla1* genes were acquired by horizontal transfer from a gammaproteobacterium and that the *fla2* genes are endogenous genes of this alphaproteobacterium. In this work, we characterized a set of mutants that were selected for swimming using the Fla2 flagella in the absence of the Fla1 flagellum (Fla2$^+$ strains). We determined that these strains have a single missense mutation in the histidine kinase domain of CckA. The expression of these mutant alleles in a Fla1$^-$ strain allowed *fla2*-dependent motility without selection. Motility of the Fla2$^+$ strains is also dependent on ChpT and CtrA. The mutant versions of CckA showed an increased autophosphorylation activity *in vitro*. Interestingly, we found that *cckA* is transcriptionally repressed by the presence of organic acids, suggesting that the availability of carbon sources could be a part of the signal that turns on this flagellar set. Evidence is presented showing that reactivation of *fla1* gene expression in the Fla2$^+$ background strongly reduces the number of cells with Fla2 flagella.**

More than 40 genes are involved in the biogenesis and functioning of the bacterial flagellum. This structure has three major subcomponents, the basal body, the hook, and the filament. The basal body contains the export apparatus, an inner membrane ring (MS ring), a periplasmic ring (P ring), and, depending on the species, an outer membrane ring (L ring). The basal body also includes the flagellar motor and a rod that expands from the MS ring and crosses the L and P rings. The hook is the first extracellular structure that is assembled; it connects the basal body with the flagellar filament that is formed by thousands of flagellin subunits (reviewed in references 1–3).

In most bacterial species, the expression of the flagellar genes is highly regulated and frequently follows a hierarchical order in which the late genes are expressed until the early genes, that are higher in the hierarchy, are expressed. At the top of the hierarchy, a transcriptional regulator is responsible for the expression of the genes required to assemble the early flagellar structures that are located in the cytoplasm (i.e., export apparatus), in the cytoplasmic membrane (i.e., MS ring), and, depending on the hierarchy, in the periplasm (i.e., P ring), the outer membrane (i.e., L ring), and the extracellular milieu (i.e., hook). Within this class, additional transcription factors are expressed. These proteins are required to transcribe the late genes, such as *fliC* (flagellin), *fliD* (filament cap), and *fliS* (secretion of FliC) (1–4).

Different regulatory mechanisms are known to be involved in the control of these hierarchies (4). The most common scheme of regulation consists of the use of different sigma factors to transcribe the genes in different tiers of the hierarchy. For instance, in the enteric bacteria *Escherichia coli* and *Salmonella*, at the top of the hierarchy the transcriptional activator $FlhD_4C_2$ and sigma-70 promote the expression of the early genes, whereas the late promoters are dependent on σ^{28}. In some species of *Vibrio* and *Pseudomonas*, σ^{54} and the activator protein FleQ promote the transcription of the genes required at the initial phases of flagellar biosynthesis, and σ^{28} expresses the late genes. In alphaproteobacteria, the flagellar hierarchy of *Caulobacter crescentus* is one of the best characterized. In this bacterium, σ^{70} and CtrA transcribe the genes encoding the proteins that form the export apparatus, the MS ring, and the regulators FliX and FlbD. Once the first flagellar structure is functional, FlbD becomes phosphorylated and activates $E\sigma^{54}$ to carry out transcription of the genes encoding the rod proteins, FlgH and FlgL (P and L rings, respectively), FlgE (the hook), and FliC (the filament). CtrA acts as a transcriptional activator when it is phosphorylated by the histidine kinase (HK) CckA and the histidine phosphotransferase ChpT (5–7). This signal transduction pathway is essential in *Caulobacterales* and *Rhizobiales* (8–11). In *C. crescentus*, the kinase/phosphatase activities of CckA are regulated by the histidine kinases PleC, DivJ, and DivL as well as by the response regulator DivK (12).

In contrast to *C. crescentus*, in many alphaproteobacteria the signaling pathway CckA/ChpT/CtrA is dispensable and the genes encoding PleC, DivJ, DivL, and DivK are not present in their genomes (13). For some species of this bacterial group, it has been

Received 22 October 2014 **Accepted** 9 December 2014

Accepted manuscript posted online 15 December 2014

Citation Vega-Baray B, Domenzain C, Rivera A, Alfaro-López R, Gómez-César E, Poggio S, Dreyfus G, Camarena L. 2015. The flagellar set Fla2 in *Rhodobacter sphaeroides* is controlled by the CckA pathway and is repressed by organic acids and the expression of Fla1. J Bacteriol 197:833–847. doi:10.1128/JB.02429-14.

Editor: J. S. Parkinson

Address correspondence to Laura Camarena, rosal@unam.mx.

Supplemental material for this article may be found at http://dx.doi.org/10.1128/JB.02429-14.

doi:10.1128/JB.02429-14

reported that CtrA does not control the cell cycle, but it controls directly or indirectly the expression of the flagellar genes (14–19). In this group of bacteria, there is no evidence regarding the control of the activity of CckA, but it has been reported that the expression of *cckA*, *chpT*, and/or *ctrA* is reduced in quorum sensing mutants in *Ruegeria* sp. strain KLH11, *Dinoroseobacter shibae*, and *Rhodobacter capsulatus* (16, 17, 19, 20). However, in *Ruegeria* sp. KLH11, the evidence suggests that this control is indirect (16). In addition, in *R. capsulatus* it was shown that *ctrA* transcription was increased 3-fold when the cultures were grown photoheterotrophically in minimal medium compared with cultures grown in YPS-rich medium (medium containing yeast extract, peptone, and salts); in addition, a reduction in the expression of *ctrA* was detected in phosphate-limited cultures but not in nitrogen- or carbon-limited cultures (20).

Rhodobacter sphaeroides is an alphaproteobacterium that has two different full sets of flagellar genes (21). The *fla1* set was initially characterized given that its expression is constitutive under the growth conditions commonly used in the laboratory (21–23). It has been shown that the *fla1* genes are transcribed in a four-tiered hierarchy. At the top of it, the master regulator FleQ activates σ^{54} to promote the expression of the *fleT-fliE-J* operon. FleT and FleQ together activate σ^{54} to transcribe the genes encoding the rest of the components of the rod, the export apparatus, the L, P, and H rings, and the hook. In this class, the genes encoding σ^{28} and the anti-sigma σ^{28} factor FlgM are also expressed. After completion of the hook-basal body (HBB), FlgM is exported out of the cell, and the genes that depend on σ^{28} are expressed (23, 24).

Bacterial taxis is achieved through the control of flagellar rotation by the chemotactic system. Fla1-dependent taxis responds to several stimuli, some of which are not directly sensed by the chemotactic proteins. For example, it has been observed that aerotaxis is controlled in part by the two-component system RegB-RegA (also known as PrrB and PrrA) (25). These proteins form a global system that responds to the redox state of the cell to control several metabolic processes that generate energy, i.e., photosynthesis, carbon and nitrogen fixation, aerobic and anaerobic respiration, electron transport, etc. (reviewed in reference 26). Under anaerobic growth conditions, RegB is active as a kinase and phosphorylates RegA; RegA-P activates the genes encoding the apoproteins of the light-harvesting and reaction center complexes (27–29). In the presence of oxygen, RegB is inactivated and the synthesis of these complexes and proteins is halted. The absence of RegB has a negative effect on the growth rate under photoheterotrophic conditions (30), and these mutant cells do not show the negative tactic response toward high concentrations of oxygen (25).

The presence of a second set of flagellar genes (*fla2*) in *R. sphaeroides* was discovered when the genomic sequence of this bacterium was released. At that time, no other flagellar structure different from the Fla1 flagellum had been observed (31). The functionality of the *fla2* genes was reported after the isolation of a mutant strain able to swim with the Fla2 flagella. This mutant, isolated in a *fla1* background, showed the presence of several polar flagella, and it was proficient to swim in liquid medium, like the wild-type strain (WS8N) that assembles the Fla1 single subpolar flagellum. Neither Fla1 nor Fla2 flagella enable swarming on surfaces, and it should be stressed that the wild-type strain grown under conditions commonly used in the laboratory does not express the *fla2* set (21).

Phylogenetic studies suggested that the *fla1* genes were acquired by an event of horizontal transfer probably from a gammaproteobacteria, whereas the *fla2* genes are the native flagellar genes of this species (21). This suggests that the *fla1* genes overtook the function of the native flagellar genes or that its presence allowed *R. sphaeroides* to swim under growth conditions where the native genes were repressed.

So far, it is not known what is the mechanism that keeps the *fla2* set transcriptionally inactive in the wild-type WS8N strain, and nothing is known about its possible regulation. In this work, we show evidence indicating that the CckA-ChpT-CtrA pathway is central to activate the *fla2* genes. Our results establish that in the absence of Fla1, an activating mutation in CckA is enough to promote the expression of the *fla2* genes and consequently the synthesis of the Fla2 flagella. In addition, we found that *cckA* is strongly repressed by a high concentration of organic acids, whereas a growth medium with a mixture of amino acids or a low concentration of succinic acid induces *cckA* and favors the synthesis of the Fla2 flagella. Evidence is also presented indicating that the expression of the *fla1* genes reduces the synthesis of Fla2.

MATERIALS AND METHODS

Plasmids, bacterial strains, and growth conditions. Plasmids and bacterial strains used in this work are listed in Table 1. *R. sphaeroides* WS8N (32) was grown at 30°C in Sistrom's minimal medium (33) or in Sistrom's minimal medium without succinic acid but supplemented as indicated below. Photoheterotrophic liquid cultures were grown under continuous illumination and in completely filled screw-cap tubes. Heterotrophic liquid cultures were incubated in the dark with shaking at 200 rpm. *Escherichia coli* was grown in LB medium (34) at 37°C. Swimming assays were carried out with bacteria grown in liquid medium or on swimming plates containing the indicated medium and 0.22% agar. When required, the following antibiotics were added: for *R. sphaeroides*, kanamycin (25 μg/ml), tetracycline (1 μg/ml), and spectinomycin (50 μg/ml); for *E. coli*, kanamycin (50 μg/ml), spectinomycin (50 μg/ml), and ampicillin (100 μg/ml).

Oligonucleotides. The oligonucleotides used in this work are listed in Table S1 in the supplemental material.

Isolation of mutant strains. To inactivate *cckA*, *chpT*, and *ctrA*, a suicide vector containing the target gene disrupted with an antibiotic resistance gene was used for allelic exchange.

To inactivate *cckA*, the oligonucleotides 454A and 454B were used to amplify by PCR a product of 2,460 bp containing the coding region of *cckA* (2,277 bp), as well as 110 and 73 bp from the downstream and upstream regions of the gene. This product was cloned into pCR2.1-TOPO plasmid, resulting in pTOPO_cckA; this plasmid was digested with EcoNI to remove most of the coding region of *cckA*. The digestion fragment, which included the complete vector and 792 bp from the 5′ end of *cckA* and 455 bp from the 3′ end, was purified and self-ligated to obtain pTOPO_ΔcckA. The allele Δ*cckA* in this plasmid was verified by sequencing. Δ*cckA*::Ω^{Spc} was obtained by cloning the Ω^{Spc} cassette as a 2-kb SmaI fragment into pTOPO_ΔcckA previously digested with EcoNI and end repaired with T4 DNA polymerase. The resultant plasmid was digested with XbaI and SacI, and the fragment carrying the allele Δ*cckA*::Ω^{Spc} was purified and cloned in the suicide plasmid pJQ200mp18 (35). The allele Δ*cckA*::*uidA-aadA* was obtained using the same procedure as described above, but instead of cloning the Ω^{Spc} cassette, the SmaI fragment from pWM5 (36) carrying *uidA-aadA* was used. This fragment allows the expression of the promotorless *uidA* gene creating a transcriptional fusion. The suicide plasmids carrying these alleles of *cckA* were introduced into *R. sphaeroides* by conjugation (37, 38). The double recombination events were selected as described previously (21).

Strain BV3 was obtained by cloning together two PCR products corresponding to the upstream and downstream regions of *chpT* in pTZ19R.

TABLE 1 Strains and plasmids used in this study

Strain or plasmid	Relevant characteristics	Source or reference
Rhodobacter sphaeroides strains		
EA1	AM1 derivative; Δ*fleQ*::Kan^r *cckA*$_{L391F}$ Δ*ctrA*::*aadA*	This work
EA2	WS8N derivative; Δ*ctrA*::*aadA*	This work
AM1	WS8N derivative; Δ*fleQ*::Kan^r *cckA*$_{L391F}$	43
BV1	WS8N derivative; Δ*fleQ*::Kan^r *cckA*$_{A387P}$	This work
BV2	WS8N derivative; Δ*fliF*::*aadA cckA*$_{F399C}$	This work
BV3	AM1 derivative; Δ*fleQ*::Kan^r *cckA*$_{L391F}$ Δ*chpT*::Ω^{Spc}	This work
BV4	WS8N derivative; Δ*fleQ*::Kan^r Δ*chpT*::Ω^{Spc}	This work
CB1	AM1 derivative; Δ*fleQ*::Kan^r Δ*cckA*::Ω^{Spc}	This work
CB2	WS8N derivative; Δ*cckA*::Ω^{Spc}	This work
CD1	WS8N derivative; Δ*fleQ*::Kan^r Δ*regB*::Ω^{Spc}	This work
CD2	AM1 derivative; Δ*fleQ*::Kan^r *cckA*$_{L391F}$ Δ*regB*::Ω^{Spc}	This work
LC5	WS8N derivative; Δ*fleQ*::Kan^r Δ*cckA*::Ω^{Spc}	This work
LC6	AM1 derivative; Δ*fleQ*::Kan^r Δ*cckA*::*uidA-aad*	This work
SP13	WS8N derivative; Δ*fleQ*::Kan^r	22
SP20	WS8N derivative; Δ*fliF*::*aadA*	Laboratory collection
WS8N	Wild-type strain; spontaneous Nal^r	24
Escherichia coli strains		
LMG194	Protein expression strain	Invitrogen
S17	*recA endA thi hsdR* RP4-2-Tc::Mu::Tn*7*; Tp^r Sm^r	30
TOP10	Cloning strain	Invitrogen
Plasmids		
pBAD/His	Expression vector of His$_6$-tagged proteins; Ap^r	Invitrogen
pBAD/His-cCckA	pBAD/HisB expressing His$_6$-cCckA	This work
pBAD/His-cCckA A387P	pBAD/HisB expressing His$_6$-cCckA A387P	This work
pBAD/His-cCckA L391F	pBAD/HisB expressing His$_6$-cCckA L391F	This work
pBAD/His-cCckA F399C	pBAD/HisB expressing His$_6$-cCckA F399C	This work
pBBMCS53	Transcriptional *uidA* fusion vector; Gm^r	34
pBBMCS53_fliL2	pBBMCS53 carrying the *fliL2* promoter	This work
pCR2.1-TOPO	Cloning vector; Ap^r Kan^r	Invitrogen
pJQ_ΔctrA::aadA	pJQ200 mp18 carrying Δ*ctrA*::*aadA*	This work
pJQ_ΔregB::Ω^{Spc}	pJQ200 mp18 carrying Δ*regB*::Ω^{Spc}	This work
pJQ200_ΔcckA::Ω^{Spc}	pJQ200 mp18 carrying Δ*cckA*::Ω^{Spc}	This work
pJQ200_ΔchpT::Ω^{Spc}	pJQ200 mp18 carrying Δ*chpT*::Ω^{Spc}	This work
pJQ200mp18	Mobilizable suicide vector for *R. sphaeroides*; Gm^r	27
pPIRL	Vector that encodes tRNAs for rare codons; Cm^r	35
pRK_cckA	pRK415 derivative expressing *cckA*	This work
pRK_cckA$_{A387P}$	pRK415 derivative expressing *cckA*$_{A387P}$	This work
pRK__cckA$_{L391F}$	pRK415 derivative expressing *cckA*$_{L391F}$	This work
pRK_cckA$_{F399C}$	pRK415 derivative expressing *cckA*$_{F399C}$	This work
pRK_chpT	pRK415 derivative expressing *chpT*	This work
pRK_ctrA	pRK415 derivative expressing *ctrA*	This work
pRK_regB$_{L267}$	pRK415 derivative expressing *regB*$_{L267}$	This work
pRK_regB$_{S267}$	pRK415 derivative expressing *regB*$_{S267}$	This work
pRK415	pRK404 derivative used for expression in *R. sphaeroides*	33
pTOPO_cckA	pCR2.1 TOPO carrying *cckA*	This work
pTOPO_ctrAup-down	pCR2.1 TOPO carrying *ctrA*updown	This work
pTOPO_ΔcckA::Ω^{Spc}	pCR2.1 TOPO carrying Δ*cckA*::Ω^{Spc}	This work
pTOPO_ΔcckA	pCR2.1 TOPO carrying Δ*cckA*	This work
pTZ_chpTup-down	pTZ19R carrying *chpT*updown	This work
pTZ_ctrAupdown	pTZ19R BamHI$^-$ carrying *ctrA*updown	This work
pTZ_ΔchpT::Ω^{Spc}	pTZ19R carrying Δ*chpT*::Ω^{Spc}	This work
pTZ_ΔctrA::*aadA*	pTZ19R BamHI$^-$ carrying Δ*ctrA*::*aadA*	This work
pTZ_ΔregB	pTZ19R carrying Δ*regB*	This work
pTZ_ΔregB::Ω^{Spc}	pTZ19R carrying Δ*regB*::Ω^{Spc}	This work
pTZ_regB$_{L267}$	pTZ19R carrying *regB*$_{L267}$	This work
pTZ_regB$_{S267}$	pTZ19R carrying *regB*$_{S267}$	This work
pTZ19R	Cloning vector	Pharmacia
pTZ19R BamHI$^-$	pTZ19R without BamHI site	Laboratory collection
pWM5	Vector source of the *uidA-aadA* cassette	28

The 610-bp product of the upstream region of *chpT* was obtained using the oligonucleotides chpTmutup1 and chpTmutup2, whereas the downstream product of 584 bp was obtained using the oligonucleotides chpTmutdown1 and chpTmutsdown2. These PCR products were joined through an EcoRV site designed in the oligonucleotides and cloned in pTZ19R. The Ω^{Spc} cassette was cloned into pTZ_chpTup-down previously digested with EcoRV. From the resultant plasmid, pTZ_ΔchpT::Ω^{Spc}, the DNA fragment carrying Δ*chpT*::Ω^{Spc} was purified and subcloned into pJQ200 mp18.

The allele Δ*ctrA*::*aadA* was obtained by cloning together in pCR2.1-TOPO two PCR products corresponding to the upstream and downstream regions of *ctrA* joined by a BamHI recognition site. The upstream region of *ctrA* (308 bp) was amplified by PCR using the oligonucleotides ctrAfor and ctrAinrev, whereas the downstream product of 294 bp was obtained using the oligonucleotides ctrAinfor and ctrArev. The upstream product encompassed 200 bp of the coding region of *ctrA* and 108 bp of the upstream region of the gene. The downstream product included 220 bp of the 3′ end of *ctrA* and 73 bp of the downstream region. These products were digested with BamHI, ligated, and cloned in pCR2.1-TOPO, resulting in pTOPO_ctrAupdown. To facilitate further manipulations, the resultant fragment (ctrAupdown) of 602 bp was subcloned into pTZ19R Bam^{-}. The resultant plasmid, pTZ_ctrAupdown, was digested with BamHI and ligated with an internal fragment of the Ω^{Spc} that only carries the *aadA* gene that confers the Spc^{r} phenotype without the transcriptional terminator sequences existent in the omega cassette (39). The *aadA* fragment was obtained by PCR using the oligonucleotides aadABam1 y aadABam2. The fragment containing the allele Δ*ctrA*::*aadA* was subcloned into pJQ200; the resultant plasmid was introduced into *R. sphaeroides*, and double-recombination events were selected.

To inactivate *regB*, the oligonucleotides regBupXbafw and regBdwSacIrv were used to amplify a product of 2,074 bp containing *regB* (1,389 bp) and its flanking regions of 300 and 385 bp upstream and downstream of *regB*, respectively. This product was cloned into pTZ19R, and the resultant plasmid (pTZ_regB) was subjected to inverse PCR using the oligonucleotides regBupEcoRVrv and regBdwEcoRVfw; this reaction removed 720 bp of the coding region of *regB* and retained 600 bp upstream and 756 bp downstream of the deletion boundary marked by an EcoRV recognition site, present in the oligonucleotides. The PCR product was purified and self-ligated to generate pTZ_ΔregB. The Ω^{Spc} cassette was cloned in the EcoRV site of the resultant plasmid as a 2-kb SmaI fragment. The plasmid pTZ_Δ*regB*::Ω^{Spc} was digested with XbaI and SacI, and the fragment carrying the allele Δ*regB*::Ω^{Spc} was subcloned into pJQ200mp18 and introduced into *R. sphaeroides* by conjugation. The double-recombination events were selected.

Motility assays. Motility was tested in soft-agar plates (0.22%) containing Sistrom's minimal medium or Sistrom's minimal medium without succinic acid but supplemented as indicated below. Plates were incubated aerobically (in a normal incubator) or anaerobically in a transparent polycarbonate anaerobic jar using the BD GasPak EZ anaerobe container system sachets and illuminated with incandescent bulbs (two at 75 W). After the desired time for each assay, motility was registered.

Isolation of Fla2^{+} strains. To isolate additional Fla2^{+} mutants, we prepared soft-agar plates containing Sistrom's minimal medium with 15 mM succinic acid. These plates were inoculated with strains SP13 and SP20 and incubated for 7 days inside an anaerobic jar and under continuous illumination. In addition, soft-agar plates containing Sistrom's minimal medium with 1 mM succinic acid were inoculated with strains SP13 and SP20 and incubated aerobically for 7 days at 30°C.

β-Glucuronidase activity. For the experiments shown in Fig. 7, strain LC6 was grown photoheterotrophically in Sistrom's minimal medium until early stationary phase. The cells were washed with medium without a carbon source, and an aliquot was used to inoculate fresh medium supplemented with a carbon source. After 14 h of photoheterotrophic growth, a 1.5-ml sample was withdrawn for analysis. For samples grown under heterotrophic conditions, aerobic cultures grown to stationary phase were diluted 10-fold and incubated at 30°C in the dark with shaking at 200 rpm until they reached an optical density at 600 nm (OD_{600}) of 0.6; at this point, 1.5 ml from each culture was collected and concentrated 6-fold. For the experiments shown in Fig. 3, the strains were grown photoheterotrophically in Sistrom's minimal medium with 0.2% Casamino Acids until exponential phase; at this point, a sample was withdrawn for analysis. β-Glucuronidase was determined from sonicated cell extracts using 4-methyl-umbelliferyl-β-D-glucuronide as the substrate and following a previously reported protocol (40). 4-Methyl-umbelliferone (Sigma) was used as a standard. In this work, specific activities are expressed as nmol of 4-methyl-umbelliferone formed min^{-1} mg^{-1} of protein.

Genetic and molecular biology techniques. Standard methods were used to obtain chromosomal or plasmid DNA (34). Restriction and other DNA-modifying enzymes were acquired from Roche, New England BioLabs (NEB), or Invitrogen. For sequencing, plasmids were purified using the Illustra plasmidPrep Mini Spin kit (GE). Chromosomal or plasmid DNA was amplified with the appropriate oligonucleotides using PrimeSTAR HS DNA polymerase (TaKaRa Bio Inc.) according to the recommendations of the manufacturer. Cloning was often carried out using the TOPO TA cloning kit or Zero Blunt TOPO PCR cloning kit (Invitrogen).

Site-directed mutagenesis. To replace the leucine codon found in *regB* at position 267 with serine, the plasmid pTZ_$regB_{L267}$ was subject to site-directed mutagenesis using the oligonucleotides Ser267regBqchfw and Ser267regBqchrv and the QuikChange protocol (Agilent Technologies, Inc.). The change was confirmed by sequencing, and the resultant plasmid was named pTZ_$regB_{S267}$. By following the same protocol and using the plasmid pBAD/His-cCckA as the substrate for site-directed mutagenesis, we obtained pBAD/His-cCckA L391F, pBAD/His-cCckA A387P, and pBAD/His-cCckA F399C. The pairs of oligonucleotides 454mutbad1 and 454mutbad2, cck A387Pfw and cck A387Prv, and cck F399Cfw and cck F399Crv were used to obtain each of these mutant versions.

Plasmids used in this work. pRK_cckA and its allelic variants were obtained by cloning into pRK415 (41) the 2.4-kb PCR product generated with the oligonucleotides 454A and 454B; in these plasmids, *cckA* is expressed from the *lac* promoter (*lacp*) present in pRK415. pTZ_$regB_{L267}$ was obtained by cloning into pTZ19R the 1.5-kb PCR product generated with the oligonucleotides regB1 and regB2. pRK_$regB_{L267}$ and pRK_$regB_{S267}$ were obtained by cloning into pRK415 the 1.5-kb XbaI-KpnI fragment obtained from pTZ_$regB_{L267}$ or pTZ_$regB_{S267}$; in the resultant plasmids, *regB* is transcribed from *lacp* present in pRK415. pRK_chpT was obtained by cloning in pRK415 the 774-bp PCR product generated with the oligonucleotides FwchpTXbaI and RvchpTSacI; *chpT* is expressed from *lacp* present in this plasmid. pRK_ctrA was obtained by cloning the 894-bp PCR product generated with the oligonucleotides ctrAfor and ctrArev into pRK415; in this construction, *ctrA* is expressed from *lacp*. The region of *cckA* encoding residues 249 to 758 was amplified by PCR using the oligonucleotides cckAHKfwpBAD and cckARR2pBAD2; the 1,558-bp product was cloned into pBAD_HisA to generate pBAD/His-cCckA. The fusion *fliL2-uidA* was obtained by cloning the regulatory region of *fliL2* into pBBMCS53; this plasmid was designed to generate transcriptional fusions using the *uidA* gene present in the plasmid (42). The 335-bp regulatory region of *fliL2* was obtained by PCR using the oligonucleotides fliFL3 and fliFL4.

Microscopy. Swimming cells were observed using a Nikon E600 microscope with a 40× objective with dark-field illumination. Immunofluorescence was carried out in cells previously fixed with 3% formaldehyde for 20 min at room temperature. The cells were centrifuged at 3,000 rpm and washed in phosphate-buffered saline (PBS) to remove the paraformaldehyde. Finally, the cells were resuspended in PBS (pH 7.4) with 1% bovine serum albumin (BSA). The primary antibody, FlgE1 previously labeled with Zenon Alexa Fluor 488 or FlgE2 labeled with Zenon Alexa Fluor 546 (Invitrogen), was added at a 1:50 dilution. After incubation for 2 to 12 h with the antibody, the cells were washed twice with PBS and

TABLE 2 Changes found in the AM1 genome

Location in WS8N[d]	WS8N (2.4.1)	AM1	WS8N[a]	ATCC17029	Amino acid in WS8N/2.4.1/WS8N[a]/AM1	Product (name or domain)
Gene name/position						
RSWS8N_04500 (RSP2804)/935763	G (A)	A	A	A	D/D/D/D	Queuine tRNA-ribosyltransferase
RSWS8N_05655 (RSP_0088)/1195392	G(A)	A	A	A	R/C/C/C	YciF; stress response protein
RSWS8N_07570 (RSP0454)/1592120	G (G)	**A**	G	G	L/L/L/F	CckA
RSWS8N_13040 (RSP1520)/2714509	C (C)	T	T	C	S/S/L/L	RegB
RSWS8N_16629 (RSP3079)/Chr II 311247	G (G)	A	A	G	G/G/D/D	Siderophore binding protein; FatB
Intercistronic region position in Chr I						
1101564	C (T)	T	T	T		Between RSWS8N_05200[b] and tRNA-Asp
3058907	C (C)	**T**	C	C		45 nt upstream of RSWS8N_14710[c]

[a] Laboratory collection since 1993.
[b] Hypothetical acetyltransferase.
[c] Hypothetical transcriptional regulator, Cro/CI family.
[d] Chr, chromosome.

incubated with 3% paraformaldehyde for 20 min at room temperature. The cells were washed twice with PBS and placed on a slide covered with a thin bed of agar. Epifluorescence images were taken using a Nikon Eclipse 600 microscope equipped with a Hamamatsu Orca-ER cooled charge-coupled-device (CCD) camera. Epifluorescent images were acquired for 3 s.

Protein overexpression and purification. Strain LMG194 was transformed with plasmid pBAD/His-cCckA, pBAD/His-cCckA L391F, pBAD/His-cCckA A387P, or pBAD/His-cCckA F399C. These strains were also transformed with the pPIRL plasmid, which increases the availability of certain tRNAs (43). Overnight cultures of these strains were diluted 1:50 and incubated at 37°C until they reached an OD_{600} of 0.5. At this point, 0.02% arabinose was added and incubation was allowed to proceed for 3 h. Cells were harvested and resuspended in 1/100 of the original volume in PBS (pH 7.4) with 20% glycerol and 10 mM imidazole. Lysozyme was added (1-mg/ml final concentration), and the mixture was incubated on ice for 15 min. The cell suspension was sonicated on ice using a microtip (3 mm), with three bursts of 10 s. Cell debris were removed by centrifugation (14,000 rpm for 5 min). The supernatant was mixed with nickel-nitrilotriacetic acid (Ni^{2+}-NTA)–agarose beads (1/250 of the original culture volume) and incubated for 1 h on ice, with mixing by occasional inversion. After this time, the sample was loaded into a polypropylene column (1 ml) and washed with 10 volumes of PBS with 25 mM imidazole. The protein was eluted using PBS with 20% glycerol and 200 mM imidazole and dialyzed overnight against PBS with 20% glycerol at 4°C. The purity of the protein was determined by SDS-PAGE (44) and Coomassie blue staining.

Phosphorylation of cCckA. A 5 μM concentration of purified His-cCckA wild type or a mutant version was incubated in HEPES buffer (pH 7.5; 33 mM HEPES, 10 mM $MgCl_2$, 50 mM KCl, 1 mM dithiothreitol [DTT], and 10% glycerol), the reaction was started by adding 6.6 μM [γ-^{32}P]ATP to a final volume of 60 μl. At the desired time points, a sample of 4 μl was withdrawn and the reaction was stopped by the addition of 4× Laemmli sample buffer (44). After SDS-PAGE, radioactivity was visualized and quantified using phosphor screens and a Typhoon scanner (GE Healthcare Life Sciences).

Genome sequence of AM1 strain and analysis. Total genomic DNA was isolated from a saturated culture of 3 ml using the GenElute bacterial genomic kit (Sigma). A library was constructed and paired-end sequenced (2 × 100 nucleotides [nt]; Illumina HiSeq 2000) using a commercial technology platform from Macrogen (Republic of Korea). Single reads were mapped against the genome of *R. sphaeroides* WS8N (45) using bowtie2. The .SAM file was converted to .bam and visualized with Artemis and SNVER (46–50) to identify the differences between the genome sequence and the mapped reads. The changes that were consistently present in all the reads at a particular position were confirmed by PCR followed by Sanger sequencing. For these confirmatory experiments, we tested genomic DNA from the wild-type WS8N and AM1 strains.

RESULTS

Analysis of the genome sequence of AM1. We have previously reported the isolation of spontaneous mutant strains able to swim with the Fla2 flagella. One of these mutants was selected in a Δ*flgC*::Kan^r background (SP18) (21), and the other was selected in a Δ*fleQ*::Kan^r background (AM1) (51). In order to establish the mutations that led to the expression of *fla2* genes, we determined the complete genome sequence of the AM1 strain. A total of 12.19 million paired reads of 100 nt were obtained and mapped against the complete genome of WS8N (45). The analysis of the mapped reads looking for single nucleotide variants (SNVs) or indels revealed the presence of the expected deletion in *fleQ* and 7 SNVs with an E value lower than E^{-150} (Table 2). To verify the identities of these positions in AM1 and also in WS8N, we amplified by PCR a fragment that included the position to be verified. The PCR products obtained from chromosomal DNA of strains WS8N and AM1 were sequenced by Sanger capillary electrophoresis. As shown in Table 2, 5 of these changes were also present in our wild-type strain (WS8N), suggesting that these mutations could have emerged in our laboratory and are not related with the Fla2$^+$ phenotype given that our wild-type strain does not have Fla2 flagella, as occurs with other wild-type WS8N strains previously studied in other laboratories (22). In an attempt to evaluate if these mutations could reflect a frequent variation present in other strains of *R. sphaeroides*, we analyzed the orthologous genes in *R. sphaeroides* 2.4.1 and *R. sphaeroides* ATCC 17029. We observed that 3 out of these 5 changes were also present in *R. sphaeroides* 2.4.1 and ATCC 17029; therefore, it is possible that these alleles commonly emerge in different strains or that they are errors in the published sequence. The other two mutations shared by our wild-type WS8N strain and AM1 resulted in amino acids changes in a siderophore receptor and in the RegB histidine kinase. Only 2 changes are specific to AM1; one is located in *cckA*, and the other is located in an intercistronic region (Table 2).

The change observed in the histidine kinase RegB deserved a closer inspection (Table 2) since it has been reported that RegB is involved in Fla1-dependent swimming (25). To determine the relevance of the *regB* allele (L267) present in our strains, we tested if the wild-type allele of *regB* (RegB S267) could affect swimming

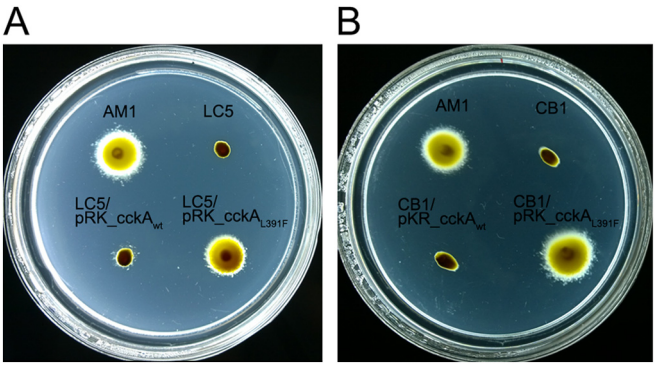

FIG 1 Swimming of strains expressing different *cckA* alleles. The swimming ability of different strains expressing different *cckA* alleles was tested. (A) Swimming of LC5 strain (WS8N Δ*fleQ*::Kan^r Δ*cckA*::Ω^{Spc}) expressing wild-type CckA or CckA L391F. AM1, positive control; LC5, negative control. (B) Swimming of strain CB1 (AM1 Δ*fleQ*::Kan^r Δ*cckA*::Ω^{Spc}) and complementation test with plasmids expressing CckA$_{wt}$ and CckA L391F. Plates were prepared with Sistrom's minimal medium containing 15 mM succinic acid and 0.22% agar. After inoculation, the plates were incubated anaerobically under continuous illumination for 60 h.

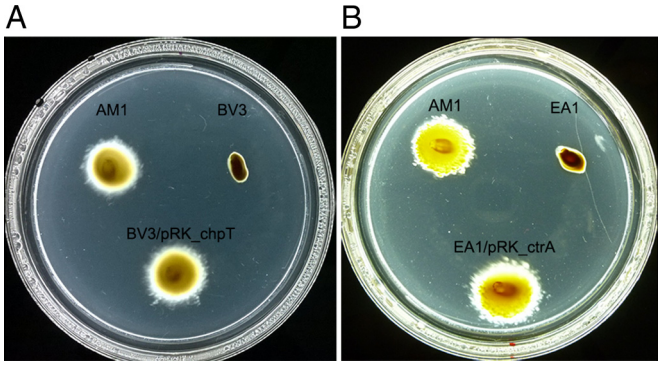

FIG 2 Influence of *chpT* and *ctrA* on the swimming behavior of AM1 cells. The swimming ability of *chpT* and *ctrA* mutant strains was tested. (A) Swimming of BV3 (AM1 Δ*fleQ*::Kan^r Δ*chpT*::Ω^{Spc}) strain, and complementation with plasmid pRK_chpT. (B) Swimming of EA1 (AM1 Δ*fleQ*::Kan^r Δ*ctrA*::*aadA*) and complementation with the plasmid pRK_ctrA. Plates were prepared with Sistrom's minimal medium containing 15 mM succinic acid and 0.22% agar. After inoculation the plates were incubated anaerobically under continuous illumination for 60 h.

of the AM1 strain or if its presence would inhibit the appearance of Fla2$^+$ strains. Under heterotrophic growth conditions, we observed a reduction of approximately 20% in the size of the swim ring of the strains lacking *regB* or expressing RegB S267 (strain CD2 [Fla2$^+$ Δ*regB*::Ω^{Spc}] or CD2/pRK_regB$_{S267}$, respectively) compared with the swim ring of AM1 or CD2/pRK_regB$_{L267}$ (see Fig. S1 in the supplemental material). However, under photoheterotrophic conditions, the strains expressing RegB S267 or L267 (AM1 [RegB L267], CD2/pRK_regB$_{S267}$, and CD2/pRK_regB$_{L267}$) formed similar swim rings (see Fig. S1). These results indicate that wild-type RegB (S267) and RegB L267 allow normal Fla2-dependent motility under anaerobic conditions and suggest that RegB L267 is insensitive to oxygen. In agreement with previous reports, the *regB* mutant CD2, grew poorly under photoheterotrophic conditions (30, 52, 53), and as a consequence, the swimming halo was barely detectable (see Fig. S1); nevertheless, from this halo it was possible to observe swimming cells under the microscope, indicating that the absence of RegB does not prevent the synthesis of Fla2 in this growth condition. In addition, the time or frequency with which Fla2$^+$ cells emerged from a selection process using CD1/pRK_regB$_{S267}$ as the parental strain is similar to that observed when the SP13 (that expresses RegB L267) strain was used. From these results, we conclude that (i) it is possible to isolate Fla2$^+$ cells in the presence of the *regB*$_{S267}$ allele (wild type) and that (ii) the Fla2-dependent swimming is slightly affected by the absence of RegB.

Effect of CckA and CckA L391F on the swimming motility of AM1. As mentioned above, the only relevant change that we observed exclusively in the genome sequence of AM1 corresponded to a single substitution in *cckA*. This mutation replaces Leu 391 with Phe. In *R. sphaeroides* WS8N, CckA has been annotated as a polypeptide of 758 residues. This protein has two transmembrane (TM) regions with a short loop in the periplasmic space. After the second TM region (after residue 58), the cytoplasmic region shows a histidine kinase (HK) domain conformed by a catalytic domain (CA) that binds ATP and phosphorylates a conserved histidine located in the DHp domain. In addition to the HK domain, this protein also has a receiver domain (REC) in the C terminus. HK and REC domains are present in the so-called hybrid histidine kinases of the two-component systems (54, 55). The mutation identified in CckA is within the HK domain and is five residues away from the conserved histidine residue that is phosphorylated (H397); the presence of this change within the HK domain suggests that the properties of CckA could have been affected by this change.

Given that CckA has been reported to be involved in the control of the flagellar genes in other alphaproteobacteria (14–16), we tested if the presence of this mutant allele of *cckA* was enough to promote swimming with Fla2 flagella. To test this possibility, we cloned the wild type and the mutant version of *cckA* into pRK415. The resultant plasmids were introduced into strain LC5 (Δ*cckA*::Ω^{Spc} Δ*fleQ*::Kan^r), and swimming was evaluated. As shown in Fig. 1A, the strain carrying the plasmid with the mutant version of *cckA* (pRK_cckA$_{L391F}$) was able to swim; in contrast, the strain that expressed the wild-type version of *cckA* only showed a few clusters of cells that did not move much from the inoculation point. The appearance of these clusters was dependent on the presence of the *cckA* gene in a multicopy plasmid, since they are not visible in the LC5 (Fig. 1) or in the SP13 (Δ*fleQ*::Kan^r) strains (data not shown). Therefore, these results indicate that CckA L391F is responsible for the Fla2$^+$ phenotype, whereas the expression of wild-type CckA from the plasmid promoter is not enough to promote swimming.

To collect further evidence supporting the role of CckA in the control of Fla2, we proceeded to inactivate *cckA* in the strain AM1 (resulting in strain CB1). As shown in Fig. 1B, the swimming ability of AM1 was completely abolished by the absence of *cckA*; the phenotype of this strain was complemented by the plasmid that expressed CckA L391F but not CckA.

Effect of mutations in CtrA and ChpT on the swimming motility of AM1. Our results show that a single mutation in CckA is able to turn on the Fla2 system and imply that the proteins homologous to CtrA and ChpT should be involved in this phenomenon. The idea that CtrA and ChpT could also control the expression of the Fla2 genes is based on the fact that these proteins together with

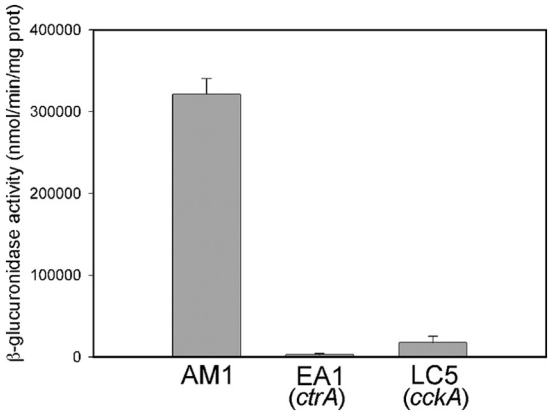

FIG 3 Transcriptional activity of *fliL2p*. β-Glucuronidase activity was determined in the following strains: AM1 (Fla2$^+$), EA1 (Δ*ctrA*::*aadA*), and LC5 (Δ*cckA*::Ω^{Spc}) carrying plasmid pBBMCS53_fliL2.

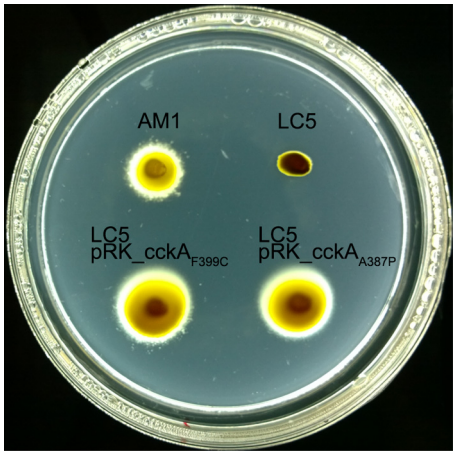

FIG 4 Swimming of LC5 (WS8N derivative, Δ*fleQ*::Kan^r Δ*cckA*::Ω^{Spc}) carrying plasmids pRK_cckA$_{F399C}$ and pRK_cckA$_{A387P}$. Plates were prepared with Sistrom's minimal medium containing 15 mM succinic acid and 0.22% agar. After inoculation, the plates were incubated anaerobically under continuous illumination for 60 h.

CckA are implicated in the expression of the flagellar genes in other bacteria (14–19). Therefore, we searched the genome of *R. sphaeroides* for genes encoding these proteins and found that RSWS8N_03320 (RSP_2621 in 2.4.1) encodes the response regulator CtrA, whereas RSWS8N_16219 (RSP_3825) encodes the homologue of the phosphotransfer protein ChpT. The gene encoding CtrA is located in chromosome I, whereas ChpT is encoded in chromosome II. Both genes were inactivated in WS8N (Fla1$^+$ Fla2$^-$) and AM1 (Fla2$^+$ Fla1$^-$) strains using the alleles Δ*ctrA*::*aadA* and Δ*chpT*::Ω^{Spc}. As shown in Fig. 2, the AM1 strain lost the ability to swim when *ctrA* or *chpT* were inactivated. In contrast, these mutant alleles did not affect the swimming motility of WS8N (see Fig. S2 in the supplemental material). Complementation using plasmids pRK_ctrA and pRK_cphT confirmed that both proteins are required for Fla2-dependent swimming (Fig. 2).

The expression level of the *fla2* genes was tested directly; for this, the reporter gene *uidA*, which encodes β-glucuronidase, was fused to the regulatory region of *fliL2* (*fliL2p*) that is the first gene of a putative operon. As shown in Fig. 3, the amount of β-glucuronidase was approximately 117-fold lower in EA1 (Δ*ctrA*::*aadA*) than in AM1 cells, indicating that CtrA is required, directly or indirectly, to express the *fla2* genes. Unexpectedly, the expression level of *fliL2p* was only 20-fold lower in LC5 (Δ*cckA*::Ω^{Spc}) cells compared with the level detected for AM1. This result suggests that CtrA-P accumulates in the Δ*cckA* strain probably due to the absence of the phosphatase activity of CckA and the phosphorylation of CtrA by a noncognate kinase or small-molecule phospho donors (56–58); alternatively, the nonphosphorylated form of CtrA could activate *fliL2p* in some degree. Given that in WS8N cells the expression of *fliL2p* is similar to that observed in EA1 cells (Δ*ctrA*::*aadA*) (data not shown), we believe that the first hypothesis is correct. Nonetheless, under any of these possibilities, the low level of expression of the *fla2* genes in LC5 (Δ*cckA*::Ω^{Spc}) cells is not enough to promote swimming.

Isolation of additional Fla2$^+$ strains with mutations in *cckA*. To further characterize the mechanisms that allow the expression of the *fla2* genes, we decided to isolate new strains showing the Fla2$^+$ phenotype. For this, we inoculated soft-agar plates with SP13 (Δ*fleQ*::Kan^r) or SP20 (Δ*fliF*::*aadA*) and incubated them under heterotrophic and photoheterotrophic growth conditions. After 7 days of incubation 13 Fla2$^+$ strains were obtained, approximately the same number of mutant strains was obtained regardless of the original phenotype or growth condition. To determine if a similar mutation to that present in the AM1 strain was responsible for the Fla2$^+$ phenotype of these strains, the DHp domain of all the *cckA* alleles was sequenced. We found two new mutations in two of them that generate CckA A387P and CckA F399C. The first change was identified in a strain isolated under photoheterotrophic growth conditions, the SP13 (Δ*fleQ*::Kan^r) strain. The second mutation was identified in a strain isolated under heterotrophic growth conditions, the SP20 (Δ*fliF*::*aadA*) strain. To verify that these *cckA* alleles were functional, the complete *cckA* gene was amplified by PCR and cloned in pRK415. As expected, these mutant versions of *cckA* expressed from the *lac* promoter present in pRK415 enabled swimming of strain LC5 (Δ*fleQ*::Kan^r Δ*cckA*::Ω^{Spc}) without any selection (Fig. 4). The *cckA* DHp domain of the remaining Fla2$^+$ strains did not show any change, and the full *cckA* gene from these strains was unable to promote swimming of LC5 (Δ*fleQ*::Kan^r Δ*cckA*::Ω^{Spc}), suggesting that *cckA* in these clones does not carry any mutation (data not shown). To determine if these strains had acquired a mutation in the CckA/ChpT/CtrA pathway that could explain the Fla2$^+$ phenotype, we sequenced the *ctrA* and *chpT* genes from each strain and 75 and 74 nt upstream of the coding regions, respectively. However, no changes were detected (data not shown). These results suggest that other proteins could be involved in the control of the Fla2 system. This control could regulate the expression or activity of CckA or CtrA. Several proteins have been reported to be involved in controlling these proteins, among them, the well-conserved SciP protein, which counteracts the activity of CtrA (15, 59, 60). In *C. crescentus*, the level of cyclic di-GMP (c-di-GMP) regulates the stability of CtrA (61), and in other bacteria, the quorum sensing systems affect the expression of *cckA* and *ctrA* (see below).

Autokinase activity of the CckA mutants. It has been reported that mutations in the DHp domain of the histidine kinases of the two-component systems usually affect the catalytic properties of the protein (62). We presume that in our case, these mutations may favor a conformation that mimics a constitutively active kinase, which would bring about activation of CtrA. To test this

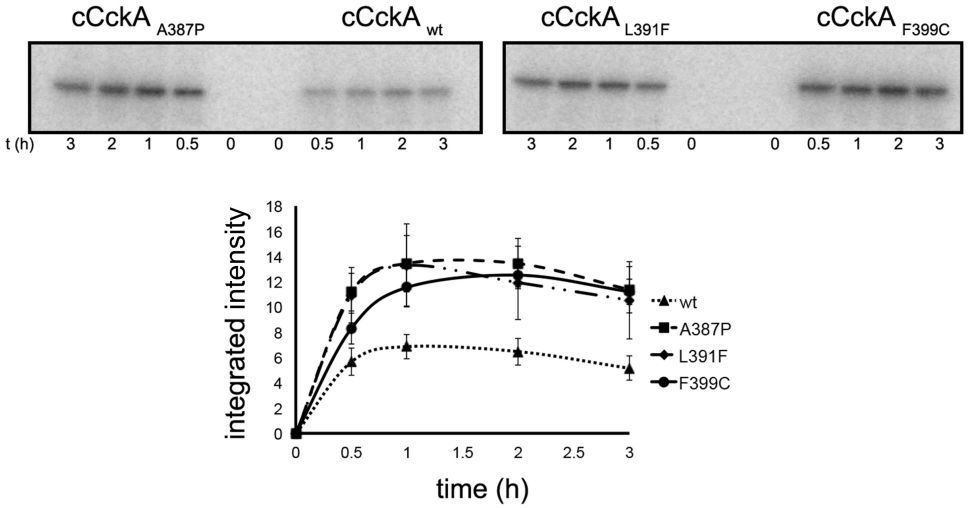

FIG 5 Autophosphorylation activity of wild-type and mutant versions of CckA. The autophosphorylation activities of the cytoplasmic fragments of different CckA versions were tested. Representative time course autoradiograms of the kinase activity of the cytoplasmic domain of wild-type CckA (cCckA) or the mutant versions are shown in the upper part. Purified proteins were incubated in the presence of [γ-^{32}P]ATP; at the indicated time points, a sample was withdrawn for SDS-PAGE analysis and quantification. The lower part shows the densitometric quantification from three independent experiments.

idea, we purified the His-tagged cytoplasmic domain of the wild-type CckA (cCckA$_{wt}$) and of the three mutant versions of the protein. The phosphorylation kinetics showed an increase in the amount of phosphorylated protein for cCckA L391F, A387P, and F399C compared to the amount of phosphorylated protein accumulated for cCckA$_{wt}$ (Fig. 5).

Effect of the culture medium on the swimming motility of AM1. The Fla2$^+$ mutants previously obtained were selected in Sistrom's minimal medium containing 34 mM succinic acid (21, 51). Later on, it was reported that AM1 cells displayed robust swarm halos and swimming in liquid Sistrom's medium with 100 μM succinic acid (51, 63); however, cells grow poorly at this low carbon source concentration, reaching a maximal OD$_{600}$ of 0.3 in liquid medium (see Fig. S3 in the supplemental material). Therefore, we tested if other carbon sources such as glycerol and Casamino Acids could promote vigorous swimming along with better growth. Soft-agar plates containing Sistrom's medium with 15 mM or 100 μM succinic acid or Sistrom's medium without succinic acid supplemented with 0.2% Casamino Acids or 0.6% glycerol were inoculated with AM1 and SP13 (Δ*fleQ*::Kan^r) cells and incubated under photoheterotrophic or heterotrophic conditions for 67 h. As shown in Fig. 6A, under photoheterotrophic conditions with Casamino Acids, AM1 forms a larger chemotactic ring (approximately 68%) than the one generated in Sistrom's minimal medium (15 mM succinic acid). This effect is also observed under heterotrophic conditions but to a lesser degree. The cell density reached in liquid cultures with Casamino Acids was significantly higher than in Sistrom's minimal medium with 100 μM succinic acid (see Fig. S3).

Unexpectedly, in the swimming plates with a low concentration of succinic acid, with glycerol and particularly with Casamino Acids as carbon sources, we detected a swimming ring around the inoculation point of SP13 (Δ*fleQ*::Kan^r), but only when the plates were incubated under photoheterotrophic conditions (Fig. 6A). To discard the possibility that suppressor mutants had appeared and formed this halo, cells from the periphery were reinoculated in swimming plates; again, these cells were able to swim in 100 μM succinic acid or 0.2% Casamino Acids only under photoheterotrophic conditions and not under aerobic conditions regardless of the carbon source. The swimming ring formed by these cells was similar to that presented in Fig. 6A (data not shown), further supporting the notion that these cells did not have a mutation that activates the Fla2 system. Therefore, we concluded that Fla2 flagella could be synthetized by SP13 cells without any additional mutation (besides Δ*fleQ*) by growing them anaerobically in either a low concentration of succinic acid or using Casamino Acids.

When AM1 and SP13 strains were grown in swimming plates containing simultaneously 0.2% Casamino Acids and a high concentration of succinic acid (15 mM), a strong reduction of the swimming ring was observed for both strains (see Fig. S4 in the supplemental material).

The fact that strain SP13 (Δ*fleQ*::Kan^r) showed Fla2-dependent motility when grown photoheterotrophically in Casamino Acids or 100 μM succinic acid could indicate that these growth conditions could be unfavorable for Fla1-dependent swimming. Therefore, to determine if the Fla1 flagellum was active when the cells were grown in 0.2% Casamino Acids or 100 μM succinic acid, the swimming of strains WS8N and CB2 (Fla1$^+$ Δ*cckA*::Ω^{Spc}) was tested in swimming plates; the results in Fig. 6B show that swimming with Fla1 flagella is not negatively affected by these growth conditions. Given that these plates were incubated for only 48 h, the Fla2-dependent swimming of SP13 (Δ*fleQ*::Kan^r) cells was still not detectable.

In spite of the swimming halo observed when the SP13 (Δ*fleQ*::Kan^r) strain was grown photoheterotrophically in 0.2% Casamino Acids (Fig. 6A), in liquid medium under these growth conditions (photoheterotrophic growth with 0.2% Casamino Acids), it was very difficult to find swimming cells in the sample. This indicates that other factors are required to fully express the *fla2* set. This result is in contrast with the fact that AM1 cells swim vigorously under these growth conditions (data not shown).

Transcriptional activity of *cckA* under different culture conditions. To correlate the swimming behavior of AM1 under different growth conditions with the expression level of *cckA*, we

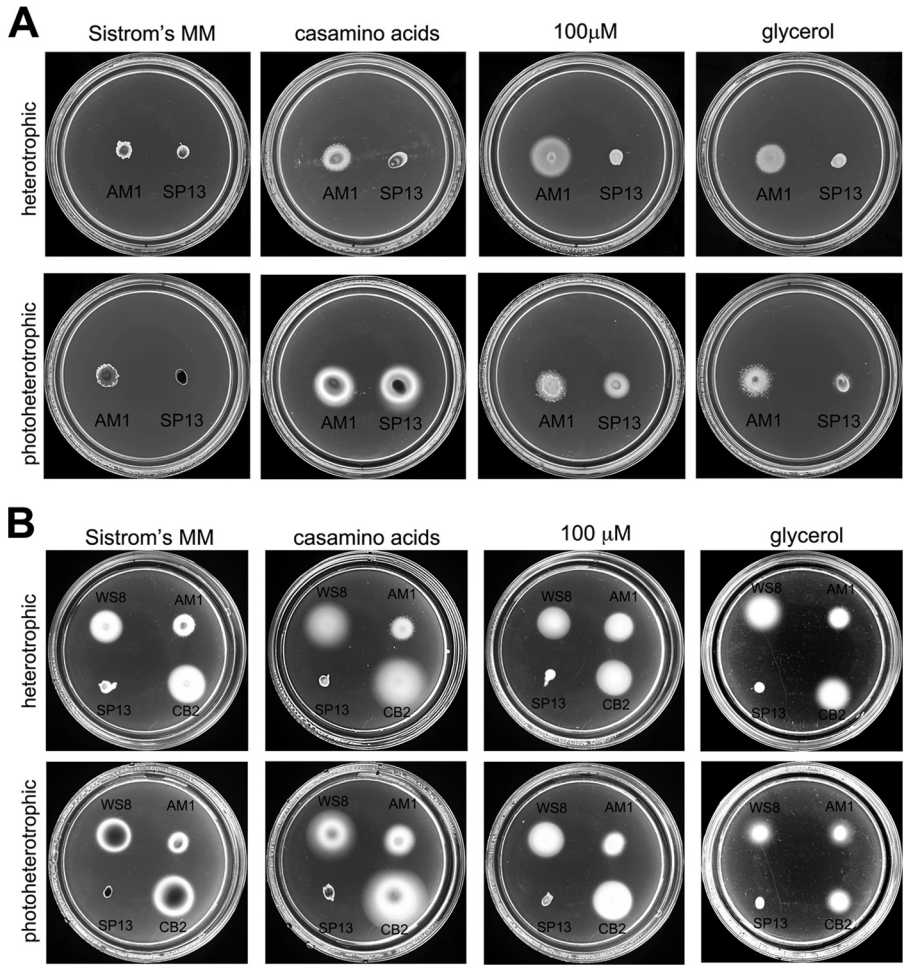

FIG 6 Effects of different carbon sources on the swimming behavior of cells expressing either Fla1 or Fla2 flagella. The relevance of the carbon source on the swimming behavior of both flagellar types was evaluated. (A) Effect of the carbon source on swimming with the Fla2 flagellum. Strains AM1 (WS8 Δ*fleQ*::Kan^r *cckA*$_{L391F}$) and SP13 (WS8N Δ*fleQ*::Kan^r) were seeded on swimming plates containing Sistrom's minimal medium with 15 mM succinic acid (Sistrom's MM), with100 μM succinic acid (100 μM), without succinic acid but supplemented with 0.2% Casamino Acids, or with 0.6% glycerol. After inoculation, the plates were incubated aerobically (upper row) or anaerobically under continuous illumination (lower row) for 60 h. (B) Effect of the carbon source on swimming with Fla1 flagella. WS8, AM1, SP13, and CB2 (AM1 Δ*cckA*::Ω^{Spc}) were seeded on swarm plates as described for panel A and incubated aerobically (upper row) or anaerobically under continuous illumination (lower row) for 48 h.

isolated a strain carrying a transcriptional fusion of the *cckA* promoter with the *uidA* gene (Δ*cckA*::*uidA-aadA*). In this strain, the amount of β-glucuronidase, encoded by *uidA*, reflects the transcriptional activity of the *cckA* promoter. The amount of β-glucuronidase was determined in total cell extracts obtained from cultures of this strain grown under different conditions. From the results shown in Fig. 7, we observed that the amount of β-glucuronidase is maximal when the extracts were obtained from cells grown in 100 μM succinic acid (this is a very low concentration of succinic acid where growth is severely limited, see Fig. S3 in the supplemental material) or 0.2% Casamino Acids. In contrast, a pronounced reduction (100-fold) was detected when strain AM1 was grown in Sistrom's minimal medium containing 15 mM succinic acid (Fig. 7). Besides, the addition of 15 mM succinic acid to the culture medium containing Casamino Acids also reduced the amount of β-glucuronidase present in the cell extracts. These results indicate that a high concentration of succinic acid represses the expression of *cckA*. To further evaluate if other organic acids from the Krebs cycle negatively affect the expression of *cckA*, we included a 15 mM concentration of either malic or fumaric acid in the culture medium containing 0.2% Casamino Acids. As shown in Fig. 7, these compounds also diminish the expression of *cckA*, as was observed with succinic acid. As expected, the activity level of β-glucuronidase was also low when the strain was grown only in 15 mM fumaric or malic acid as a carbon source (Fig. 7). To test a different carbon source, we added glycerol to the culture medium with Casamino Acids. Glycerol did not affect the induction of *cckA* produced by the presence of Casamino Acids (Fig. 7).

Presence of Fla2 flagella in a Fla1$^+$ Fla2$^+$ strain. To select for the presence of Fla2 flagella, it was necessary to eliminate the swimming motility mediated by the Fla1 flagella. However, to explore whether or not a single cell can display both types of flagella, we introduced the plasmid pRK_*fleQ*$^+$ in AM1 (Δ*fleQ*::Kan^r *cckA*$_{L391F}$) cells. It was previously demonstrated that this plasmid restores the Fla1$^+$ phenotype of the Fla1$^-$ strain carrying the Δ*fleQ*::Kan^r allele (SP13) (23).

AM1/pRK_fleQ$^+$, as well as AM1, WS8N, and SP13 (Δ*fleQ*::Kan^r) cells, were grown photoheterotrophically in Sistrom's min-

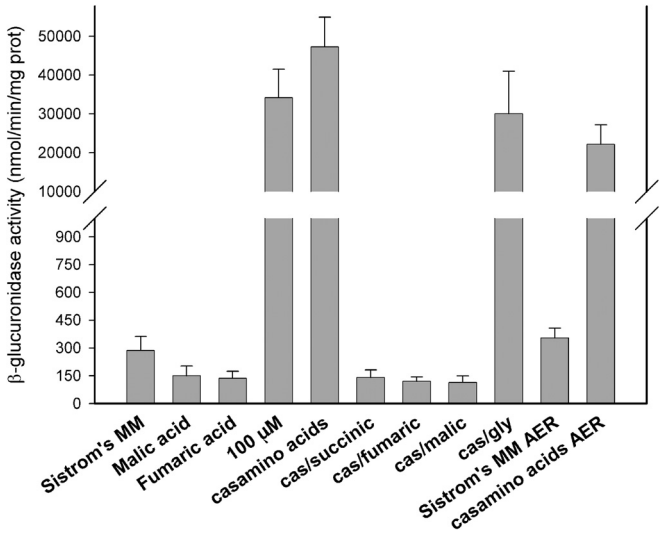

FIG 7 Effects of organic acids on the transcriptional activity of *cckA*. Shown are the β-glucuronidase activities of strain LC6 (Δ*fleQ*::Kan^r Δ*cckA*::*uidA-aad*) grown with different carbon sources: Sistrom's minimal medium supplemented with 15 mM or 100 μM succinic acid (Sistrom's MM or 100 μM, respectively), Sistrom's minimal medium without succinic acid but supplemented with 0.2% Casamino Acids (casamino acids) or with 0.2% Casamino Acids (cas) and the indicated organic acid to a final concentration of 15 mM, or 0.6% glycerol (gly). Cultures were grown anaerobically in screw-cap tubes or aerobically (AER). Values are the means of three independent measurements. The standard deviation is also shown.

imal medium until early stationary phase. The cultures were washed in medium without carbon source, and an aliquot was used to inoculate fresh medium supplemented with 100 μM succinic acid, 0.2% Casamino Acids, or 15 mM succinic acid. After 14 h of photoheterotrophic growth; cells were collected, fixed, and tested separately with anti-FlgE1 or anti-FlgE2 antibody, previously stained with Alexa Fluor 488 or 546, respectively.

Three independent experiments were carried out, and representative images obtained from one of these experiments are shown in Fig. 8, as is a quantification of a total of 3,000 cells for each strain and for each condition. From these experiments, we determined that in Sistrom's medium supplemented with 15 mM succinic acid, approximately 45% of the wild-type WS8N cells showed a single fluorescent focus corresponding to the Fla1 flagellum; whereas no signal was detected for the Fla2 flagella. In contrast, 84% of AM1 cells grown in 100 μM succinic acid showed a fluorescent focus when tested with anti-FlgE2, but no signal was detected using anti-FlgE1. As expected, SP13 cells did not show the presence of Fla1 or Fla2 when grown in 15 mM or 100 μM succinic acid or in 0.2% Casamino Acids (Fig. 8), showing that our methodology is appropriate for the detection of both types of flagella. Therefore, we tested the presence of Fla1 and Fla2 in AM1/pRK_fleQ$^+$ cells. When this strain was grown in 15 mM succinic acid, we detected 43% of cells with a single fluorescent focus corresponding to the Fla1 flagella and 0.7% of the cells with Fla2. The same strain grown in 100 μM succinic acid showed 17% of the cells with Fla1 flagella and 11% of cells with Fla2 flagella. When this strain was grown in 0.2% Casamino Acids the same trend was observed, i.e., a dominance of Fla1 (39%) over Fla2 (3%) (Fig. 8). Interestingly, even at 100 μM succinic acid we were unable to detect a single cell showing simultaneous fluorescent signals for FlgE1 and FlgE2. This suggests a mutual exclusion between the two flagellar systems in a single cell but not in the population.

From these experiments, we also observed that for WS8N the numbers of cells with Fla1 flagella were reduced approximately 2- and 14-fold when the strain was grown under culture conditions that promote the expression of *cckA*, i.e., Sistrom's minimal medium with 0.2% Casamino Acids or 100 μM succinic acid (Fig. 8). Similarly, the number of cells with Fla2 flagella decreased drastically when the AM1 strain was complemented with *fleQ*, further supporting the exclusion of the flagellar systems.

DISCUSSION

In this work, we show that the two-component system formed by CckA, ChpT, and CtrA regulates the expression of the *fla2* genes in *R. sphaeroides*. The genome sequence of mutants able to swim in the absence of the Fla1 flagella revealed that a single mutation in *cckA* is enough to turn on the expression of *fla2* under growth conditions that do not normally enable transcription of these flagellar genes (21, 22). The presence of the Fla2 flagella in strains that express these gain-of-function versions of CckA is dependent on the presence of ChpT and CtrA, indicating that the mutations in *cckA* do not alter the specificity of the kinase and that the signaling occurs through the known components of the pathway. Therefore, CtrA should activate the expression of the *fla2* genes in *R. sphaeroides*, similar to the situation previously reported for other alphaproteobacteria that do not have a second flagellar gene set (14–16, 19).

Previously, it has been reported that mutations in the DHp domain of HKs such as EnvZ, NtrB, CrdS, and AgrC can affect the kinase, phosphatase activity, or both (62, 64–66). In this work, we show that CckA L391F, A387P, and F399C autophosphorylate faster than wild-type CckA; *in vivo*, this should result in a higher level of CtrA-P and hence the expression of *fla2*. It remains to be demonstrated that autophosphorylation of wild-type CckA is the only rate-limiting step in the phosphorylation of CtrA.

A transcriptional fusion of *fliL2p* with a reporter gene showed that in the absence of *cckA*, this promoter is expressed at a higher level than in the *ctrA* strain or in WS8N, suggesting that CtrA could be phosphorylated by a noncognate histidine kinase, as has been observed for other response regulators (56, 58), or by small phospho donors such as acetyl phosphate (57); in WS8N, the phosphatase activity of CckA seems to reduce the level of CtrA-P, given that the expression of *fliL2p* is as low as that observed in the *ctrA* strain.

Intriguingly, we did not isolate a gain-of-function *ctrA* mutant even though we were able to isolate three independent mutants with changes in CckA that yield a Fla2$^+$ phenotype, as well as 11 independent mutants with the Fla2$^+$ phenotype with changes that did not affect *cckA*, *chpT*, or *ctrA*. It is possible that a constitutive mutation in CtrA could result in the repression of the *fla2* genes, or perhaps an unknown gene under the control of CtrA could affect cell growth negatively. On the other hand, the fact that we were able to isolate strains with a Fla2$^+$ phenotype without affecting the CckA pathway suggest that other elements might control the expression of the *fla2* genes. It will be interesting to identify these mutations and determine if they act through the CckA pathway or independently.

In addition to the CckA pathway, our results show that the redox sensor RegB could be involved in the regulation of the *fla2* genes. We noticed that under aerobic conditions, the swim ring

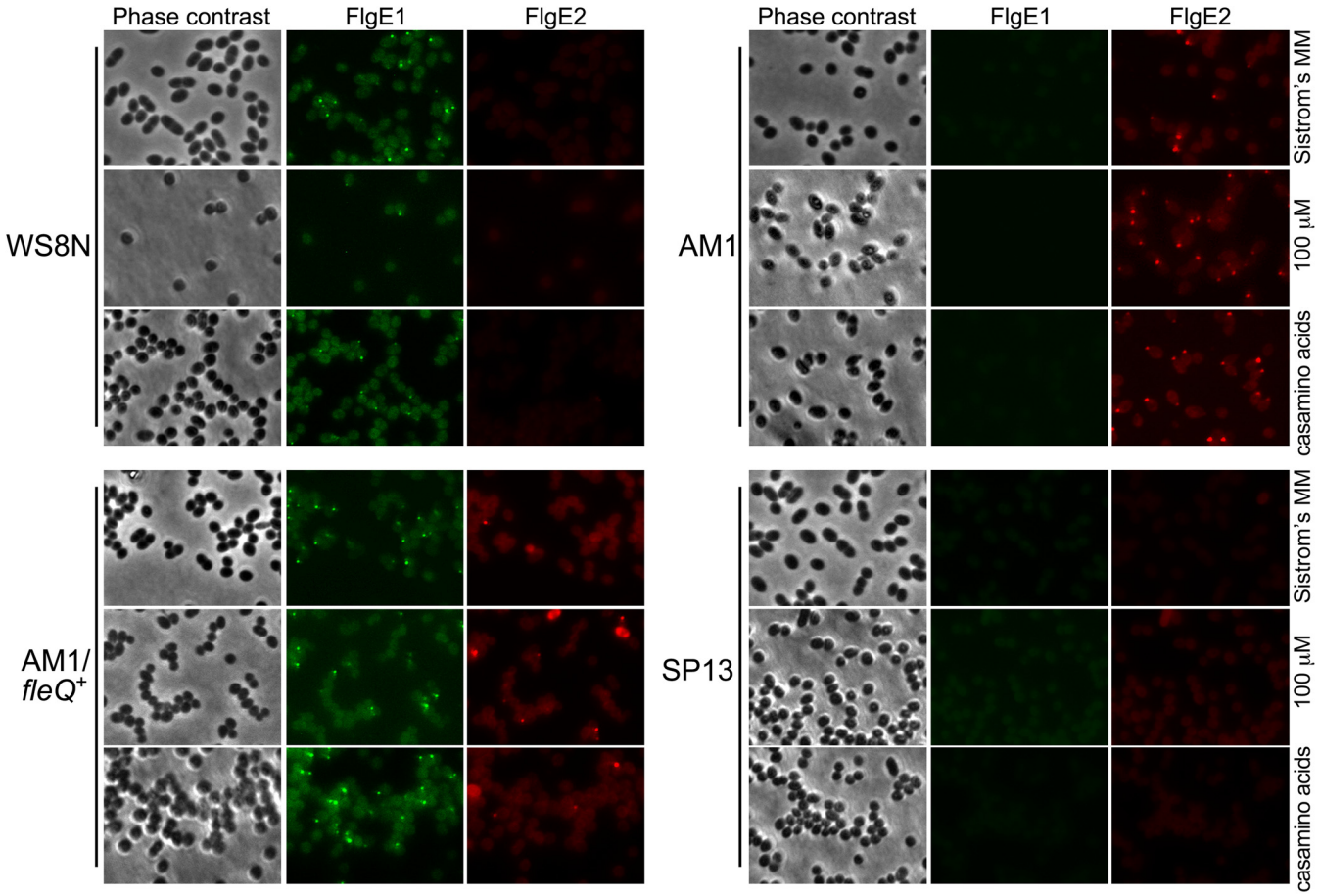

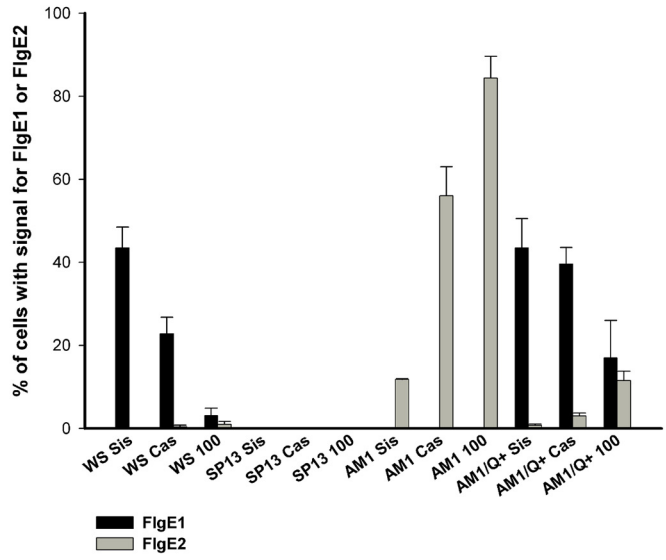

FIG 8 *In situ* detection of Fla1 and Fla2 flagella. Bacterial cells obtained from the indicated culture medium were incubated in the presence of anti-FlgE1 or anti-FlgE2 labeled with Zenon Alexa Fluor 488 or Alexa Fluor 546, respectively. In the lower part, the percentage of cells showing signal for FlgE1 or FlgE2 for each condition is indicated. The graph shows the average from three independent experiments. The standard deviation is also shown.

generated by AM1 is reduced by approximately 20% if *regB* is deleted or when the wild-type $regB_{S267}$ allele is expressed in the CD2 (AM1 Δ*regB*::Ω^{Spc}) strain. However, under photoheterotrophic conditions where RegB is active (26), the CD2 (AM1 Δ*regB*::Ω^{Spc}) strain carrying pRK_$regB_{S267}$ or pRK_$regB_{L267}$ showed a similar swim ring. It has been reported that under oxidizing conditions, the kinase activity of RegB is inactivated by the formation of cysteine sulfenic acid at position 265 (67), explaining

the reduction of the swarm ring when RegB S267 is expressed under aerobic conditions. Conversely, under anaerobic conditions, RegB acts as a kinase (26), and in this state, RegB S267 promotes swimming with Fla2 flagella. However, when RegB L267 is expressed, swimming is enhanced under aerobic growth conditions, suggesting that this mutation renders RegB insensitive to oxygen. In a search for possible RegA binding sites, the cognate response regulator of RegB, using its proposed recognition sequence (26), did not reveal any positive hits in the noncoding regions upstream of *cckA* and *ctrA*, indicating that control of *fla2* expression by the Reg system could be indirect or that the binding site of RegA in these regions is not conserved. Alternatively, RegB could influence the aerotactic response mediated by Fla2.

In this work, we also show that *cckA* transcription is strongly repressed by the presence of a high concentration of organic acids in the culture medium (i.e., 15 mM succinic, malic, and fumaric acids) but is strongly induced when 0.2% Casamino Acids or a low concentration of succinic acid (100 μM) is used as a carbon source. Cell growth is compromised in the presence of 100 μM succinic acid (see Fig. S3 in the supplemental material), but the cultures reach a high OD_{600} in 0.2% Casamino Acids, suggesting that the induction of *cckA* is not dependent on the cell density of the culture. However, it cannot be discarded that the quorum sensing system of *R. sphaeroides* that is controlled by the proteins CerR and CerI (homologs of LuxR and LuxI, respectively) (68) could influence *cckA* expression, as occurs in other alphaproteobacteria (16, 20).

The repression of *cckA* and the consequent absence of Fla2 flagella mediated by the presence of organic acids is contrary to what has been reported for *R. capsulatus*, in which *ctrA* is expressed in a higher level when the cells are grown in minimal medium containing malic acid as a carbon source than in peptone-based rich medium (20). In agreement with this, a recent comparison of the expression profiles of orthologous genes between *R. capsulatus* and *R. sphaeroides* showed that the expression pattern of *cckA* is not conserved (69).

C_4-dicarboxylates are a preferred carbon source for *Pseudomonas aeruginosa* and *Sinorhizobium meliloti* and cause catabolite repression of degradative pathways for other carbon sources (70–72). Catabolite repression in *P. aeruginosa* is mediated by the global regulator Crc, which represses the translation of genes involved in the uptake and catabolism of several nonpreferred carbon sources. In the presence of less preferred carbon sources, the two-component system CbrA/CbrB activates the transcription of one small RNA that binds Crc, relieving translational repression (73). In *S. meliloti* a histidine kinase is required to maintain a strong succinate-mediated catabolite repression (74), but the kinases of *P. aeruginosa* and *S. meliloti* are not similar. Therefore, it is difficult at this point to predict how succinate and other C_4-dicarboxylic acids could repress the expression of *cckA* in *R. sphaeroides*.

R. sphaeroides is commonly grown in Sistrom's minimal medium that includes 34 or 17 mM succinic acid, partially explaining why the Fla2 flagella had not been detected previously in the wild-type strain. Nevertheless, relieving the repression exerted by organic acids is not enough to observe swimming with the Fla2 flagella, suggesting that swimming with Fla2 may require activation of CckA by an unknown mechanism. Given that *R. sphaeroides* does not carry the genes encoding DivL, DivK, or DivJ, which are known to control CckA activity in *C. crescentus*, it is possible that other proteins are involved in controlling CckA activity.

We observed that vigorous swimming of a *fla1* strain with the wild-type *cckA* allele requires growth in soft-agar plates containing Casamino Acids as a carbon source and incubation under photoheterotrophic conditions; swimming was not detected when the same type of plates was incubated aerobically in the dark or when cells were grown photoheterotrophically in 0.2% Casamino Acids but in liquid medium. These results show that is possible to detect Fla2-dependent swimming on wild-type *cckA* when photoheterotrophic growth using Casamino Acids as a carbon source is combined with an unknown signal or stimuli generated during the growth in soft-agar plates. The most obvious explanation would imply that this hypothetical signal could be related with the nutrient gradient formed by cell growth. It remains to be determined if these conditions synergistically increase the expression of *cckA* or if other mechanisms could exist, such as CckA activation.

Independently of the hypothetical mechanism that may mediate CckA activation, our results indicate that transcriptional activation of *cckA* is an important step to enable the expression of the *fla2* genes.

The control of *fla2* genes in *R. sphaeroides* is particularly relevant, given that this bacterium could have developed additional mechanisms to control *fla2* after acquiring the *fla1* set. We present evidence that indicates that the expression of *fla2* is somehow incompatible with the synthesis of the Fla1 flagellum. This idea is based on the observations that 84% of the cells of the AM1 strain grown in 100 μM succinic acid have Fla2 flagella and that, when this strain was complemented with *fleQ*$^+$, a notable reduction in the number of cells that express Fla2 occurred, together with an important increase in the number of cells with Fla1 flagella. Individual cells with both flagella where not observed. This result suggests that in a single cell, the synthesis of Fla2 is incompatible with synthesis of Fla1. These results suggest that *R. sphaeroides* has a mechanism that ensures the expression of only one flagellar set per cell. Even though the presence of Fla1 in WS8N, or of Fla2 in AM1, follows an opposite trend depending on the culture conditions, a more complex regulation should exist, given that growth in the presence of Casamino Acids or 100 μM succinic acid does not hinder the synthesis of Fla1 in the AM1/pRK_fleQ$^+$ strain, indicating that Fla1 somehow inhibits the synthesis of Fla2 flagella in individual cells.

It has been commonly observed in bacteria that have a polar flagellum and inducible lateral flagella (required for swarming) that lateral flagella are expressed only under conditions of increased viscosity (75), However, it was recently reported that under planktonic conditions *Shewanella oneidensis* has the polar flagellum and, sporadically, one or two lateral flagella are formed. In this case, the simultaneous expression of both types of flagella allows a more efficient spreading in swimming plates because the lateral flagella modify the swimming pattern (76). Although we were unable to detect *R. sphaeroides* cells with both types of flagella when grown in liquid media, it is still possible that this type of cells was present in swimming plates. If this is the case, Fla2 does not contribute to cell spreading, since we did not observe a reduction in the swimming halo of Fla1$^+$ Fla2$^-$ cells even in plates incubated photoheterotrophically with Casamino Acids (Fig. 6B). In *R. sphaeroides*, the existence of two types of flagella that are mutually exclusive could be advantageous because of a possible specialization for each type of flagellum depending on the environmental

conditions. In addition, since each of these flagella has its own chemotactic system, it is possible that the advantage of having two flagellar systems is related with a better browsing of attractants in the environment at a population level.

As mentioned above, *R. capsulatus*, which is closely related to *R. sphaeroides*, is motile in a medium containing malic acid as a carbon source, as well as in rich medium (20). To our knowledge, there are no reports of a growth condition under which this bacterium becomes nonmotile, indicating that the CckA pathway must be functional in all the growth conditions tested so far. In contrast, in *R. sphaeroides* we observed that this pathway seems to be inactive under several growth conditions. Therefore, it is expected that profound differences should exist in the control of these proteins in order to produce such a different outcome. It is possible that the acquisition of the Fla1 set reshaped the regulatory circuit that controls this signal transduction system. A similar situation has been reported regarding the multiple σ^{54} factors present in *R. sphaeroides* that show unique features (77, 78).

ACKNOWLEDGMENTS

We thank Aurora Osorio, Teresa Ballado, and Javier de la Mora for technical support. We also thank Andrés de Sandozequi Mijares for the gift of the FlgE1 protein and Georgina Hernández for valuable help with antibody production. We thank the IFC Molecular Biology Unit for sequence facilities.

A.R. was supported by a fellowship from CONACyT (239738). This work was partially supported by grants from PAPIIT (IN204614) and CONACyT (235996).

REFERENCES

1. **Berg HC.** 2003. The rotary motor of bacterial flagella. Annu Rev Biochem **72:**19–54. http://dx.doi.org/10.1146/annurev.biochem.72.121801.161737.
2. **Macnab RM.** 2003. How bacteria assemble flagella. Annu Rev Microbiol **57:**77–100. http://dx.doi.org/10.1146/annurev.micro.57.030502.090832.
3. **Terashima H, Kojima S, Homma M.** 2008. Flagellar motility in bacteria structure and function of flagellar motor. Int Rev Cell Mol Biol **270:**39–85. http://dx.doi.org/10.1016/S1937-6448(08)01402-0.
4. **Smith TG, Hoover TR.** 2009. Deciphering bacterial flagellar gene regulatory networks in the genomic era. Adv Appl Microbiol **67:**257–295. http://dx.doi.org/10.1016/S0065-2164(08)01008-3.
5. **Curtis PD, Brun YV.** 2010. Getting in the loop: regulation of development in *Caulobacter crescentus*. Microbiol Mol Biol Rev **74:**13–41. http://dx.doi.org/10.1128/MMBR.00040-09.
6. **Tsang J, Hoover TR.** 2014. Themes and variations: regulation of RpoN-dependent flagellar genes across diverse bacterial species. Scientifica **2014:** 681754. http://dx.doi.org/10.1155/2014/681754.
7. **Chen YE, Tsokos CG, Biondi EG, Perchuk BS, Laub MT.** 2009. Dynamics of two phosphorelays controlling cell cycle progression in *Caulobacter crescentus*. J Bacteriol **191:**7417–7429. http://dx.doi.org/10.1128/JB.00992-09.
8. **Quon KC, Marczynski GT, Shapiro L.** 1996. Cell cycle control by an essential bacterial two-component signal transduction protein. Cell **84:** 83–93. http://dx.doi.org/10.1016/S0092-8674(00)80995-2.
9. **Biondi EG, Reisinger SJ, Skerker JM, Arif M, Perchuk BS, Ryan KR, Laub MT.** 2006. Regulation of the bacterial cell cycle by an integrated genetic circuit. Nature **444:**899–904. http://dx.doi.org/10.1038/nature05321.
10. **Kim J, Heindl JE, Fuqua C.** 2013. Coordination of division and development influences complex multicellular behavior in *Agrobacterium tumefaciens*. PLoS One **8:**e56682. http://dx.doi.org/10.1371/journal.pone.0056682.
11. **Barnett MJ, Hung DY, Reisenauer A, Shapiro L, Long SR.** 2001. A homolog of the CtrA cell cycle regulator is present and essential in *Sinorhizobium meliloti*. J Bacteriol **183:**3204–3210. http://dx.doi.org/10.1128/JB.183.10.3204-3210.2001.
12. **Tsokos CG, Perchuk BS, Laub MT.** 2011. A dynamic complex of signaling proteins uses polar localization to regulate cell-fate asymmetry in *Caulobacter crescentus*. Dev Cell **20:**329–341. http://dx.doi.org/10.1016/j.devcel.2011.01.007.
13. **Brilli M, Fondi M, Fani R, Mengoni A, Ferri L, Bazzicalupo M, Biondi EG.** 2010. The diversity and evolution of cell cycle regulation in alphaproteobacteria: a comparative genomic analysis. BMC Syst Biol **4:**52. http://dx.doi.org/10.1186/1752-0509-4-52.
14. **Belas R, Horikawa E, Aizawa S, Suvanasuthi R.** 2009. Genetic determinants of *Silicibacter* sp. TM1040 motility. J Bacteriol **191:**4502–4512. http://dx.doi.org/10.1128/JB.00429-09.
15. **Mercer RG, Quinlan M, Rose AR, Noll S, Beatty JT, Lang AS.** 2012. Regulatory systems controlling motility and gene transfer agent production and release in *Rhodobacter capsulatus*. FEMS Microbiol Lett **331:**53–62. http://dx.doi.org/10.1111/j.1574-6968.2012.02553.x.
16. **Zan J, Heindl JE, Liu Y, Fuqua C, Hill RT.** 2013. The CckA-ChpT-CtrA phosphorelay system is regulated by quorum sensing and controls flagellar motility in the marine sponge symbiont *Ruegeria* sp. KLH11. PLoS One **8:**e66346. http://dx.doi.org/10.1371/journal.pone.0066346.
17. **Wang H, Ziesche L, Frank O, Michael V, Martin M, Petersen J, Schulz S, Wagner-Dobler I, Tomasch J.** 2014. The CtrA phosphorelay integrates differentiation and communication in the marine alphaproteobacterium *Dinoroseobacter shibae*. BMC Genomics **15:**130. http://dx.doi.org/10.1186/1471-2164-15-130.
18. **Greene SE, Brilli M, Biondi EG, Komeili A.** 2012. Analysis of the CtrA pathway in *Magnetospirillum* reveals an ancestral role in motility in alphaproteobacteria. J Bacteriol **194:**2973–2986. http://dx.doi.org/10.1128/JB.00170-12.
19. **Miller TR, Belas R.** 2006. Motility is involved in *Silicibacter* sp. TM1040 interaction with dinoflagellates. Environ Microbiol **8:**1648–1659. http://dx.doi.org/10.1111/j.1462-2920.2006.01071.x.
20. **Leung MM, Brimacombe CA, Beatty JT.** 2013. Transcriptional regulation of the *Rhodobacter capsulatus* response regulator CtrA. Microbiology **159:**96–106. http://dx.doi.org/10.1099/mic.0.062349-0.
21. **Poggio S, Abreu-Goodger C, Fabela S, Osorio A, Dreyfus G, Vinuesa P, Camarena L.** 2007. A complete set of flagellar genes acquired by horizontal transfer coexists with the endogenous flagellar system in *Rhodobacter sphaeroides*. J Bacteriol **189:**3208–3216. http://dx.doi.org/10.1128/JB.01681-06.
22. **Armitage JP, Macnab RM.** 1987. Unidirectional, intermittent rotation of the flagellum of *Rhodobacter sphaeroides*. J Bacteriol **169:**514–518.
23. **Poggio S, Osorio A, Dreyfus G, Camarena L.** 2005. The flagellar hierarchy of *Rhodobacter sphaeroides* is controlled by the concerted action of two enhancer-binding proteins. Mol Microbiol **58:**969–983. http://dx.doi.org/10.1111/j.1365-2958.2005.04900.x.
24. **Martin AC, Gould M, Byles E, Roberts MA, Armitage JP.** 2006. Two chemosensory operons of *Rhodobacter sphaeroides* are regulated independently by sigma 28 and sigma 54. J Bacteriol **188:**7932–7940. http://dx.doi.org/10.1128/JB.00964-06.
25. **Romagnoli S, Packer HL, Armitage JP.** 2002. Tactic responses to oxygen in the phototrophic bacterium *Rhodobacter sphaeroides* WS8N. J Bacteriol **184:**5590–5598. http://dx.doi.org/10.1128/JB.184.20.5590-5598.2002.
26. **Elsen S, Swem LR, Swem DL, Bauer CE.** 2004. RegB/RegA, a highly conserved redox-responding global two-component regulatory system. Microbiol Mol Biol Rev **68:**263–279. http://dx.doi.org/10.1128/MMBR.68.2.263-279.2004.
27. **Eraso JM, Kaplan S.** 1994. *prrA*, a putative response regulator involved in oxygen regulation of photosynthesis gene expression in *Rhodobacter sphaeroides*. J Bacteriol **176:**32–43.
28. **Swem LR, Elsen S, Bird TH, Swem DL, Koch HG, Myllykallio H, Daldal F, Bauer CE.** 2001. The RegB/RegA two-component regulatory system controls synthesis of photosynthesis and respiratory electron transfer components in *Rhodobacter capsulatus*. J Mol Biol **309:**121–138. http://dx.doi.org/10.1006/jmbi.2001.4652.
29. **Swem LR, Kraft BJ, Swem DL, Setterdahl AT, Masuda S, Knaff DB, Zaleski JM, Bauer CE.** 2003. Signal transduction by the global regulator RegB is mediated by a redox-active cysteine. EMBO J **22:**4699–4708. http://dx.doi.org/10.1093/emboj/cdg461.
30. **Eraso JM, Kaplan S.** 1996. Complex regulatory activities associated with the histidine kinase PrrB in expression of photosynthesis genes in *Rhodobacter sphaeroides* 2.4.1. J Bacteriol **178:**7037–7046.
31. **Mackenzie C, Choudhary M, Larimer FW, Predki PF, Stilwagen S, Armitage JP, Barber RD, Donohue TJ, Hosler JP, Newman JE, Shapleigh JP, Sockett RE, Zeilstra-Ryalls J, Kaplan S.** 2001. The home stretch, a first analysis of the nearly completed genome of *Rhodobacter sphaeroides* 2.4.1. Photosynth Res **70:**19–41. http://dx.doi.org/10.1023/A:1013831823701.

32. **Sockett RE, Foster JCA, Armitage JP.** 1990. Molecular biology of the *Rhodobacter sphaeroides* flagellum. FEMS Symp **53:**473–479.
33. **Sistrom WR.** 1962. The kinetics of the synthesis of photopigments in *Rhodopseudomonas spheroides*. J Gen Microbiol **28:**607–616. http://dx.doi.org/10.1099/00221287-28-4-607.
34. **Ausubel FM, Brent R, Kingston RE, Moore DD, Seidman JG, Smith JA, Struhl K.** 1987. Current protocols in molecular biology. John Wiley and Sons, New York, NY.
35. **Quandt J, Hynes MF.** 1993. Versatile suicide vectors which allow direct selection for gene replacement in Gram-negative bacteria. Gene **127:**15–21. http://dx.doi.org/10.1016/0378-1119(93)90611-6.
36. **Metcalf WW, Wanner BL.** 1993. Construction of new β-glucuronidase cassettes for making transcriptional fusions and their use with new methods for allele replacement. Gene **129:**17–25. http://dx.doi.org/10.1016/0378-1119(93)90691-U.
37. **Davis J, Donohue TJ, Kaplan S.** 1988. Construction, characterization, and complementation of a Puf− mutant of *Rhodobacter sphaeroides*. J Bacteriol **170:**320–329.
38. **Simon R, Priefer U, Pühler A.** 1983. A broad host range mobilization system for in vivo genetic engineering: transposon mutagenesis in Gram-negative bacteria. Biotechnology (NY) **1:**37–45.
39. **Ballado T, Camarena L, Gonzalez-Pedrajo B, Silva-Herzog E, Dreyfus G.** 2001. The hook gene (*flgE*) is expressed from the *flgBCDEF* operon in *Rhodobacter sphaeroides*: study of an *flgE* mutant. J Bacteriol **183:**1680–1687. http://dx.doi.org/10.1128/JB.183.5.1680-1687.2001.
40. **Jefferson RA, Burgess SM, Hirsh D.** 1986. β-Glucuronidase from *Escherichia coli* as a gene-fusion marker. Proc Natl Acad Sci U S A **83:**8447–8451. http://dx.doi.org/10.1073/pnas.83.22.8447.
41. **Keen NT, Tamaki S, Kobayashi D, Trollinger D.** 1988. Improved broad-host-range plasmids for DNA cloning in Gram-negative bacteria. Gene **70:**191–197. http://dx.doi.org/10.1016/0378-1119(88)90117-5.
42. **Girard L, Brom S, Davalos A, Lopez O, Soberon M, Romero D.** 2000. Differential regulation of *fixN*-reiterated genes in *Rhizobium etli* by a novel *fixL-fixK* cascade. Mol Plant Microbe Interact **13:**1283–1292. http://dx.doi.org/10.1094/MPMI.2000.13.12.1283.
43. **Bao K, Cohen SN.** 2001. Terminal proteins essential for the replication of linear plasmids and chromosomes in *Streptomyces*. Genes Dev **15:**1518–1527. http://dx.doi.org/10.1101/gad.896201.
44. **Laemmli UK.** 1970. Cleavage of structural proteins during the assembly of the head of bacteriophage T4. Nature **227:**680–685. http://dx.doi.org/10.1038/227680a0.
45. **Porter SL, Wilkinson DA, Byles ED, Wadhams GH, Taylor S, Saunders NJ, Armitage JP.** 2011. Genome sequence of *Rhodobacter sphaeroides* strain WS8N. J Bacteriol **193:**4027–4028. http://dx.doi.org/10.1128/JB.05257-11.
46. **Goecks J, Nekrutenko A, Taylor J, Galaxy T.** 2010. Galaxy: a comprehensive approach for supporting accessible, reproducible, and transparent computational research in the life sciences. Genome Biol **11:**R86. http://dx.doi.org/10.1186/gb-2010-11-8-r86.
47. **Blankenberg D, Von Kuster G, Coraor N, Ananda G, Lazarus R, Mangan M, Nekrutenko A, Taylor J.** 2010 Galaxy: a web-based genome analysis tool for experimentalists. Curr Protoc Mol Biol **89:**19.10.1–19.10.21. http://dx.doi.org/10.1002/0471142727.mb1910s89.
48. **Giardine B, Riemer C, Hardison RC, Burhans R, Elnitski L, Shah P, Zhang Y, Blankenberg D, Albert I, Taylor J, Miller W, Kent WJ, Nekrutenko A.** 2005. Galaxy: a platform for interactive large-scale genome analysis. Genome Res **15:**1451–1455. http://dx.doi.org/10.1101/gr.4086505.
49. **Wei Z, Wang W, Hu P, Lyon GJ, Hakonarson H.** 2011. SNVer: a statistical tool for variant calling in analysis of pooled or individual next-generation sequencing data. Nucleic Acids Res **39:**e132. http://dx.doi.org/10.1093/nar/gkr599.
50. **Carver T, Harris SR, Berriman M, Parkhill J, McQuillan JA.** 2012. Artemis: an integrated platform for visualization and analysis of high-throughput sequence-based experimental data. Bioinformatics **28:**464–469. http://dx.doi.org/10.1093/bioinformatics/btr703.
51. **del Campo AM, Ballado T, de la Mora J, Poggio S, Camarena L, Dreyfus G.** 2007. Chemotactic control of the two flagellar systems of *Rhodobacter sphaeroides* is mediated by different sets of CheY and FliM proteins. J Bacteriol **189:**8397–8401. http://dx.doi.org/10.1128/JB.00730-07.
52. **Zeilstra-Ryalls J, Gomelsky M, Eraso JM, Yeliseev A, O'Gara J, Kaplan S.** 1998. Control of photosystem formation in *Rhodobacter sphaeroides*. J Bacteriol **180:**2801–2809.
53. **Laratta WP, Choi PS, Tosques IE, Shapleigh JP.** 2002. Involvement of the PrrB/PrrA two-component system in nitrite respiration in *Rhodobacter sphaeroides* 2.4.3: evidence for transcriptional regulation. J Bacteriol **184:**3521–3529. http://dx.doi.org/10.1128/JB.184.13.3521-3529.2002.
54. **Stock AM, Robinson VL, Goudreau PN.** 2000. Two-component signal transduction. Annu Rev Biochem **69:**183–215. http://dx.doi.org/10.1146/annurev.biochem.69.1.183.
55. **Laub MT, Goulian M.** 2007. Specificity in two-component signal transduction pathways. Annu Rev Genet **41:**121–145. http://dx.doi.org/10.1146/annurev.genet.41.042007.170548.
56. **Siryaporn A, Goulian M.** 2008. Cross-talk suppression between the CpxA-CpxR and EnvZ-OmpR two-component systems in *E. coli*. Mol Microbiol **70:**494–506. http://dx.doi.org/10.1111/j.1365-2958.2008.06426.x.
57. **Lukat GS, McCleary WR, Stock AM, Stock JB.** 1992. Phosphorylation of bacterial response regulator proteins by low molecular weight phosphodonors. Proc Natl Acad Sci U S A **89:**718–722. http://dx.doi.org/10.1073/pnas.89.2.718.
58. **Guckes KR, Kostakioti M, Breland EJ, Gu AP, Shaffer CL, Martinez CR, III, Hultgren SJ, Hadjifrangiskou M.** 2013. Strong cross-system interactions drive the activation of the QseB response regulator in the absence of its cognate sensor. Proc Natl Acad Sci U S A **110:**16592–16597. http://dx.doi.org/10.1073/pnas.1315320110.
59. **Tan MH, Kozdon JB, Shen X, Shapiro L, McAdams HH.** 2010. An essential transcription factor, SciP, enhances robustness of *Caulobacter* cell cycle regulation. Proc Natl Acad Sci U S A **107:**18985–18990. http://dx.doi.org/10.1073/pnas.1014395107.
60. **Gora KG, Tsokos CG, Chen YE, Srinivasan BS, Perchuk BS, Laub MT.** 2010. A cell-type-specific protein-protein interaction modulates transcriptional activity of a master regulator in *Caulobacter crescentus*. Mol Cell **39:**455–467. http://dx.doi.org/10.1016/j.molcel.2010.06.024.
61. **Abel S, Chien P, Wassmann P, Schirmer T, Kaever V, Laub MT, Baker TA, Jenal U.** 2011. Regulatory cohesion of cell cycle and cell differentiation through interlinked phosphorylation and second messenger networks. Mol Cell **43:**550–560. http://dx.doi.org/10.1016/j.molcel.2011.07.018.
62. **Willett JW, Kirby JR.** 2012. Genetic and biochemical dissection of a HisKA domain identifies residues required exclusively for kinase and phosphatase activities. PLoS Genet **8:**e1003084. http://dx.doi.org/10.1371/journal.pgen.1003084.
63. **Martínez-del Campo A, Ballado T, Camarena L, Dreyfus G.** 2011. In *Rhodobacter sphaeroides*, chemotactic operon 1 regulates rotation of the flagellar system 2. J Bacteriol **193:**6781–6786. http://dx.doi.org/10.1128/JB.05933-11.
64. **Pioszak AA, Ninfa AJ.** 2003. Genetic and biochemical analysis of phosphatase activity of *Escherichia coli* NRII (NtrB) and its regulation by the PII signal transduction protein. J Bacteriol **185:**1299–1315. http://dx.doi.org/10.1128/JB.185.4.1299-1315.2003.
65. **Geisinger E, Muir TW, Novick RP.** 2009. *agr* receptor mutants reveal distinct modes of inhibition by staphylococcal autoinducing peptides. Proc Natl Acad Sci U S A **106:**1216–1221. http://dx.doi.org/10.1073/pnas.0807760106.
66. **Hsing W, Russo FD, Bernd KK, Silhavy TJ.** 1998. Mutations that alter the kinase and phosphatase activities of the two-component sensor EnvZ. J Bacteriol **180:**4538–4546.
67. **Wu J, Cheng Z, Reddie K, Carroll K, Hammad LA, Karty JA, Bauer CE.** 2013. RegB kinase activity is repressed by oxidative formation of cysteine sulfenic acid. J Biol Chem **288:**4755–4762. http://dx.doi.org/10.1074/jbc.M112.413492.
68. **Puskas A, Greenberg EP, Kaplan S, Schaefer AL.** 1997. A quorum-sensing system in the free-living photosynthetic bacterium *Rhodobacter sphaeroides*. J Bacteriol **179:**7530–7537.
69. **Peña-Castillo L, Mercer RG, Gurinovich A, Callister SJ, Wright AT, Westbye AB, Beatty JT, Lang AS.** 2014. Gene co-expression network analysis in Rhodobacter capsulatus and application to comparative expression analysis of *Rhodobacter sphaeroides*. BMC Genomics **15:**730. http://dx.doi.org/10.1186/1471-2164-15-730.
70. **Collier DN, Hager PW, Phibbs PVJ.** 1996. Catabolite repression control in the *Pseudomonads*. Res Microbiol **147:**551–561. http://dx.doi.org/10.1016/0923-2508(96)84011-3.
71. **Ucker DS, Signer ER.** 1978. Catabolite-repression-like phenomenon in *Rhizobium meliloti*. J Bacteriol **136:**1197–1200.
72. **Valentini M, Lapouge K.** 2013. Catabolite repression in *Pseudomonas*

aeruginosa PAO1 regulates the uptake of C4 -dicarboxylates depending on succinate concentration. Environ Microbiol **15:**1707–1716. http://dx.doi.org/10.1111/1462-2920.12056.

73. **Rojo F.** 2010. Carbon catabolite repression in *Pseudomonas*: optimizing metabolic versatility and interactions with the environment. FEMS Microbiol Rev **34:**658–684. http://dx.doi.org/10.1111/j.1574-6976.2010.00218.x.
74. **Garcia PP, Bringhurst RM, Arango Pinedo C, Gage DJ.** 2010. Characterization of a two-component regulatory system that regulates succinate-mediated catabolite repression in *Sinorhizobium meliloti*. J Bacteriol **192:** 5725–5735. http://dx.doi.org/10.1128/JB.00629-10.
75. **McCarter LL.** 2004. Dual flagellar systems enable motility under different circumstances. J Mol Microbiol Biotechnol **7:**18–29. http://dx.doi.org/10.1159/000077866.
76. **Bubendorfer S, Koltai M, Rossmann F, Sourjik V, Thormann KM.** 2014. Secondary bacterial flagellar system improves bacterial spreading by increasing the directional persistence of swimming. Proc Natl Acad Sci U S A **111:**11485–11490. http://dx.doi.org/10.1073/pnas.1405820111.
77. **Poggio S, Osorio A, Dreyfus G, Camarena L.** 2002. The four different σ^{54} factors of *Rhodobacter sphaeroides* are not functionally interchangeable. Mol Microbiol **46:**75–85. http://dx.doi.org/10.1046/j.1365-2958.2002.03158.x.
78. **Poggio S, Osorio A, Dreyfus G, Camarena L.** 2006. Transcriptional specificity of RpoN1 and RpoN2 involves differential recognition of the promoter sequences and specific interaction with the cognate activator proteins. J Biol Chem **281:**27205–27215. http://dx.doi.org/10.1074/jbc.M601735200.

AMERICAN SOCIETY FOR MICROBIOLOGY | mBio®

RESEARCH ARTICLE

The Histidine Kinase CckA Is Directly Inhibited by a Response Regulator-like Protein in a Negative Feedback Loop

Benjamín Vega-Baray,[a] Clelia Domenzain,[a] Sebastián Poggio,[a] Georges Dreyfus,[b] Laura Camarena[a]

[a]Instituto de Investigaciones Biomédicas, Universidad Nacional Autónoma de México, Mexico City, Mexico
[b]Instituto de Fisiología Celular, Universidad Nacional Autónoma de México, Mexico City, Mexico

ABSTRACT In alphaproteobacteria, the two-component system (TCS) formed by the hybrid histidine kinase CckA, the phosphotransfer protein ChpT, and the response regulator CtrA is widely distributed. In these microorganisms, this system controls diverse functions such as motility, DNA repair, and cell division. In *Caulobacterales* and *Rhizobiales*, CckA is regulated by the pseudo- histidine kinase DivL, and the response regulator DivK. However, this regulatory circuit differs for other bacterial groups. For instance, in *Rhodobacterales,* DivK is absent and DivL consists of only the regulatory PAS domain. In this study, we report that, in *Rhodobacter sphaeroides*, the kinase activity of CckA is inhibited by Osp, a single domain response regulator (SDRR) protein that directly interacts with the transmitter domain of CckA. *In vitro*, the kinase activity of CckA was severely inhibited with an equimolar amount of Osp, whereas the phosphatase activity of CckA was not affected. We also found that the expression of *osp* is activated by CtrA creating a negative feedback loop. However, under growth conditions known to activate the TCS, the increased expression of *osp* does not parallel Osp accumulation, indicating a complex regulation. Phylogenetic analysis of selected species of *Rhodobacterales* revealed that Osp is widely distributed in several genera. For most of these species, we found a sequence highly similar to the CtrA-binding site in the control region of *osp*, suggesting that the TCS CckA/ChpT/CtrA is controlled by a novel regulatory circuit that includes Osp in these bacteria.

IMPORTANCE The two-component systems (TCS) in bacteria in its simplest architecture consist of a histidine kinase (HK) and a response regulator (RR). In response to a specific stimulus, the HK is activated and drives phosphorylation of the RR, which is responsible of generating an adaptive response. These systems are ubiquitous among bacteria and are frequently controlled by accessory proteins. In alphaproteobacteria, the TCS formed by the HK CckA, the phosphotransferase ChpT, and the RR CtrA is widely distributed. Currently, most of the information of this system and its regulatory proteins comes from findings carried out in microorganisms where it is essential. However, this is not the case in many species, and studies of this TCS and its regulatory proteins are lacking. In this study, we found that Osp, a RR-like protein, inhibits the kinase activity of CckA in a negative feedback loop since *osp* expression is activated by CtrA. The inhibitory role of Osp and the similar action of the previously reported FixT protein, suggests the existence of a new group of RR-like proteins whose main function is to interact with the HK and prevent its phosphorylation.

KEYWORDS *Rhodobacter sphaeroides*, CckA, two-component systems, Osp, bacterial signal transduction, hybrid histidine kinase, *Roseobacteraceae*

In bacteria, two component systems (TCS) are used to perceive and transduce many different input signals and provide adaptive responses to extracellular and intracellular cues. In its simplest form, TCS are formed by a sensor histidine kinase (SHK) and a

Editor Susan Gottesman, National Cancer Institute

Address correspondence to Laura Camarena, rosal@unam.mx, or Georges Dreyfus, gdreyfus@ifisiol.unam.mx.

The authors declare no conflict of interest.

Received 27 May 2022
Accepted 23 June 2022
Published 25 July 2022

response regulator (RR). The stimulus perceived by a specific sensor domain of the SHK, results in autophosphorylation of the conserved histidine (H) residue present in the transmitter domain, which includes both the catalytic (CA), and the dimerization and histidine phosphotransfer domains (DHp). The phosphoryl group is transferred to a conserved aspartic acid (D) residue present in the receiver domain (REC) of the RR, which elicits an appropriate cellular response. Frequently the RR protein is a transcription factor that modifies the expression of a set of genes to accomplish the proper response. A variation of this basic scheme involves hybrid histidine kinases (SHHK) in which a REC domain is fused to the SHK; in these cases, the presence of an additional phosphotransfer (HPt) domain that either can be an independent polypeptide or be part of the SHHK, is required to achieve phosphorylation of the RR protein (1–3).

The TCS formed by the membrane SHHK CckA, the Hpt protein ChpT, and the RR CtrA is widely distributed in alphaproteobacteria (4), and it has been extensively characterized in the dimorphic bacterium *Caulobacter crescentus* where progression of its cell cycle is controlled by CtrA (5–7). In this bacterium, each cell division is asymmetrical, resulting in a swarmer cell unable to replicate its DNA and a replicatively active stalked cell. After division, the stalked cell can initiate a new cycle of DNA replication, while the swarmer cell needs to differentiate into a stalked cell after a determined period of time. Cell cycle progression is controlled by a complex program in which the CckA/ChpT/CtrA system integrates the information from different regulatory proteins (8). The temporal and spatial presence of the phosphorylated form of CtrA (CtrA-P) controls the fate of the daughter cells by activating and repressing genes with critical roles in cell cycle progression and cell development (9, 10).

In *C. crescentus*, different proteins control the output of this TCS. These regulators alter CtrA stability, determine if CckA functions as a kinase or a phosphatase and, in consequence, control the spatial distribution of CtrA-P (11–15). One of these regulatory modules consists of the pseudo-HK DivL, the RR DivK, and the kinase/phosphatase DivJ and PleC proteins (16–18). Specifically, DivL stimulates the kinase activity of CckA in the flagellated pole, where the allosteric regulator of DivL, named DivK, is actively dephosphorylated by PleC. In contrast, in the stalked cell pole, DivK is maintained in its phosphorylated form by DivJ (19). The interaction between DivK-P and DivL alters the CckA-DivL interaction and favors the phosphatase activity of CckA (16, 17, 20). In addition, the second messenger c-di-GMP that drives the swarmer-stalked transition binds directly to CckA switching its activity from kinase to phosphatase (21, 22).

A bioinformatic analysis revealed that several regulators of CckA such as DivJ and DivK, are absent in *Rhodobacterales*, *Rickettsiales,* and several species of *Rhodospirillales*, suggesting that CckA could be controlled by other proteins (4).

In *Rhodobacter sphaeroides* the TCS CckA/ChpT/CtrA is required for the expression of the Fla2 flagellar system (23). This bacterium has two different flagellar systems of different phylogenetic origin, which are controlled by different transcription factors (23–26). Under the standard growth conditions used in the laboratory, only the single subpolar Fla1 flagellum is assembled whereas the *fla2* genes are not expressed, indicating that the TCS CckA/ChpT/CtrA is inactive (24). Expression of the *fla2* genes has been reported in double mutants that carry a gain of function mutation in CckA, and another mutation that blocks the synthesis of the Fla1 flagellum. A single mutation preventing the expression of the *fla1* genes does not result in the expression of *fla2* (23, 24, 27, 28).

Transcriptomic profiling of the genes controlled by CtrA in *R. sphaeroides* revealed that at least 321 genes are regulated by CtrA, which are distributed across many functional categories. In particular, CtrA affects specific pathways such as *fla2*-dependent motility, chemotaxis, gas vesicle formation, photosynthesis, etc. (29). In contrast to many studied species of α- proteobacteria, in *R. sphaeroides,* this TCS is not essential and, in fact, its expression is turned off under many different growth conditions. The signals that activate or repress CckA/ChpT/CtrA in this bacterium are largely unknown, but it has been reported that photoheterotrophic growth using a poor carbon source

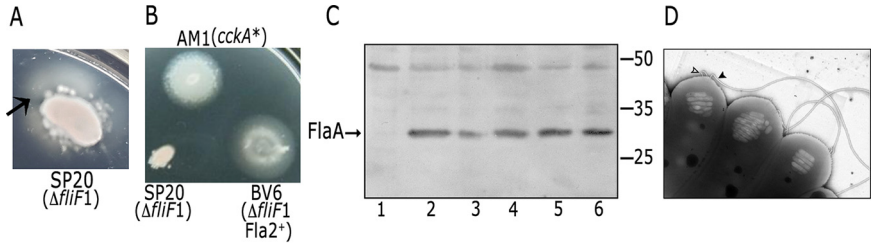

FIG 1 (A) Isolation of a spontaneous Fla2 mutant + from a non-motile strain (SP20) inoculated on a soft agar plate and incubated for 7 days at 30°C. The arrow indicates the bulge caused by the swimmer cells emerging from the colony. (B) Swimming phenotype of the Fla2+ mutant strain BV6 after purification, as controls strains AM1 and SP20 were included. The AM1 strain expresses the constitutive version of CckA, $CckA_{L391F}$. The gene encoding this mutant version of CckA is represented as *cckA**. Plates containing Sistrom's minimal medium with 0.1 mM succinic acid as a carbon source were inoculated with cells from a saturated culture and incubated for 60 h. (C) Anti-FlaA Western blot analysis of total cell extracts of strains LC7 (Δ*ctrA*::Hyg) (lane 1), AM1 (lane 2), BV6 to BV9 (lanes 3 to 6). Migration of the molecular mass markers is shown at the right and values expressed in kDa. (D) Transmission electron microscopy of BV6 cells showing the presence of flagella. For the cell on the left, the flagellar filament is indicated with a black arrowhead and an open arrowhead indicates the presence of two flagellar hooks that remain attached to the cell body when the flagellar filament was broken during manipulation.

in the culture medium such as 0.1 mM succinic acid or cas amino acids favors activation of the system (23, 30).

In this study, we report the existence of a new type of CckA regulator that directly inhibits its kinase activity by binding to its transmitter domain. In its absence, activation of CckA brings about the expression of the genes activated by CtrA-P. The wide distribution of the gene encoding this negative regulator across *Rhodobacterales* suggests that this mechanism of regulation is prevalent in several genera of this Order. A comprehensive characterization of the role of this protein in *R. sphaeroides* is presented in this study.

RESULTS

Isolation of mutant strains with an active CckA/ChpT/CtrA TCS. To obtain new insights regarding the mechanisms that control activation of the CckA/ChpT/CtrA TCS in *R. sphaeroides*, we isolated mutants that had an altered output of the system. We took advantage that under the growth conditions commonly used in the laboratory, this TCS is turned off, so we proceeded to select mutant strains able to swim with the Fla2 flagellum. For this, a mutant strain in the master regulator of the Fla1 system, FleQ (SP13 strain) (25), or a mutant defective in an early protein required for Fla1 biogenesis, such as the membrane protein FliF (SP20 strain, *fliF*1::*aadA*), were inoculated on soft agar plates. These strains are non-motile; however, after 7 days of incubation, irregular flares emerged, indicating the presence of motile cells (Fig. 1A). Four independent isolates, two from each parental strain, were selected and purified; these strains were inoculated on soft agar plates, and it was observed that they spread uniformly, indicating the presence of a homogeneous population (Fig. 1B). For comparison, the AM1 strain carrying a gain of function version of CckA ($CckA_{L391F}$, and labeled in Fig. 1B as *cckA**) was used as a positive control (23, 27). Western blotting of total cell extracts of these strains revealed the presence of the Fla2 flagellar filament protein (FlaA) (Fig. 1C). Therefore, the phenotype of these spontaneous mutants was assigned as Fla2+. Electron microscopy analysis of one of these Fla2+ strains, BV6, revealed the presence of polar flagella, a distinctive feature of the Fla2 flagellation pattern (Fig. 1D). For AM1 and other strains with an active Fla2 system, it has been reported the presence of several polar flagella with an average of 4.5 flagella per cell (24, 31). In Fig. 1D, it was also possible to observe the presence of gas vesicles, detected as electron-lucent bodies in the cytoplasm. It was previously shown that the formation of these structures is also dependent on CtrA (29).

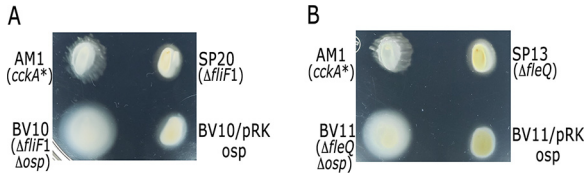

FIG 2 Swimming plates of mutant strains SP20 (A) and SP13 (B) carrying the *osp*::Hyg allele. Mutant strains were complemented using plasmid pRK_osp. Control strains carry the empty plasmid pRK415. The AM1 strain expresses the constitutive version of CckA, $CckA_{L391F}$. The gene encoding this mutant version of CckA is represented as *cckA**. Plates containing Sistrom's minimal medium supplemented with 1 μg mL^{-1} tetracycline and 0.1 mM succinic acid as a carbon source were incubated for 60 h under photoheterotrophic conditions. The diameter of the swimming rings was determined from at least three independent experiments. For panel A, AM1 = 1.85 cm SD $\pm$ 0.11; SP20 = 1.3 cm SD $\pm$ 0.04; BV10 = 2.58 cm SD $\pm$ 0.12; BV10/pRK_osp = 1.48 cm SD $\pm$ 0.05. A significant difference of $P < 0.01$ for SP20, BV10 and BV10/pRK_osp versus AM1 and BV10 versus BV10/pRK_osp was determined by one-way analysis of variance. For panel B, AM1 = 1.87 cm SD $\pm$ 0.03; SP13 = 1.33 cm SD $\pm$ 0.14; BV11 = 1.97 cm SD $\pm$ 0.05; BV11/pRK_osp = 1.49 cm SD $\pm$ 0.19. A significant difference of $P < 0.01$ for SP13, and BV11/pRK_osp versus AM1; and BV11 versus BV11/pRK_09785 was determined using the same statistical test.

Formation of Fla2 flagella indicates that the TCS CckA/ChpT/CtrA is active in the BV6 strain and strongly suggests that, in the other strains that were isolated, this would also be the case. However, no mutations were found after sequencing *cckA*, *chpT* and *ctrA*, in BV6 to BV9 strains. Therefore, the complete genome sequence of the BV6 strain was obtained and compared with the genome sequence of the wild-type WS8N strain. From this analysis, the only mutation identified corresponds to a transversion in the gene RSWS8N_09785 that encodes for a protein of 120 residues that is predicted to be a SDRR. This mutation causes the substitution of His115 for Asp.

The absence of RSWS8N_09785 is responsible of the activation of the TCS CckA/ChpT/CtrA. We learned that the RSWS8N_09785 homologous gene in *R. sphaeroides* 2.4.1 was previously reported to be a positive regulator of photosynthesis but in that report, no relationship with the TCS CckA/ChpT/CtrA was established. This gene was named *osp* that stands for optimal synthesis of the photosynthetic apparatus (32).

Therefore, to ascertain that the product of RSWS8N_09785 from here on *osp* was related with the observed phenotypes, we replaced the chromosomal gene by the mutant allele *osp*::Hyg in the strain SP20. In contrast to the parental strain that was unable to swim, it was observed that the loss of *osp* makes swimming of the resultant strain possible (Fig. 2A). The introduction of the wild-type gene in plasmid pRK415 (pRK_osp) restores the parental phenotype confirming that the Osp protein is solely responsible of the observed phenotype in the original mutant strain (Fig. 2A). The same results were observed using SP13 as parental strain (Fig. 2B). It should be noted that the swimming ability of the strain carrying a mutation in *osp* was dependent on the presence of CckA, ChpT, and CtrA indicating that, in this strain, the Fla2+ phenotype is still dependent on the 3 components of the system (data not shown).

We also established that Osp negatively affects the gain of function version of CckA that is expressed in the AM1 strain ($CckA_{L391F}$) given that swimming of these cells was severely reduced by the presence of a plasmid expressing this protein (Fig. 3A). Deletion of *osp* in AM1 cells caused a slight increment in swimming, and this effect was counteracted by the presence of pRK_osp (Fig. 3A).

The hypothesis that Osp is a negative regulator of the TCS CckA/ChpT/CtrA was additionally supported by measuring the expression of the CtrA-dependent *mcpB* gene in the AM1 derivative strain carrying the reporter fusion *mcpB*::*uidA-aadA* (29). *mcpB* is part of the chemotactic operon 1 (*che*Op1) and it was previously demonstrated that its expression is directly controlled by CtrA; therefore, it represents a reliable reporter of CtrA activation (26). As shown in Fig. 3B, β-glucuronidase activity (encoded by *uidA*) was severely reduced by the presence of pRK_osp. This result agrees with the notion that Osp limits CtrA activation.

In accordance with the idea that inactivation of *osp* induces the Fla2+ phenotype, we found that the remaining mutants also carried mutations in this gene. We observed

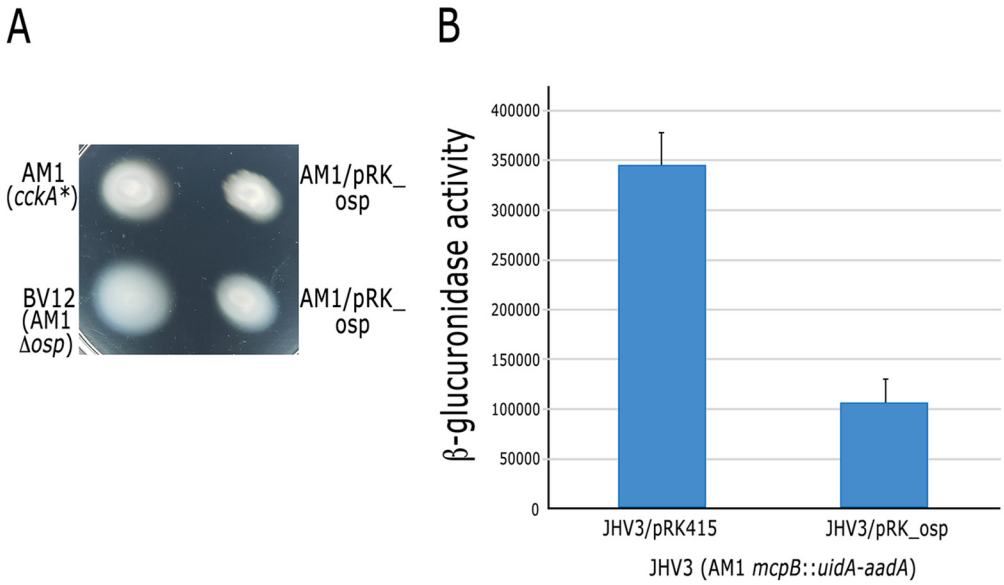

FIG 3 (A) Swimming plate of AM1 and its derivative BV12 (AM1 *osp*::Hyg) strains carrying an empty plasmid pRK415 or pRK_osp. Plates containing Sistrom's minimal medium supplemented with 1 μg mL^{-1} tetracycline and 0.1 mM succinic acid as a carbon source were incubated for 60 h. The diameter of the swimming rings was determined from at least three independent experiments. AM1 = 1.89 cm SD $\pm$ 0.06; AM1/pRK_osp = 1.17 cm SD $\pm$ 0.05; BV12 = 2.59 cm SD $\pm$ 0.28; BV12/pRK_osp = 1.68 cm SD $\pm$ 0.24. A significant difference of $P < 0.01$ for AM1/pRK_osp versus AM1; BV12/pRK_osp versus BV12 and BV12 versus AM1 was determined by one-way analysis of variance. (B) β-glucuronidase activity driven by the chromosomal fusion *mcpB*::*uidA-aadA* present in JHV3 was determined from strains carrying pRK415 or pRK_osp. Total cell extracts were obtained from cultures grown photoheterotrophically in Sistrom's minimal medium supplemented with 0.2% cas amino acids as a carbon source. Activity is expressed as picomoles of methylumbelliferone formed per minute per milligram of protein. A significant difference of $P < 0.01$ for JHV3/pRK415 versus JHV3/pRK_osp was determined using a two-tailed *t* test.

for strain BV7 an insertion of a single nucleotide that shifted the open reading frame of *osp* generating a truncated protein of only 77 amino acids; for strain BV8 an insertion of 6 nucleotides that adds the amino acids A and V after residue 63, and for strain BV9 a deletion of a single nucleotide that shifted the open reading frame after residue 11. These strains were successfully complemented with the plasmid pRK_osp (data not shown).

Osp is similar to a SDRR and its expression is dependent on CtrA. Osp is similar in structure to a SDRR, showing the typical topology (β/α)5, and it also shows the phosphorylatable aspartic residue at the end of the β3 strand (D51). However, relevant residues that are present in bona fide response regulators are missing such, as 2 acid residues (D) after the β1 strand that are required for Mg^{2+} coordination, and the conserved lysine (K) at the end of β5 are absent (33, 34) (Fig. 4A). The absence of these conserved residues suggest that this protein is not phosphorylated. In this regard, it was previously observed that *in R. sphaeroides* 2.4.1 the mutant version Osp D51A promoted the expression of the photosynthetic genes as wild-type Osp did (32).

To test if the swimming phenotype was also supported by a non-phosphorylated version of Osp, residue D51 was replaced by asparagine (N) by site-directed mutagenesis. It was previously shown that this substitution also results in a non-phosphorylatable RR, and in consequence, it cannot accomplish the role of the phosphorylated protein (35–38). The plasmid expressing the D51N version of Osp was introduced to the BV12 strain, and we observed a severe reduction in swimming, suggesting that this protein is functional in a non-phosphorylated state (Fig. 4B).

The *osp* gene is found 243 bp downstream of a gene encoding a putative transcriptional regulator of the TetR family, and 111 bp upstream of a gene encoding a conserved hypothetical protein (Fig. 4C). Considering the intercistronic distances between these genes, *osp* is presumably transcribed as a monocistronic mRNA. In agreement with this idea, previously reported transcriptomic data of the genes controlled by CtrA

FIG 4 (A) Amino acid alignment of Osp and CheY from *E. coli*. The secondary structure features that conform the canonical structure of typical RRs is shown above and below the amino acid sequences of Osp and CheY. Conserved functional residues present in RRs are boxed in pink. The blue bars represent α-helixes, and yellow arrows β-strands. Secondary structure predictions were obtained using Psipred (84) and protein homology was evaluated using Swiss-Model (85) and the crystal structure of CheY (PDB 6TG7). (B) Swimming plate of BV12 strain carrying pRK_osp or pRK_osp D51N. Strains AM1 and BV12 carrying pRK415 were included as controls. Plates containing Sistrom's minimal medium supplemented with 1 μg mL^{-1} tetracycline and 0.1 mM succinic acid as a carbon source were incubated for 60 h. The diameter of the swimming rings was determined from at least three independent experiments, AM1 = 1.82 cm SD $\pm$ 0.13; BV12 = 2.5 cm SD $\pm$ 0.25; BV12/pRK_osp = 1.64 cm SD $\pm$ 0.25; BV12/pRK_osp D51N = 1.12 cm SD $\pm$ 0.1. A significant difference of $P < 0.01$ for BV12/pRK_osp and BV12/pRK_osp D51N versus BV12 was determined by one-way analysis of variance. (C) Genomic context of RSWS8N_09785 (*osp*). NCBI BLASTP and HHpred (86) analyses for homology detection were performed.

in *R. sphaeroides*, showed that *osp* is activated by CtrA but not the contiguous genes (29). To further support this result, a transcriptional fusion of the control region of *osp* with the reporter gene *uidA* was cloned in pRK415 and the resulting plasmid was introduced to strains AM1 and LC7 (AM1Δ*ctrA*::Hyg). As shown in Fig. 5A, very low expression of β-glucuronidase in the absence of CtrA was observed. We detected higher activities when the AM1 strain was grown photoheterotrophically and using a low concentration of succinic acid (0.1 mM) as a carbon source, a condition known to activate the CckA/CtrA system (23). As expected, in SP13 and its derivative strain BV17 (Δ*ctrA*), this plasmid promoted a low level of activity similar to that observed for the LC7 ($cckA_{L391F}$ Δ*ctrA*) strain under all tested growth conditions (Fig. S1). A sequence similar to the CtrA-binding site (TAA N7 TTAA) (10, 29, 39) was identified 54 bp upstream of the start codon of Osp (ATG) (Fig. 5B). In *C. crescentus*, a global transcriptomic study revealed that promoters activated by CtrA have this CtrA-binding motif positioned near the -35 promoter region, considering the transcriptional start site as the +1 position (40). The regulatory regions of *osp* from species closely related to *R. sphaeroides*, also show the CtrA-binding motif and several conserved bases downstream that may represent the -35 and the -10 promoter regions. A conserved purine is at a proper distance to be considered the putative transcriptional start site (Fig. 5C). This conserved architecture further supports the idea that *osp* is directly activated by CtrA.

Osp inhibits CckA autophosphorylation and CtrA phosphorylation. Given that Osp has a negative effect on the expression of the genes under the control of the CckA/ChpT/CtrA system, we evaluated the autophosphorylation of the cytoplasmic domain of CckA in the presence of Osp (the domain architecture of CckA is presented in Fig. 10). As shown in Fig. 6A, CckA phosphorylation is severely inhibited by the presence of Osp. It was determined that a molar ratio of 0.25 between Osp/CckA is enough to reduce CckA phosphorylation by ca. 50% (Fig. 6B), and a molar ratio of 1 practically achieved near complete inhibition. To investigate if Osp inhibits nonspecifically other HKs, we tested the kinase activity of the cytoplasmatic domain of the HK PhoR (41) in the absence and presence of Osp. This experiment showed that Osp inhibition is specific toward CckA (Fig. S2). In addition, we also demonstrated that CckA kinase activity was not affected by including in the assay a nonspecific protein containing a REC domain such as the REC domain of DctR, an active response regulator required for the transport of C4-dicarboxylic acids in *R. sphaeroides* (30).

In the presence of Osp, the phosphorelay from CckA to ChpT and CtrA was not observed, showing that the presence of the complete phosphorelay pathway did not

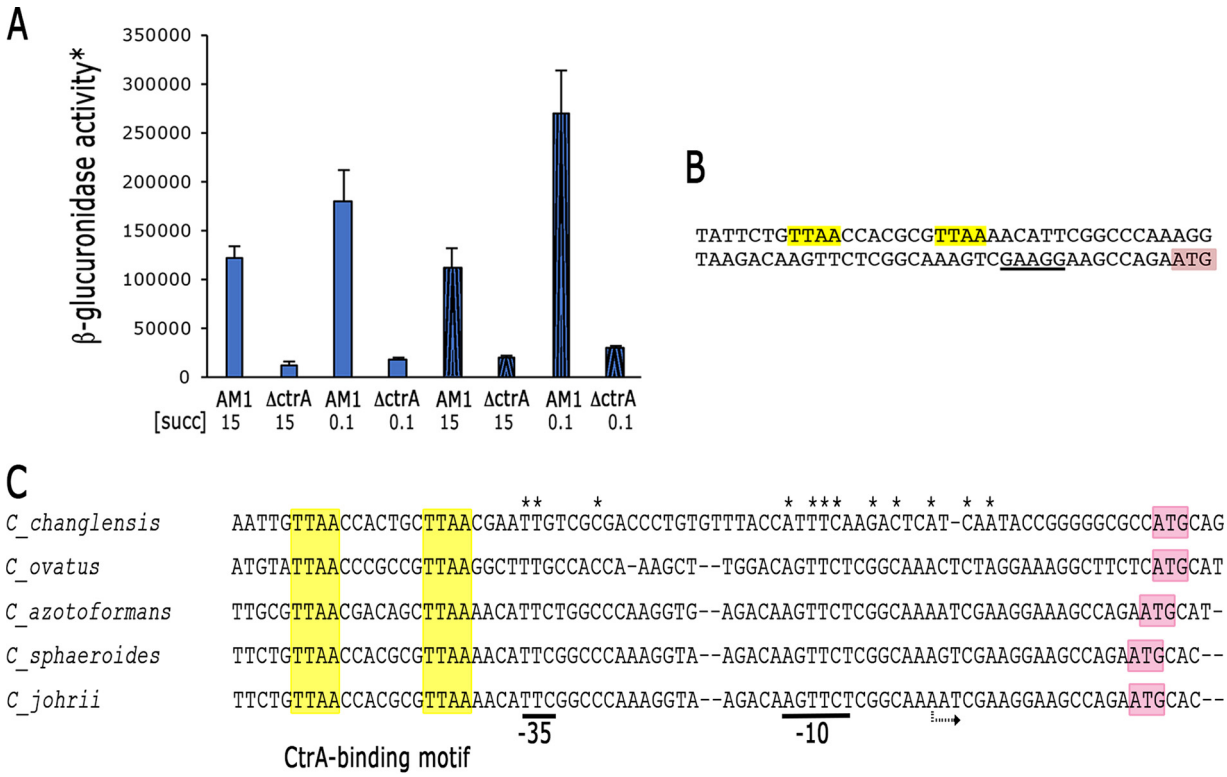

FIG 5 (A) β-glucuronidase activity expressed from the regulatory region of *osp* fused to the reporter gene *uidA*, in pRK415. The plasmid carrying this fusion was introduced into strains AM1 and LC7 (Δ*ctrA*::Hyg), and the amount of β-glucuronidase was determined from three independent assays. Cell extracts were obtained from cultures grown heterotrophically (solid filled columns) or photoheterotrophically (pattern filled columns) in Sistrom's minimal medium containing 15 or 0.1 mM succinic acid as a carbon source. *Activity is expressed as picomoles of methylumbelliferone formed per minute per milligram of protein. Standard deviations are shown. A significant difference of $P < 0.01$ for LC7/pRK_osp::uidA-aadA versus AM1/pRK_osp::uidA-aadA under all growth conditions was determined by one-way analysis of variance. (B) Sequence of the upstream region of *osp* showing the putative CtrA-binding site (yellow boxes). The predicted ribosome-binding site is underlined, and the start translation site is shown (pink box). (C) Alignment of the regulatory region of *osp* in the indicated organisms. The sequences matching with the consensus CtrA-binding site are highlighted in yellow. The translation codon is highlighted in pink. The conserved nucleotides after the CtrA-binding motif are indicated by an asterisk. Conserved nucleotides of the putative -35 and -10 promoter regions are underlined. The possible transcriptional start site is indicated by a curved arrow.

affect the inhibition of CckA phosphorylation by Osp (Fig. 7). In addition, when CckA was previously phosphorylated and subsequently mixed with ChpT and CtrA or ChpT, CtrA and Osp, we did not observe a significant difference (Fig. S3), supporting the notion that Osp mainly acts by inhibiting the kinase activity of CckA.

We also evaluated the dephosphorylation of phospho-CckA in the presence or absence of Osp. It was observed that dephosphorylation of CckA was not affected by the equimolar presence of Osp (Fig. 8). Moreover, the addition of Osp to the previously phosphorylated proteins CckA, ChpT, and CtrA did not affect dephosphorylation of CckA (Fig. S4).

$CckA_{L391F}$ is partially resistant to Osp. It was previously reported that it was possible to obtain Fla2+ strains just by the presence of a gain of function mutation in CckA, such as the one characterized for the AM1 strain i.e., $CckA_{L391F}$ (23, 42). Nonetheless, the strong inhibition of the CckA kinase activity by Osp raised the question of how a single mutation in *cckA* can generate a Fla2+ phenotype, given that in this strain, *osp* has a wild-type sequence. Therefore, it follows that $CckA_{L391F}$ must be somewhat refractory to the action of Osp. To test this possibility, we carried out a phosphorylation assay using $CckA_{L391F}$ and an equimolar concentration of Osp. As shown in Fig. 9A, phosphorylation of $CckA_{L391F}$ is still detectable as compared with wild-type CckA. As expected from this result, in the presence of Osp, CtrA-P was still clearly detected when $CckA_{L391F}$ was used in the phosphorelay assay (Fig. 9B). To evaluate if inhibition of $CckA_{L391F}$ could require a higher concentration of Osp, increased amounts of this

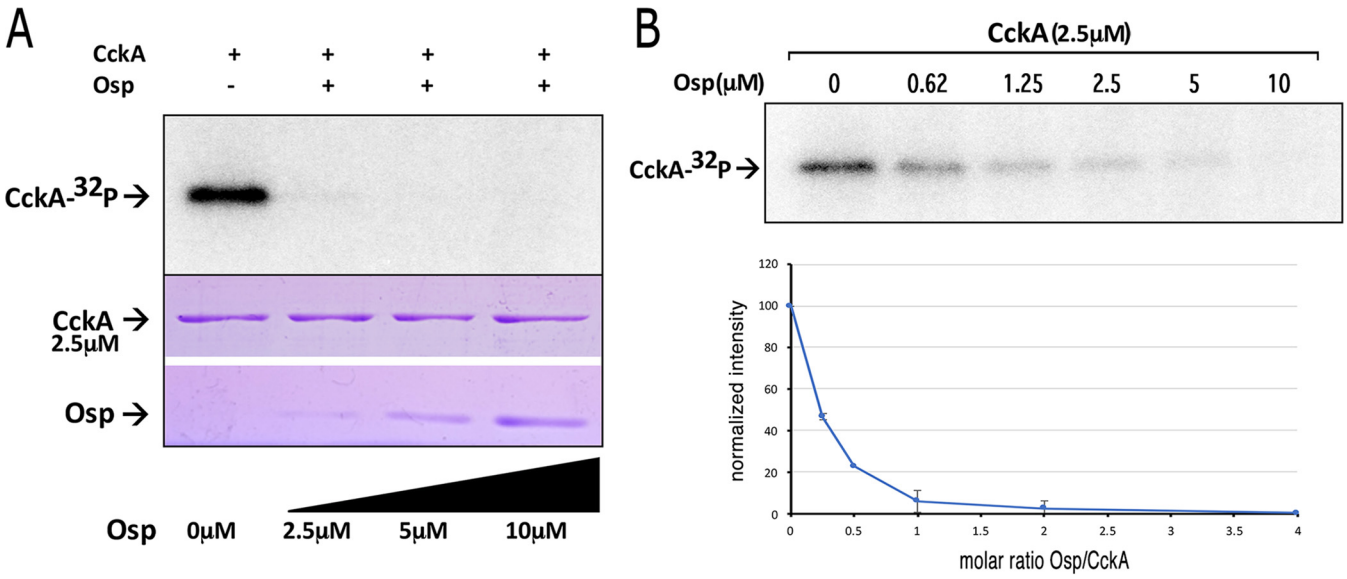

FIG 6 CckA phosphorylation using [γ-^{32}P]ATP in the presence of different concentrations of Osp. (A) 2.5 μM CckA was incubated with increasing concentrations of Osp (0, 2.5 μM, 5 μM and 10 μM) and [γ-^{32}P]ATP for 30 min and subjected to SDS-PAGE. The presence of CckA-^{32}P was detected by phosphorImager visualization (upper part of the figure). The proteins used for the experiment were mixed, and an aliquot was analyzed by SDS-PAGE followed by Coomassie brilliant blue staining (shown below). (B) 2.5 μM CckA was incubated with increasing concentrations of Osp (0, 0.625 μM, 1.25 μM, 2.5 μM, 5 μM, and 10 μM) and [γ-^{32}P]ATP for 30 min the mixture was subjected to SDS-PAGE. Quantification of the amount of CckA phosphorylated in the presence of the indicated concentration of Osp. The images shown correspond to representative experiments from three independent assays.

protein were included in the phosphorylation assay. This experiment revealed that inhibition of $CckA_{L391F}$ required a concentration approximately four times higher of Osp than that required to inhibit wild-type CckA (Fig. 9C).

Osp interacts with the transmitter domain of CckA. To obtain evidence of the physical interaction between CckA and Osp, we carried out a yeast double hybrid assay using different domains of CckA fused to the DNA binding domain (BD domain) of the transcriptional activator Gal4, whereas Osp was fused to the activation domain (AD domain) of Gal4. In this assay, a positive interaction between the proteins to be tested brings together the AD and the BD domains of Gal4 creating a functional activator that promotes expression of HIS3 and ADE2. It has been reported that HIS3 has a leaky expression (43); therefore, testing the expression of HIS3 and ADE2 simultaneously reli-

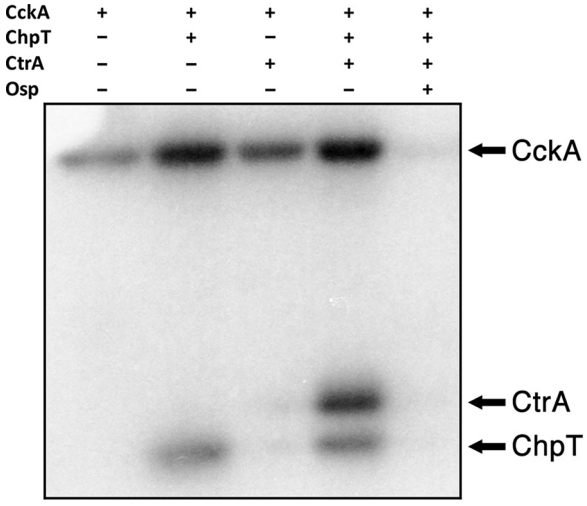

FIG 7 Phosphorelay reconstitution in the presence or absence of Osp. 2.5 μM of the purified components were mixed and the reaction was initiated by adding [γ-^{32}P]ATP. The presence or absence of the various proteins in the reaction medium is indicated by a plus or a minus symbol. The image shown corresponds to a representative experiment from three independent assays.

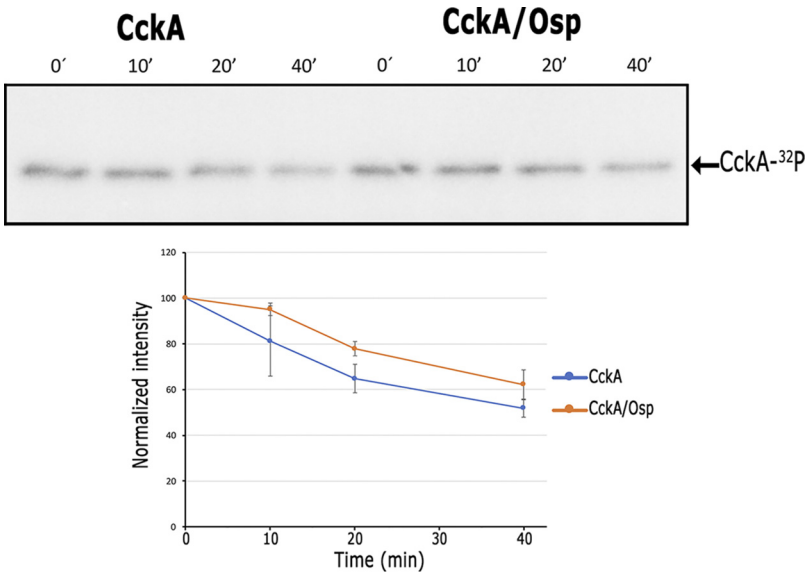

FIG 8 Time course assay of CckA dephosphorylation in the absence or presence of Osp. The presence of CckA-^{32}P was detected by phosphorImager visualization. 2.5 μM CckA was phosphorylated and remaining ATP was removed by column-filtration chromatography, the protein was mixed with buffer or with 2.5 μM Osp, and at the indicated time points, samples were analyzed by SDS-PAGE. Quantification of CckA-P is expressed as the ratio between the signal at a determined time divided by the signal at t = 0. The image shown corresponds to a representative experiment from three independent assays. A non-significant difference of P = 0.75 was determined for the slopes of the linear regression curves analyzed by a two-tailed t test.

ably indicates a strong interaction between the tested proteins (*idem*). In the yeast strain AH109, the absence of leucine (L) and tryptophan (W) selects the presence of the plasmids encoding the fusion proteins, and the expression of the reporter genes HIS3 and ADE2 is detected by histidine (H) and adenine (A) prototrophy. The experiments showed a robust growth on plates without histidine and adenine (LWHA) for cells expressing Osp and CckA protein fusions, indicating a strong interaction between these proteins. This interaction is mediated by the transmitter domain of CckA given that the PAS and the REC domains were dispensable (Fig. 10).

It should be noted that the binding assay did not reveal significant differences between the interactions of Osp with CckA or with $CckA_{L391F}$, suggesting that either the assay is not sensitive enough to differentiate in affinity or that the $CckA_{L391F}$ mutation does not interfere with Osp binding but makes the protein less sensitive to its inhibitory effect.

To explore if these results could be explained by an unspecific interaction between CckA and any protein containing a REC domain, we fused the AD domain of GAL4 to the REC domain of the transcriptional activator DctR. We did not detect interaction between CckA and the REC domain of DctR supporting the idea of a specific interaction between the transmitter domain of CckA and Osp (Fig. 10). A slight growth in the absence of H and A was detected for the cells expressing CckA (REC) and Osp (Fig. 10). However, a low level of auto-activation promoted by pGBKT7_cckA-REC could explain this residual growth (Fig. S5). The expression of the fusion proteins in these experiments was confirmed by Western blotting (data not shown).

The interaction between CckA and Osp was further corroborated by the co-purification of a non-tagged version of Osp along with His_6-CckA by Ni-NTA affinity chromatography (Fig. 11).

Accumulation of Osp does not mirror its transcriptional expression pattern. The expression of *osp* is activated by CtrA, and Osp inhibits the kinase activity of CckA, creating a negative feedback loop. However, previous evidence suggests that *osp* is expressed at low levels even in the absence of CtrA (29). These observations raise the question of how the TCS CckA/ChpT/CtrA reaches a high level of activity. The simplest

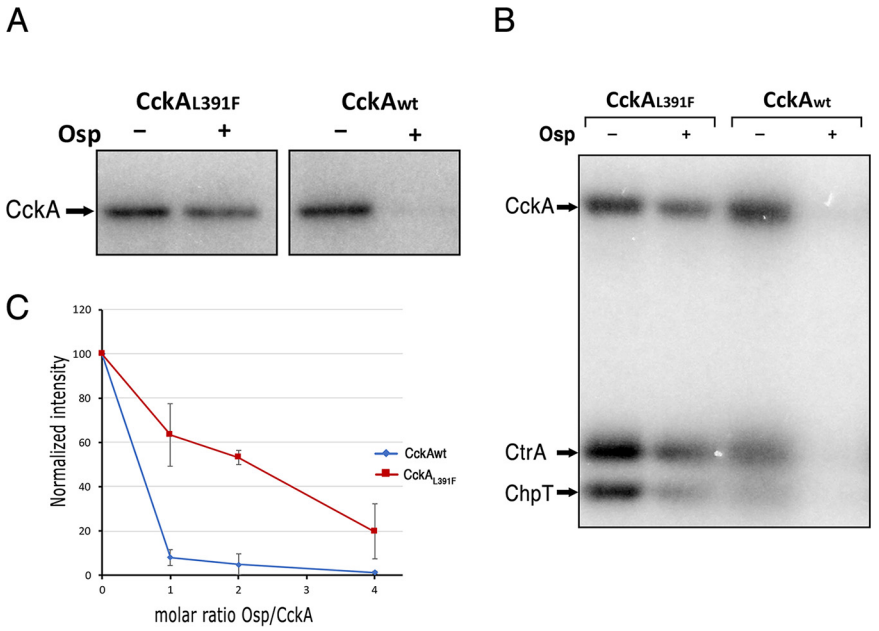

FIG 9 (A) Effect of the presence of Osp on the phosphorylation reaction of $CckA_{L391F}$ and wild-type CckA. For these experiments, Osp was added at a 1:1 molar ratio to CckA. (B) Effect of Osp on the phosphorelay of the purified proteins CckA/ChpT/CtrA using $CckA_{L391F}$ or wild-type CckA. For this experiment, 2.5 μM each protein was used. (C) 2.5 μM CckA or CckAL391F was incubated with increasing concentrations of Osp (0, 2.5 μM, 5 μM and 10 μM) and [γ-^{32}P]ATP for 30 min and subjected to SDS-PAGE. Quantitation by phosphorImager analysis of the amount of phosphorylated CckA or CckAL391F in the presence of the indicated Osp/CckA molar ratio. The images shown correspond to representative experiments from three independent assays.

solution would be to avoid Osp accumulation when the TCS needs to be activated. Therefore, we tested if the presence of Osp in total cell extracts mirrors its transcription profile. To reveal the presence of Osp, we carried out a Western blot analysis using an anti-FLAG antibody that allowed us to recognize an N-terminal tagged version of Osp. Importantly this version of the protein that is fairly functional (Fig. S6) is expressed from its native position in the chromosome and uses the same translational start site of Osp. As shown in Fig. 12A, Osp was strongly detected in cells grown aerobically in 15 mM succinic acid, but it was barely detected in cells grown in 0.1 mM succinic acid and under photoheterotrophic growth, irrespectively of the succinic acid concentration. As a control of the CckA/ChpT/CtrA TCS activity, the same samples were tested with an antibody that recognizes the flagellar hook protein FlgE2. As expected for a protein encoded by a gene controlled by CtrA-P, FlgE2 was clearly detected when the cells were grown in 0.1 mM succinic acid and severely reduced in 15 mM (Fig. 12B). In general, this result reveals that the presence of Osp does not follow the same pattern to that observed for a CtrA-activated gene, suggesting that Osp stability could be regulated to maintain a low level when the TCS CckA/ChpT CtrA is activated.

Osp is conserved in specific clades of the *Rhodobacterales*. The TCS CckA/ChpT/CtrA is present in alphaproteobacteria but the regulatory proteins that control this system show adaptations in specific clades of this group (4). A search for the *osp* gene in different bacteria revealed its presence in species closely related to *Rhodobacter sphaeroides* (now *Cereibacter sphaeroides*) and in species of the *Defluviimonas* genus. However, it is conspicuously absent in other species within the *Rhodobacteraceae* family. In contrast, *osp* is widely distributed in species of the *Roseobacteraceae* family (Fig. 13, species with Osp are shaded in blue), and it was not found in any other genera of alphaproteobacteria. Interestingly, the presence of Osp in *Amylibacter kogurei* that diverges before the division between *Rhodobacteraceae* and *Roseobacteraceae* and the narrow distribution of the *osp* gene in the *Rhodobacteraceae* family, suggests a complex evolution in which the gene could have been lost in several genera of this family and retained only

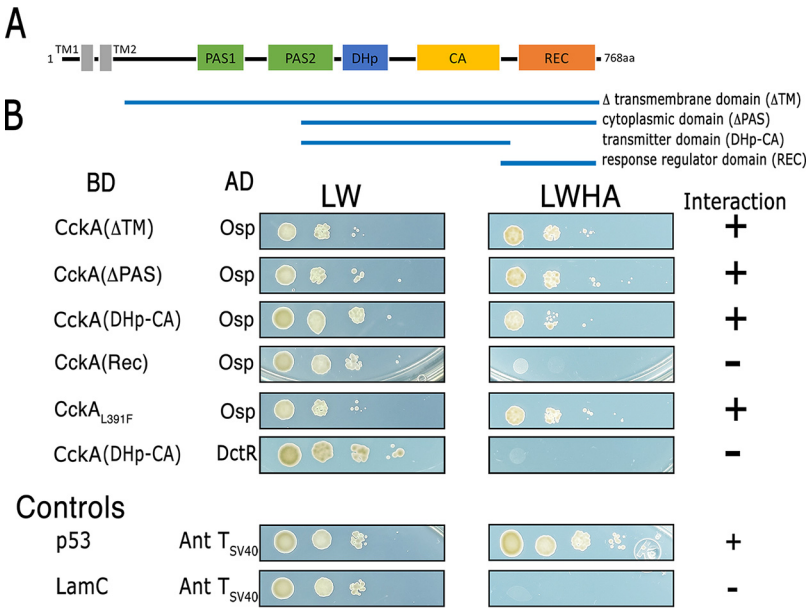

FIG 10 (A) Domain architecture of CckA, the domains present in each construct are indicated below. (B) Interaction of Osp with CckA tested by the yeast double hybrid assay. Yeast cells were transformed with the pair of plasmids carrying the DNA binding domain of GAL4 (BD) fused to a CckA domain, and the activation domain (AD) of GAL4 fused to Osp. Under the column labeled BD, the CckA domain cloned in pGBKT7 plasmid is indicated. Protein-protein interactions were evaluated by testing histidine (H) and adenine (A) prototrophy. The letters L, W, H and A indicate the nutrient that is absent in the culture medium. LW indicates the absence of leucine and tryptophan in the culture medium. LWHA indicates the absence of leucine, tryptophan, histidine, and adenine. Positive and negative interactions between Osp and CckA are summarized at the far-right. Below the positive and negative interaction controls represented by GAL4AD-T (simian virus 40 large antigen T) and GAL4BD-Lam (lamin C) (−), and GAL4AD-T and GAL4BD-p53 (+) pairs are shown. The control experiments using AH109 yeast cells expressing the different versions of Gal4BD-CckA and GAL4AD-T (SV40 T-antigen) are shown in Fig. S5.

in a few of them i.e., *Cereibacter* and *Defluviimonas*. A more consistent distribution of *osp* among the different genera of the *Roseobacteraceae* family was observed.

Interestingly, for many of these bacterial species, we found a sequence similar to the CtrA-binding site in the regulatory region of *osp* (Fig. 13, purple stars and Fig. S7). If these sites are functional, the regulatory circuit that controls the TCS CckA/ChpT/CtrA in these bacterial species will also include Osp, probably creating a negative feedback loop of the system as occurs in *R. sphaeroides*.

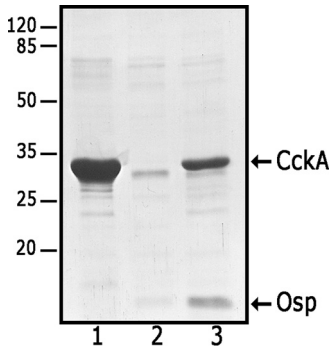

FIG 11 *In vivo* pull-down of Osp using His_6-CckA. A cell extract obtained from *E. coli* cells over-expressing only His_6-CckA (lane 1); only Osp without a His6X-tag (lane 2); or simultaneously both proteins i.e., His_6-CckA and Osp without a His6X-tag (lane 3) were used to purify His_6-CckA by affinity chromatography using Ni-NTA-agarose. The purified proteins were subjected to SDS-PAGE and visualized by Coomassie brilliant blue staining. It should be stressed that the over-expression of these proteins was carried out using the T7 promoter cloned upstream of each gene. Migration of the molecular mass markers is shown at the left and expressed in kDa.

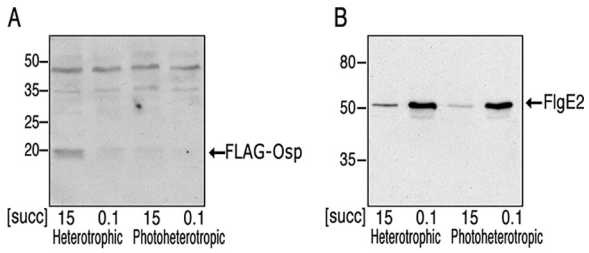

FIG 12 Total cell extracts obtained from BV18 cells grown under the indicated conditions, were subjected to SDS-PAGE and tested by Western blotting analysis using anti-FLAG (A) and anti-FlgE (B) antibodies. The growth condition, and the concentration of succinic acid (mM) used as carbon source is indicated below. The migration of the molecular mass markers (kDa) is indicated at the left.

As reported, a short version of the DivL that lacks the pseudo-histidine kinase domain and the absence of its interacting partner, the protein DivK, are a common trait in *Rhodobacterales* (4, 44, 45) (Fig. 13).

Noteworthy, we found a possible progression of events that seem to have preceded the appearance of Osp. Initially, following the loss of DivK (Fig. 13), we observed two versions of DivL i.e., in the group represented by *Oceanicella actignis* and *Albimonas pacifica*, we detected the presence of a large version of DivL, although its HK and CA domains were degenerated but still identified in a bioinformatic prediction, and for the rest of the *Rhodobacterales*, we detected the presence of a short version of DivL. After the loss of DivK and truncation of DivL, Osp could have appeared early (Fig. 13, purple dot) and subsequently be lost, or could have appeared at a later point and horizontally acquired by other species.

Interestingly, from this analysis, a possible horizontal transfer was detected in *Thalassobius mediterraneum* (*Roseobacteraceae*) in which the short version of DivL was present but, in contrast to other related bacteria, DivK was also present. The presence of DivK in this microorganism seems to be the product of a horizontal transfer event given that no other species in the Order have DivK. Comparison of DivK of *T. mediterraneum* by BLAST showed that DivK from *Henricella marina* (*Hypomonadaceae*) is the most similar sequence, suggesting that this may be the possible origin of the gene. Furthermore, in these organisms *divK* is found upstream of *pleD* and PleD from *H. marina* is also the best hit of PleD from *T. mediterraneum*.

DISCUSSION

The negative control of TCSs in bacteria is frequently carried out by diverse proteins that modulate HKs. For instance, in *Escherichia coli*, the HK NtrB (NRII) is switched to its phosphatase state upon binding of the sensor protein PII (46, 47). In *Bacillus subtilis*, the HK KinA is inhibited by SdA and KipI (48, 49). These inhibitory proteins do not share structural similarity, but all of them bind to the transmitter domain of their cognate HK (49–53). Regarding its structure, PII is a β-α-β homotrimer (54); in contrast, Sda is a 46-residue protein that adopts an antiparallel hairpin structure (55, 56), and the 240 residues long KipI belongs to the cyclophilin-like domain superfamily (57, 58). These examples illustrate that, often, inhibition of the HKs is accomplished by structurally unrelated proteins.

FixT, a SDRR has been reported to act as a negative regulator of the SHK FixL in *Sinorhizobium meliloti* and *C. crescentus* (59–61). It was demonstrated that FixT inhibits autophosphorylation of FixL without affecting its dephosphorylation rate (60, 62). Given that phosphorylation of FixT was not observed, it was ruled out that it could act as a phosphate sink (60, 62).

In this study, we showed that Osp a SDRR, is responsible of inhibiting the TCS CckA/ChpT/CtrA in *R. sphaeroides*. An inactivating mutation in *osp* causes the expression of the CtrA-activated genes, such as the flagellar and chemotactic genes. Consistent with this result, *in vitro* phosphorylation assays showed that Osp directly inhibits phosphorylation of the HHK CckA, whereas its dephosphorylation rate is not affected. The

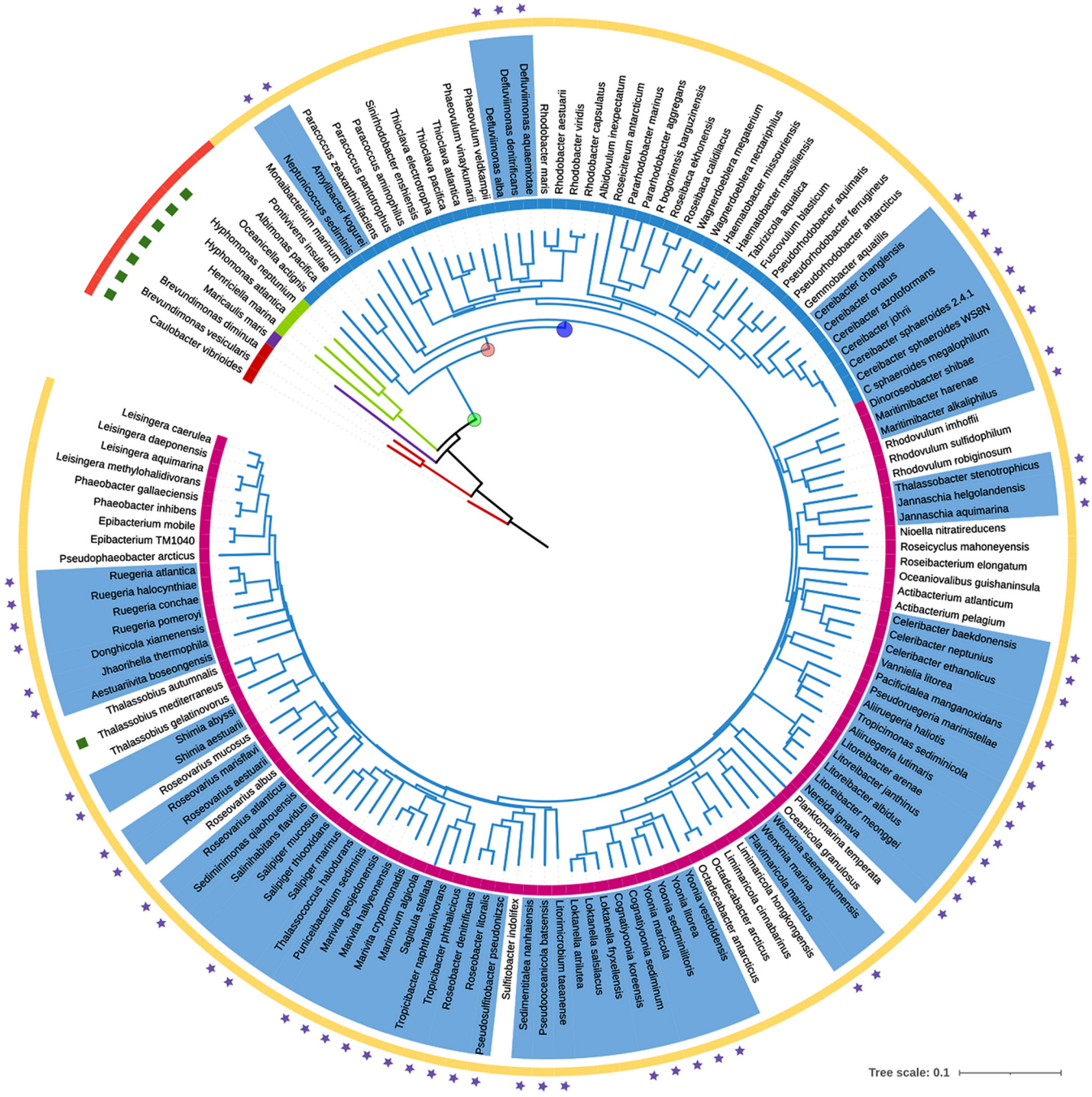

FIG 13 Phylogenetic distribution of *osp* in *Rhodobacterales*. Species phylogeny based on RpoC, the tree was generated by the neighbor joining method using clustal simple phylogeny and edited with iTOL. From inside to outside, color of the branches indicates the Order: *Caulobacterales* (red), *Maricaulales* (purple); *Hyphomonadales* (green), *Rhodobacterales* (blue). Circle below the species name indicates the Family: *Caulobacteraceae* (red), *Maricaulaceae* (purple), *Hyphomonadaceae* (green), *Rodobacteraceae* (blue), and *Roseobacteraceae* (magenta). In the circle depicting the species names, the presence of Osp is indicated by a blue background. The presence of DivK is represented by green squares above the species names, the presence of a long DivL (red) or a short DivL (yellow). The stars represent the presence of a putative CtrA-binding site in the regulatory region of *osp*. Green dot possible point of DivK loss, pink dot truncation of DivL (short DivL), blue dot represents earliest possible appearance of Osp. Complete information for each species, the GenBank accession number for each genome, the accession number for RpoC, Osp, and DivK are included in Table S2.

presence of ChpT and CtrA did not relieve this inhibition and phosphorylation of Osp was not observed.

The effect of FixT and Osp indicate that inhibition of HKs by SDRRs could be a common mechanism and that it can also be implicated in regulating HHKs that are structurally more complex than canonical HKs.

We also determined that Osp interacts with the transmitter domain of CckA. Since Osp is a RR and it interacts with the transmitter domain of CckA, it is tempting to propose that the interaction between these two proteins occurs through the same protein regions that mediate the interaction between other HKs and their cognate RRs. If this is the case, binding of Osp may then interfere with the access of the CA domain to the phosphorylatable His residue. Furthemore, we observed that Osp was able to inhibit CckA autophosphorylation when present in a substoichiometric ratio, raising the possibility that Osp could bind a CckA dimer and cause a conformational change that would prevent its phosphorylation. In this regard, it should be stressed that most of the SHK commonly exists as dimers and structural studies support the view that, in the autokinase state, the packing of the DHp helixes is different for each monomer and, in consequence, only one CA domain is found in close proximity to the phosphorylatable histidine (63–65). It is possible that Osp could have a higher affinity for this protomer and, from this position, it could prevent the rearrangement of the other protomer. Determination of the crystal structure of the complex would help to clarify the stoichiometry of the complex.

We observed that Osp was not phosphorylated; we believe that the absence of two acid residues before the α-helix 1 could account for this. The lack of these acid residues is also observed for the FixT proteins of *S. meliloti* and *C. crescentus*, neither of which are phosphorylated (60, 62).

Regarding the transcriptional control of *osp*, a global transcriptomic analysis of the CtrA-dependent genes revealed that *osp* transcription is activated by CtrA but in its absence, *osp* expression is still detectable (29). We confirmed this result using a transcriptional fusion of the regulatory region of *osp* to the *uidA* reporter gene. Transcriptional activation of *osp* by CtrA generates a negative feedback loop that limits the activity of the system; the basal expression of *osp* will maintain the system inactive until an unknown signal promotes Osp degradation. This postranscriptional control may be enough to turn on and keep the system active. Increasing the expression of *osp* from a plasmid significantly reduced the swimming ability of the AM1 strain and, therefore, we presume that a precise balance of Osp concentration, based on transcriptional and posttranslational mechanisms, is essential to control the TCS CckA/ChpT/CtrA in *R. sphaeroides*.

Proteolysis of FixT and Sda is also the release mechanism of their respective SHK from inhibition (62, 66), showing that this molecular strategy is commonly used to reduce the intracellular amount of an inhibitor.

The presence of Osp in many different genera of bacteria that lack the DivK/DivL system suggests that a negative control of the TCS CckA/ChpT/CtrA must be physiologically important. In these cases, Osp would accomplish an analogous role to that of DivK-P of *C. crescentus*. In bacteria where DivK and DivL have been characterized, such as in *C. crescentus* and in a few species of *Rhizobiales*, the TCS CckA/ChpT/CtrA is essential, and its activity is modulated by different proteins that are mainly controlled by internal cues, such as DNA replication or cell division (5, 67–69). In this context, Osp represents a powerful alternative solution that could make the system sensitive to environmental signals.

MATERIALS AND METHODS

Bacterial strains and growth conditions. The strains used in this work are listed in Table 1. *R. sphaeroides* strains were grown in Sistrom's minimal medium (70), without cas amino acids and supplemented with 15 mM or 0.1 mM succinic acid as carbon source. Growth conditions were reported previously (29). *Saccharomyces cerevisiae* was grown at 30°C in YPDA or in synthetic defined minimal medium (Clontech).

Molecular biology techniques. Standard methods were used to obtain chromosomal or plasmid DNA (71). DNA was amplified with the appropriate oligonucleotides (Table S1) using Prime Star *Taq* DNA polymerase (TaKaRa) according to the recommendations of the manufacturer. Standard methods were used for transformation, ligation, and other related techniques.

Motility assays. Motility was tested in soft agar plates (0.22%) as described previously (29).

Genome sequence of BV6 and analysis. A genomic library was constructed and subjected to 2 × 76-bp pair-end sequencing on the Illumina NexSeq 500 platform. Reads were mapped against the genome of *R. sphaeroides* WS8N using bowtie2 (72). A BCF file was created using SAMtools, variants

TABLE 1 Strains and plasmids

Strain or plasmid	Description	Source
Rhodobacter sphaeroides strains		
AM1	SP13 derivative; Δ*fleQ*::Kan, *cckA*L391F	27
BV6	SP20 derivative; Δ*fliF1*::*aadA, osp*H115D	This study
BV7	SP13 derivative; Δ*fleQ*::Kan, *osp*77aa	This study
BV8	SP20 derivative; Δ*fliF1*::*aadA*, *osp*AV+	This study
BV9	SP13 derivative; Δ*fleQ*::Kan, *osp*11shift	This study
BV10	SP20 derivative; Δ*fliF1*::*aadA*, Δ*osp*::Hyg	This study
BV11	SP13 derivative; Δ*fleQ*::Kan, Δ*osp*::Hyg	This study
BV12	AM1 derivative; Δ*fleQ*::Kan, *cckA*L391F, Δ*osp*::Hyg	This study
BV13	SP13 derivative; Δ*fleQ*::Kan, Δ*osp*::Hyg, Δ*ctrA*::*aadA*	This study
BV14	BV11 derivative; Δ*ctrA*::*aadA*	This study
BV15	BV11 derivative; Δ*chpT*::*aadA*	This study
BV16	BV6 derivative; Δ*cckA*::Hyg	This study
BV17	SP13 derivative; Δ*ctrA*::Hyg	This study
BV18	AM1 derivative; FLAG-*osp*	This study
BV19	SP13 derivative; FLAG-*osp*	This study
JHV3	AM1 derivative; Δ*fleQ*::Kan, *cckA*L391F, *mcpB*::*uidA-aadA*	29
LC7	AM1 derivative; Δ*fleQ*::Kan, *cckA*L391F, Δ*ctrA*::Hyg	Laboratory collection
SP13	WS8N derivative; Δ*fleQ*::Kan	25
SP20	WS8N derivative; Δ*fliF1*::*aadA*	Laboratory collection
Escherichia coli strains		
LMG194	Protein expression strain	Invitrogen
TOP10	Cloning strain	Invitrogen
Rosetta	Protein expression strain	Novagen
Yeast strains		
AH109	Reporter strain for two-hybrid screening *HIS3*, *ADE2,* and *lacZ*	Clontech
Plasmids		
pBAD HisB	Expression vector of His6X-tagged proteins; Ap	Invitrogen
pBAD_chpT	pBAD/HisB expressing His6-ChpT	Laboratory collection
pBAD_ctrA	pBAD/HisA expressing His6-CtrA	87
pBAD/His-CckA	pBAD/HisB expressing the cytoplasmic domain of CckA fused to His6x	23
pBAD/His-CckA L391F	pBAD/HisB expressing the cytoplasmic domain of CckAL391F fused to His6x	23
pBADHis-dctR	pBAD-His expressing DctR fused to His6x	30
pET28a	Expression vector for His6x-tagged proteins, Kan	Novagen
pET28A_6XHis-cckA_osp	pET28 expressing the transmitter domain of CckA fused to His6x, and Osp	This study
pET28A_6xHis-cckA	pET28 expressing the transmitter domain of CckA fused to His6x	This study
pET28a_His6x-PhoR	pET28a expressing the cytoplasmic domain of PhoR fused to His6x	This study
pET28a_osp	pET28a expressing Osp	This study
pET28a_osp6xHis	pET28a expressing Osp fused to His6x	This study
pGADT7	Plasmid for double hybrid assay with the Gal4 activation domain *LEU2*	Clontech
pGADT7_osp	pGADT7 expressing the fusion Gal4AD-Osp	This study
pGADT7_REC-DctR	pGADT7 expressing the fusion Gal4AD-REC-DctR	This study
pGBKT7	Plasmid for double hybrid assay with the Gal4 DNA binding domain *TRP1*	Clontech
pGBKT7_cckA_DHp-CA	pGBKT7 expressing the fusion of GAL4AD-CckA DHp domain	This study
pGBKT7_cckA-REC	pGBKT7 expressing the fusion of Gal4AD-CckA-REC	This study
pGBKT7_cckADPas	pGBKT7 expressing the fusion Gal4BD-CckAΔPAS	This study
pGBKT7_cckAΔTM	pGBKT7 expressing the fusion Gal4BD-CckAΔTM	This study
pIJ963	Plasmid source of the Hyg cassette	88
pJQ200mp18	Suicide vector for *R. sphaeroides*	89
pJQ200_Δosp::Hyg	pJQ200mp18 carrying Δ*osp*::Hyg	This study
pRK415	Expression vector used in *R. sphaeroides*, Tc	90
pRK_osp	pRK415 expressing Osp	This study
pRK_osp D51N	pRK415 expressing Osp D51N	This study
pRK_osp::uidA-aadA	pRK415 arring the transcriptional fusion *osp-uidA*	This study
pSUP11	Plasmid for epitope tagging	91
pTZ18R_Δosp::Hyg	pTZ18R carrying Δ*osp*::Hyg	This study
pTZ18R_ospUPDW	pTZ18R carrying the upstream and downstream regions of osp	This study
pTZ18R/19R	Cloning vectors, Ap	92
pTZ19R Bam-	pTZ19R without BamHI site	Laboratory collection
pTZospFLAG_1.7	pTZ19RBamHI- containing the upstream and coding region of FLAG-osp	This study
pWM5	Vector source of the *uidA-aadA* cassette	93

(SNPs and indels) were called using BCF tools (73, 74). Changes were confirmed by PCR followed by Sanger sequencing.

β-glucuronidase assay. Enzymatic activities were performed following previously reported protocols (29, 75). Protein content was determined with a Bio-Rad protein assay kit.

Strains isolated in this work. The strains isolated for this work were obtained following the procedures described in the supplementary methods (Text S1).

Protein overexpression and purification. Proteins were overexpressed and purified using standard methods (23, 76). Details of the procedures are described in supplementary methods (Text S1).

Phosphorylation reactions. His_6-CckA or the mutant version, His_6-$CckA_{L391F}$, was adjusted to 2.5 μM in HEPES buffer (33 mM HEPES, 10 mM $MgCl_2$, 50 mM KCl, 1 mM dithiothreitol, and 10% glycerol pH 7.5). Osp-His_6 was added as required at the indicated concentration. The phosphorylation reaction was started by adding 500 μM ATP with 1 μL of [γ-^{32}P]ATP to a final volume of 30 μL. At the desired time points, a sample of 5 μL was withdrawn, and the reaction was stopped by the addition of 5 μL of Laemmli sample buffer (4X) (77). After SDS-PAGE, radioactivity was visualized and quantified using phosphorimaging screens. The phosphotransfer reactions were performed by mixing His_6-CckA, or His_6-CckA and 2.5 μM Osp-His_6, together with purified His_6-ChpT (2.5 μM), and His_6-CtrA (2.5 μM) in HEPES buffer. The phosphorylation reaction was started by adding 500 μM ATP with 1 μL of [γ-^{32}P]ATP to a final volume of 30 μL. After 20 min the reaction was stopped by the addition of 30 μL of Laemmli sample buffer (4X). Alternatively, for the experiment shown in Fig. S3, 2.5 μM CckA was phosphorylated with [γ-^{32}P]ATP for 30 min and subject to size exclusion chromatography. The elution volume was divided in two and mixed with 2.5 μM ChpT and CtrA or with 2.5 μM ChpT, CtrA, and Osp. After mixing, samples were taken at the indicated times and subjected to SDS-PAGE.

Phosphatase activity of CckA. 2.5 μM His_6-CckA was phosphorylated using [γ-^{32}P]ATP for 20 min. After this time, the remaining ATP was removed by size exclusion chromatography. The elution volume of 40 μL was divided in two and mixed either with buffer or with 2.5 μM Osp-His_6 to a final volume of 30 μL. After mixing, samples were taken every 10 min and the reaction was stopped using 5 μL of Laemmli sample buffer (4X). Alternatively, phosphatase activity was also evaluated, initiating the reaction with 2.5 μM CckA, ChpT, and CtrA, previously phosphorylated with [γ-^{32}P]ATP for 30 min and subject to size exclusion chromatography. The elution volume was divided in two and mixed either with buffer or 2.5 μM Osp-His_6. Samples were taken at the indicated times and analyzed by SDS-PAGE.

Yeast double hybrid assays. Protein interactions were tested using the Matchmaker GAL4 system 3 following the instructions of the manufacturer (Clontech).

Western blot. Total cell extracts were subjected to SDS-PAGE (77). Proteins were transferred onto a nitrocellulose membrane and probed using anti-FLAG (1:10,000), anti-FlgE2, or anti FliA (1:30,000) immunoglobulins (78, 79). Detection was done with a secondary antibody conjugated to alkaline phosphatase and developed with CDPStar (Applied Biosystems).

Phylogenetic analysis. The *Rhodobacterales* species were selected if their genomes were complete or nearly complete >95% with low level of contamination <5% as outlined in CheckM (80). The RpoC protein was identified by BLASTP. The RpoC proteins were aligned with Muscle version 3.8 (81). The phylogenetic tree was constructed by neighbor joining method (82).

Bioinformatic analysis of the sequences. For each genome in Fig. 13, the intergenic region between *osp* and the upstream gene was obtained from the NCBI database. These sequences were searched for the presence of DNA motifs using MEME version 5.4.1 (83). For analysis of the sequences in Fig. 4, secondary structure predictions were carried out using Psipred (84) and protein homology was evaluated using Swiss-Model (85) and the crystal structure of CheY (PDB 6TG7).

SUPPLEMENTAL MATERIAL

Supplemental material is available online only.

TEXT S1, DOCX file, 0.03 MB.

FIG S1, TIF file, 2.8 MB.

FIG S2, TIF file, 1.6 MB.

FIG S3, TIF file, 2.6 MB.

FIG S4, TIF file, 2.7 MB.

FIG S5, TIF file, 2.7 MB.

FIG S6, TIF file, 2.4 MB.

FIG S7, DOCX file, 0.4 MB.

TABLE S1, DOCX file, 0.1 MB.

TABLE S2, DOCX file, 0.04 MB.

ACKNOWLEDGMENTS

We thank Tzipe Govezensky Zack for valuable help with statistical analysis, Aurora Osorio, Teresa Ballado, and Javier de la Mora for technical support, Daniel Garzón for his help with antibody production and animal care, and the Molecular Biology Unit IFC-UNAM for sequencing facilities. We thank the RAI, CIC-UNAM-INCMNSZ for the electron

microscopy facilities. We thank Cindie Capel Durán for construction of the pBAD-chpT plasmid.

This study is part of the requisites to obtain a doctoral degree by Benjamín Vega-Baray (Doctorado en Ciencias Biomédicas, Universidad Nacional Autónoma de México).

This work was partially supported by DGAPA-PAPIIT grant IG200420 to G.D. and L.C. Benjamín Vega-Baray was supported during his studies by a fellowship from CONACyT (becario 587609).

REFERENCES

1. Gao R, Stock AM. 2009. Biological insights from structures of two-component proteins. Annu Rev Microbiol 63:133–154. https://doi.org/10.1146/annurev.micro.091208.073214.
2. Laub MT, Goulian M. 2007. Specificity in two-component signal transduction pathways. Annu Rev Genet 41:121–145. https://doi.org/10.1146/annurev.genet.41.042007.170548.
3. Buschiazzo A, Trajtenberg F. 2019. Two-component sensing and regulation: how do histidine kinases talk with response regulators at the molecular level? Annu Rev Microbiol 73:507–528. https://doi.org/10.1146/annurev-micro-091018-054627.
4. Brilli M, Fondi M, Fani R, Mengoni A, Ferri L, Bazzicalupo M, Biondi EG. 2010. The diversity and evolution of cell cycle regulation in alpha-proteobacteria: a comparative genomic analysis. BMC Syst Biol 4:52. https://doi.org/10.1186/1752-0509-4-52.
5. Quon KC, Marczynski GT, Shapiro L. 1996. Cell cycle control by an essential bacterial two-component signal transduction protein. Cell 84:83–93. https://doi.org/10.1016/s0092-8674(00)80995-2.
6. Quon KC, Yang B, Domian IJ, Shapiro L, Marczynski GT. 1998. Negative control of bacterial DNA replication by a cell cycle regulatory protein that binds at the chromosome origin. Proc Natl Acad Sci U S A 95:120–125. https://doi.org/10.1073/pnas.95.1.120.
7. Leicht O, van Teeseling MCF, Panis G, Reif C, Wendt H, Viollier PH, Thanbichler M, Casadesus J, Casadesus J, Casadesus J, Casadesus J. 2020. Integrative and quantitative view of the CtrA regulatory network in a stalked budding bacterium. PLoS Genet 16:e1008724. https://doi.org/10.1371/journal.pgen.1008724.
8. Tsokos CG, Laub MT. 2012. Polarity and cell fate asymmetry in *Caulobacter crescentus*. Opin Microbiol 15:744–750. https://doi.org/10.1016/j.mib.2012.10.011.
9. Reisenauer A, Quon K, Shapiro L. 1999. The CtrA response regulator mediates temporal control of gene expression during the *Caulobacter* cell cycle. J Bacteriol 181:2430–2439. https://doi.org/10.1128/JB.181.8.2430-2439.1999.
10. Laub MT, Chen SL, Shapiro L, McAdams HH. 2002. Genes directly controlled by CtrA, a master regulator of the *Caulobacter* cell cycle. Proc Natl Acad Sci U S A 99:4632–4637. https://doi.org/10.1073/pnas.062065699.
11. Jenal U, Fuchs T. 1998. An essential protease involved in bacterial cell-cycle control. EMBO J 17:5658–5669. https://doi.org/10.1093/emboj/17.19.5658.
12. Ozaki S, Schalch-Moser A, Zumthor L, Manfredi P, Ebbensgaard A, Schirmer T, Jenal U. 2014. Activation and polar sequestration of PopA, a c-di-GMP effector protein involved in *Caulobacter crescentus* cell cycle control. Mol Microbiol 94:580–594. https://doi.org/10.1111/mmi.12777.
13. Iniesta AA, McGrath PT, Reisenauer A, McAdams HH, Shapiro L. 2006. A phospho-signaling pathway controls the localization and activity of a protease complex critical for bacterial cell cycle progression. Proc Natl Acad Sci U S A 103:10935–10940. https://doi.org/10.1073/pnas.0604554103.
14. Joshi KK, Berge M, Radhakrishnan SK, Viollier PH, Chien P. 2015. An adaptor hierarchy regulates proteolysis during a bacterial cell cycle. Cell 163:419–431. https://doi.org/10.1016/j.cell.2015.09.030.
15. Guzzo M, Sanderlin AG, Castro LK, Laub MT. 2021. Activation of a signaling pathway by the physical translocation of a chromosome. Dev Cell 56:2145–2159. https://doi.org/10.1016/j.devcel.2021.06.014.
16. Hecht GB, Lane T, Ohta N, Sommer JM, Newton A. 1995. An essential single-domain response regulator required for normal-cell division and differentiation in *Caulobacter crescentus*. EMBO J 14:3915–3924. https://doi.org/10.1002/j.1460-2075.1995.tb00063.x.
17. Lam H, Matroule JY, Jacobs-Wagner C. 2003. The asymmetric spatial distribution of bacterial signal transduction proteins coordinates cell cycle events. Dev Cell 5:149–159. https://doi.org/10.1016/s1534-5807(03)00191-6.
18. Matroule JY, Lam H, Burnette DT, Jacobs-Wagner C. 2004. Cytokinesis monitoring during development: rapid pole-to-pole shuttling of a signaling protein by localized kinase and phosphatase in *Caulobacter*. Cell 118:579–590. https://doi.org/10.1016/j.cell.2004.08.019.
19. Paul R, Jaeger T, Abel S, Wiederkehr I, Folcher M, Biondi EG, Laub MT, Jenal U. 2008. Allosteric regulation of histidine kinases by their cognate response regulator determines cell fate. Cell 133:928–928. https://doi.org/10.1016/j.cell.2008.05.018.
20. Childers WS, Xu Q, Mann TH, Mathews II, Blair JA, Deacon AM, Shapiro L. 2014. Cell fate regulation governed by a repurposed bacterial histidine kinase. PLoS Biol 12:e1001979. https://doi.org/10.1371/journal.pbio.1001979.
21. Dubey BN, Lori C, Ozaki S, Fucile G, Plaza-Menacho I, Jenal U, Schirmer T. 2016. Cyclic di-GMP mediates a histidine kinase/phosphatase switch by noncovalent domain cross-linking. Sci Adv 2:e1600823. https://doi.org/10.1126/sciadv.1600823.
22. Lori C, Ozaki S, Steiner S, Bohm R, Abel S, Dubey BN, Schirmer T, Hiller S, Jenal U. 2015. Cyclic di-GMP acts as a cell cycle oscillator to drive chromosome replication. Nature 523:236–239. https://doi.org/10.1038/nature14473.
23. Vega-Baray B, Domenzain C, Rivera A, Alfaro-Lopez R, Gomez-Cesar E, Poggio S, Dreyfus G, Camarena L. 2015. The flagellar set Fla2 in *Rhodobacter sphaeroides* is controlled by the CckA pathway and is repressed by organic acids and the expression of Fla1. J Bacteriol 197:833–847. https://doi.org/10.1128/JB.02429-14.
24. Poggio S, Abreu-Goodger C, Fabela S, Osorio A, Dreyfus G, Vinuesa P, Camarena L. 2007. A complete set of flagellar genes acquired by horizontal transfer coexists with the endogenous flagellar system in *Rhodobacter sphaeroides*. J Bacteriol 189:3208–3216. https://doi.org/10.1128/JB.01681-06.
25. Poggio S, Osorio A, Dreyfus G, Camarena L. 2005. The flagellar hierarchy of *Rhodobacter sphaeroides* is controlled by the concerted action of two enhancer-binding proteins. Mol Microbiol 58:969–983. https://doi.org/10.1111/j.1365-2958.2005.04900.x.
26. Hernandez-Valle J, Domenzain C, de la Mora J, Poggio S, Dreyfus G, Camarena L. 2017. The master regulators of the Fla1 and Fla2 flagella of *Rhodobacter sphaeroides* control the expression of their cognate CheY proteins. J Bacteriol 199:e00670-16. https://doi.org/10.1128/JB.00670-16.
27. del Campo AM, Ballado T, de la Mora J, Poggio S, Camarena L, Dreyfus G. 2007. Chemotactic control of the two flagellar systems of *Rhodobacter sphaeroides* is mediated by different sets of CheY and FliM proteins. J Bacteriol 189:8397–8401. https://doi.org/10.1128/JB.00730-07.
28. Camarena L, Dreyfus G. 2020. Living in a foster home: the single subpolar flagellum Fla1 of *Rhodobacter sphaeroides*. Biomolecules 10:774. https://doi.org/10.3390/biom10050774.
29. Hernandez-Valle J, Sanchez-Flores A, Poggio S, Dreyfus G, Camarena L. 2020. The CtrA regulon of *Rhodobacter sphaeroides* favors adaptation to a particular life style. J Bacteriol 202:e00678-19. https://doi.org/10.1128/JB.00678-19.
30. Sanchez-Ortiz VJ, Domenzain C, Poggio S, Dreyfus G, Camarena L. 2021. The periplasmic component of the DctPQM TRAP-transporter is part of the DctS/DctR sensory pathway in *Rhodobacter sphaeroides*. Microbiology 167. https://doi.org/10.1099/mic.0.001037.
31. de la Mora J, Uchida K, del Campo AM, Camarena L, Aizawa S, Dreyfus G. 2015. Structural characterization of the Fla2 flagellum of *Rhodobacter sphaeroides*. J Bacteriol 197:2859–2866. https://doi.org/10.1128/JB.00170-15.
32. Oh JI, Ko IJ, Kaplan S. 2003. Digging deeper: uncovering genetic loci which modulate photosynthesis gene expression in *Rhodobacter sphaeroides* 2.4.1. Microbiology 149:949–960. https://doi.org/10.1099/mic.0.26010-0.
33. Bourret RB. 2010. Receiver domain structure and function in response regulator proteins. Curr Opin Microbiol 13:142–149. https://doi.org/10.1016/j.mib.2010.01.015.
34. Gao R, Bouillet S, Stock AM. 2019. Structural basis of response regulator function. Annu Rev Microbiol 73:175–197. https://doi.org/10.1146/annurev-micro-020518-115931.

35. Janausch IG, Garcia-Moreno I, Lehnen D, Zeuner Y, Unden G. 2004. Phosphorylation and DNA binding of the regulator DcuR of the fumarate-responsive two-component system DcuSR of *Escherichia coli*. Microbiology 150:877–883. https://doi.org/10.1099/mic.0.26900-0.
36. Plate L, Marletta MA. 2012. Nitric oxide modulates bacterial biofilm formation through a multicomponent Cyclic-di-GMP signaling network. Mol Cell 46:449–460. https://doi.org/10.1016/j.molcel.2012.03.023.
37. Hernandez-Eligio A, Andrade A, Soto L, Morett E, Juarez K. 2017. The unphosphorylated form of the PilR two-component system regulates *pilA* gene expression in *Geobacter sulfurreducens*. Environ Sci Pollut Res Int 24:25693–25701. https://doi.org/10.1007/s11356-016-6192-5.
38. Merighi M, Majerczak DR, Stover EH, Coplin DL. 2003. The HrpX/HrpY two-component system activates *hrpS* expression, the first step in the regulatory cascade controlling the Hrp regulon in *Pantoea stewartii* subsp stewartii. Mol Plant Microbe Interact 16:238–248. https://doi.org/10.1094/MPMI.2003.16.3.238.
39. Ouimet MC, Marczynski GT. 2000. Analysis of a cell-cycle promoter bound by a response regulator. J Mol Biol 302:761–775. https://doi.org/10.1006/jmbi.2000.4500.
40. Zhou B, Schrader JM, Kalogeraki VS, Abeliuk E, Dinh CB, Pham JQ, Cui ZZ, Dill DL, McAdams HH, Shapiro L. 2015. The global regulatory architecture of transcription during the *Caulobacter* cell cycle. PLoS Genet 11:e1004831. https://doi.org/10.1371/journal.pgen.1004831.
41. Hsieh YJ, Wanner BL. 2010. Global regulation by the seven-component Pi signaling system. Curr Opin Microbiol 13:198–203. https://doi.org/10.1016/j.mib.2010.01.014.
42. Martinez-del Campo A, Ballado T, Camarena L, Dreyfus G. 2011. In *Rhodobacter sphaeroides*, chemotactic operon 1 regulates rotation of the flagellar system 2. J Bacteriol 193:6781–6786. https://doi.org/10.1128/JB.05933-11.
43. James P, Halladay J, Craig EA. 1996. Genomic libraries and a host strain designed for highly efficient two-hybrid selection in yeast. Genetics 144:1425–1436. https://doi.org/10.1093/genetics/144.4.1425.
44. Westbye AB, Kater L, Wiesmann C, Ding H, Yip CK, Beatty JT. 2018. The protease ClpXP and the PAS domain protein DivL regulate CtrA and gene transfer agent production in *Rhodobacter capsulatus*. Appl Environ Microbiol 84:e00275-18. https://doi.org/10.1128/AEM.00275-18.
45. Mann TH, Childers WS, Blair JA, Eckart MR, Shapiro L. 2016. A cell cycle kinase with tandem sensory PAS domains integrates cell fate cues. Nat Commun 7:11454–11466. https://doi.org/10.1038/ncomms11454.
46. Jiang P, Ninfa AJ. 1999. Regulation of autophosphorylation of *Escherichia coli* nitrogen regulator II by the PII signal transduction protein. J Bacteriol 181:1906–1911. https://doi.org/10.1128/JB.181.6.1906-1911.1999.
47. Jiang P, Atkinson MR, Srisawat C, Sun Q, Ninfa AJ. 2000. Functional dissection of the dimerization and enzymatic activities of *Escherichia coli* nitrogen regulator II and their regulation by the PII protein. Biochemistry 39:13433–13449. https://doi.org/10.1021/bi000794u.
48. Burkholder WF, Kurtser I, Grossman AD. 2001. Replication initiation proteins regulate a developmental checkpoint in *Bacillus subtilis*. Cell 104:269–279. https://doi.org/10.1016/s0092-8674(01)00211-2.
49. Wang L, Grau R, Perego M, Hoch JA. 1997. A novel histidine kinase inhibitor regulating development in *Bacillus subtilis*. Genes & Dev 11:2569–2579. https://doi.org/10.1101/gad.11.19.2569.
50. Pioszak AA, Jiang P, Ninfa AJ. 2000. The *Escherichia coli* PII signal transduction protein regulates the activities of the two-component system transmitter protein NRII by direct interaction with the kinase domain of the transmitter module. Biochemistry 39:13450–13461. https://doi.org/10.1021/bi000795m.
51. Martinez-Argudo I, Salinas P, Maldonado R, Contreras A. 2002. Domain interactions on the *ntr* signal transduction pathway: two-hybrid analysis of mutant and truncated derivatives of histidine kinase NtrB. J Bacteriol 184:200–206. https://doi.org/10.1128/JB.184.1.200-206.2002.
52. Cunningham KA, Burkholder WF. 2009. The histidine kinase inhibitor Sda binds near the site of autophosphorylation and may sterically hinder autophosphorylation and phosphotransfer to Spo0F. Mol Microbiol 71:659–677. https://doi.org/10.1111/j.1365-2958.2008.06554.x.
53. Whitten AE, Jacques DA, Hammouda B, Hanley T, King GF, Guss JM, Trewhella J, Langley DB. 2007. The structure of the KinA-Sda complex suggests an allosteric mechanism of histidine kinase inhibition. J Mol Biol 368:407–420. https://doi.org/10.1016/j.jmb.2007.01.064.
54. Cheah E, Carr PD, Suffolk PM, Vasudevan SG, Dixon NE, Ollis DL. 1994. Structure of the *Escherichia coli* signal transducing protein P_{II}. Structure 2:981–990. https://doi.org/10.1016/s0969-2126(94)00100-6.
55. Rowland SL, Burkholder WF, Cunningham KA, Maciejewski MW, Grossman AD, King GF. 2004. Structure and mechanism of action of Sda, an inhibitor of the histidine kinases that regulate initiation of sporulation in *Bacillus subtilis*. Mol Cell 13:689–701. https://doi.org/10.1016/s1097-2765(04)00084-x.
56. Jacques DA, Streamer M, Rowland SL, King GF, Guss JM, Trewhella J, Langley DB. 2009. Structure of the sporulation histidine kinase inhibitor Sda from *Bacillus subtilis* and insights into its solution state. Acta Crystallogr D Struct Biol 65:574–581. https://doi.org/10.1107/S090744490901169X.
57. Jacques DA, Langley DB, Jeffries CM, Cunningham KA, Burkholder WF, Guss JM, Trewhella J. 2008. Histidine kinase regulation by a cyclophilin-like inhibitor. J Mol Biol 384:422–435. https://doi.org/10.1016/j.jmb.2008.09.017.
58. Jacques DA, Langley DB, Hynson RMG, Whitten AE, Kwan A, Guss JM, Trewhella J. 2011. A novel structure of an antikinase and its inhibitor. J Mol Biol 405:214–226. https://doi.org/10.1016/j.jmb.2010.10.047.
59. Foussard M, Garnerone AM, Ni F, Soupene E, Boistard P, Batut J. 1997. Negative autoregulation of the *Rhizobium meliloti fixK* gene is indirect and requires a newly identified regulator, FixT. Mol Microbiol 25:27–37. https://doi.org/10.1046/j.1365-2958.1997.4501814.x.
60. Garnerone AM, Cabanes D, Foussard M, Boistard P, Batut J. 1999. Inhibition of the FixL sensor kinase by the FixT protein in *Sinorhizobium meliloti*. J Biol Chem 274:32500–32506. https://doi.org/10.1074/jbc.274.45.32500.
61. Crosson S, McGrath PT, Stephens C, McAdams HH, Shapiro L. 2005. Conserved modular design of an oxygen sensory/signaling network with species-specific output. Proc Natl Acad Sci U S A 102:8018–8023. https://doi.org/10.1073/pnas.0503022102.
62. Stein BJ, Fiebig A, Crosson S. 2020. Feedback control of a two-component signaling system an Fe-S-binding receiver domain. mBio 11:e03383-19. https://doi.org/10.1128/mBio.03383-19.
63. Bhate MP, Molnar KS, Goulian M, DeGrado WF. 2015. Signal transduction in histidine kinases: insights from new structures. Structure 23:981–994. https://doi.org/10.1016/j.str.2015.04.002.
64. Mechaly AE, Sassoon N, Betton JM, Alzari PM. 2014. Segmental Helical Motions and Dynamical Asymmetry Modulate Histidine Kinase Autophosphorylation. PLoS Biol 12:e1001776. https://doi.org/10.1371/journal.pbio.1001776.
65. Cai YF, Su MY, Ahmad A, Hu XJ, Sang JY, Kong LY, Chen XQ, Wang C, Shuai JW, Han AD. 2017. Conformational dynamics of the essential sensor histidine kinase WalK. Acta Crystallogr DStruct Biol 73:793–803. https://doi.org/10.1107/S2059798317013043.
66. Ruvolo MV, Mach KE, Burkholder WF. 2006. Proteolysis of the replication checkpoint protein Sda is necessary for the efficient initiation of sporulation after transient replication stress in *Bacillus subtilis*. Mol Microbiol 60:1490–1508. https://doi.org/10.1111/j.1365-2958.2006.05167.x.
67. Barnett MJ, Hung DY, Reisenauer A, Shapiro L, Long SR. 2001. A homolog of the CtrA cell cycle regulator is present and essential in *Sinorhizobium meliloti*. J Bacteriol 183:3204–3210. https://doi.org/10.1128/JB.183.10.3204-3210.2001.
68. Kim J, Heindl JE, Fuqua C. 2013. Coordination of division and development influences complex multicellular behavior in *Agrobacterium tumefaciens*. PLoS One 8:e56682. https://doi.org/10.1371/journal.pone.0056682.
69. Francis N, Poncin K, Fioravanti A, Vassen V, Willemart K, Ong TA, Rappez L, Letesson JJ, Biondi EG, De Bolle X. 2017. CtrA controls cell division and outer membrane composition of the pathogen *Brucella abortus*. Mol Microbiol 103:780–797. https://doi.org/10.1111/mmi.13589.
70. Sistrom WR. 1962. The kinetics of the synthesis of photopigments in *Rhodopseudomonas sphaeroides*. J Gen Microbiol 28:607–616. https://doi.org/10.1099/00221287-28-4-607.
71. Ausubel FM, Brent R, Kingston RE, Moore DD, Seidman JG, Smith JA, Struhl K. 1987. Current protocols in molecular biology. p 1.6.4-1.6.5; 1.7.1-1.7.3; 2.4.1-2.4.5 John Wiley, New York, NY.
72. Langmead B, Salzberg SL. 2012. Fast gapped-read alignment with Bowtie 2. Nat Methods 9:357–359. https://doi.org/10.1038/nmeth.1923.
73. Li H, Handsaker B, Wysoker A, Fennell T, Ruan J, Homer N, Marth G, Abecasis G, Durbin R, 1000 Genome Project Data Processing Subgroup. 2009. The sequence alignment/map format and SAMtools. Bioinformatics 25:2078–2079. https://doi.org/10.1093/bioinformatics/btp352.
74. Danecek P, Bonfield JK, Liddle J, Marshall J, Ohan V, Pollard MO, Whitwham A, Keane T, McCarthy SA, Davies RM, Li H. 2021. Twelve years of SAMtools and BCFtools. Gigascience 10. https://doi.org/10.1093/gigascience/giab008.
75. Jefferson RA, Burgess SM, Hirsh D. 1986. beta-Glucuronidase from *Escherichia coli* as a gene-fusion marker. Proc Natl Acad Sci U S A 83:8447–8451. https://doi.org/10.1073/pnas.83.22.8447.
76. Bornhorst JA, Falke JJ. 2000. Purification of proteins using polyhistidine affinity tags, p 245–254. *In* Bornhorst JA, Falke JJ, Simon M (ed), Applications of Chimeric Genes and Hybrid proteins, Pt A (electronic). Academic Press, Cambridge, MA.

77. Laemmli UK. 1970. Cleavage of structural proteins during the assembly of the head of bacteriophage T*4*. Nature 227:680–685. https://doi.org/10.1038/227680a0.
78. Towbin H, Staehelin T, Gordon J. 1979. Electrophoretic transfer of proteins from polyacrylamide gels to nitrocellulose sheets: procedure and some applications. Proc Natl Acad Sci U S A 76:4350–4354. https://doi.org/10.1073/pnas.76.9.4350.
79. Harlow E, Lane D. 1988. Antibodies. A laboratory manual. p 471–510. Cold Spring Harbor Laboratory Press, Cold Spring Harbor, New York.
80. Parks DH, Imelfort M, Skennerton CT, Hugenholtz P, Tyson GW. 2015. CheckM: assessing the quality of microbial genomes recovered from isolates, single cells, and metagenomes. Genome Res 25:1043–1055. https://doi.org/10.1101/gr.186072.114.
81. Edgar RC. 2004. MUSCLE: multiple sequence alignment with high accuracy and high throughput. Nucleic Acids Res 32:1792–1797. https://doi.org/10.1093/nar/gkh340.
82. Saitou N, Nei M. 1987. The neighbor-joining method: a new method for reconstructing phylogenetic trees. Mol Biol Evol 4:406–425. https://doi.org/10.1093/oxfordjournals.molbev.a040454.
83. Bailey TL, Boden M, Buske FA, Frith M, Grant CE, Clementi L, Ren J, Li WW, Noble WS. 2009. MEME SUITE: tools for motif discovery and searching. Nucleic Acids Res 37:W202–W208. https://doi.org/10.1093/nar/gkp335.
84. Buchan DWA, Jones DT. 2019. The PSIPRED protein analysis workbench: 20 years on. Nucleic Acids Res 47:W402–W407. https://doi.org/10.1093/nar/gkz297.
85. Waterhouse A, Bertoni M, Bienert S, Studer G, Tauriello G, Gumienny R, Heer FT, de Beer TAP, Rempfer C, Bordoli L, Lepore R, Schwede T. 2018. SWISS-MODEL: homology modelling of protein structures and complexes. Nucleic Acids Res 46:W296–W303. https://doi.org/10.1093/nar/gky427.
86. Soding J, Biegert A, Lupas AN. 2005. The HHpred interactive server for protein homology detection and structure prediction. Nucleic Acids Res 33:W244–W248. https://doi.org/10.1093/nar/gki408.
87. Rivera-Osorio A, Osorio A, Poggio S, Dreyfus G, Camarena L. 2018. Architecture of divergent flagellar promoters controlled by CtrA in *Rhodobacter sphaeroides*. BMC Microbiol 18:129. https://doi.org/10.1186/s12866-018-1264-y.
88. Lydiate DR, Ashby AM, Henderson DJ, Kieser T, Hopwood DA. 1989. Physical and genetic characterization of chromosomal copies of the *Streptomyces coelicolor* mini-circle. J Gen Microbiol 135:941–955. https://doi.org/10.1099/00221287-135-4-941.
89. Quandt J, Hynes MF. 1993. Versatile suicide vectors which allow direct selection for gene replacement in Gram-negative bacteria. Gene 127:15–21. https://doi.org/10.1016/0378-1119(93)90611-6.
90. Keen NT, Tamaki S, Kobayashi D, Trollinger D. 1988. Improved broad-host-range plasmids for DNA cloning in Gram-negative bacteria. Gene 70:191–197. https://doi.org/10.1016/0378-1119(88)90117-5.
91. Uzzau S, Figueroa-Bossi N, Rubino S, Bossi L. 2001. Epitope tagging of chromosomal genes in *Salmonella*. Proc Natl Acad Sci U S A 98:15264–15269. https://doi.org/10.1073/pnas.261348198.
92. Mead DA, Szczesna-Skorupa E, Kemper B. 1986. Single-stranded-DNA blue-T7 promoter plasmids - a versatile tandem promoter system for cloning and protein engineering Protein Eng 1:67–74. https://doi.org/10.1093/protein/1.1.67.
93. Metcalf WW, Wanner BL. 1993. Construction of new β-glucuronidase cassettes for making transcriptional fusions and their use with new methods for allele replacement. Gene 129:17–25. https://doi.org/10.1016/0378-1119(93)90691-u.